Development and improvement of pre-treatment technologies to enhance ferrochrome production

ELJ Kleynhans

20278241

MEng in Development and Management Engineering (cum laude), MSc in Chemistry (cum laude), BSc Industrial Science in Chemical Technology

Thesis submitted for the degree ***Philosophiae Doctor*** in ***Chemical Engineering*** at the Potchefstroom Campus of the North-West University

Supervisor:	Prof JP Beukes
Co-supervisor:	Dr PG van Zyl
Assistant supervisor:	Prof JR Bunt

November 2016

NORTH-WEST UNIVERSITY
YUNIBESITI YA BOKONE-BOPHIRIMA
NOORDWES-UNIVERSITEIT

It all starts here ™

SOLEMN DECLARATION

I, ***Ernst Lodewyk Johannes Kleynhans***, declare herewith that the thesis entitled:

Development and improvement of pre-treatment technologies to enhance ferrochrome production,

which I herewith submit to the North-West University (NWU) as completion of the requirements set for the ***PhD in Chemical Engineering*** degree, is my own work, unless specifically indicated to the contrary in the text, has been text edited as required and has not been submitted to any other tertiary institution other than the NWU.

Signature of student: E.L.J. Kleynhans University-number: **20278241**

Signed at **Potchefstroom** on **Sunday, 09 April 2017**

ACKNOWLEDGEMENTS

"The words of the wise are as goads, and as nails fastened by the masters of assemblies, which are given from one shepherd. And further, by these, my son, be admonished: of making many books there is no end; and much study is a weariness of the flesh. Let us hear the conclusion of the whole matter: Fear God, and keep his commandments: for this is the whole duty of man. For God shall bring every work into judgment, with every secret thing, whether it be good, or whether it be evil." Ecc 12:11-14 (KJV)

† *My Heavenly Father, thank you for blessing me daily and giving me the ability and perseverance to successfully complete this research. Thank you for your grace and love, for keeping an eye on me and guiding me throughout my life.* †

It is my honour and privilege to acknowledge and convey my sincerest gratitude to the following important contributors to my PhD degree:

The National Research Foundation (NRF) for financial assistance towards this research (Grant No. 96995 and 84451). The opinions expressed and conclusions arrived at, are those of the author and are not necessarily to be attributed to the NRF.

My supervisor and mentor, Prof Paul Beukes, and co-supervisor, Dr Pieter van Zyl. I am sincerely thankful for the part both of you played in my professional and personal growth and development. Thank you for the opportunity, input, guidance, support and encouragement. I would also like to acknowledge Prof John Bunt for his contribution to my success.

My parents, Ernst and Yvette, and my siblings Albert and Ingrid, thank you for your love, never-ending support and encouragement.

My best friend and wife, Anzel Kleynhans

We have been together since the onset of our post-graduate studies and I will forever treasure the time we studied together. Thank you for your unconditional and never-ending love, support, advice and encouragement. You kept me focused on what I wanted to achieve and helped me to persevere. I am truly grateful to have you in my life.

"I may not have everything I want in life but I'm blessed enough to have all that I need!"

PREFACE

Introduction

This thesis was submitted in article format, as allowed by the North-West University (NWU) under the General Academic Rules (A-rules) set for post-graduate curriculums (NWU, 2015). The A-rules prescribe that "...where a candidate is permitted to submit a thesis in the form of a published research article or articles or as an unpublished manuscript or manuscripts in article format and more than one such article or manuscript is used, the thesis must still be presented as a unit, supplemented with an inclusive problem statement, a focused literature analysis and integration and with a synoptic conclusion...." Due to the afore-mentioned the articles included in this PhD thesis were added as they were drafted for submission, submitted, accepted for publication, or published, depending at which stage a specific article was when the thesis was submitted for examination. The conventional experimental, as well as results and discussions chapters are therefore excluded from this thesis, since the relevant information is summarised in the articles. Separate motivation and objectives, literature and project evaluation chapters will be included, along with the articles, as set out in the Manual for Post Graduate Studies' guidelines for submitting a thesis in article format (NWU, 2016). As some of the information included in the motivation and objectives, literature and project evaluation chapters were summarised in the articles, this will result in some repetition of ideas/similar text in some of the chapters and in the articles itself (NWU, 2015; NWU, 2016). This minor repetition is therefore as a result of the format in which the thesis is submitted and is beyond the control of the candidate. The fonts, numbering and layout of Chapters 3 to 7 (containing the research articles) are also not consistent with the rest of the thesis, since they were added in the formats published, submitted or prepared for submission as required by the journals.

Rationale in submitting thesis in article format

Although submitting a thesis in article format is allowed by the NWU, it is currently not a requirement under the A-rules of the NWU. However, it is prescribe in the A-rules that with the submission of any thesis, which is not submitted in article format, faculty rules may require proof that at the time of submitting the thesis for examination, the candidate prepared a draft article ready for submission or, with the concurrence of the promoter, must submit proof that a research article has already been submitted to an accredited journal. However, in practice, many of these draft papers are never published in an accredited journal. At the time when this thesis was submitted for examination, two article (Chapters 3 and 5) had already been published in the journal *Minerals Engineering* (ISSN: 0892-6875), while the papers included in Chapter 4 and 6 was accepted for publication in *Metallurgical and Materials Transactions B* (ISSN: 1073-5615)

and the *Journal of the South African Institute of Mining and Metallurgy* (ISSN: 2225-6253), respectively.

There are several advantages to write a thesis in article format:

- It resolves the conflict between preparing the thesis for examination and preparing papers for publication, as they amount to the same outcome. Generally writing of the thesis enjoys priority, which results in a lot of work in theses not getting published, preventing such data from greater exposure to the peer reviewed public domain.

- It increases the probability that the work conducted for the purpose of the degree is published. This is not only to the advantage of the candidate, but also for the supervisor(s), contributors and the university in general.

- If the candidate submits and receives reviewers' comments on the article(s) before submitting the thesis for examination, the candidate can use this feedback to improve the thesis. This not only improves the quality of the thesis, but also gives the candidate a greater confidence in the work conducted. By the time the thesis is submitted for examination, the core part of the thesis has already been subjected to the scrutiny of experts other than the candidate and his supervisor(s).

- Having part of the work published prior to examination establishes it as worthy of publications, which is one of the requisite criteria for a PhD degree, but not a master's degree. Therefore the larger the portion that is published, the easier it is for the examiners of the thesis and the Board of the Graduate Research entity to recognise that the work has made a scientific contribution.

ABSTRACT

Ferrochrome (FeCr) is a vital alloy mostly used for the production of stainless steel. It is produced from chromite ore, the only economically exploitable natural chromium (Cr) resource, through carbothermic smelting in submerged arc or direct current furnaces. FeCr production is an energy-intensive process. FeCr producers strive towards lower overall energy consumption due to increases in costs, efficiency and environmental pressures. In South Africa, in particular, higher electricity prices have placed pressure on FeCr producers. Currently, the pelletised chromite pre-reduction process, also referred to as solid state reduction of chromite, is most likely the FeCr production process with the lowest specific electricity consumption (SEC), i.e. MWh/t FeCr produced.

The unique process considerations of clay binders in the pelletised chromite pre-reduction process were highlighted and demonstrated utilising two case study clays (Chapter 3). It was demonstrated that the clay binder has to impart high compressive and abrasion resistance strengths to the cured pellets in both oxidising and reducing environments (corresponding to the oxidised outer layer and pre-reduced core of industrially produced pellets), while ensuring adequate hot strength of pellets during the curing process. The possible effects of the clay binder selection and the amount of binder addition on the degree of chromite pre-reduction achieved were also investigated, since it could have substantial efficiency and economic implications. The case study results presented in this paper indicated that it is unlikely that the performance of a specific clay binder in this relatively complex process can be predicted, based only on the chemical, surface-chemical and mineralogical characterisation of the clay.

The effects of carbonaceous reductant selection on chromite pre-reduction and cured pellet strength were investigated (Chapter 4). Multiple linear regression analysis was employed to evaluate the effect of reductant characteristics on the aforementioned two parameters. This yielded mathematical solutions that can be used by FeCr producers to select reductants more optimally in future. Additionally, the results indicated that hydrogen (H)- (24% contribution) and volatile content (45.8% contribution) were the most significant contributors to predicting variance in pre-reduction and compressive strength, respectively. The role of H within this context is postulated to be linked to the ability of a reductant to release H that can induce reduction. Therefore, contrary to the current operational selection criteria, the authors believe that thermally untreated reductants (e.g. anthracite, as opposed to coke or char), with volatile contents close to the currently applied specification (to ensure pellet strength), would be optimal, since it would maximise the H content that would enhance pre-reduction.

The pre-oxidation of chromite ore prior to milling, agglomeration and pre-reduction was explored (Chapter 5) and found to significantly enhance the level of chromite pre-reduction achieved in the pelletised chromite pre-reduction process. This resulted in substantial decreases in both the SEC and lumpy carbonaceous reductants required for furnace smelting. The optimum pre-oxidation temperature was established as the temperature where a balance was achieved between maximising iron (Fe) migration to the surface of ore particles that were pre-oxidised, while avoiding the formation of free eskolaite (Cr_2O_3). For the case study metallurgical grade chromite ore considered, the optimum pre-oxidation temperature was found to be 1000 °C. Utilising such pre-oxidised ore could theoretically lead to an improvement of approximately 8.5% in the SEC and a 14% decrease in the lumpy carbonaceous material required during submerged arc furnace smelting of pelletised chromite pre-reduced feed. Therefore, the techno-economic feasibility of integrating chromite pre-oxidation into the pre-reduction process was investigated (Chapter 6). Financial modelling yielded a net present value (NPV) at a 10% discount rate of ~ZAR 900 million and an internal rate of return (IRR) of ~30.5% after tax, suggesting that the implementation of pre-oxidation prior to pelletised pre-reduction may be viable from an investment perspective. Sensitivity analyses indicated that the parameter with the greatest influence on the project NPV and IRR is the level of pre-reduction achieved. This indicated that the relationship between maintaining the optimum pre-oxidation temperature and the degree of pre-reduction achieved is critical to maximise process efficiency and financial viability.

FeCr producers are only paid per mass unit of Cr content in the FeCr, i.e. in US¢/lb contained Cr, according to the current global FeCr markets pricing structure. Consequently, FeCr producers transport a large fraction of their product weight, i.e. the Fe content of the FeCr, without any benefit. The Fe content in the FeCr produced depend on the chromite spinel chromium-to-iron (Cr/Fe) ratio. Therefore, the selective removal of Fe from the chromite spinel using different combinations of chromite pre-oxidation, pre-reduction and sulphuric acid leaching were also investigated (Chapter 7). The Cr/Fe ratio of the case study ores could be increased from 1.57 up to ~23.4. However Cr recovery decreased significantly under experimental conditions to achieve such high Cr/Fe ratios. More desirable Cr/Fe ratios of >2 up to ~4.28 were achieved, while maintaining Cr recoveries of >90%.

Keywords: Chromite, ferrochromium or ferrochrome (FeCr), pre-reduction, solid state reduction, pelletisation, clay binder, reductant selection, multi-linear regression, pre-oxidation, specific electricity consumption (SEC), discounted cash flow (DCF) model, techno-economic feasibility chromium-to-iron (Cr/Fe) ratio, sulphuric acid leaching

TABLE OF CONTENTS

LIST OF TABLES

The tables in the articles and appendix are no listed here

LIST OF FIGURES

The figures in the articles and appendix are no listed here

CHAPTER 1: MOTIVATION AND OBJECTIVES

In this chapter, an overview of the project motivation for developing and improving pre-treatment technologies to enhance ferrochrome production is briefly discussed in Section 1.1, while general aims and specific objectives of this study are listed in Section 1.2.

1.1 Motivation

Chromium (Cr) is an irreplaceable component in all grades of stainless steels and high end super-alloys (Cramer *et al.*, 2004; Murthy *et al.*, 2011). It is the key element that renders steel "stainless" and is present in alloys ranging in amounts from 12% to about 35% Cr, making it corrosion-, oxidation- and heat resistant. Generally, the higher the Cr content, the more corrosion-, oxidation- and heat resistant is the alloy. Chromite ores, containing Cr in the characteristic spinel mineral form, are the only commercially-viable source of large volumes of new Cr units. The vast majority, approximately 90-95%, of mined chromite ores are processed into intermediate products called high-carbon and charge grade ferrochrome (FeCr), a crude Cr-iron (Fe) alloy, containing roughly >48-65% Cr, about 4-8% carbon (C) and varying amounts (0-4%) of silicon (Si), depending on the process used, with the majority of the balance made up by Fe. Approximately 80-90% of FeCr produced serves as feedstock for the Argon Oxygen Decarburiser (AOD) process, which is a modified steel converter and the first step in producing a low carbon Cr and Fe melt. Additional alloying elements like Nickel (Ni) and Molybdenum (Mo) are then added to the melt before the liquid steel is cast into plates and then rolled into sheets. These sheets form the bulk of the primary stainless steel market, and are the feed for the myriad of stainless steel products. The demand for chromite ore and FeCr are driven primarily by the demand for stainless steel. While the market is showing signs of slowing, it is still expected that global stainless steel production growth will average +5.5% p.a. to the end of the decade, driven mainly by China and India with Europe and the US markets showing signs of recovery (Murthy *et al.*, 2011; ICDA, 2013d; ICDA, 2013c; ICDA, 2013a; Oberholzer & Daly, 2014; Barnes *et al.*, 2015).

FeCr is primarily produced during the pyrometallurgical carbo-thermic reduction of chromite, mainly in alternating current (AC) submerged arc furnaces (SAF) and direct current arc furnaces (DCF) (Beukes *et al.*, 2010; Dwarapudi *et al.*, 2013; Neizel *et al.*, 2013). This smelting production process consumes not only high quantities of electricity, but also large amounts of coal based reductants. The carbo-thermic reduction of chromite ore to produce different grades of FeCr is consequently among the most energy intensive metal extraction processes currently being

performed, not only due to the highly endothermic nature of the reduction reactions occurring in these processes, but also as a result of the very high operating temperatures required for the smelting operation to separate the Cr-containing alloy from the discard gangue material contained in the slag (Barnes *et al.*, 2015).

It is generally accepted that South Africa, with the world's largest known chromite deposits located in its Bushveld Igneous Complex (BIC), holds ~72% of global chromite reserves (~82% if the upper group two (UG2) reserves of the platinum mines is added) and ~68% of the global resource not including reserves (see Section 2.2.1 for definitions) (Venmyn Rand Pty Ltd, 2010). In the course of the last two decades, chromite production from the BIC has virtually tripled. During this period, South Africa's FeCr industry has grown to such an extent that there are currently 14 separate FeCr smelting facilities in existence with an estimated FeCr production capacity of 5.2 million t/y (Beukes *et al.*, 2012; Jones, 2015). As a result, the value of the country's export earnings from FeCr has increased more than 30-fold. Traditionally, South Africa produced chromite ore mainly for its own requirements, being the main FeCr producer globally at the time. Until 2011, South Africa was the largest FeCr producer in the world, with about 33% of global production. However, in 2012, South Africa relinquished its position as the world's leading FeCr producer, as its production decreased to about 30% of the world's output, becoming the second-largest FeCr producer after China who doubled their production from 2009-2012. This shift was largely driven by a deterioration of historical cost competitiveness and recent electricity supply constraints in South Africa, which in tum sparked a surge in chromite ore exports to supply the demand of a rapid growing Chinese FeCr and stainless steel industry. In 2012, South Africa produced the majority of the world's chromite ore, accounting for ~41% of the global production. However, ~55% of the ~10 million tonnes of chromite ore South Africa produced in 2012 were exported, implying that ~28% of ore consumed in the rest of the world in 2012 originated from South Africa (ICDA, 2013d; ICDA, 2013c; ICDA, 2013b; ICDA, 2013a; Oberholzer & Daly, 2014).

While South Africa hold approximately three quarters of the global chromite reserves and resources, the majority of the local chromite ores have relatively low chromium-to-iron (Cr/Fe) ratios. The major deposits in the western and eastern Bushveld, where resources are vast, have Cr/Fe ratios of 1.5 to 1.6 which is typical of South Africa's metallurgical grade ore. The local ferrochrome industry also receives significant volumes of UG2 chromite, which is a process residue from the platinum group metals (PGM) industry in South Africa (Cramer et al., 2004). This UG2 chromite ore usually has Cr/Fe ratios of 1.3 to 1.4. Due to South Africa's electricity constrained FeCr industry and the growing Chinese market, mines increased their export of metallurgical grade ore, while South African FeCr producers increasingly exploited the low cost UG2 chromite ores in order to reduce production costs (Howat, 1986; Cramer *et al.*, 2004).

The typical operational costs of FeCr smelters can be divided into four cost categories, i.e. chromite ore (30%), carbonaceous reductant (20%), electricity (30%) and other production costs (20%) (Daavittila *et al.*, 2004). However, the cost distribution for South African FeCr smelters varies slightly from smelters in European conditions; with chromite ore and reductants each accounting for approximately 30%, electricity accounting for 25-30% of the production costs, while factors such as maintenance, labour and waste disposal accounts for the remaining 10-15% (Biermann *et al.*, 2012; FAPA, 2016). Considering that electricity consumption is one of the single largest cost component in FeCr production (Daavittila *et al.*, 2004), instability in supply and cost increases are extremely significant. While electricity supply constraints are expected to be somewhat alleviated as 28% is expected to be added to South Africa's generating capacity over the next 5 years, the cost of electricity will be an ongoing challenge for South African FeCr producers competitiveness. Given Eskom's (South Africa's sole electricity supplier) funding constraints and cost inflation (particularly coal); electricity prices is predicted to increasing at 12% nominal (~6% real) up to 2018/19. This is higher than the 8% (9.5% for industrial users) set forward under the National Energy Regulator of South Africa's (NERSA) MYPD3 programme. This will result in electricity as a % of average South African FeCr production costs nearly doubling, increasing from approximately 25% to around 40% over the next four years (NERSA, 2009b; NERSA, 2009a; Eskom, 2011; Eskom, 2012; Oberholzer & Daly, 2014; FAPA, 2016).

Four relatively well-defined process combinations are utilised by the South African FeCr producers, i.e. i) conventional semi-closed furnace operation, ii) closed furnace operation utilising mostly oxidative sintered pelletised feed (Outotec), iii) closed furnace operation with pre-reduced pelletised feed (pelletised chromite pre-reduction), and iv) DCF operation (Beukes *et al.*, 2010). The pelletised chromite pre-reduction process is considered to be the process option with the lowest specific electricity consumption (SEC) currently being utilised industrially (Naiker & Riley, 2006b; Naiker, 2007; Ugwuegbu, 2012; Hu *et al.*, 2016). In this process, fine chromite (<6 mm), a clay binder and a carbon reductant are dry milled, pelletised, pre-heated and pre-reduced, before the hot pre-reduced pellets are fed along with additional reductants and fluxes into an closed SAF (Beukes *et al.*, 2010). The SEC of the pelletised chromite pre-reduction process is approximately 2.4 MWh/t FeCr (Naiker & Riley, 2006b; Naiker, 2007; Neizel *et al.*, 2013). When comparing this to the SEC for DCF operations of >4.5 MWh/t FeCr (Greyling *et al.*, 2010), the oxidative sintered process of ≥3.1 MWh/t FeCr (Botha, 2003; Naiker, 2007) and conventional SAF production of 3.9-4.2 MWh/t FeCr (Weber & Eric, 2006; Naiker, 2007), it becomes clear that the pelletised chromite pre-reduction process option holds significant SEC advantages, especially within the South African context with rapidly increasing electricity costs (Oberholzer & Daly, 2014). Other advantages associated with pelletised pre-reduced feed are, i.e. i) the ability to consume fine chromite, providing an agglomerate feed to the SAF, ii) the use of lower cost fine reductants as opposed to lumpy reductants, iii) the use of oxygen as an energy source, iv) Cr recoveries in

the order of 90% and v) the ability to produce a low silicon containing FeCr product (Botha, 2003; Naiker & Riley, 2006b; Naiker, 2007). It can therefore only be assumed that this process option will become more commonly applied as the pressure on energy consumption and environmental consciousness increases.

FeCr is mostly produced in SAFs in which, historically, the use of fine chromite ore (usually <6 mm) is limited, since fine materials increase the tendency of the surface layer of the SAF to sinter. This traps evolving process gas, which can result in so-called bed turnovers or blowing of the furnace that could have disastrous consequences (Riekkola-Vanhanen, 1999; Beukes *et al.*, 2010). The majority of South African chromite ore is relatively friable (Gu & Wills, 1988; Cramer *et al.*, 2004; Beukes *et al.*, 2010; Glastonbury *et al.*, 2010) and for this reason mostly fine metallurgical grade ore (<1 mm) and additional fine UG2 ores residue are available to FeCr producers. Consequently, an agglomeration step prior to feeding these ores into a FeCr SAF is required. Agglomerated furnace feed, which is one of the advantages of the chromite pre-reduction process mentioned previously, ensures a permeable furnace bed, without which gas eruptions, bed turnovers, reduced efficiencies and increased downtime are common (Beukes *et al.*, 2010).

Considering the extent of South Africa's chromite reserves, the unique characteristics of these reserves and the size of the local FeCr industry, processes to increase chromite pre-reduction levels could be of significant local (but also of international) interest. Data published by Niayesh and Fletcher (1986) clearly indicated how the SEC of the smelting furnace is decreased as the level of chromite pre-reduction and material feed temperature is increased. To enhance the pre-reduction process of the chromite ore, as well as its following reduction process in the arc furnace, various strategies have been investigated. A literature survey shows that the methods used by the researchers fall in two categories, i.e. i) microstructure modification of the chromite ore spinel structure and ii) flux or additive addition to enhance the rate and level of chromite pre-reduction (Sundar Murti *et al.*, 1983; Dawson & Edwards, 1986; Katayama *et al.*, 1986; Van Deventer, 1988; Nunnington & Barcza, 1989; Weber & Eric, 1992; Weber & Eric, 1993; Neuschiitz *et al.*, 1995; Ding & Warner, 1997a; Ding & Warner, 1997b; Lekatou & Walker, 1997; Duong & Johnston, 2000; Tathavakar *et al.*, 2005; Weber & Eric, 2006; Takano *et al.*, 2007; Kapure *et al.*, 2010; Zhao & Hayes, 2010; Kapure *et al.*, 2013; Beukes *et al.*, 2015; Wang *et al.*, 2015; Hu *et al.*, 2016).

In the pelletised chromite pre-reduction process, a clay binder and carbonaceous reductant, as secondary components, forms part of the raw material mixture along with the primary chromite ore component, as indicated earlier. It is highly likely that characteristics of specific clay binders and carbonaceous reductant raw materials utilised by the industry will have significant and varying effects on the level of achievable pre-reduction, either by being ineffectual, improving or impairing pre-reduction. However, it is not only the level of pre-reduction that needs to be considered in

the industrial application of the pelletised pre-reduction process, but also the physical attributes of the pellets, e.g. green pellet strength, cured pellet compressive and abrasion strengths, hot pellet strength. Without these characteristics, the pelletised material would break down, causing sintering on the surface of the SAF burden material and possible furnace eruptions. The hot pellet strength is equally important, since the breakdown of pellets that are pre-reduced in the rotary kiln results in the build-up of dam rings (material sticking to inside of kiln), which could significantly reduce kiln efficiencies. However, as far as the candidate could asses, the effect of different secondary raw materials, i.e. the clay binder and carbonaceous reductant, on the unique process requirement of the pre-reduction process have not been considered.

In order to alter the microstructure of the chromite spinel, a hydrometallurgical method, pyrometallurgical method or a combination of both, such as leaching, oxidative roasting, pre-reduction, smelting or chlorination must be employed. Tathavakar *et al.* (2005) studied the thermal decomposition behaviour of South African chromite ores in order to relate the influence of oxygen potential with the likely product phases formed. They identified that by treating chromite ore at high temperature in an oxidising atmosphere, oxidation of Fe^{2+} ensues and promotes the formation of an intermediate metastable maghemite-type defective or altered spinel phase, which then transforms into a sesquioxide phase at high temperatures. Oxidation as a treatment prior to smelting in the SAF is a commercially applied process. In the oxidative sintering process (Outotec, 2015), which has been the most commonly applied process over the last decade in the South African FeCr industry, milled chromite ore is sintered in pelletised form. This sintering process is essentially a partial oxidative process, during which the small amount of carbon present in the uncured pellets is oxidised to sinter the pellets (Niemelä *et al.*, 2004; Beukes *et al.*, 2010). SEC for SAF FeCr production with oxidative sintered pellets is ≥3.1 MWh/t FeCr as previously mentioned, which is an improvement from the conventional SAF smelting of ores. It is thus possible that pre-oxidation of chromite ore, prior to being used in the pelletised pre-reduction process, can potentially have significant SEC advantages.

As stated earlier, the Cr/Fe ratio of South African chromite ore is low. The Cr/Fe ratio is the primary determining factor of the Cr grade in the ferrochrome product produced (Fowkes, 2014). Current pricing practises in the world FeCr industry dictate that FeCr producers are only paid for the Cr content, i.e. in US¢/lb contained Cr (Cramer *et al.*, 2004). The argument therefore follows that shipping higher grade FeCr, i.e. ~65% vs. 48-52% Cr content, is more efficient in that you are transporting less "waste", i.e. the Fe content in the FeCr, without any benefit and ultimately is more sustainable in the long run (Oberholzer & Daly, 2014). It would thus be beneficial to the South African FeCr industry to remove Fe from the chromite ore and consequently increase the Cr/Fe ratio which would raise the Cr content in the FeCr that is ultimately produced. However, the Fe in chromite ores are contained in the spinel and not in the gangue material, making it

particularly difficult to separate. In order for the Fe to be removed, the spinel structure has to be structurally dissociated. Since microstructural modification of the chromite spinel to improve pre-reduction is one possible approach to enhance the growth and profitability South Africa's FeCr industry, it would be beneficial to further explore possibilities of improving the Cr/Fe ratio as well.

1.2 Objectives

The aims and objectives of this study were to:

1. Investigate the effect of secondary raw materials, i.e. i) the clay binder and ii) carbonaceous reductant, on the unique process requirements of the chromite pre-reduction process to ultimately assist FeCr producers in optimising the selection of their raw materials.

2. Evaluate whether pre-oxidation of chromite ore, prior to being used in the pelletised pre-reduction process, can improve the extent of pre-reduction, which will further improve the SEC of the SAF. The specific objectives were to i) present the new suggested process, i.e. pre-oxidation of chromite ore prior to pelletised pre-reduction, ii) assess how to optimise pre-oxidation conditions to maximise the benefit of using pre-oxidised chromite ore iii) indicate the possible practical advantages and disadvantages of this process option by considering factors such as SEC, carbonaceous reductant consumption, breaking- and abrasion strengths, as well as the formation of hexavalent chromium, Cr(VI), which is considered a human carcinogen and iv) asses the techno-economic feasibility of implementing the proposed pre-oxidation process prior to the chromite pre-reduction process.

3. Identify an appropriate method(s) to alter the chromite spinel and improve the Cr/Fe ratio of low grade chromite ore.

CHAPTER 2: LITERATURE SURVEY

In this chapter, an overview of relevant literature is provided. This consists of general information on chromium (Section 2.1), the importance of ferrochrome within the South African context as well as factors impacting on the industry (Section 2.2), the main processes and techniques utilised during chromite beneficiation and ferrochrome production (Section 2.3), chromite pre-reduction as an energy saving process option (Section 2.4), pre-oxidation as a pre-treatment method (Section 2.5) and different approaches to change the spinel structure of chromite (Section 2.6). Finally, a concluding summary is provided to end the chapter (Section 2.7).

2.1 General information on chromium

2.1.1 Historical perspective

The known history of chromium (Cr) began over 200 years ago, though some speculation exist that it was known to ancient civilisations. However, such early uses of Cr (e.g. in ancient civilisations) would have been accidental, since the attributes of Cr metal and its other forms were never documented and thus unknown at that stage. A historical chronology of Cr is presented in Table 2-1. The history of Cr started in 1762, when J.G. Lehmann described in a letter an orange-yellow mineral he obtained from the Beresof gold mines in Siberia's Ural Mountains, which he called crocoite because it resembled the yellow colour of egg yolk (*krokos* in Greek). In 1797, a French chemist named Nicolas-Louis Vauquelin identified a new metallic element in crocoite. After further research, Vauquelin found that trace elements of the metallic element give rubies their characteristic red colour and emeralds, serpentine and Cr mica their distinctive green colour. He called the metallic element "chromium", after the Greek *khrōma*, meaning colour, because of its colourful compounds. By this time, the yellow concentrate obtained by means of crushing crocoite was already utilised as a paint pigment. Chromium's versatility became even more evident as time progressed, however, paint remained the main application for many years. In the 19th century potassium dichromate was found to help dyes attach and adhere to fabric and was introduced as a mordant in the textile industry. A few years later, Cr salts were introduced in tanning leather. The use of Cr as a timber preservative dates back to the early 20th century. In the 1920s, the process of Cr electroplating was developed. This gave the metal surface certain properties, including abrasion and wear resistance, corrosion protection, lubricity and aesthetic qualities. Cr's use in refractory bricks began late in the 19th century and its use in foundry sands, for moulding, did not transpire until the 20th century. The first patent for the use of Cr in steel was granted in 1865. However, the large-scale use of Cr in metals was not realised until the

development of the electric arc furnace in the early 1900s, which made it possible to smelt chromite, the principal ore of Cr, into ferrochrome (FeCr). Although Cr occur in many minerals, chromite is the only Cr mineral of economic importance for FeCr production. At this stage, i.e. in the early 1900s, Cr was used to produce Cr metal – an "alloy" composed almost entirely of Cr. Then, with the discovery of stainless steel, the Cr industry started to grow rapidly. At the beginning of the 20th century, global production of chromite was less than 100 000 tpa. In 2000 it reached 16 million tpa and in 2010 it had climbed to 25 million tpa (IETEG, 2005).

Table 2-1: Chronology of Cr (IETEG, 2005; ICDA, 2016)

1762	Lehmann discovers crocoite while visiting the Beresof mines located on the eastern slopes of the Ural Mountains in Siberia.
1798	Vauquelin identifies metallic Cr.
1811	First known major chromite discovery in the USA (exploited immediately).
1820	Potassium dichromate first used as a tanning mordant and Koechlin introduces Cr yellow in calico printing.
1830	Norway starts mining chromite.
1846	Small chromite deposits discovered in Canada.
1848	Important chromite discovery in Turkey.
1849	Chromite discovered in India (but is only exploited 50 years later).
1858	Cr leather tanning invented.
1860	Turkey becomes world leader of chromite production.
1865	Important discovery of chromite in South Africa and Zimbabwe (but is only exploited 50 years later). First patent for the use of Cr in steel.
1879	First recorded use of Cr in refractory applications.
1882	Chromite discovered in Australia.
1892	First commercial discovery of chromite on Russian territory.
1893	FeCr is first produced by Moissan in an electric fumace. First use in armour plating (Germany).
1897	America produces its first commercial high-carbon (HC) FeCr.
1898	First production of pure Cr by aluminothermy.
1906	Cr ore is found in Brazil and Cuba. First industrial production of FeCr in USA by UCAR.
1935	Chromated copper arsenate first used as a wood preservative in timber treatment.
1937	Discovery of chromite deposits in Albania and the Philippines.
1942	First production of HC, medium carbon (MC) and low carbon (LC) FeCr in South Africa.
1943	First FeCr smelter in the USSR (Kazakhstan) (Serov, 2010).
1960	First use of chromite as a specialist foundry sand (South Africa).
1963	First furnace for charge grade FeCr production in South Africa.
1966	Soviet Union becomes the most important FeCr producer.
1983	First direct current (DC) plasma arc fumace for FeCr in South Africa.
1999	South Africa becomes the world's most important producer of charge grade FeCr.

2.1.2 Properties, geology and mineralogy

Pure metallic Cr is lustrous and silver-like in colour, hard but brittle, malleable and can take a high polish. It has a high melting and boiling point of ~1857 °C and ~2672 °C, respectively. It has a density near room temperature (20 °C) of 7.15 g/cm^3 and a liquid density of 6.3 g/cm^3 at its melting point. The heat of fusion of Cr is 21 kJ/mol, its heat of vaporisation is 339.5 kJ/mol and it has a specific heat capacity of 23.35 J/mol.K at 25 °C. Cr is a member of the transition metals (IETEG, 2005; Roza, 2008; Lide, 2009). The oxidation states of Cr currently known to science range from –2 to +6, but it most commonly occurs as Cr^0, Cr^{2+}, $Cr^{3+}$and Cr^{6+}. Chromium in the 2+ oxidation state is, however, rather unstable and is rapidly oxidised to the 3+ state, thus only the trivalent and hexavalent forms are found in nature. The natural occurring isotopes for Cr are ^{50}Cr (4.3%), ^{52}Cr (83.8%), ^{53}Cr (9.6%), and ^{54}Cr (2.4%). Cr is the ninth most abundant compound on earth and exists in a number of mineral forms, however its distribution varies considerably. Therefore, as with all minerals, economic deposits occur only in nature where the specific element has significantly concentrated. Rock in the earth's crust contain an average of 400 ppm of Cr by mass, seawater 0.6 ppb, stream water 1 ppb, and humans 30 ppb. Cr(III) is not considered to be toxic and is in fact a vital micro nutrient. In contrast, airborne Cr(VI) is considered to be carcinogenic (IETEG, 2005; Loock *et al.*, 2014; Loock-Hattingh *et al.*, 2015). Chromite, an iron(II)-Cr(III) oxide, is the main source of Cr. Chromite is a weakly magnetic, silvery black to brownish black mineral of igneous origin. It occurs solely in peridotite of plutonic rocks formed by the intrusion and solidification of molten lava or magma, which is very rich in heavy, iron containing minerals such as pyroxenes and olivines. Inside these rocks, often referred to as ultramafic igneous rocks, Cr occurs in a spinel structure, a highly complex isometric crystal system. In its basic form, it contains magnesium as MgO as well as aluminium as Al_2O_3. The Cr spinel is therefore represented in its simplest form as (IETEG, 2005):

$$(Fe,Mg)O.(Cr,Fe,Al)_2O_3 \qquad 2\text{-}1$$

Chromite spinel fits to cubic coordination, shown in Figure 2-1, in which the 32 oxygen atoms stack in the central plane of the large cubic cell, forming 64 tetrahedral cavities and 32 octahedral cavities. Amongst these cavities, for the classic chromite spinel, eight tetrahedral sites are occupied by Fe^{2+} and 16 octahedral sites are occupied by Cr^{3+}. In chromite ores occurring in nature, part of the Fe^{2+} can be replaced by Mg^{2+} and a part of the Cr^{3+} can be replaced by Al^{3+} or Fe^{3+}. Thus, $(Fe,Mg)O.(Cr,Fe,Al)_2O_3$ as the Cr-bearing phase is isomorphic, in which Mg^{2+} and Fe^{2+} occupy the tetrahedral sites of the lattice, whereas Cr^{3+}, Al^{3+}, and Fe^{3+} occupy the octahedral sites (Zhang *et al.*, 2016).

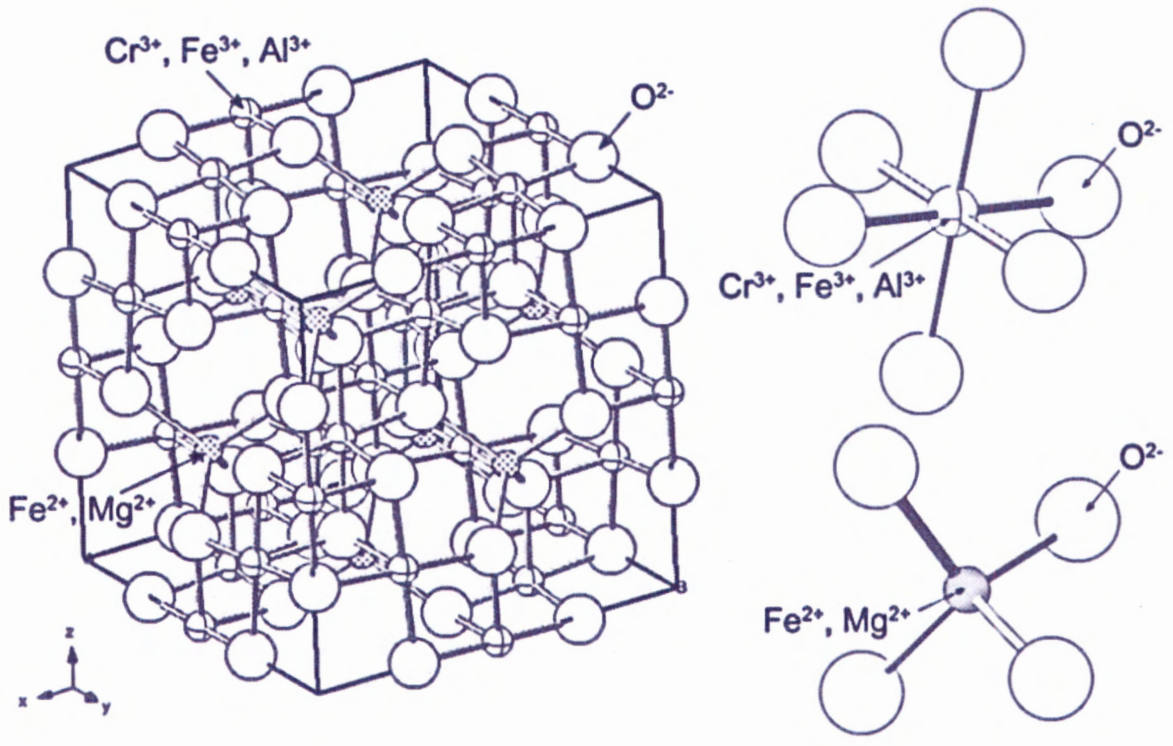

Figure 2-1: Crystalline structure of chromite spinel (Zhang *et al.*, 2016)

Large variations in the total and relative amounts of Cr and Fe in the lattice occur in different deposits. These affect the ore grade, not only in terms of the Cr_2O_3 content, but also in the chromium-to-iron (Cr/Fe) ratio which determines the Cr content of the FeCr produced. The variations also affect the reducibility (relative ease of reduction) of the ore. For example, increasing amounts of magnesium compared with iron in the divalent site will make the spinel more difficult to reduce. On the other hand, increasing amounts of iron in the trivalent site, replacing aluminium, will increase the reducibility of the spinel. Hence, chromite ore can be given a refractory index, i.e. its relative resistance to reduction, as shown in Equation 2-2 (IETEG, 2005).

$$Refractory\ index = \frac{wt.\%\ Cr_2O_3 + MgO + Al_2O_3}{(Total\ Fe\ as\ FeO) + SiO_2} \qquad 2\text{-}2$$

Chromite has also been identified in serpentinites, which may be developed through hydrothermal alteration of a peridotite. Uvarovite, the Cr garnet, is commonly associated with chromite. The Mohs hardness of chromite is 5.5 and the specific gravity is 4.3 to 5.0. Because of these physical characteristics of chromite it is occasionally concentrated in placer deposits (Schroeder, 1970; National Academy of Sciences, 1974; IETEG, 2005).

2.1.3 Uses

Chromium is a strategic metal of the twentieth century, but it is also used in dozens of industrial processes creating a vast number of consumer products. A breakdown of the global use of Cr is shown in Figure 2-2 (Heinz H. Pariser, 2013; ICDA, 2013c).

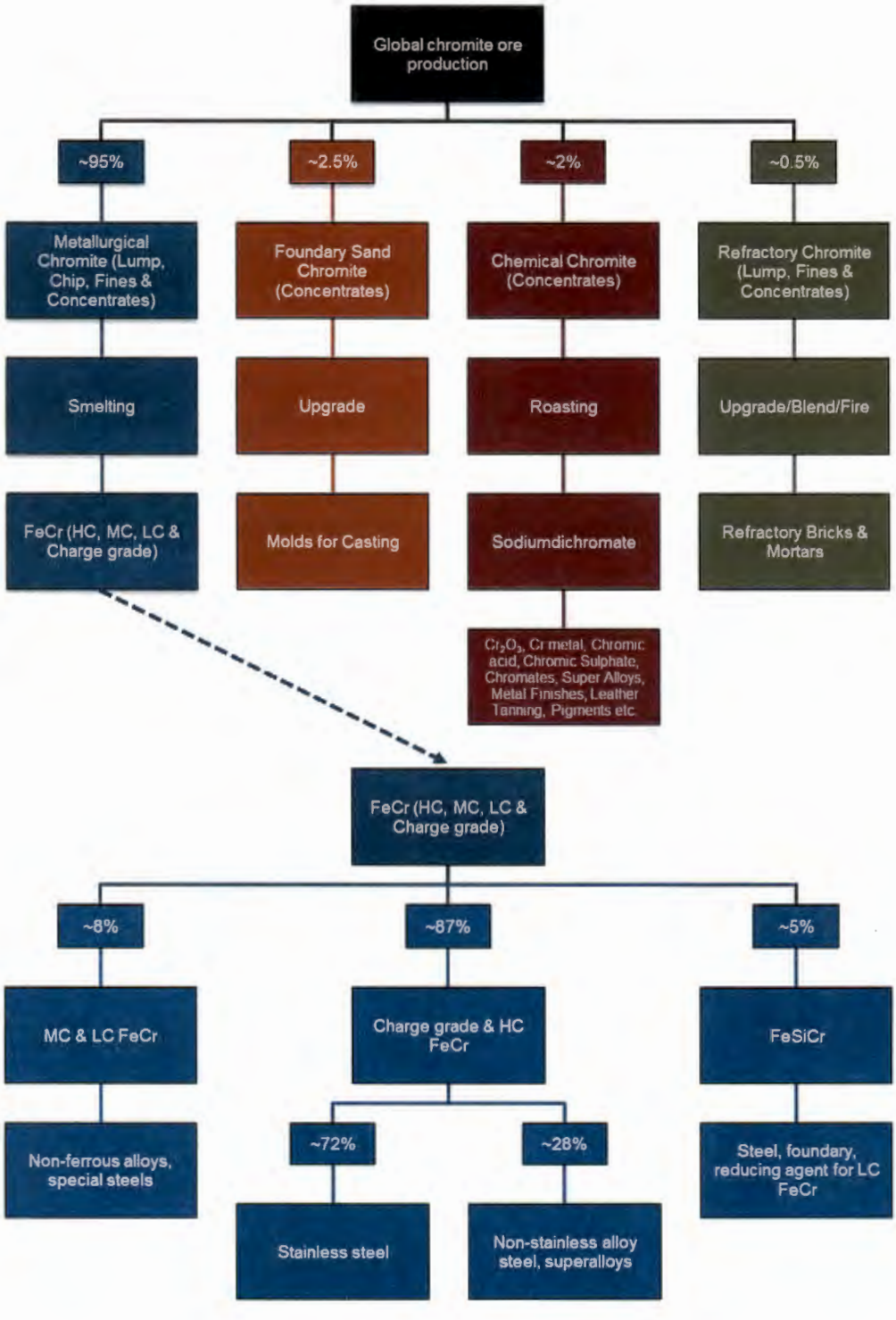

Figure 2-2: Breakdown of the industrial uses of Cr (Pariser, 2013)

The FeCr market accounts for most of the world's demand for Cr, but several niche markets use Cr in applications related to the foundry, refractory and chemical industries. According to the United States Geological Survey (USGS), Cr in the form of chromite ore has no substitute in the production of FeCr, Cr chemicals, or chromite refractories (Kogel *et al.*, 2006; USGS, 2015). Furthermore, Cr in the form of FeCr has no substitutes in super-alloys or in stainless steels, which is the largest use of FeCr. Until the early 1900s, chromite was mainly used in the manufacturing of chemicals. In the early 1900s, chromite became widely used in the manufacturing of metallurgical and refractory products, notably in stainless steels and basic refractory bricks. Refractory bricks and shapes formed of chromite are useful owing to the high melting temperature, moderate thermal expansion, and the general stability of the chromite crystalline structure. Cr containing steels have no substitute when combined characteristics such as high-temperature rigidity, as well as resistance to tarnish and abrasion are required, as in the case of roller bearings or in the aerospace and machine tool industries (IETEG, 2005). Table 2–2 provides a summary of the typical compositions of chromite generally required for various types of end-uses.

Table 2–2: General compositions of various grades of chromite (Riekkola-Vanhanen, 1999; Kogel *et al.*, 2006; Venmyn Rand Pty Ltd, 2010)

Use	%Cr_2O_3	%C	Cr/Fe ratio	%SiO_2
HC FeCr	>60	4-10	2.0-3.6	2-4
Charge grade FeCr	48-55	6-8	1.3-2.0	
MC FeCr	>55	0.5-4		
LC FeCr	>55	0.01-0.5		<1.0
Chemical	40-46		<2.1	
Refractory	>60 (plus Al_2O_3)			0.7

2.2 South Africa's ferrochrome industry

2.2.1 Chromite ore resources

Historically, there was sufficient high-grade metallurgical chromite ore to meet demand, however with the rapid growth of the stainless and other alloy steel industries, the much larger reserves of the lower grade-higher Fe containing ores had to be exploited. Through the years, various terms have been used to describe and classify mineral resources. It is therefore important to correctly

define these classifications, before these terms are used. The USGS define resources, reserve base, reserves, and shipping-grade chromite ore as follows (USGS, 2015):

Resource – a mineral in such a form that economic extraction of a commodity from the concentration is currently or potentially feasible.
Reserve base – the part of an identified resource that meets specified minimum physical and chemical criteria related to current mining and production practices, including those for grade, quality, thickness, and depth.
Reserve – the part of the reserve base which could be economically extracted or produced at the time of determination. The term reserves need not signify that extraction facilities are in place and operative.
Shipping-grade chromite – the reserve deposit quantity and grade normalised to 45% Cr_2O_3.

Global chromite resources are estimated by different sources to be between 7.5 and 12 billion tons (including or excluding reserves), which is sufficient to meet demand for centuries (Kogel *et al.*, 2006; Papp, 2009a; Venmyn Rand Pty Ltd, 2010; OCC, 2014). The global chromite mineral reserves and mineral resources (exclusive of reserves) are presented in Table 2–3 (Venmyn Rand Pty Ltd, 2010; Pariser, 2013), along with the geographical locations and size of major chromite resource deposits, obtained from Kogel *et al.* (2006) and illustrated in Figure 2-3.

Table 2–3: Global chromite mineral resources and mineral reserves in million tonnes (Mt) (Venmyn Rand Pty Ltd, 2010; Pariser, 2013)

	Reserves		Rank	Resources		Rank
Country	Mt	%		Mt	%	
South Africa	3 100	84.56%	1	5 500	68.73%	1
Kazakhstan	320	8.73%	2	320	4.00%	3
Zimbabwe	140	3.82%	3	1 000	12.50%	2
Finland	41	1.12%	4	120	1.50%	5
India	27	0.74%	5	67	0.84%	6
Canada	NA	-	-	220	2.75%	4
Turkey	NA	-	-	220	2.75%	4
Others	38	1.04%	-	555	6.94%	-
Total	3 666	100%		8 002	100%	

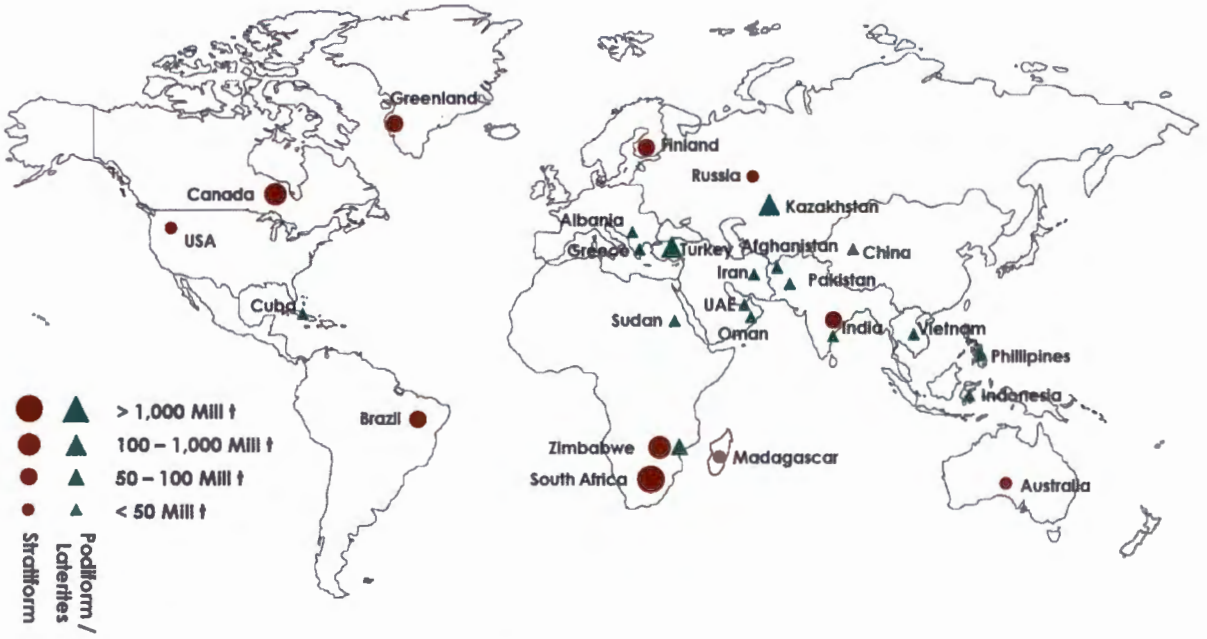

Figure 2-3: Geographical location, geologic type and size of major chromite ore resource deposit (Kogel *et al.*, 2006; Pariser, 2013; OCC, 2014)

According to various sources South Africa holds between 68 to 80% of the world's economically viable chromite ore resources (Riekkola-Vanhanen, 1999; Cramer *et al.*, 2004; Basson *et al.*, 2007; Lungu, 2010; Pariser, 2013; OCC, 2014). Large resources and reserves are also located in Zimbabwe, with smaller resource deposits situated in Canada, Finland, India, Kazakhstan and Turkey.

The total world shipping-grade chromite ore reserves were estimated by the USGS at around 480 million tonnes (Mt) (Basson *et al.*, 2007; Papp, 2008; USGS, 2015), while the International Chromium Development Association (ICDA) estimates that world chromite reserves total 3.6 billion tonnes (Table 2–3).

Chromite spinel is a heavy mineral (i.e. high specific density) and thus concentrates through gravity separation from most of the other molten material in the magma during cooling and crystallisation. Geologically the world's commercial chromite ore resources are found in either podiform or stratiform deposits. Podiform-type chromite deposits occur in irregular shapes like pods or lenses, while stratiform-type chromite deposits occur as parallel seams in large, layered igneous rock complexes (Gu & Wills, 1988; Paktunc, 1990; Papp & Lipin, 2000; Cramer *et al.*, 2004). The layering is regular and there is large lateral continuity. The largest and best example of this type of deposit is the Kaapvaal and Zimbabwe cratons in Southern Africa, characterised by the presence of large mafic to ultramafic layered complexes. By far the most important and economically viable of these is the Bushveld Igneous Complex (BIC), which was intruded 2.06

billion years ago into the rocks of the Transvaal Supergroup along the unconformity between the Magaliesburg quartzites and the overlying Rooiberg felsites. The total estimated area of the BIC is 66,000 km^2, about 55% of which is covered by younger formations. The mafic rocks of the BIC can be divided into a number of units according to their representative gravity anomalies. These include the north-western and south-western lobes, separated by the Pilanesberg Alkaline Complex, and the north-eastem and south-eastern lobes that are separated by the Steelpoort fault. The geology and stratigraphy of the BIC is presented in Figure 2-4. The mafic rocks, collectively known as the Rustenburg Layered Suite (RLS), can be divided into five zones, i.e. Upper Zone (UZ), Main Zone (MZ), Critical Zone (CZ), Lower Zone (LZ), and Marginal/Bordering Zone (BZ) (from the top downwards, as shown in Figure 2-4). At the base, the Marginal Zone consists of generally finer-grained rocks than those of the interior of the complex and contains an abundance of xenoliths. It is highly variable in thickness, may be completely absent in some areas and contains no economic mineralisation (Venmyn Rand Pty Ltd, 2010).

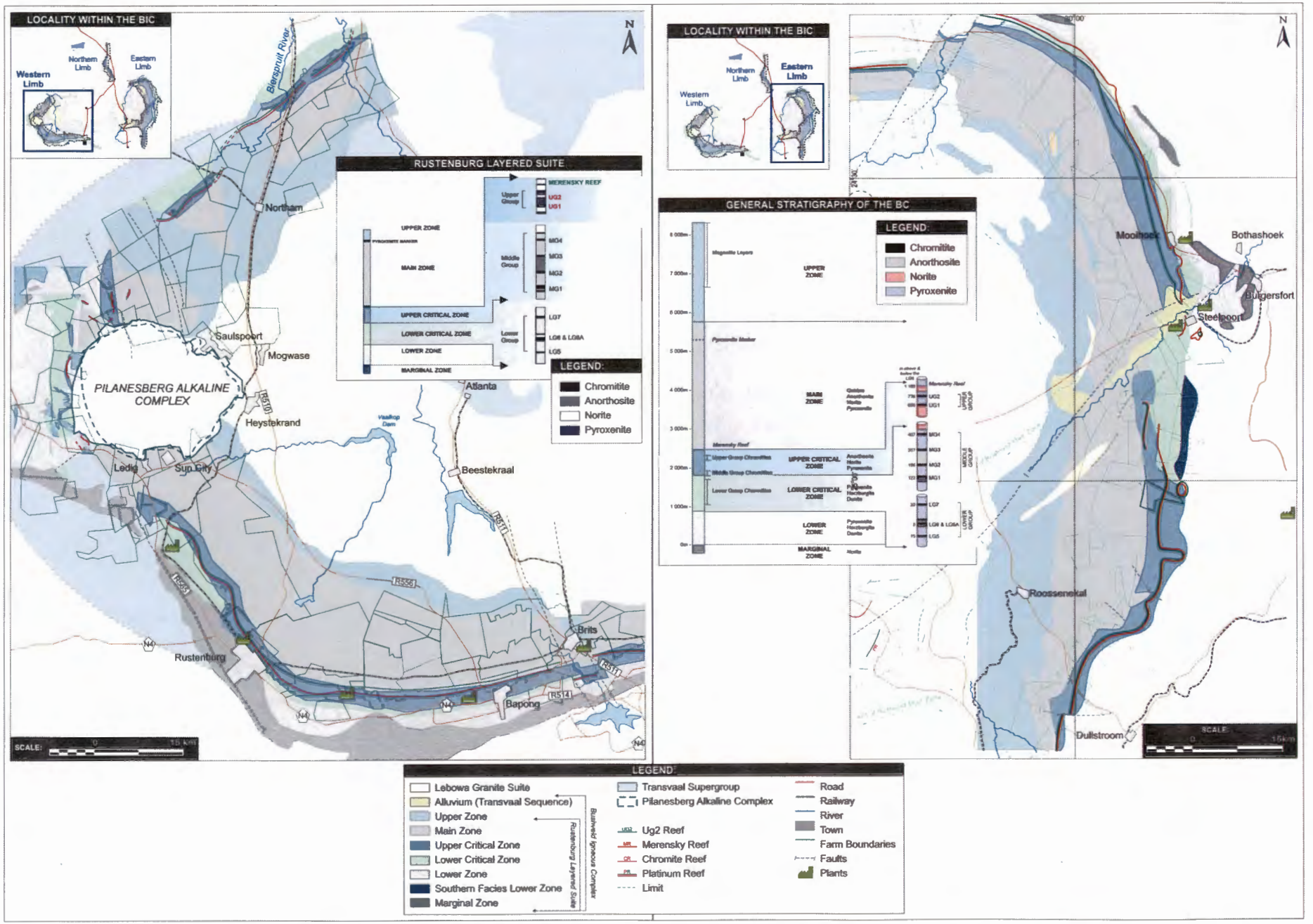

Figure 2-4: Regional location of the western and eastern BIC and related chromite mineral seam deposits (Venmyn Rand Pty Ltd, 2010)

As previously stated, South Africa's entire chromite ore resources are located within the BIC where several chromite seams exist (Cramer *et al.*, 2004). The chromite layers are confined to the Critical Zone and are subdivided into Lower, Middle, and Upper Groups. All the layers of the Lower Group (LG) occur within the pyroxenites of the Lower Critical Zone. The Middle Group (MG) of layers occur at the transition from the Lower to the Upper Critical Zone, at a level where plagioclase first becomes persistently cumulus within the whole BIC sequence. The MG chromite layers are either hosted by pyroxenites or by plagioclase-rich norites and anorthosites. The Upper Group (UG) of layers occur within the Upper Critical Zone below the Merensky Reef. The LG contains seven layers and the MG four in the western and eastern BIC, while the UG consist of two layers in the western BIC and three layers in the eastern BIC (Venmyn Rand Pty Ltd, 2010). South Africa's most productive economically exploitable seams are the lower group 6 (LG6) with a Cr/Fe ratio of 1.5-2, the middle group 1 and 2 (MG1 and MG2) with a Cr/Fe ratio of 1.5-1.8 and the upper group 2 (UG2) with a Cr/Fe ratio of 1.3-1.4. The last of these is not of interest as a source of chromite alone, but primarily as a source of platinum group metals (PGMs). Chromite ores in South Africa are therefore associated with PGMs. The major reserves of PGMs are the UG2 and Merensky reefs, which are the largest deposits of Cr, vanadium and platinum in the world (Howat, 1986; Cramer, 2001; Cramer *et al.*, 2004; Xiao & Laplante, 2004; Basson *et al.*, 2007). UG2 chromite ore is gaining acceptance as a source for charge grade FeCr production with the utilisation of several technological innovations (Basson *et al.*, 2007). One should take note that South Africa's *in situ* chromite ores are largely low grade (<45% Cr_2O_3) with low Cr/Fe ratios (<1.6) and are generally brittle. South Africa's main chromite ores are not devalued *per se* by a low Cr content, but rather by the low Cr/Fe ratio of the ores. This is illustrated in Figure 2-5, showing the typical Cr_2O_3 content and Cr/Fe ratios of selected chromite ores. Comparing South Africa's primary metallurgical grade and UG2 chromite ore with typical Indian, Zimbabwean and Turkish ore, it is observed that the Cr_2O_3 content of the ores are similar, however the Indian, Zimbabwean and Turkish ores has higher Cr/Fe ratios. This is as a result of a higher Fe content in South African ores. The relationship between the grades of FeCr that can be produced from chromite ores with different Cr/Fe ratios is presented in Figure 2-6. The resulting alloys produced from South African chromite ores are mostly normal or low charge grade FeCr with a Cr content of <55%, compared to HC FeCr (Cr content >60%) produced from Turkish chromite ore with a Cr/Fe of 3. The production of charge grade FeCr, with lower Cr content, influences the transport cost per Cr unit adversely (Basson *et al.*, 2007), since FeCr producers are only paid for the Cr content.

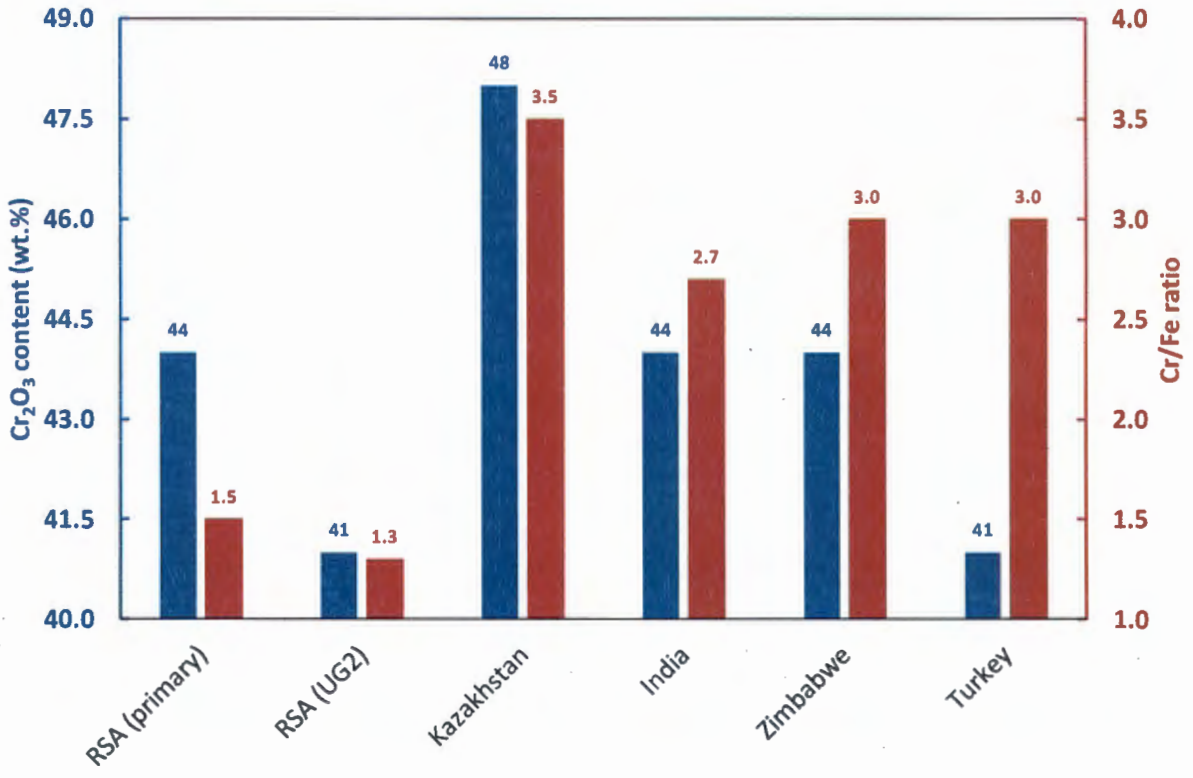

Figure 2-5: **Average/typical Cr_2O_3 content and Cr/Fe ratios of selected chromite ores (Fowkes, 2014)**

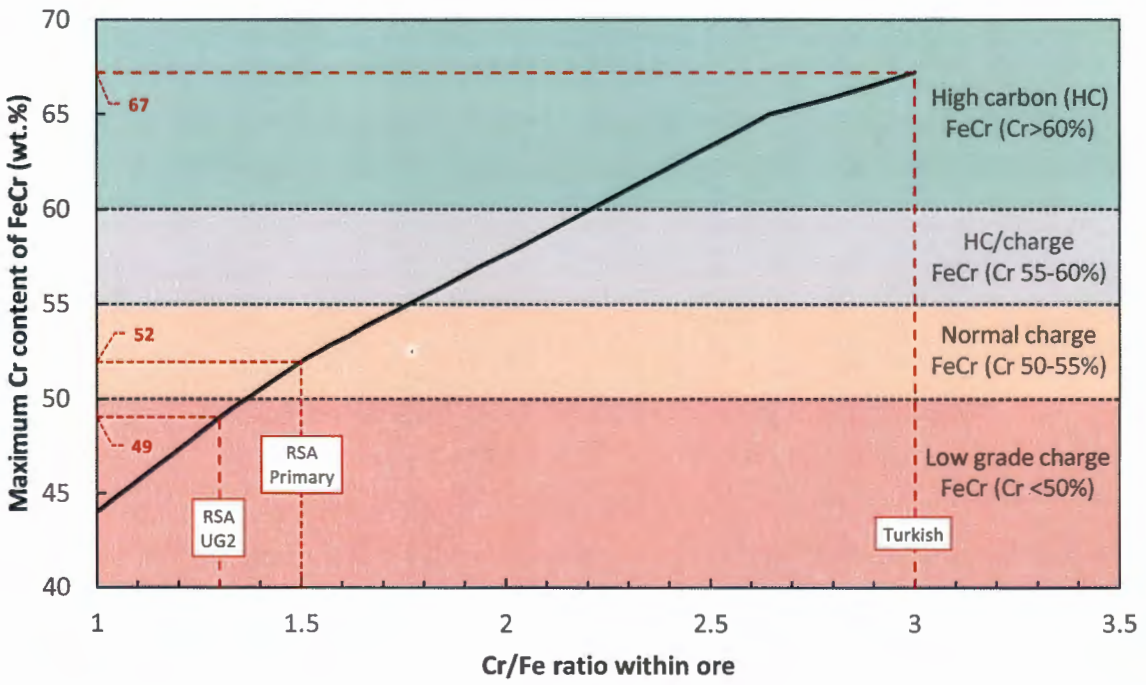

Figure 2-6: **The relationship between the grades of FeCr which can be produced from chromite ores with different Cr/Fe ratio (Fowkes, 2014)**

2.2.2 Economic and market considerations

Worldwide chromite ore demand is primarily dependent upon the usages of FeCr in the stainless and alloy steel manufacturing process. As previously mentioned chromite ore also has some uses in the chemical, refractory and foundry industries, but they provide a far smaller proportion of demand than FeCr production (ICDA, 2013a). In 2011, in spite of steady growth in stainless steel and FeCr production over the previous 5 years (2007-2011), chromite ore prices were lower in nominal terms than they were at the start of 2007. Accounting for inflation during this period, metallurgical grade chromite ore prices actually declined in real terms (ICDA, 2013a). This has been attributed to oversupply with a number of reasons being responsible for ore consumption growing more slowly than aggregate supply over this period, i.e. i) FeCr furnaces have become more efficient, ii) technological advances have allowed FeCr smelters to use greater quantities of what once would have been considered low-quality ore (i.e. ore with comparatively low Cr content or low Cr/Fe ratio) and iii) FeCr producers have also lowered their consumption of lumpy chromite ore, substituting it with pelletised concentrate or, in some cases, directly charging their furnaces with fines. Lower-grade chromite ore is, normally, in greater abundance in addition to being easier and cheaper to produce than higher-grade lumpy ore that it has replaced. As a result, relatively inexpensive supply sources (e.g. UG2) have been developed, and contributed to the excessive supply capacity (ICDA, 2013a).

Chromite ore is mined in over twenty countries, but the majority, approximately 82% of the production, originates from five countries, i.e. on average during 2001-2012 South Africa accounted for ~41% of the world's production, Kazakhstan and India accounted for ~17% and ~15%, respectively, Turkey for ~6% and Brazil for ~3% (Papp, 2008; Papp, 2009b; ICDA, 2010; ICDA, 2013d). The chromite ore production of these five countries is presented in Figure 2-7. The trade flow of chromite ore concentrate for 2012 is shown in Figure 2-8. In 2012, ~24.7 million Mt chromite ore concentrates was produced globally. Approximately 48% (11.8 million Mt) of the chromite ore produced was exported by the producing countries. China imported ~9.3 million Mt, which means ~38% of the chromite ore produced in 2012 globally was consumed by them. South Africa exported ~5.6 million Mt of ore concentrate in 2012, hence ~23% of the ore used globally (excluding South Africa's own use) where South African chromite ore.

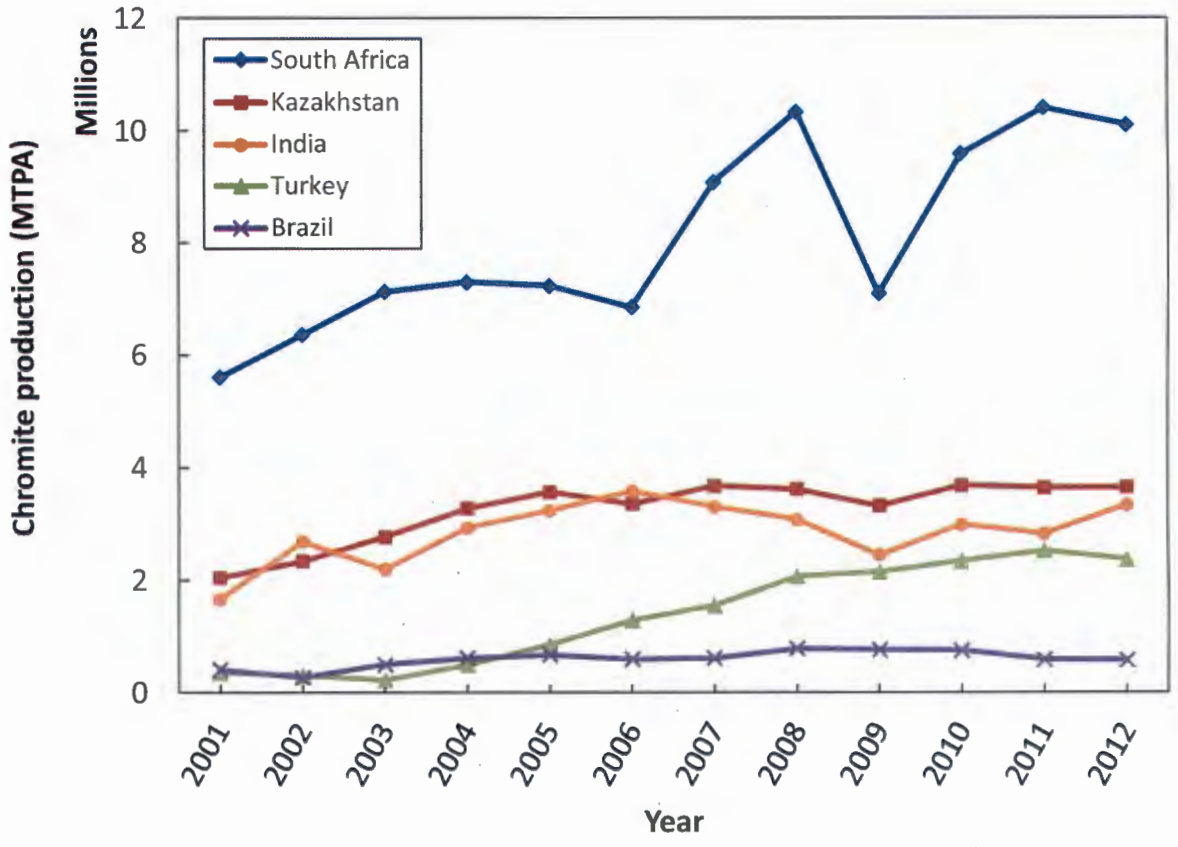

Figure 2-7: **Chromite production in million metric tons per annum (MTPA) for 1990-2012 (ICDA, 2013d)**

Figure 2-8: **Chromite ore concentrate trade flow for 2012, in '000 tpa (Pariser, 2013)**

As previously mentioned, the majority of chromite is converted into FeCr, which in turn is mostly consumed for stainless steel production (CRU, 2010; ICDA, 2010). It is therefore useful to consider the correlation between chromite, FeCr and stainless steel production volumes. Figure 2-9 indicates that there is a direct correlation, with some lags, between the production volume trends of these commodities. From Figure 2-9 it is observed that if the demand for stainless steel increases the demand for FeCr and ultimately chromite ore will automatically follow suit. This will either lead to a supply deficiency and a rise in FeCr prices or an increase in FeCr production, or both.

Cr materials are not openly traded. Purchase contracts are confidential between buyer and seller; however, trade journals report composite prices based on interviews with buyers and sellers, and traders declare the value of materials they import or export. Thus, industry publications and international trade statistics are sources of Cr material prices and values, respectively (Papp, 2008).

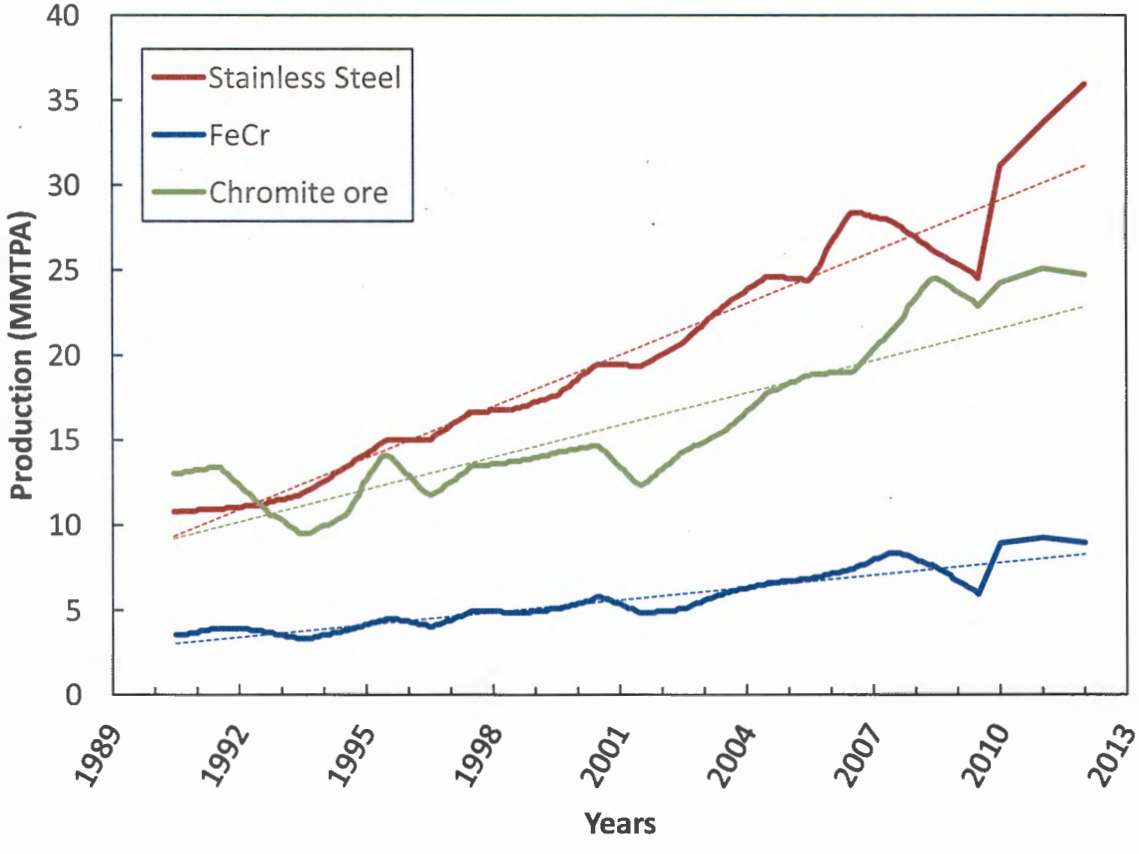

Figure 2-9: World production in million metric tons per annum (MMTPA) for 1990-2012 (Ideas 1st Research, 2010; ICDA, 2013d)

FeCr prices are usually negotiated every quarter by South African producers for European and Asian consumers, irrespective of the volume and tenure of the contracts. This price is a benchmark for all other contracts including spot market contracts, barring a few instances. Depending on the demand-supply situation at the time, the movement of spot prices is generally in tandem with quarterly contractual prices. The benchmark South African contracts are priced as US cents/lb of Cr content (Ideas 1st Research, 2010). Historically, it is observed that the prices of chromite ore, FeCr, and chromite ore move in tandem. Figure 2-10 indicates the correlation between the chromite ore price and the stainless steel and FeCr price indexes. Long term contracts in the stainless steel market are priced in two parts namely base value and alloy surcharge. Normally base values are kept constant for the duration of the contract, while the alloy surcharge prices are revised on a recurring basis to compensate for the volatility in the alloy mix. The alloy surcharge price is decided by the major components in stainless steel. They are chromium, nickel, molybdenum and manganese. The price fluctuation of nickel influences the grade production of stainless steel, as 60% of the total stainless steel produced contains nickel while the balance 40% has a very low nickel content (Ideas 1st Research, 2010). The expansions of both the Chinese and Indian economies were thought to be the main influences for the increase in Cr prices from 2007 through to part of 2008. The global financial meltdown in the late 2008 caused the prices to dramatically decline (Papp, 2008).

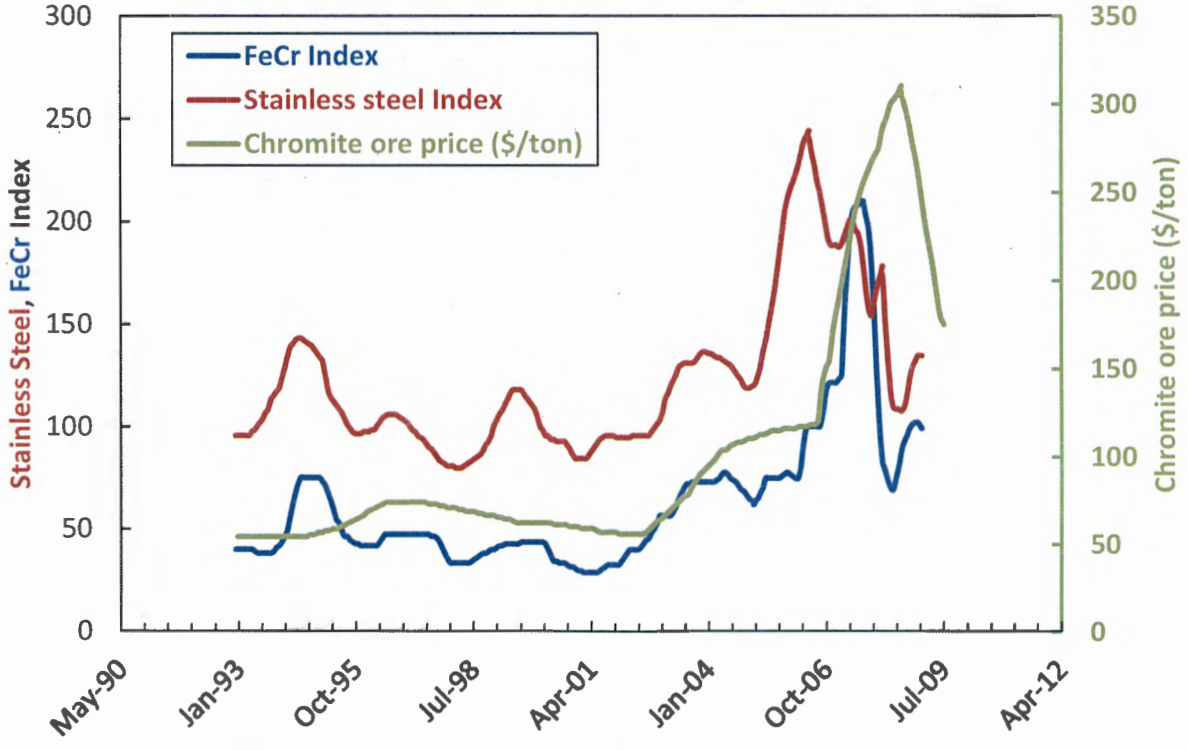

Figure 2-10: Chromite ore price ($/ton) and the stainless steel (SS) and FeCr price indexes (CRU, 2010; Ideas 1st Research, 2010)

The South African Rand exchange rate is a potentially significant factor in the price of chromite ore and FeCr because South Africa is a leading producer of these materials (Papp, 2008). South Africa is also the largest and second largest exporter of platinum and gold respectively, thus it is expected that these two markets would have a significant influence on South Africa's currency (Ideas 1st Research, 2010). Figure 2-11 shows the monthly average South African Rand (ZAR) per U.S. Dollar (US$) exchange rate in comparison with the historical FeCr prices (ZAR/kg) (Antweiler, 2016). From these exchange rate fluctuations the volatility and possible financial effect on the South African FeCr industry are evident.

Figure 2-11: Monthly average exchange rates: South African Rand (ZAR) per U.S. Dollar (US$) and the FeCr price (ZAR/kg) (Antweiler, 2016)

2.2.3 Carbonaceous Reductants

Another factor that has a significant impact on the South African FeCr industry is the availability of suitable reductants. Anthracite, char and coke are the main carbon reductants used (Makhoba & Hurman Eric, 2010). Coke is produced by driving off the volatile components of coal in an oven using heat, leaving behind a hard but porous carbonaceous mass known as coke. Not all coals will transform to coke and not all coke can be classed as metallurgical coke. Metallurgical coke

is characterised by its ability to retain its strength and size under cold conditions outside the furnace where it is being handled and under hot condition inside the furnace where is subjected to degradation by a number of different mechanisms. Coke is produced in batteries, either by-product batteries or non-recovery batteries. A typical layout of a by-product coke plant is shown in Figure 2-12. The layout of a non-recovery coke plant is similar, except for the absence of the by-product plant (Osborne, 2013).

Metallurgical coals broadly cover those coals which are classified as either semi-soft, soft, hard, semi-hard, pulverised coal injection (PCI) coals or anthracite. The relationship between each coal classification can be seen in Figure 2-13 (Osborne, 2013).

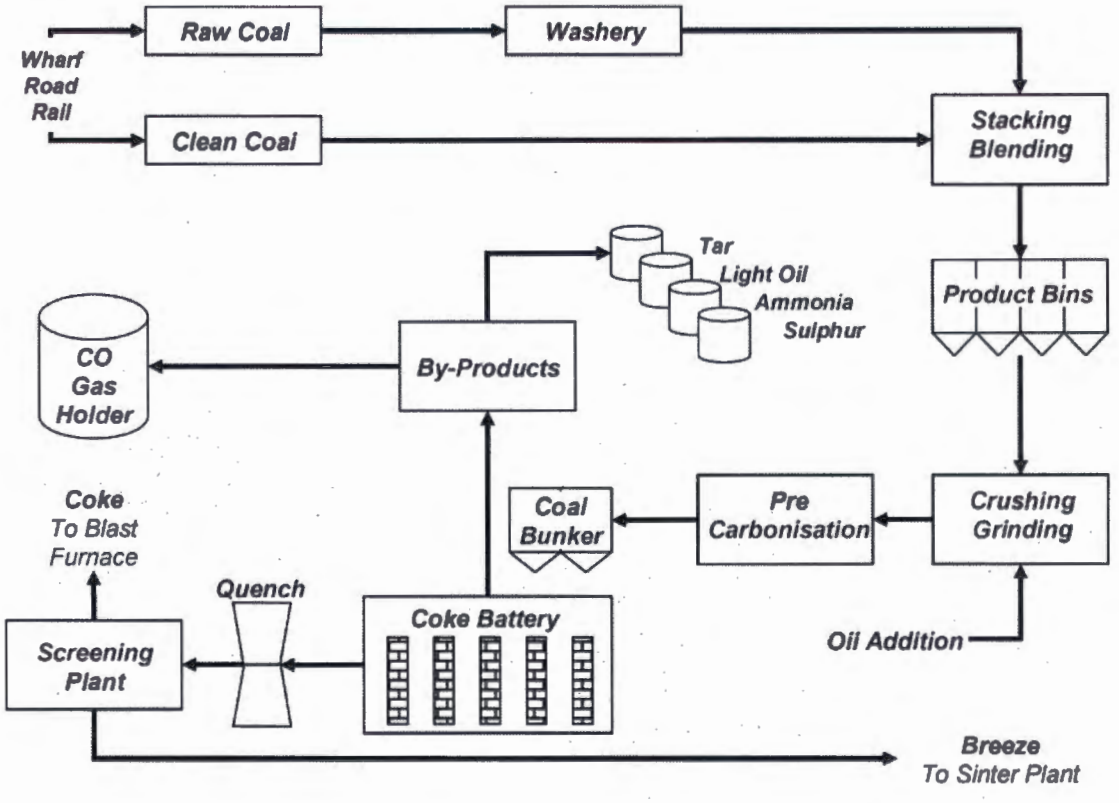

Figure 2-12: Schematic diagram of a by-product coke plant (Osborne, 2013)

It is important to recognise that the actual utilisation of an individual coal is determined by a number of factors, therefore the boundaries between all classification zones in Figure 2-13 are blurred as there are no clear cut-offs. For FeCr production a reductant with a low ash, low phosphorus and low sulphur content is required (Basson *et al.*, 2007; Ideas 1st Research, 2010; Makhoba & Hurman Eric, 2010). Due to the specific properties required, reductant availability is a cause of concern for FeCr producers. Moreover, there is no regulation within reductant markets and therefore over-supply or shortages may occur regularly resulting in enormous price fluctuations. In addition, the steel industry has a major influence on the dynamics of coking coal

prices (Ideas 1st Research, 2010; Makhoba & Hurman Eric, 2010). Typical properties of reductants for ferro alloy production are presented in Table 2–4 (Basson *et al.*, 2007).

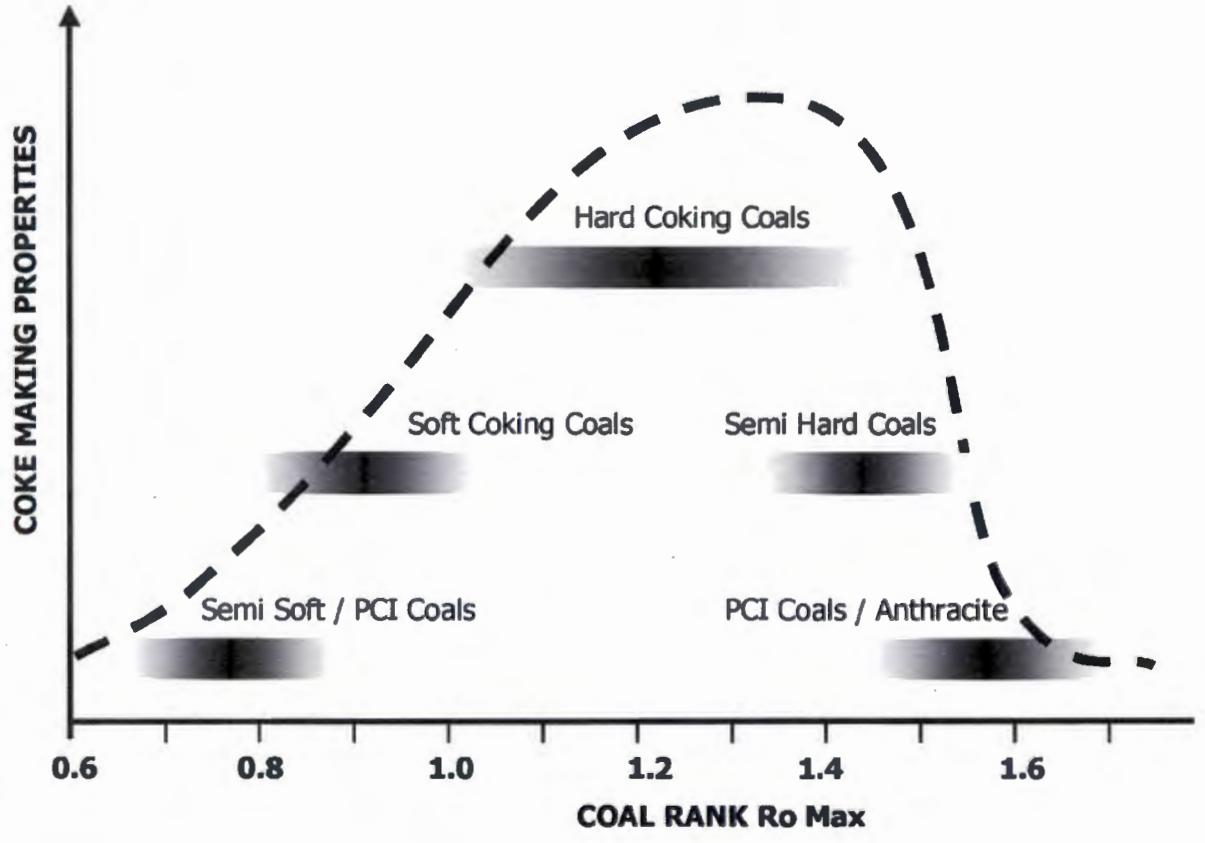

Figure 2-13: Simplified Classification of Metallurgical Coals (Osborne, 2013)

Table 2–4: Typical properties of selected carbon reductants used in ferro alloy production (Basson *et al.*, 2007)

Characteristic	Anthracite	Char/Gas coke	Coal	Chinese charge grade FeCr coke	SA charge grade FeCr coke
Volatile %	6-10	1-2	18-25	<1	<1
Ash %	15	19	11	14	16
Fixed carbon %	80	80	56	85	83
Sulphur %	0.6	0.2	0.8	0.6	0.7
Phosphorus %	0.004	0.009	0.009	0.013	0.009

Around 50-60% of coking coal requirement in South Africa over the past years were met through long-term contracts, but these were reset to an on spot basis. Low ash and phosphorous grade coking coal come with premiums, which makes price negotiations for FeCr producers difficult. With this in mind it is clear that coking coal prices will have an impact on FeCr production and prices in the near future (Ideas 1st Research, 2010).

South Africa has enough resources and has been self-sufficient for many years with respect to reductants for ferro alloy production (Basson *et al.*, 2007; Ideas 1st Research, 2010). Substantial coal reserves are located in five major basins and recoverable coal and anthracite materials were estimated to be around 61 000 Mt (Barcza *et al.*, 1982; Featherstone & Barcza, 1982). In recent years it has however become necessary to import reductants for alloy production. Metallurgical coke is mostly imported from China for FeCr production and Zimbabwe for manganese alloy production. The rapid increase in South Africa's ferro alloy production capacity along with no growth in coke production capacity in recent years is the main reason for importation. The trend towards closed furnaces, mostly for environmental reasons, generally require a larger fraction of coke in the reductant mixture, which also contributed to coke shortages (Basson *et al.*, 2007; 2010; Pan, 2013). Specific coke and char consumption for charge grade FeCr production has increased by 0.02 t/t FeCr over the last few years at the expense of coal. Ferro alloy producers are also looking to increase the usage of anthracite in ferro alloy production. Anthracite has mainly been applied in DC charge grade FeCr furnaces and smaller AC charge grade FeCr and manganese alloy furnaces. For economic reasons the usage of metallurgical coal is maximised within the constraints that are experienced with the use of coal on larger, closed furnaces. The number 1, 2 lower and 5 coal seams in the Witbank basin are currently the primary source of metallurgical coal. It typically has a sulphur and phosphorous content of <0.7 and <0.012%, respectively (Basson *et al.*, 2007; Pan, 2013).

With respect to reductants, there are two challenges the South African FeCr industry are facing at the moment. From the facts mentioned in the previous paragraph it can be concluded that the first problem is that producers are importing coke because of a lack in local coke production capacity. The second problem is supply constraints of low phosphorus and sulphur coals for use as such, or for conversion of these coals into coke, gas coke and char. As far as the former is concerned, Mittal Coke and Chemical expanded their coke capacity to 450 000 t/a primarily for FeCr and ferromanganese production in South Africa. There were also indications of coke production from other major players. As far as the latter is concerned, it is believed that deposits of metallurgical grade coal that belonged to big mining companies that did not exploit these resources will be allocated to small black economical empowered (BEE) entrepreneurs because of the Mineral and Petroleum Resource development Act (Act 28 of 2008). This small scale mining of coal resources will make reductants available to the ferro alloy industry, instead of being

lost to steam coal exports and feedstock to power stations. Over the next 5 years the existing coalfields will be depleted and production of coal will shift to the vast Waterberg reserves located in the Northern Province. Thus, as far as the foreseeable future, South Africa will have enough carbon reductants at its disposal (Basson *et al.*, 2007).

2.2.4 Electricity supply

Electricity supply depend on three functions, i.e. generation, transmission and distribution. Generation is the production of electricity in power stations. Eskom, South Africa's state owned electricity supplier, provides over 95% of the generation, the rest coming from small municipal power stations and some independent power producers (IPPs). Until recently, these IPPs have usually been factories or plants, which generate electricity for their own use, or as a by-product of their production processes, but occasionally sell some of it to Eskom. Transmission is the wholesale transfer of electricity from power stations to centres of demand. Eskom does 100% of South Africa's transmission. South Africa's transmission lines are sometimes more than 1 500km long (as between the coal stations in the north and Cape Town in the south). For this, very high voltages are utilised to minimise losses. Distribution is the transfer of electricity from substations at centres of demand (at the ends of the transmission lines) to final customers, such as factories, plants, offices and households. The substations are responsible for decreasing the voltage to the standard voltage (e.g. 220 V for household use) used by end consumers. About 50% of distribution is done by Eskom and 50% by municipalities. The municipalities mark up the price of the electricity they buy from Eskom and provide to their customers, this mark-up being a major source of revenue for them.

South Africa's electricity consumption is as high as in many European countries and far higher than in any other African country. Compared with Europe (~32%), the South African industry consumes a much higher proportion (~53%) of total electricity than other sectors. Over 92% of South Africa's electricity is from coal, while nuclear contributes only about 6%. Although South Africa's gas turbines have a greater capacity (2 426 MW) than the Koeberg nuclear power station (1 910 MW). However, Koeberg produces far more electricity because it is a baseload supplier with very low production costs.

With a change in governance in 1994, no clear-sighted, well-planned strategy was implemented for continued expansion of generation capacity in line with economic growth rates. South Africa's electricity demand started to gradually catch up with its electricity generating capacity (Baker, 2006). The historic supply-demand overview of electricity in South Africa up to 2015 is shown in Figure 2-15 (Basson *et al.*, 2007). From this it is clear that the availability of surplus generation capacity has significantly been eroded. In 2004 Eskom recognised that it had a serious problem and began planning to build two large new coal stations, i.e. Medupi (Limpopo Province, South

Africa) and Kusile (Mpumalanga Province). Nevertheless, this was too late. By 2007, Eskom had run out of electricity and couldn't meet the rising demands any more. The erosion of surplus generation capacity, indicated in Figure 2-15, has led to a dramatic increase in electricity prices, compared to other BRICS countries, that is set to continue in the foreseeable future (Pfister, 2006; Basson *et al.*, 2007). In the period 1980 to 2005 the nominal electricity price in South Africa increased steadily at a rate of roughly 0.58 South African cents/kWh per year (NERSA, 2009b). According to statistics from the National Energy Regulator of South Africa (NERSA), the nominal price of electricity increased by 174% from 2007 to 2010 (NERSA, 2009a; NERSA, 2009b). NERSA subsequently granted Eskom a three-year rate increase resulting in electricity costs of 41.57 South African cents/kWh for 2010/11, 52.30 South African cents/kWh for 2011/12 and 65.85 South African cents/kWh for 2012/13 (NERSA, 2009a; Eskom, 2011). NERSA since allowed Eskom to raise tariffs by an average 8% for 5 years (2014-2018), however, recently they approved an annual average price increase of 12.7% for 2015/16 and 16.6% for 2016/17, which is made up of the 8% annual price increase approved in the original MYPD 3 decision and an additional 4.7% and 8.6% as allowed through the revenue clearing account (RCA) mechanism which forms part of the NERSA regulatory methodology (Figure 2-16). The electricity price increases is well above the inflation rate when considering South Africa's CPI (Figure 2-16). Within the energy market in South Africa, the FeCr sector is one of the most intensive electricity consumers. Of the approximately 63% that the industrial sector contribute to total key customer sales, the FeCr sector contributes approximately 23% (Nedzingahe *et al.*, 2010). Considering that electricity consumption is the single largest cost component in FeCr production (Daavittila *et al.*, 2004), the afore-mentioned cost increases are extremely significant. The average portion that electricity is accounting for in FeCr production costs, indicated in Figure 2-16, increased from ~23% in 2008 to ~40% in 2016. However, the pressure on South African FeCr producers is not unique, since globally lower SEC (MWh/t FeCr) and a decreased carbon footprint have become driving factors.

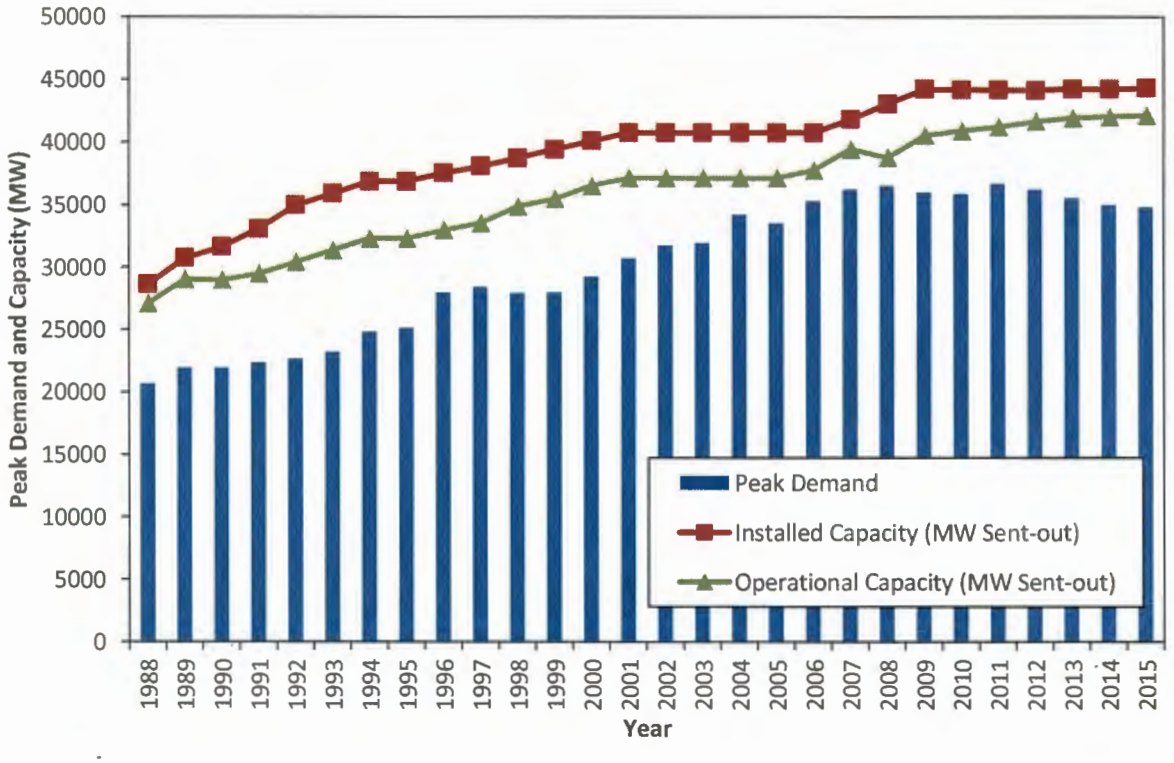

Figure 2-14: Electricity demand overview for South Africa (Pfister, 2006; Basson *et al.*, 2007)

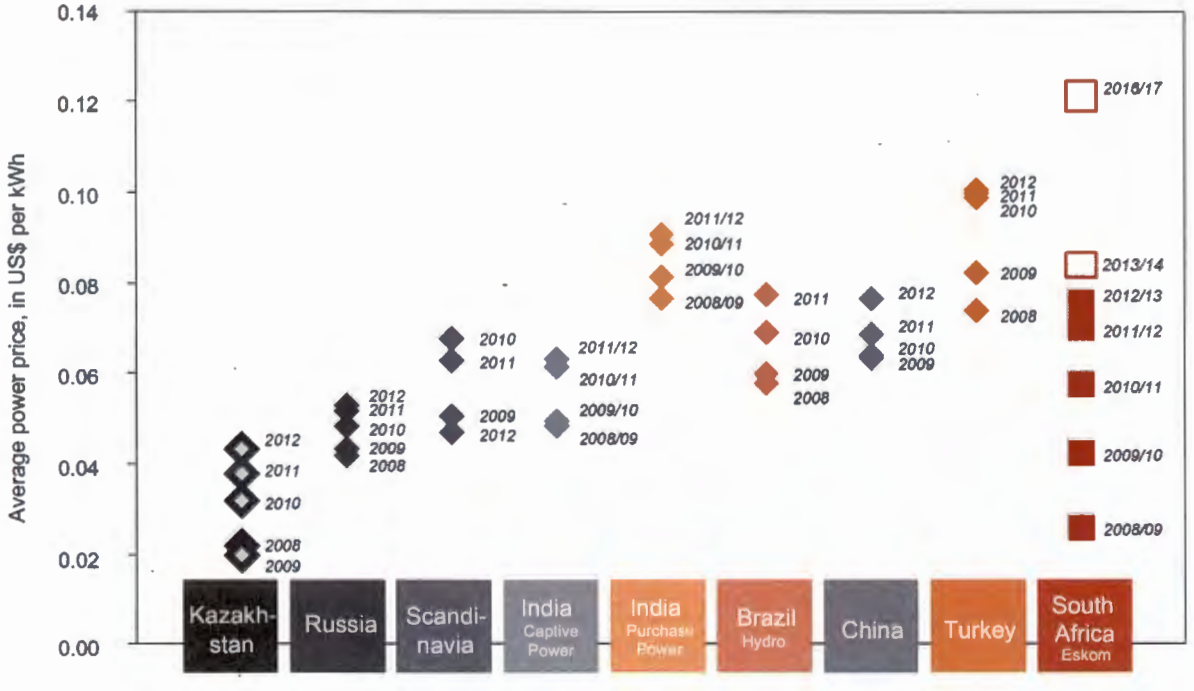

Figure 2-15: Comparison of electricity prices in selected countries (All data based on average power prices and exchange rates for the years stated. South African projection based on 2012 exchange rate.) (Merafe-Resources, 2012)

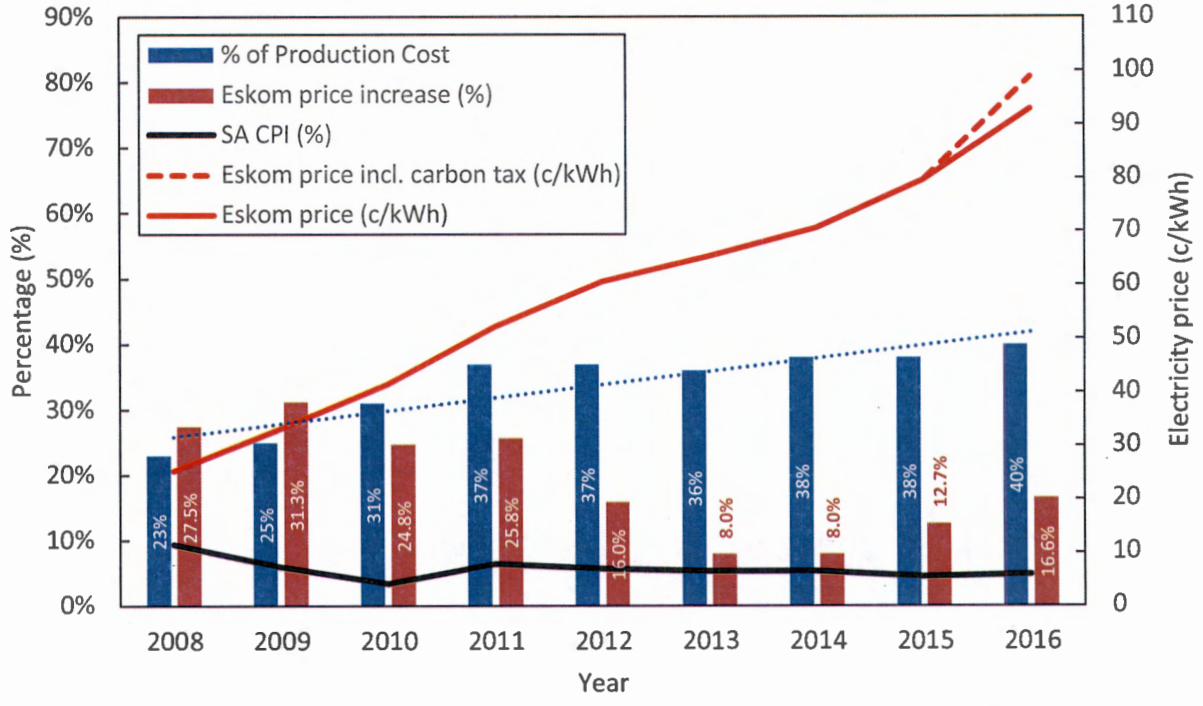

Figure 2-16: The association between Eskom's electricity price and South Africa's CPI and the effect on FeCr production cost (FAPA, 2016)

2.2.5 Ferrochrome production

The advent of argon-oxygen decarburisation 50 years ago triggered the expansion of South Africa's FeCr industry, which lead to South Africa becoming the world leader in FeCr production (Featherstone & Barcza, 1982; Basson *et al.*, 2007). This can be ascribed to an abundance of good quality raw materials (ore, reductants and fluxes), historically relatively low electricity costs, adequate infrastructure and reasonably low-cost capital (Basson *et al.*, 2007). However, the last decade has seen South Africa relinquish its position as the world's leading FeCr producer to China. The shift has primarily been driven by reduced cost competitiveness and electricity supply constraints, which in turn have spurred a surge in chromite ore exports to feed the rapid growth in Chinese FeCr capacity. In 2002, South Africa produced over 50% of the world's FeCr, mainly as charge grade. As a result of South Africa's electricity crisis, South Africa's portion in global FeCr production declined at an average rate of 5% year-on-year from 2004. This was mainly due to agreements South African FeCr producers reached with Eskom to sell back electricity that they would have used in their furnaces, thus impacting on production levels. In 2012, South Africa produced 32.31% of the ~8.9 million metric tonnes of FeCr produced world-wide. At the time, South Africa was producing only at 56% of its total production capacity. The summarised production capacities of South Africa's FeCr smelter plants as of 2016 are shown in Table 2–5 (Basson *et al.*, 2007; Bonga, 2009; Jones, 2010; Beukes *et al.*, 2012).

Table 2–5: Production capacity of South African FeCr producers adapted from Jones (2015)

Plant	Locality	Production capacity (t/a)
ASA Metals Dilokong	Burgersfort	400 000
Assmang Chrome	Machadodorp	300 000
Ferrometals	Witbank	550 000
Hernic Ferrochrome	Brits	420 000
TC smelter	Mooinooi	267 000
Middelburg Ferrochrome	Middelburg	285 000
Mogale Alloys	Krugersdorp	130 000
Tata Ferrochrome	Richards Bay	135 000
Tubatse Ferrochrome	Steelpoort	380 000
Glencore Alloys Lydenburg	Lydenburg	400 000
Glencore Alloys Boshoek	Rustenburg-Sun City	240 000
Glencore Alloys Lion	Steelpoort	720 000
Glencore Alloys Rustenburg	Rustenburg	430 000
Glencore Alloys Wonderkop	Rustenburg-Brits	545 000
TOTAL		~5 202 000

When considering statistics of the International Chromium Development Association (ICDA) Statistical Bulletin 2013, depicted in Figure 2-17, it is evident that South Africa's stake in charge grade FeCr production went down by 18.71% from 51.02% in 2002 to 32.31% in 2012. China increased its production of FeCr by an average of 31% year-on-year to 3.1 million tonnes in 2012, facilitated by the increased availability of chromite ore from South Africa, due to South African FeCr producer not being able to utilise the ore themselves. The Compound Annual Growth Rate (CAGR) for FeCr production over the period 2002-2012 of selected countries are shown in Figure 2-18. Consequently South Africa, the largest producer of FeCr for the last decade, with ~30% of global production in 2012, was overtaken by China who doubled their production in the last 3 years, filling the stainless steel industry's rapid growing demand for FeCr (ISSF, 2011; ICDA, 2013c).

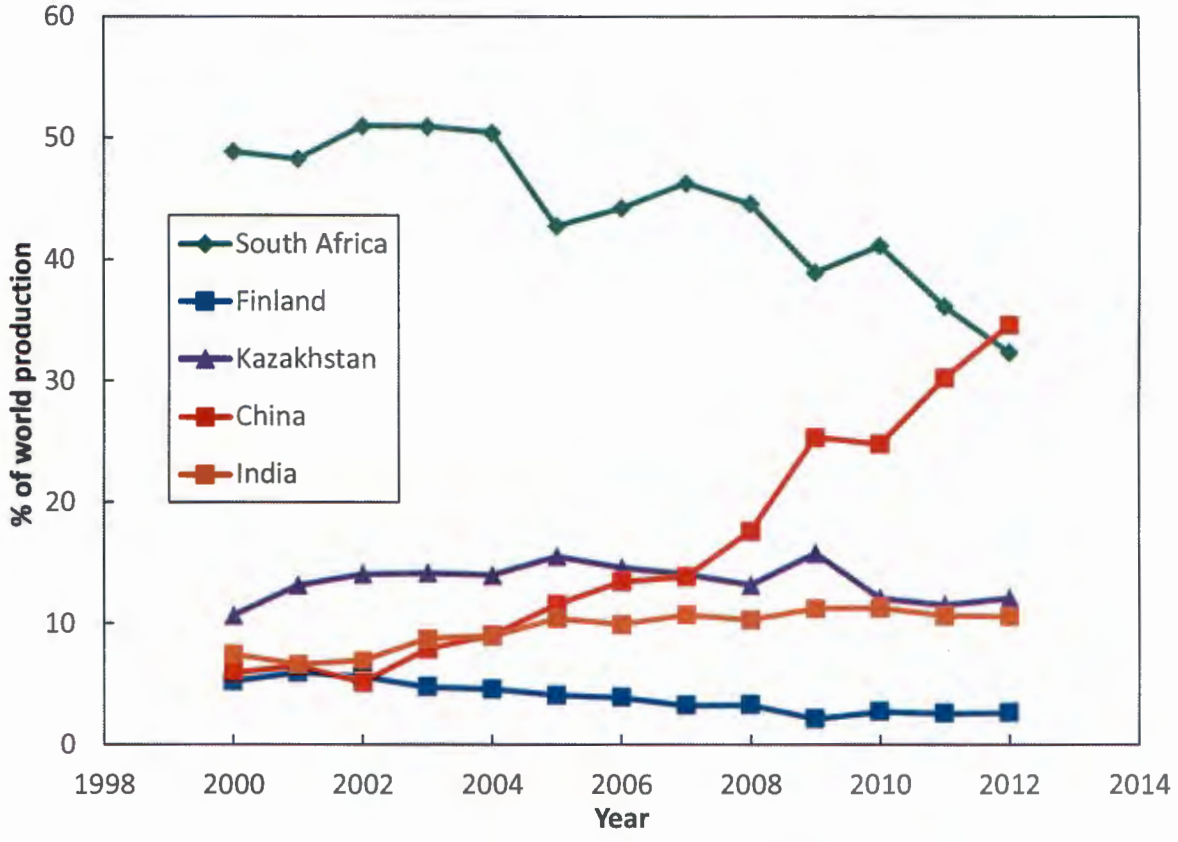

Figure 2-17: High-carbon charge grade FeCr production 2000-2014 (ICDA, 2010; ICDA, 2013d)

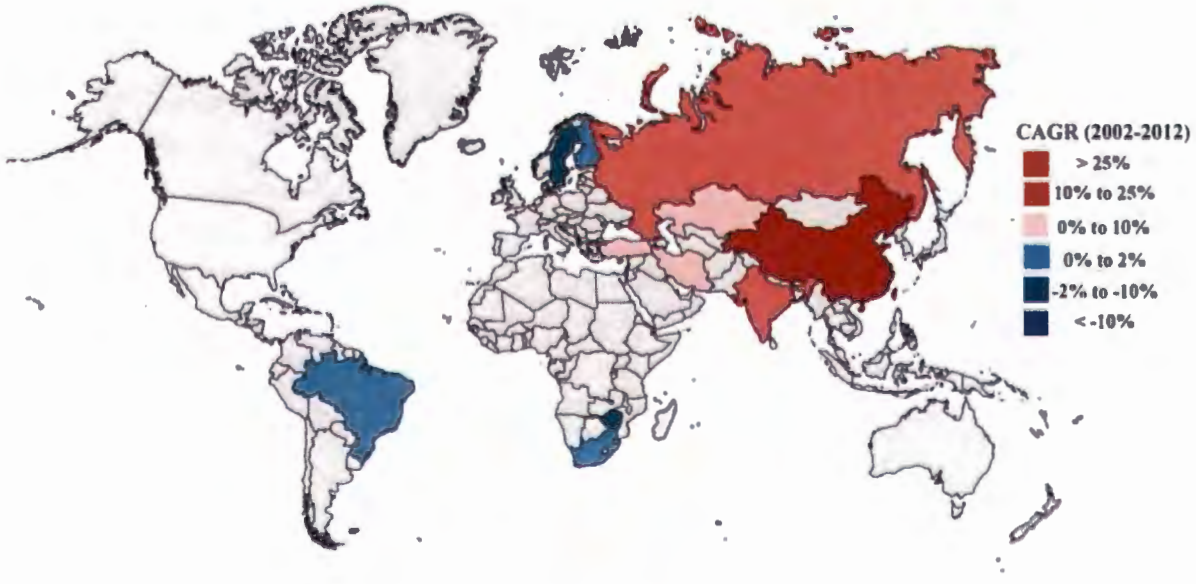

Figure 2-18: The Compound Annual Growth Rate (CAGR) for FeCr production over the period 2002-2012 of selected countries (Yuksel, 2013)

2.3 Main processes and techniques

2.3.1 Mining and beneficiation of chromite ores

Open-cast mining as well as underground mining techniques are used to obtain raw chromite ore. Specific mining techniques vary widely depending on the local resources and materials (Nafziger, 1982; Gediga & Russ, 2007).

The purpose of beneficiation is to render the ore physically (granulometry) and chemically suitable for subsequent treatments. Operations typically serve to separate and concentrate mineral values from waste materials, remove the impurities or prepare the ore for further refinement. Beneficiation activities do not change the mineral values themselves other than reducing (crushing and grinding) or enlarging (pelletising and briquetting) particle size to facilitate further processes. Chromite ore is beneficiated for processing using several methods. The ore source, end use sector requirements, mineral characteristics of the ore deposits, gangue mineral assemblage and the degree of dissemination of constituent minerals determine the beneficiation practices and methods that are used. A general representation of a chromite ore beneficiation process is shown in Figure 2-19 and consists of two sections, i.e. comminution (preparing the material for subsequent unit operations) and concentration (Abubakre *et al.*, 2007; Murthy *et al.*, 2011).

In the feed preparation section the run-of-mine ore is screened from ±220 mm to 75 mm. This is followed by a primary and secondary crushing stage separated by screening to produce an offset of less than 3 mm. The secondary crushers offset is recycled back and rescreened. The crushed ore is then further grounded to less than 1 mm. In the concentration section the ore is upgraded using conventional gravity techniques, e.g. spiral concentrators (Murthy *et al.*, 2011).

Though gravity techniques are well established and widely accepted for the concentration of chromite ore, such techniques become inefficient and complex while treating very fine size particles of less than 75 µm. Recovery is a concern particularly in finely disseminated ores due to its inherent complexities. Each gravity separation technique delivers its maximum efficiency under specific operating conditions and particle size range (Murthy *et al.*, 2011).

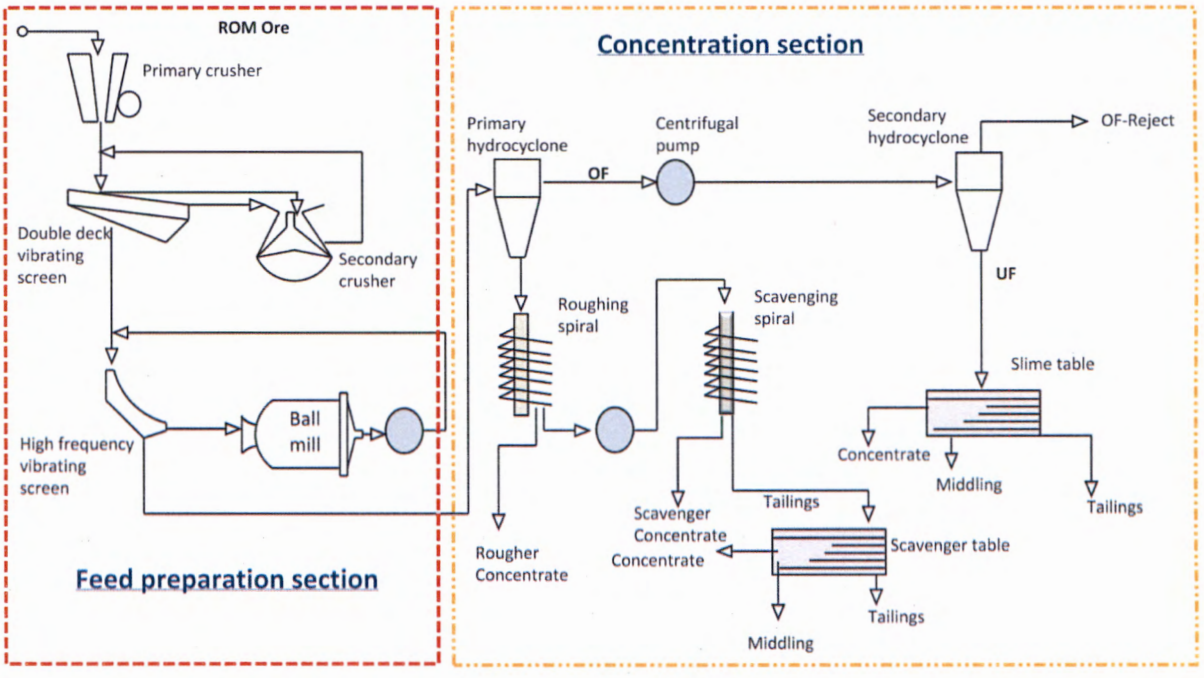

Figure 2-19: General process flow sheet for chromite ore beneficiation (Murthy *et al.*, 2011)

Heavy medium and gravity concentration methods are the most commonly used beneficiation processes. Heavy medium separation is the most economical method when coarse particles ranging between 10 to 100 mm need to be treated. In the case of finer particles, jigs, spirals and shaking tables are used. Spirals are, however, the most important among gravity concentrators and are currently the preferred choice. Cr can be recovered within the range of 80 to 85% when using these processes (Howat, 1986; Gu & Wills, 1988).

Gravity separation methods predominate over flotation techniques (Nafziger, 1982). Flotation is thus not a major method of beneficiation for chromite ores. In some instances fatty acids, such as oleic acid, have been used where flotation has been adopted as a method of separation. Chromite ores from different locations exhibit a wide variation in surface properties which is a major difficulty when making use of flotation (Gu & Wills, 1988).

All chromite ores are paramagnetic at room temperature. Their magnetic capacity is dependent on the Fe^{2+} content (Owada & Harada, 1985). It has been speculated that this paramagnetism is predominantly present in the sections more concentrated with Fe^{2+} because of the non-uniform distribution of magnetic ions in the crystalline structure. Low-intensity magnetic separation (about 0.1 T) is used to reject the magnetite from paramagnetic chromite material, but is inefficient in separating the chromite ores that are present in fine intergrowths with other materials. In a high-intensity magnetic field (about 1 T) chromite can be extracted as a magnetic product from the gangue material (Nafziger, 1982; Gu & Wills, 1988).

South African chromite ores are relatively friable and easily break down to the size of the chromite crystals (Gu & Wills, 1988). Due to this friability, it is common to only recover 10 to 15% lumpy ore (≥15 mm and <150 mm) and 8 to 12% chip or pebble ores (≥6 mm and <15 mm) during the beneficiation process employed after chromite mining. The remaining ore would typically be in the <6 mm fraction, which would usually be crushed and/or milled to <1 mm and then upgraded utilising typical gravity separation techniques (e.g. spiral concentrators) to approximately 45% Cr_2O_3 content. This upgraded <1 mm ore is commonly known as metallurgical grade chromite ore (Glastonbury *et al.*, 2010).

2.3.2 Ferrochrome production processes

A generalised process flow diagram, which indicates the most common process steps utilised by South African FeCr producers, is shown in Figure 2-20 (Beukes *et al.*, 2010).

In general, four relatively well-defined process combinations are utilised by South African FeCr producers (Beukes *et al.*, 2010):

A) **Conventional open or semi-closed SAF operations, with bag filter off-gas treatment.** This is the oldest technology applied in South Africa, but still accounts for a substantial fraction of overall production (Gediga & Russ, 2007). In this type of operation, coarse (lumpy and chips/pebble ores) and a small fraction of fine ores can be smelted without an agglomeration process undertaken to increase the size of fine ores. Although it has been stated that fine ores cannot be fed directly into a SAF without causing dangerous blow-outs or bed turnovers (Riekkola-Vanhanen, 1999), fine ores are in fact fed into some semi-closed SAF in the South African FeCr industry. With reference to the process flow diagram indicated in Figure 2-20, the process steps followed are 5, 7, 8, 9 and 10. Some semi-closed SAF do consume pelletized feed, in which case process steps 1-4 would also be included. Most of semi-closed SAFs used in South Africa are operated on an acid slag, with a basicity factor smaller than 1. Equation 2-3 defines the basicity factor (BF) (Beukes *et al.*, 2010):

$$BF = \frac{\%CaO + \%MgO}{\%SiO_2} \qquad 2\text{-}3$$

Some semi-closed furnaces might operate on BF >1, but these are less common and such operations are sometimes only temporarily undertaken to compensate for refractory linings being in poor condition (since basic slag has a higher liquidus temperature than

acid slag), or if enhanced sulphur removing capacity by the slag is required (since more basic cation associated sulphite is formed in the slag) (Beukes *et al.*, 2010).

B) Closed furnace operation, usually utilising an oxidative sintered pelletised feed (Outotec, 2015).

This has been the technology most commonly employed in South Africa, with the majority of green and brown field expansions utilising this combination of process steps during the last decade. Process steps usually include steps 1-5, 7-9 and 11, with or without 6. In all green field FeCr developments the pelletising and sintering (steps 2 and 3) sections were combined with closed SAF. However, pelletising and sintering sections have also been constructed at plants where the pelletised feed is utilised by conventional semi-closed furnaces. These furnaces are usually operated on an acid slag (BF <1) (Beukes *et al.*, 2010).

C) Closed furnace operation with pre-reduced pelletised feed (Botha, 2003; Naiker, 2007).

The process steps include steps 1-5, 7-9 and 11. The pelletised feed differs substantially from the oxidative sintered type due to the fact that the pellets are pre-reduced and mostly fed hot, directly after pre-reduction, into the furnaces. The furnaces are closed and operate on a basic slag (BF >1). At present, two South African FeCr smelter plants use this process.

D) DCF operation (Denton *et al.*, 2004; Curr, 2009).

For this type of operation, the feed can consist exclusively of fine material. Currently three such furnaces are in routine commercial operation for FeCr production in SA and typically utilize a basic slag regime (BF >1). Process steps include 5, 7 (with a DC, instead of a SAF), 8, 9 and 11. Drying (process step 6) might also be included.

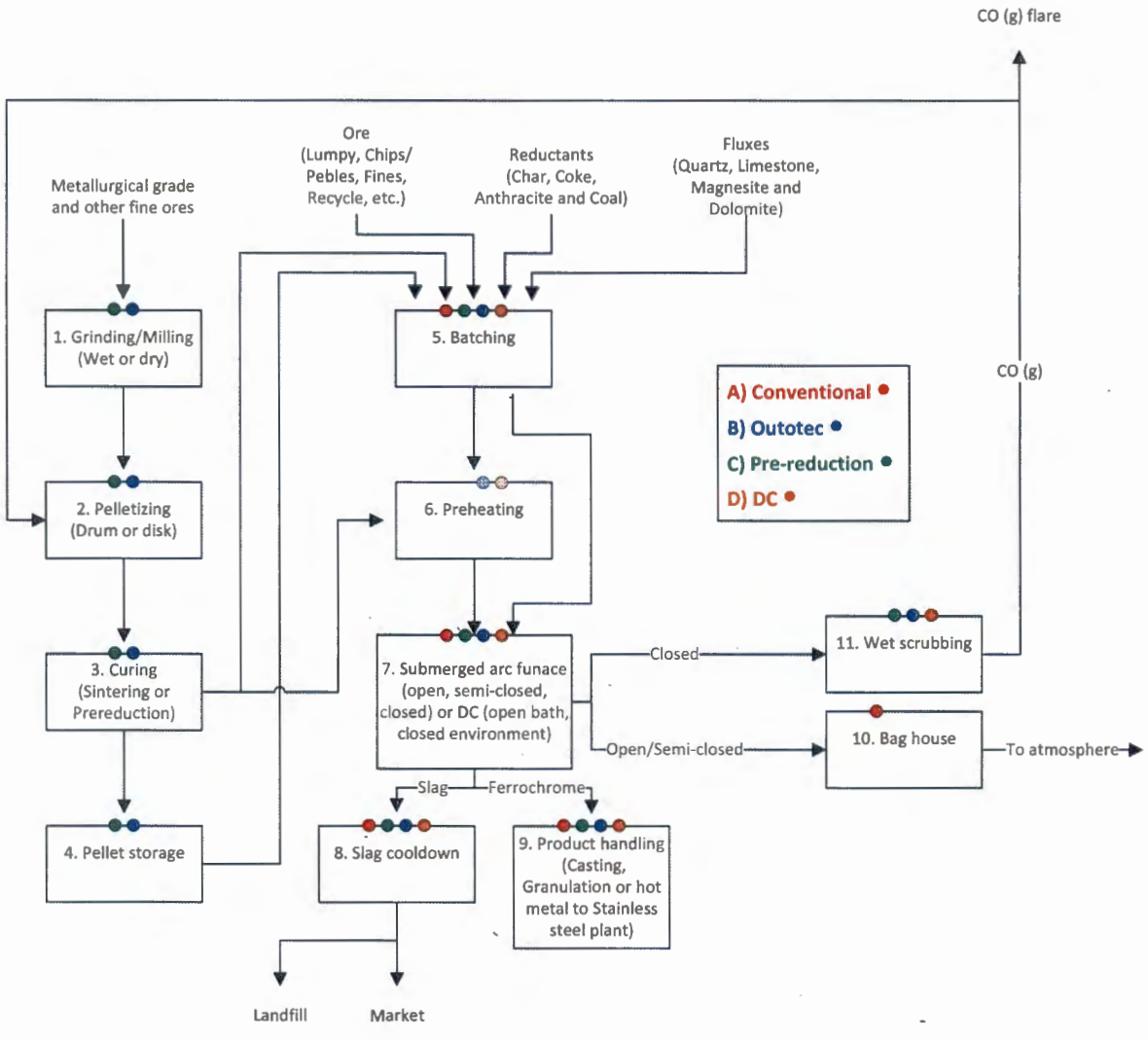

Figure 2-20: A flow diagram adapted by Beukes *et al.* (2010) from Riekkola-Vanhanen (1999), indicating the most common process steps utilised for FeCr production in South Africa

2.4 Chromite pre-reduction

2.4.1 Extent of pre-reduction technology commercialisation

Pre-reduction technology has been around for a number of years, with the pre-reduction of Fe ore being a more commonly utilised process. Remarkably, pre-reduction of chromite has not been widely used on a commercial scale; however, it is a very well-established practice in South Africa and has been utilised since 1975 (Dawson & Edwards, 1986; Basson *et al.*, 2007; Naiker, 2007; McCullough *et al.*, 2010). It is currently the second most commonly employed technology in the South African FeCr industry (Beukes *et al.*, 2010). A number of studies have been conducted on the pre-reduction of chromite ore utilising different reductant sources including

coke, anthracite, carbon monoxide, methane and hydrogen. This has led to a few processes being partially developed, as well as implemented on a commercial scale.

The solid-state reduction of chromite (SRC) process developed by Showa Denko in Japan was the first commercially successful process (Naiker, 2007). In this process, chromite ore fines are milled in a ball mill, pelletised using a clay binder with coke added as reductant, dried in a travelling grate kiln, and fired in a rotary kiln to approximately 1400 °C. The kiln is heated by a burner using pulverised coal, CO or oil as fuel (Riekkola-Vanhanen, 1999). The SRC process has been employed with success at two commercial facilities, i.e. the Shunan Denko Plant in Japan and the Glencore Lydenburg smelter (previously Consolidated Metallurgical Industries, CMI) in the Mpumalanga Province, South Africa. These two facilities have proved to be the most energy efficient FeCr production plants (Naiker, 2007). When Xstrata purchased the CMI plant in 1998 from the Johannesburg Consolidated Industries (JCI) group, they wanted to decrease cost structures at the Lydenburg plant. Therefore, between 1998 and 2001, they developed the Premus process, based on the SRC process, mainly by in-plant trials. Xstrata made a fundamental change in the operating philosophy of the process in that the Premus process sought to maximize the energy output from the kiln, while still achieving the required efficiencies and therefore increasing furnace output, while the original CMI process's main objective was to maximize metallisation in the pellets (Naiker, 2007). In 2006 third quarter Xstrata increased their FeCr capacity with the commissioning of its Lion FeCr smelter plant which also makes use of a pre-reduction stage utilising Xstrata's Premus technology (Basson *et al.*, 2007; McCullough *et al.*, 2010). In 2010 Xstrata announced the seconded phase expansion of the Lion plant that involved the construction of another 360 000 t/y capacity smelter, raising their total FeCr production capacity above 2.3 million t/y (Creamer, 2010; Wait, 2011).

Alternative processes that have been used or have been partly developed include the Krupp-Codir CDR (Chromium Direct Reduction Process) and Rotary Hearth Furnace (RHF) that was later acquired by Polysius, as well as Outokumpu's pre-treatment process (McCullough *et al.*, 2010).

The CDR process uses un-agglomerated ore fines. Self-agglomeration of the fines occurs inside the rotary kiln in the high temperature zone. A temperature of approximately 1500 °C is used and the kiln feed consists of chromite concentrate, a siliceous flux, and a large excess of reductant. Coal is used as both energy source and reductant (Dawson & Edwards, 1986; Riekkola-Vanhanen, 1999). A big disadvantage of this process is that the excess reductant must be separated from the metal-slag mixture before smelting can commence. To achieve this, the kiln discharge must be cooled which results in a substantial loss of enthalpy (Dawson & Edwards, 1986). SAMANCOR installed the CDR pre-reduction process at its Middelburg FeCr Plant with the process involving the partial fluxing of Cr ore fines (not pellets) and the use of oxygen

enrichment to attain temperatures of around 1500 °C, but ran into problems in particular with dam ring build-up (material sticking to the inside of the rotary kiln) and refractory wear.

INMETCO developed its Direct Reduced Iron (DRI) Technology process utilizing a RHF and applied it with great success to stainless steel dust recycling. However, attempts to apply the RHF process to chromite ore pre-reduction were only partly successful, the main problem being the re-oxidation of the pre-reduced pellets (McCullough *et al.*, 2010). Tenova Pyromet in co-operation with its technical partners, Paul Wurth and Tenova LOI Italimpianti, has recently developed a pre-reduction process for FeCr ores based on using Rotary Hearth Furnace technology fired with closed furnace off-gas, but the process has not yet been industrially applied (Dos Santos, 2010).

Outokumpu studied its pre-reduction process for about ten years in the laboratory and on pilot scale, as well as for two years in a commercial scale operation. The process consisted of a rotary kiln with a length of 55 m and inner diameter of 2.3 m. The major problem that they encountered was to maintain an even pre-reduction degree. Consequently, the furnace operations became difficult to maintain and efficiency were not good enough to make the operation viable, so they returned to using the equipment for preheating (Daavittila *et al.*, 2004).

2.4.2 Strategic advantages of chromite pre-reduction

Although various processes are utilised in the production of FeCr, the use of pelletised chromite pre-reduction has a number of key advantages over other processes:

a) Pre-reduction's most important advantage is certainly the reduction of the overall process electric energy consumption. At present, high-carbon/charge grade FeCr is generally produced in electric arc furnaces. A major disadvantage of this process is the amount of electrical energy required for the reduction of the metal oxides to the metallic state. In order to minimize energy consumption and consequently improve cost efficiency, solid-state carbothermic pre-reduction of chromite has become a necessary option, since it requires the lowest SEC for operation of all FeCr production processes (Weber & Eric, 2006; Neizel, 2010). With pre-reduction levels of up to 90% for the Fe and 50% achieved for Cr, electrical energy consumption is reduced by approximately 40% from around 3.9 MWh/t required in conventional ore fed processes down to 2.4 MWh/t (McCullough *et al.*, 2010). The net SEC as a function of the degree of chromite pre-reduction achieved and then charged into an arc furnace at different temperatures was reconstructed from Takano *et al.* (2007) and Niayesh and Fletcher (1986) and is presented in Figure 2-21.

b) The process utilises 100% fine chromite ore, therefore taking maximum advantage of friable chromite ore available in South Africa (Naiker & Riley, 2006a).

c) Providing an agglomerate feed to furnaces thus reducing the risk of bed turnovers and blowouts occurring (Naiker & Riley, 2006a).

d) Although pre-reduction capital cost is higher than the capital incurred for a conventional process, it is still the lowest capital cost per annualised ton of FeCr (Naiker, 2007).

e) High recoveries of metallic oxides (90%).

f) Production of a low silicon product (<3%).

g) The use of lower cost fine reductants instead of lumpy reductants and the use of oxygen as an energy source (Botha, 2003; Naiker & Riley, 2006a; Naiker, 2007).

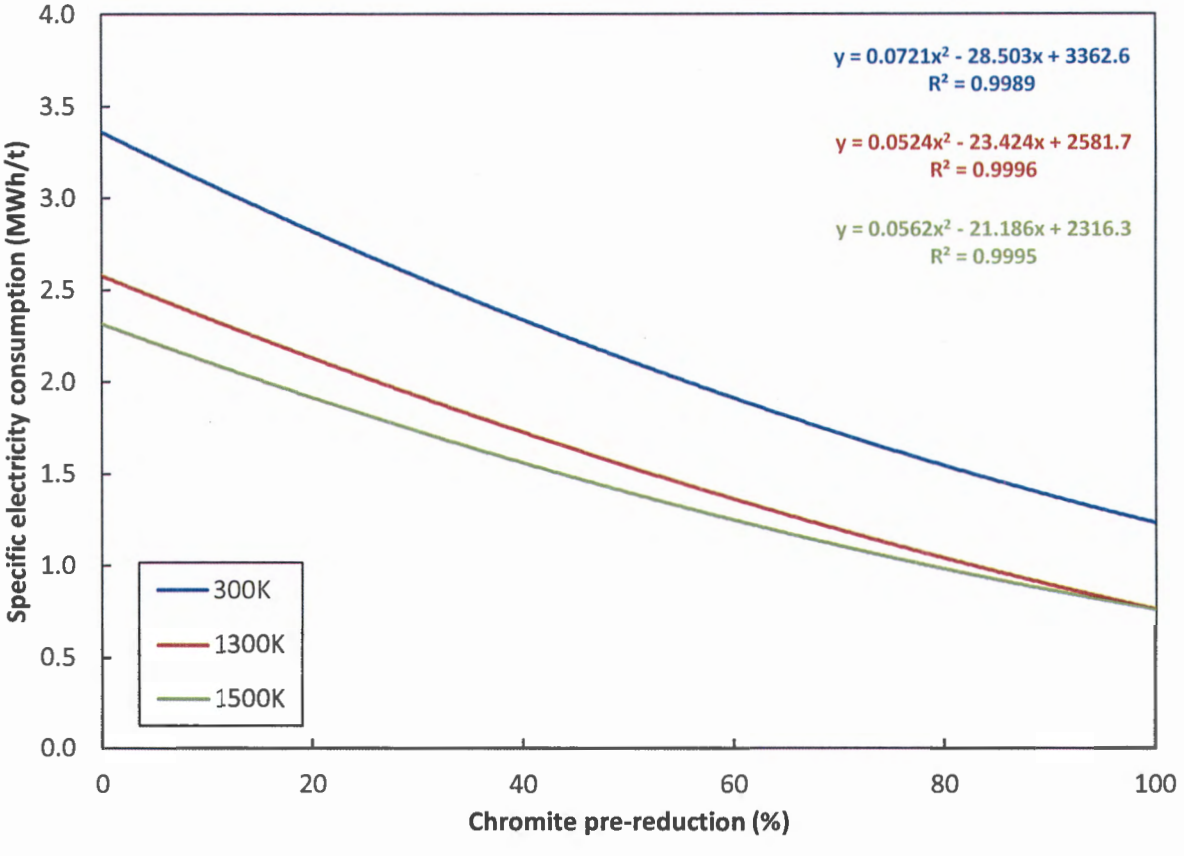

Figure 2-21: Net energy requirement for the production of 1 ton of FeCr as a function of the degree of pre-reduction achieved and charging temperature (Niayesh & Fletcher, 1986; Takano *et al.*, 2007)

2.4.3 Fundamental aspects of chromite pre-reduction

In a chromite pre-reduction process certain terms are used to describe the reduction rate and extent of reduction and metallisation. It is therefore necessary to define these terms before going into further discussions. Barnes *et al.* (1983) proposed definitions for the terms "degree of reduction" and "metallisation" which have since been used by some researchers (Soykan *et al.*, 1991b; Weber & Eric, 2006). Given that the removal of oxygen is associated with reduction, the extent of reduction, R(%), was defined as (Barnes *et al.*, 1983):

$$R(\%) = \frac{Mass\ of\ oxygen\ removed}{Original\ removable\ oxygen} \times 100 \qquad 2\text{-}4$$

In the pre-reduction process solid carbon is used as a reductant and CO is thus formed as a reduction reactions product (illustrated in Equation 2-7, Equation 2-8 and Equation 2-9), with 1 mole of CO forming for 1 mole of oxygen removed from the ore oxides. The extent of reduction can thus also be defined as (Barnes *et al.*, 1983):

$$R(\%) = \frac{Mass\ of\ CO\ evolved}{\frac{28}{16} \times Original\ removable\ oxygen} \times 100 \qquad 2\text{-}5$$

The amount of removable oxygen used to define Equation 2-4 and Equation 2-5 is determined from the oxygen loss associated with the metal oxides Fe_2O_3, FeO and Cr_2O_3.

The extent of metallisation, M(%), is defined as (Barnes *et al.*, 1983):

$$M(\%) = \frac{Cr^0 + Fe^0}{Cr_{tot} + Fe_{tot}} \qquad 2\text{-}6$$

Where: Cr^0 is the amount of Cr reduced to the metal state

Fe^0 is the amount of Fe reduced to the metal state

Cr_{tot} is the total Cr amount

Fe_{tot} is the total Fe amount

Since complete oxygen removal corresponds to complete metallisation, 100% reduction corresponds to 100% metallisation. The relationship between metallisation and reduction is, however, not linear and Barnes *et al.* (1983) attributed this to the following factors:

1) In the early stages of reduction, Fe_2O_3 is reduced to FeO without any metallisation:

$$Fe_2O_3 + C \rightarrow 2FeO + CO \qquad 2\text{-}7$$

2) FeO is reduced to Fe^0, producing 1 mol of CO for every mole of Fe^0 produced:

$$FeO + C \rightarrow Fe + CO \qquad 2\text{-}8$$

3) Cr_2O_3 is reduced to Cr^0, producing 1.5 mol of CO per mole of Cr produced:

$$Cr_2O_3 + 3C \rightarrow 2Cr + 3CO \qquad 2\text{-}9$$

Dawson and Edwards (1986) illustrated the individual difference in metallisation and reduction of Fe and Cr, confirming the above mentioned factors proposed by Barnes *et al.* (1983). A graphic illustration of this relationship between reduction and metallisation were reconstructed form Dawson and Edwards (1986) and shown in Figure 2-22.

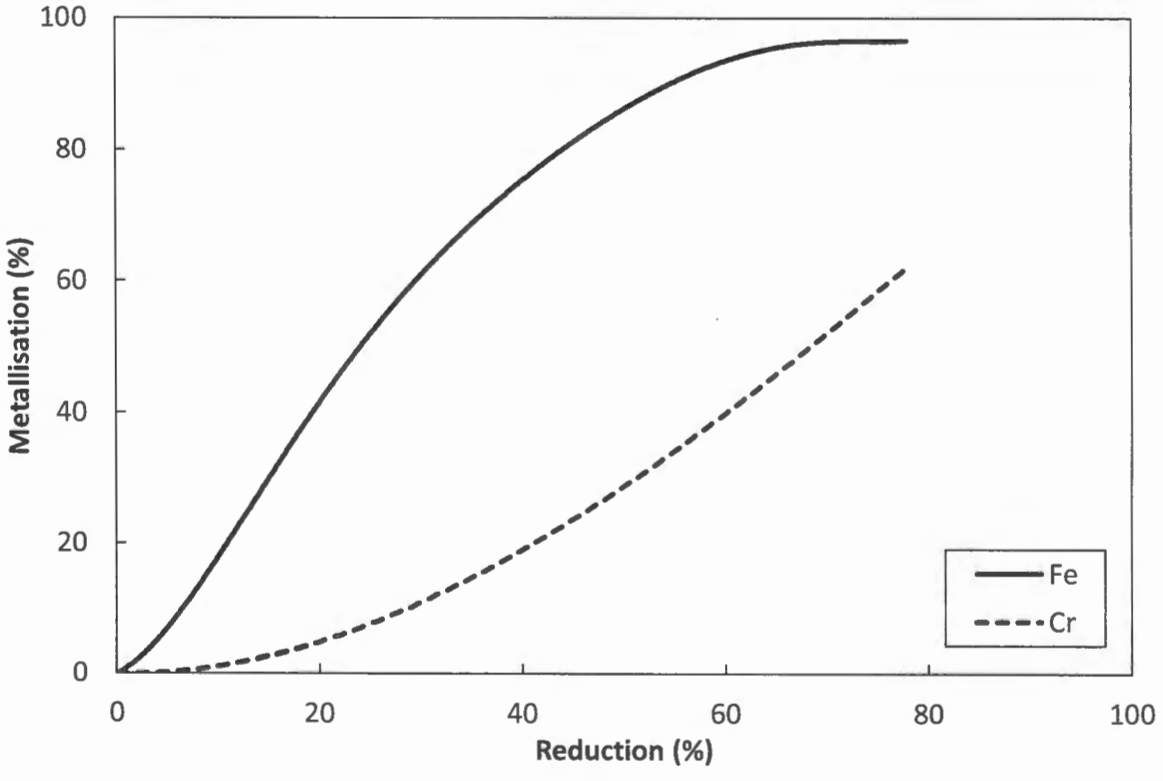

Figure 2-22: The relationship between reduction and metallisation, based on South African LG-6 chromite treated at 1200 °C (Dawson & Edwards, 1986)

Chromite ore is primarily composed of $FeO{\cdot}Cr_2O_3$, $MgO{\cdot}Cr_2O_3$, $MgO{\cdot}Al_2O_3$, $(Cr,Al)_2O_3$, forming a complex spinel structure and may also hold a certain amount of free Fe, not contained inside the spinel (Takano *et al.*, 2007). The general formula for specifically South African chromite ore located in the BIC is $(Fe^{2+}_{0.74}Mg_{0.27})_{\Sigma=1.01}(Cr_{1.42}Al_{0.40}Fe^{3+}_{0.15}Ti_{0.01}V_{0.01})_{\Sigma=1.99}O_4$. The reduction mechanism for chromite is therefore much more complex, due to the number of metal oxides, slag components (SiO_2, TiO_2, Al_2O_3, MgO, CaO, including gaseous Mg and SiO) and alkalis contained inside the spinel structure or existing as free compounds (Niemelä *et al.*, 2004).

Takano *et al.* (2007) identified three ways in which high temperature reduction of chromite using a carbon reductant can generally occur, i.e. i) solid chromite is reduced by solid or gaseous reductant; ii) direct reaction at the interface between the slag and metal, where the dissolved chromite in the slag are reduced by carbon dissolved in the metal phase; and iii) direct reaction between dissolved chromite in the slag and the carbon particles floating on it. In SAF mechanisms ii and iii should be predominant, while in the chromite pre-reduction process a large portion of chromite is expected to reduce by solid or gaseous reductants before liquid phase formation. The reduction of oxides is based on the reaction with solid carbon and carbon monoxide gas. The relevant solid carbon and CO gas interaction reactions are indicated in Equation 2-10 and Equation 2-11 (Niemelä *et al.*, 2004).

$$2C + O_2(g) \rightarrow 2CO(g) \qquad 2\text{-}10$$

$$2CO(g) + O_2(g) \rightarrow 2CO_2(g) \qquad 2\text{-}11$$

Niemelä *et al.* (2004) investigated the formation, characterisation and utilisation of CO-gas formed during the carbothermic reduction of chromite. According to the Ellingham diagram calculations the authors conducted (indicated in Figure 2-23) they showed that solid carbon reduces Fe_2O_3 to Fe_3O_4 at around 250 °C. The reduction of Fe_3O_4 to FeO occurs at temperatures above approximately 710 °C with solid carbon and carbon monoxide. FeO is reduced to the Fe^0 state at relatively low temperatures, around 710 °C and above with solid carbon, while the reduction of Cr_2O_3 with solid carbon occurs at higher temperatures of 1250 °C and above. Carbon monoxide reduces Fe_2O_3 to Fe_3O_4 over the whole calculated temperature range, but as mentioned earlier reduction of Fe_3O_4 to FeO occurs kinetically above 710 °C. Although it is not shown in Figure 2-23, a high CO/CO_2 ratio would also be required for such reduction to take place. Form the calculations it is evident that the reduction of Cr_2O_3 and $(FeO{\cdot}Cr_2O_3)$ is not possible with carbon monoxide alone.

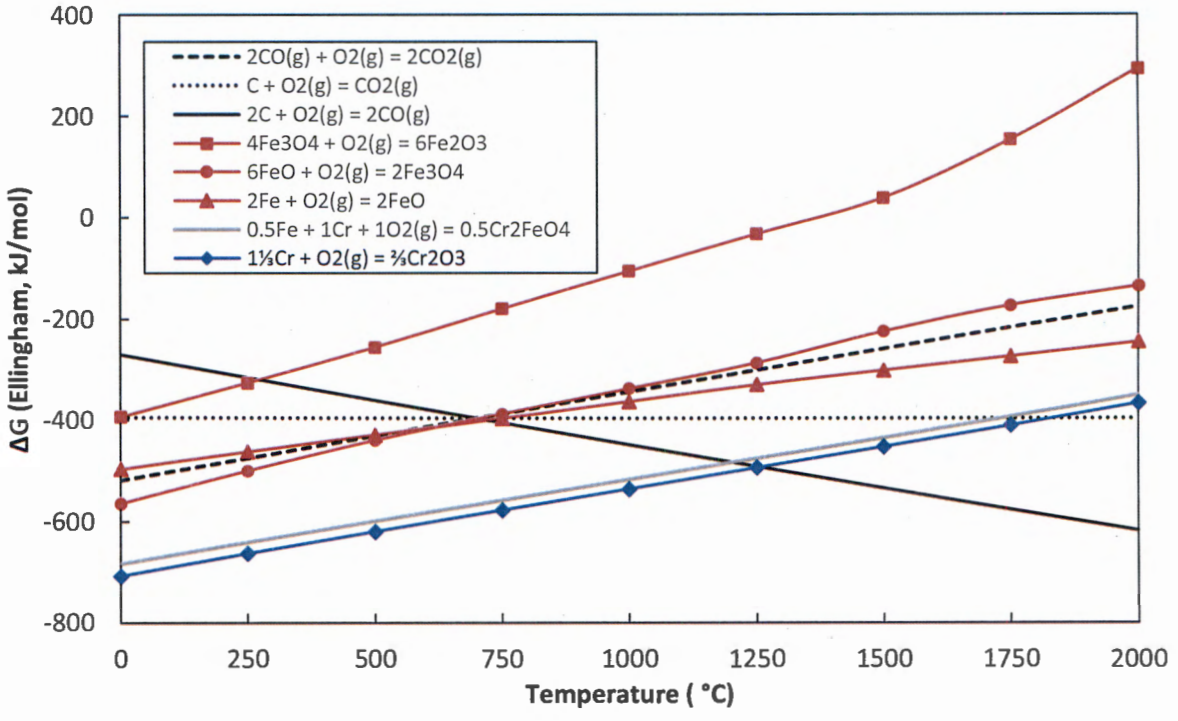

Figure 2-23: Standard free energies of reduction of metal oxides with carbon and carbon monoxide (Niemelä *et al.*, 2004)

The mechanisms and kinetics of the reduction of South African chromite ores have been studied by numerous researchers. A comprehensive reference list of these investigations is given by Hayes (2004). Significant results on the solid-state carbothermic reduction mechanism and kinetics of chromite from the LG6 layer of the BIC treated at 1400 °C have been published by Soykan *et al.* (1991b; 1991a). Soykan *et al.* (1991b; 1991a) proposed a stoichiometric ionic diffuse reduction model involving somewhat complex reactions among the solid carbon reductant, altered chromite spinel phases, and various ionic species. It also included site-exchange mechanisms between Fe^{2-} and Cr^{3+} ions, with the Cr^{3+} being placed in octahedral sites due to its very high affinity for octahedral coordination (Soykan *et al.*, 1991b; Soykan *et al.*, 1991a; Weber & Eric, 1993; Weber & Eric, 2006). The proposed mechanism, furthermore, included a swap mechanism between the Cr^{2+} ions of the surface unit cell and the Fe^{2+} ions of the unit cell just below the surface. Soykan *et al.* (1991b; 1991a) observed that localisation occurred in partially reduced chromite and that all the oxygen are removed from the surface as Fe and Cr is reduced. The inner cores were found to be rich in Fe, whereas the outer cores were depleted of Fe. A graphic representation, shown in Figure 2-24, of the reduction of chromite was proposed by Ding and Warner (1997b) correlating to the observations of Soykan *et al.* (1991b; 1991a). Soykan *et al.* (1991b; 1991a) revealed that, within the outer core (Reduced area, Figure 2-24), Fe^{2+} and Cr^{3+} ions diffused outward, whereas Cr^{2+}, Al^{3+} and Mg^{2+} ions diffused inward. Initially, Fe^{3+} and Fe^{2+} ions at the surface of chromite particle (Interface 1, Figure 2-24) were reduced to the metal state.

This was followed immediately by the reduction of Cr^{3+} ions to the 2+ oxidation state. Cr^{2+} ions diffusing toward the inner core of the particle reduced the Fe^{3+} ions in the spinel under the surface of the particle to Fe^{2+} at the interface (Reduced area, Figure 2-24) between the inner and outer cores. Fe^{2+} ions diffuse toward the surface, where they were reduced to metallic Fe. After the Fe had been completely reduced, Cr^{3+} and any Cr^{2+} that was present were reduced to the metal state, leaving a Fe and Cr free spinel, $MgAl_2O_4$. The metallised Fe and Cr carburised during the reduction into $(Fe,Cr)_7C_3$, according to Equation 2-12 and Equation 2-13.

$$7Cr_2O_3 + 27C \rightarrow 2Cr_7C_3 + 21CO \qquad 2\text{-}12$$

$$7FeO + 10C \rightarrow Fe_7C_3 + 7CO \qquad 2\text{-}13$$

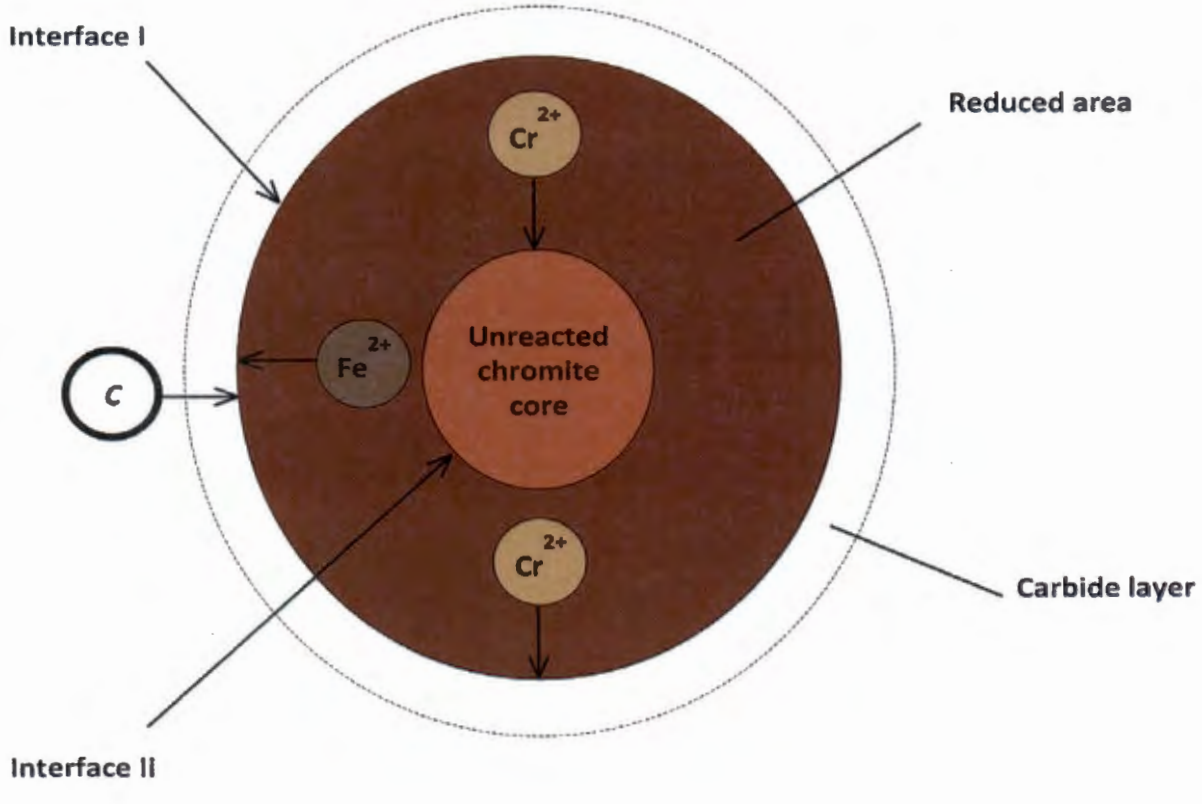

Figure 2-24: Schematic representation of the reduction mechanism of chromite (Ding & Warner, 1997b)

2.4.4 Factors influencing the pre-reduction of chromite

2.4.4.1 Effect of time and temperature

The extent of chromite pre-reduction achieved in industrial operations is seldom more than 60%. This involves nearly complete metallisation of the iron and typically less than 30% metallisation of the chromium. The low metallisation of the chromium, therefore, limits the potential further reduction in electrical energy required, as mentioned in Paragraphs 2.4.2 and 2.4.3. The relatively low degree of pre-reduction obtained in current industrial operations is a result of the slow reduction kinetics of chromium species occurring in the chromite. The kinetics is determined by the temperature of operation, which is limited to a maximum of about 1350 °C. At temperatures above 1350 °C, partial melting of the pellets occurs, that consequently causes dam-ring formation in the kiln and hence a decrease in operation efficiency (Dawson & Edwards, 1986). The effect of time and temperature on the pre-reduction of chromite concentrates with a low Cr/Fe ratio, studied by Barnes *et al.* (1983), is indicated in Figure 2-25.

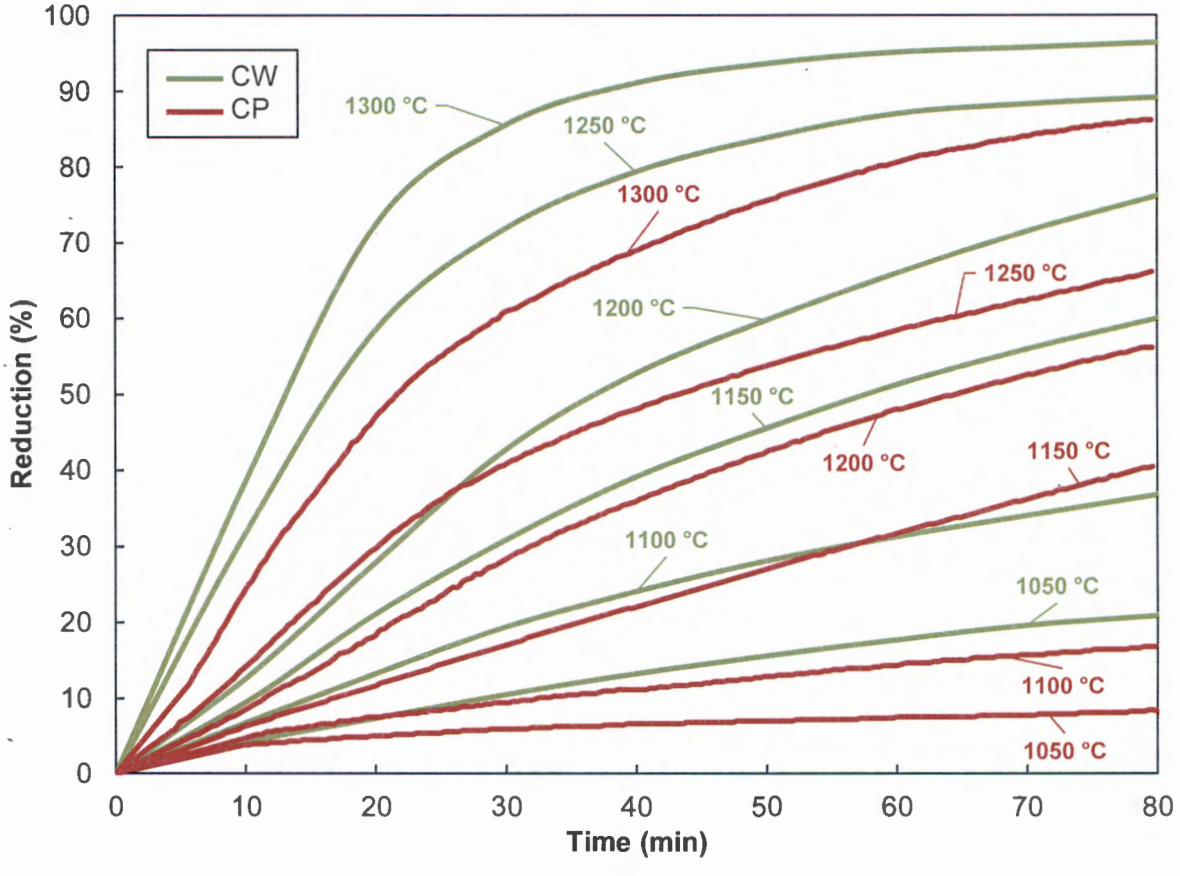

Figure 2-25: The effect of time and temperature on the rate of chromite reduction of two samples of ore, designated CW and CP, from different ore bodies in the UG2 layer (Barnes *et al.*, 1983)

2.4.4.2 Effects of additives on pre-reduction

The reduction of chromite in the presence of various additives and fluxes with the aim of improving the pre-reduction of chromite has been a subject of several investigations in recent years.

- Sundar Murti *et al.* (1983) studied the effect of 8% CaO addition on the reduction of synthetic and natural chromites at 1200-1300 °C using graphite as a reductant. They found that the reduction was enhanced by the additive and attributed this to the CaO diffusing into the spinel and then releasing the FeO, thereby increasing the chromite reducibility.

- Katayama *et al.* (1986) proved that 1 wt.% addition of $Na_2B_4O_7$, NaF, NaCl, CaB_4O_7, B_2O_3 and CaF_2 improved the reduction rate of Russian chromium ore; while the same wt.% $CaCl_2$ addition inhibited the reduction rate the longer it was exposed to the experimental temperature of 1200 °C. The effect that these salt additives had on the reduction rate of Russian chromium ore at 1200 °C where reconstructed from (Katayama *et al.*, 1986) and illustrated in Figure 2-26.

- Dawson and Edwards (1986) investigated the addition of a fluxing agent, CaF_2, and a eutectic mixture, NaF-CaF_2, on the reduction rate of chromite. While a moderate addition of CaF_2 was found to be beneficial for chromite reduction, the eutectic mixture of NaF-CaF_2 were much more effective than using only CaF_2.

- Van Deventer (1988) studied the effect of K_2CO_3, Na_2O_2, CaO, SiO_2, Fe^0, Cr^0, Al_2O_3 and MgO additions on the reduction of Kroondal chromite at 1400 °C by graphite. K_2CO_3, Na_2O_2, CaO, SiO_2 and Fe^0 were found to enhance the rate of reduction, while Al_2O_3 and MgO inhibited the reaction. Cr^0 additions had little influence on reduction rates.

- Nunnington and Barcza (1989) found that the addition of granite and fluorospar to act as fluxing agents in the pre-reduction of chromite ore pellets under oxidising conditions improved reduction rates.

- Weber and Eric studied the carbothermic reduction of chromite in the presence of silica flux extensively and found that reduction was enhanced at and above 1400 °C (Weber & Eric, 1992; Weber & Eric, 1993; Weber & Eric, 2006).

- Lekatou and Walker (1997) also researched the effect of SiO_2 additions on the solid state reduction of chromite concentrates.

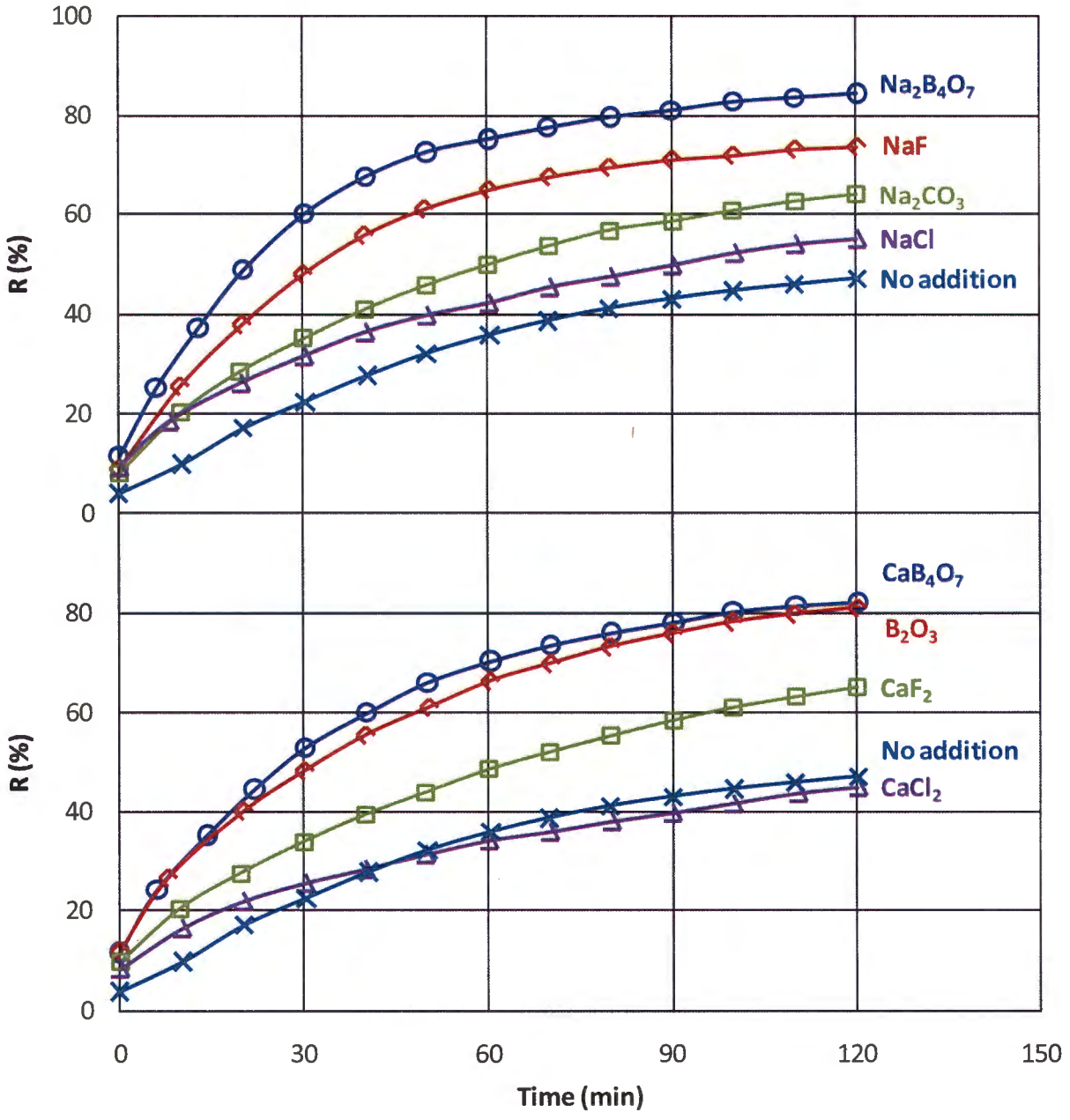

Figure 2-26: The effect of various salt additives (1 wt.% addition) on the reduction rate of Russian chromium ore at 1200 °C (Katayama et al., 1986)

- Ding and Warner investigated the catalytic effect of both lime and SiO_2 additions on the reduction of ground South African chromite concentrates. SiO_2 was found to have an enhanced effect on the reduction rate at and above 1380 °C, but only if reduction levels are higher than 40%, constituting the formation of a liquid slag (Ding & Warner, 1997b). Experiments on the catalytic reduction of carbon chromite composite pellets by lime were carried out at 1270-1433 °C and the reduction rate and extent were found to increase with increasing reduction temperature and lime addition (Ding & Warner, 1997a).

- Takano *et al.* (2007) utilised Portland cement, hydrated lime and silica as additives and proved that composite pellets containing these compounds had enhanced chromite reduction rates.

- Neizel *et al.* (2013) proved that $CaCO_3$ addition could significantly enhance the level of chromite pre-reduction achieved in the pelletised chromite pre-reduction process. From a theoretical point of view this could have a corresponding positive effect on the SEC requirements during FeCr production. However, Neizel *et al.* (2013) showed that $CaCO_3$ addition results in severe decreases in both the compressive and abrasion strengths of pre-reduced pellets. Practically, this renders this technique much less useful for SAF FeCr production, since excessive fines in the feed material is likely to result in increased gas eruptions and bed turnovers with an associated increased safety risk, as well as associated decrease in furnace efficiencies and equipment damage.

- Wang *et al.* (2015) studied the isothermal reductions of synthetic chromite ($FeCr_2O_4$) with additions of CaO, MgO, Al2O3 and SiO2 at 1400 °C. Compared to reduction without additions, the rate and degree of reduction was improved with additions of CaO and Al_2O_3. Wang *et al.* (2015) attributed this to CaO and Al_2O_3 improving Cr^{3+} diffusion in the solid phase. MgO was found to inhibit reduction due to the formation of $MgCr_2O_4$, which Wang *et al.* (2015) indicated as a more stable phase than $FeCr_2O_4$. With additions of SiO_2, the degree of reduction reached was the same as without any addition, however the rate of reduction lowered due to the formation of a CrO-SiO_2 liquid phase.

The above-mentioned investigations indicate that the addition of certain additives could have an effect on the reduction of chromite, either positive or negative. The list given above are by no means comprehensive, but it does provide some insight into past research activities.

2.5 Pre-oxidation of chromite ore

Pre-oxidation as a pre-treatment prior to smelting in the SAF is a commercially applied process. In the Outotec Steel Belt Sintering (SBS) process (Figure 2-27, process combination B, Section 2.3.2), which has been the most commonly applied process over the last decade in the South African FeCr industry, milled chromite ore is sintered in a pelletised form. This sintering process is basically an oxidative process, during which the fixed carbon content (~2 wt.%) present in the pellets, which is significantly lower compared to chromite pre-reduction (~15 wt.%), is oxidised to sinter the pellets (Niemelä *et al.*, 2004; Kleynhans *et al.*, 2012; Glastonbury *et al.*, 2015).

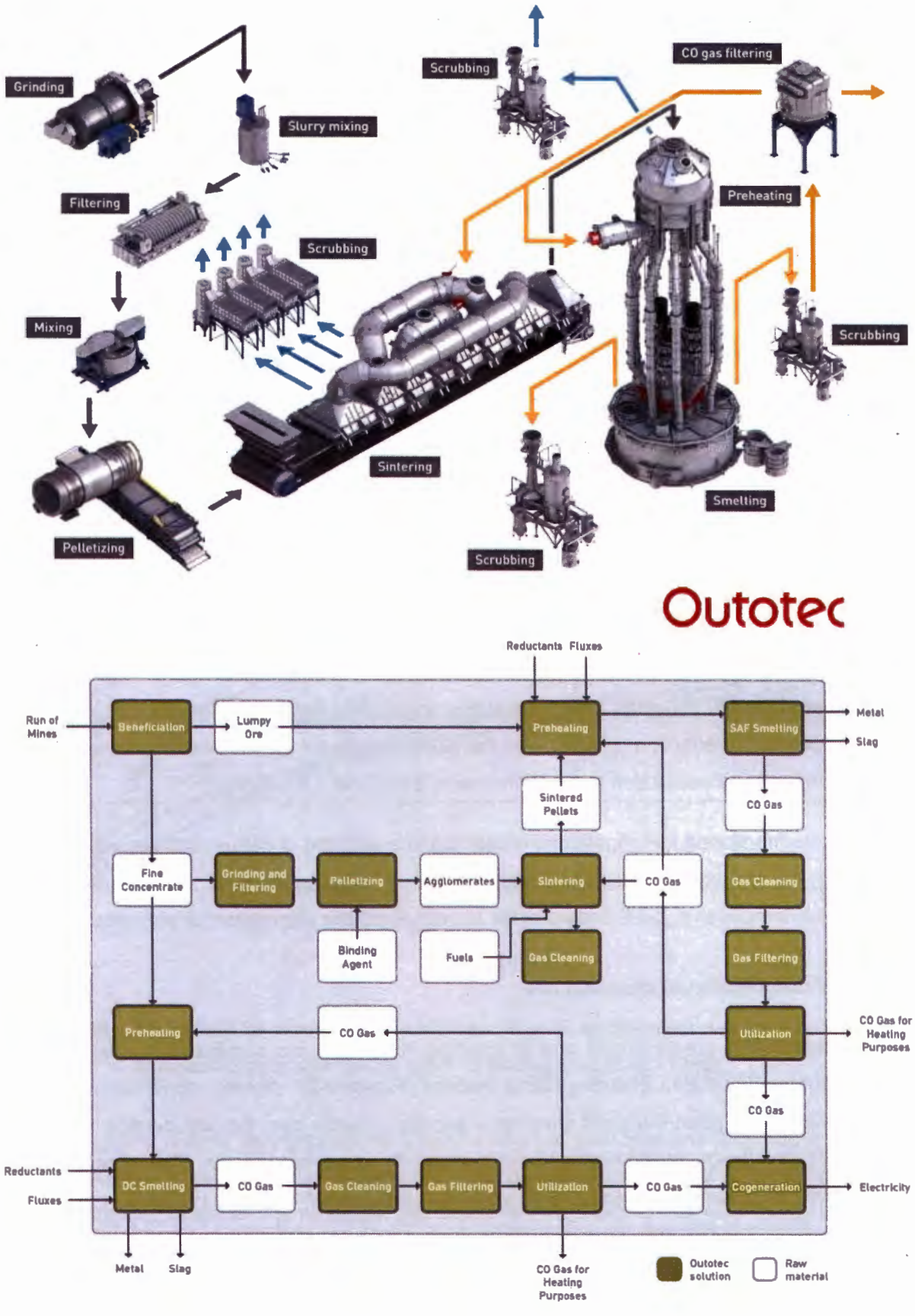

Figure 2-27: Outotec Steel Belt Sintering (SBS) process (Outotec, 2015)

Zhao and Hayes (2010) investigated the effects of oxidation on the microstructure and reduction (as occurring in the smelting process) of chromite pellets. They found that by pre-heating the pelletised ore at temperatures between 1000 and 1200 °C in air, it increased the reducibility of the chromite in the smelting furnace. They attributed this increased reducibility to the increase in surface area created due to the shear mechanism generating smaller particles, i.e. the transformation of Fe_3O_4 to Fe_2O_3 (Zhao & Hayes, 2010). The rapid transformation to the M_2O_3 phase occurs through a solid state shear mechanism that results in the preferential growth on the planes in the crystals. The strain induced at the Fe_3O_4/Fe_2O_3 phase boundary and the preferential reduction of Fe_2O_3 can result in the mechanical break-up of the crystal grains, thereby increasing the effective surface area for reduction (Zhao & Hayes, 2010).

Kapure *et al.* (2010; 2013) studied the reduction of pre-oxidised Indian chromite ore (from Sukinda) composite pellets using coal reductant at high temperature (1500 °C). Chromite ore oxidised in air at 900 °C for a duration 2 hours was used as the material for carrying out the reduction studies. Kapure *et al.* (2010) identified that during pre-oxidation of chromite ore, the FeO present in chromite spinel oxidises to Fe_2O_3 (sequioxide) in the form of exholved precipitate on the surface of chromite grains and generates cation vacancies. SEM micrographs and SEM-EDS analysis of raw (un-oxidised) chromite (A) and a pre-oxidised chromite particle (B) are shown in Figure 2-27. Kapure *et al.* (2010) showed from Figure 2-28B that after pre-oxidation of chromite the Fe_2O_3 sequioxide phase has precipitated on the surface of chromite particle in a characteristic Widmanstätten pattern. The lighter grey colour lines are iron enriched phases and the darker grey colour matrix is an Mg rich phase. Kapure *et al.* (2010) also identified from these results that Fe is precipitating from the matrix on [111] crystallographic planes. The pre-oxidation of chromite causing a typical Widmanstätten pattern to form on the surface of chromite grain is in keeping with the well-recognised theory of oxidation and precipitation of sesquioxide phase minerals (Tathavakar *et al.*, 2005).

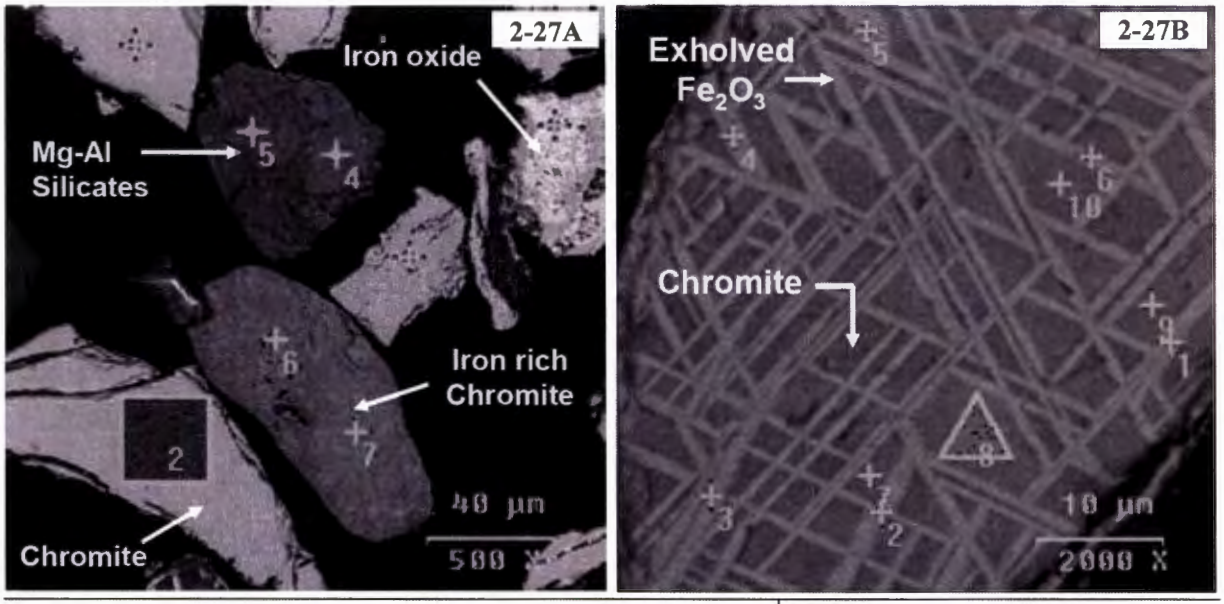

Figure 2-28A							Figure 2-28B			
Point	O	Mg	Al	Si	Cr	Fe	Point	Mg	Cr	Fe
1	22.7	11.7	8.4	0.5	46.9	7.7	1	7.3	45.9	15.5
2	23.3	10.3	7.9	0.6	46.4	10.9	2	4.2	47.1	28.8
3	21.2	0.0	1.7	2.7	2.4	71.3	3	3.3	47.2	20.2
4	31.9	10.6	3.5	32.0	0.3	11.3	4	2.0	47.8	22.5
5	32.2	11.1	1.7	34.1	0.4	12.1	5	0.0	46.6	26.1
6	26.4	0.5	7.3	3.1	30.9	30.0	8	12.5	46.8	9.3
7	24.5	0.0	7.7	2.9	37.2	25.8	9	12.6	46.7	8.8
8	22.7	10.2	7.0	0.7	47.8	10.2	10	13.3	47.4	8.6

Figure 2-28: SEM micrographs and SEM-EDS analysis of raw (un-oxidised) chromite (A) and a pre-oxidised chromite particle (B) (Kapure *et al.*, 2010)

A schematic structure of the moving AB_2O_4/B_2O_3 interface with a small rotation along a close-packed direction, accommodated by vacancies are shown in Figure 2-29 (Tathavakar *et al.*, 2005). According to this theory, the favoured crystallographic orientation of Widmanstätten lamellae is along the [111] plane of the spinel matrix phase. The [111] planes of spinel and the [0001] planes of sesquioxide have a related close packing arrangement of oxygen ions, which account for the common orientation of sesquioxide lamellae along the [111] plane of the spinel matrix. Tapered terminals develop at the intersection of two or more lamellae, which are indicative of a diffusion-controlled process. Furthermore, in an oxidising environment, in addition to the inherent driving force for phase transformation, the imposed oxygen chemical potential encourages the diffusion of Fe^{2+} ion from the central core of chromite particle towards the solid-gas interface on the surface of the particle (Tathavakar *et al.*, 2005; Kapure *et al.*, 2010; Kapure *et al.*, 2013).

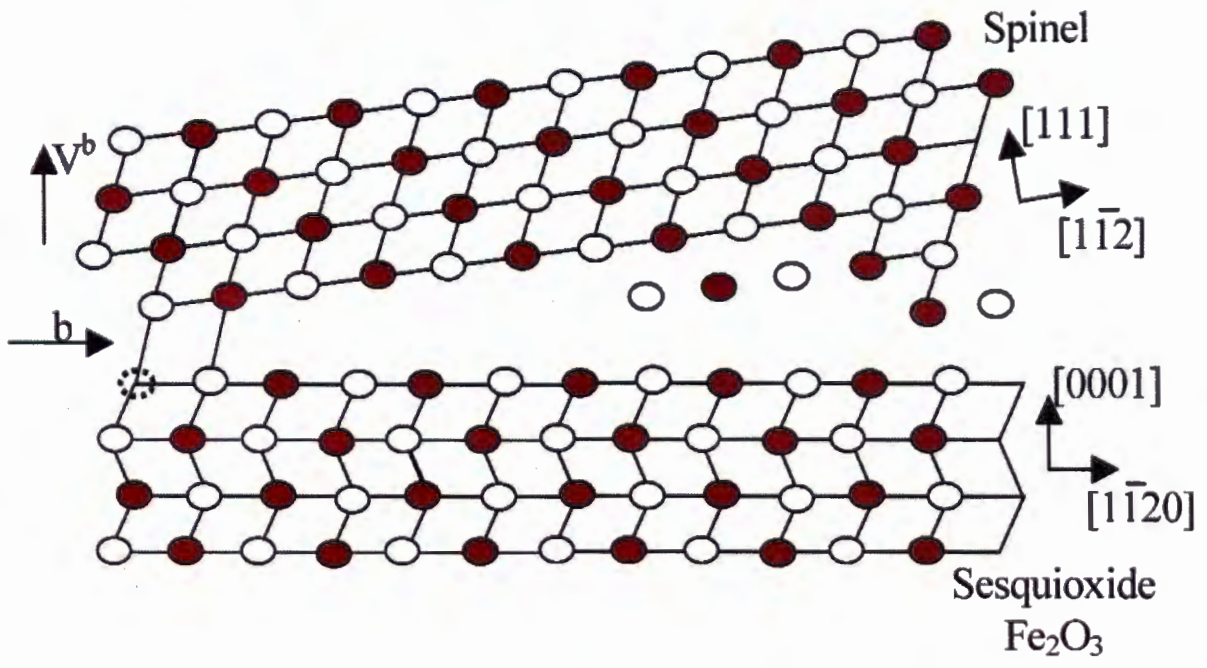

Figure 2-29: A schematic structure of the moving AB_2O_4/B_2O_3 interface with a small rotation along a close-packed direction, accommodated by vacancies (Tathavakar *et al.*, 2005)

This diffusion of Fe^{2+} cations to the outside of the chromite particle together with the oxidation to Fe^{3+} cations takes place via following reactions (Tathavakar *et al.*, 2005; Kapure *et al.*, 2010):

$$\frac{1}{2}O_2 \xrightarrow{T} O_o^{2-} + V_{cat}^{n} + 2 \cdot h^{\bullet} \qquad 2\text{-}14$$

$$2Fe^{2+} \xrightarrow{T} 2Fe^{2+} + 2 \cdot e' \qquad 2\text{-}15$$

Where O_o^{2-} represents oxygen anions on the cubic closed packed lattice, V_{cat}^{n} is the cation vacancy, $h^{\bullet}$ is the hole, and e' is the electron. Oxidation of chromite ore causes the spinel structure to open up and subsequently newly formed Fe_2O_3 phase along with the additional vacancies generated during oxidation improves the reactivity of chromite ore and helps in liquid slag formation at lower temperatures during reduction (Tathavakar *et al.*, 2005; Kapure *et al.*, 2010).

Tathavakar *et al.* (2005) studied the thermal decomposition behaviour of South African chromite ores in order to relate the influence of oxygen to likely product phases formed. In this investigation Tathavakar *et al.* (2005) calculated the free energies of decomposition of binary spinels using

FACT-Sage 5 (thermochemical software) and plotted free energy change (ΔG) against temperature (T). A reconstruction of this data is shown in Figure 2-30. It is clear from Figure 2-30 that the chromite spinels ($FeCr_2O_4$ and $MgCr_2O_4$) with higher ΔG values are more stable compared to the other spinels. However, in an oxidising environment, the decomposition of FeO-based spinels is thermodynamically favoured compared to MgO based spinels. Tathavakar *et al.* (2005) also determined values of free energy changes for the oxidation reaction (Equations 2-16 to 2-22) of FeO and FeO-based spinels to Fe_3O_4 and Fe_2O_3, and these results are plotted in Figure 2-31. From the graph in Figure 2-31, it can be reasoned that FeO oxidises to Fe_3O_4 and then to Fe_2O_3, which is also accurate for all FeO-based spinels. It is obvious from the Gibbs energy plots for the oxidation reactions of Fe^{2+} spinels in Figure 2-31 that all Fe^{2+} spinels are unstable. Consequently, the metastable maghemite-type spinel formed during the first stage of oxidation of the chromite spinel starts to decompose into a stable hematite phase, due to the presence of high oxygen partial pressure ($P_{O_2} = 0.2\ atm$) and temperature (above 600 °C) (Tathavakar *et al.*, 2005).

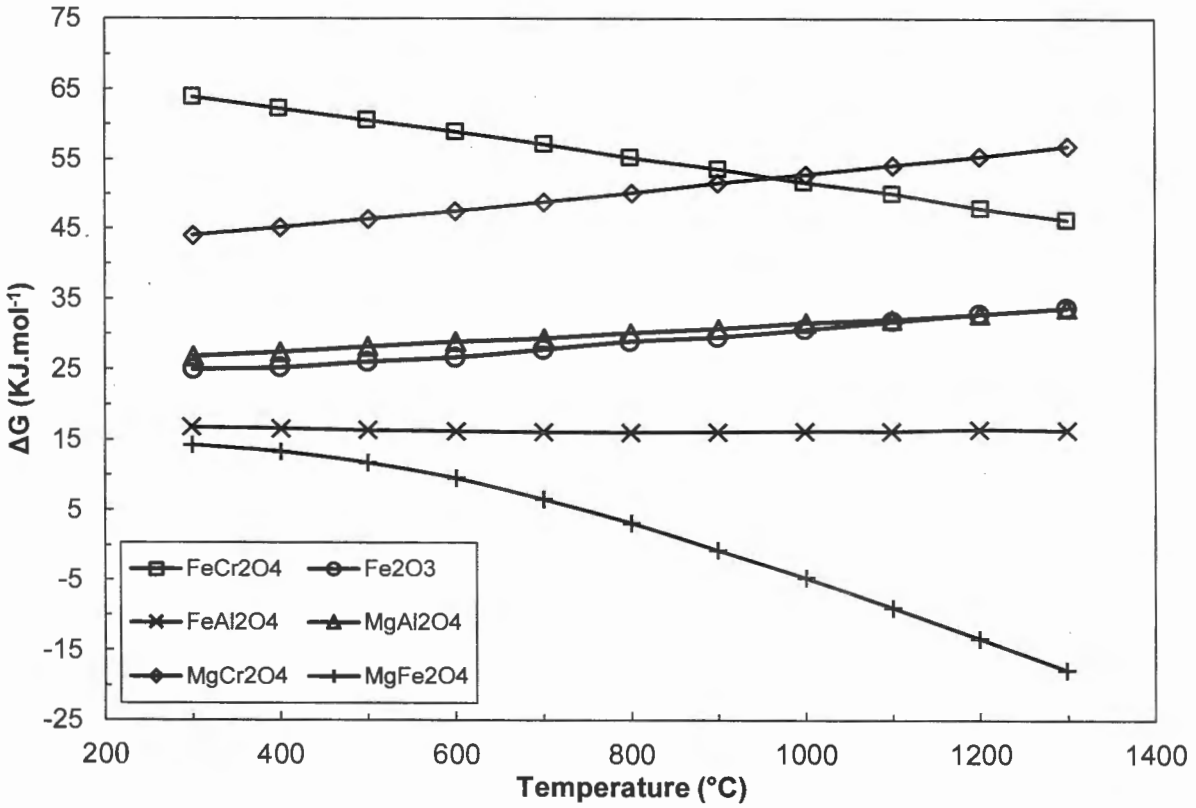

Figure 2-30: A plot calculated using the FACT-Sage 5 program of the Gibbs energy for the decomposition of pure spinels against temperature reconstructed from Tathavakar *et al.* (2005)

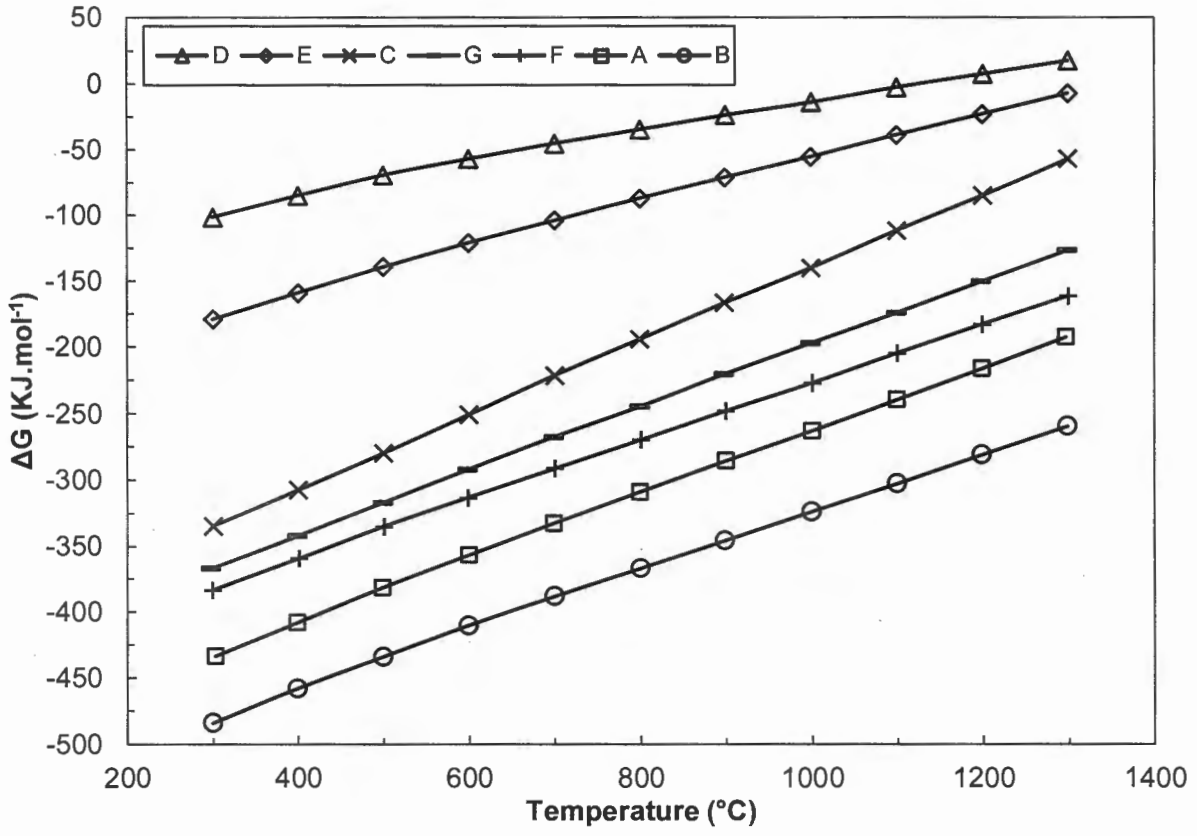

$$A: 4FeO + O_2 \xrightarrow{T} 2Fe_2O_3 \quad \text{2-16}$$

$$B: 6FeO + O_2 \xrightarrow{T} 2Fe_3O_4 \quad \text{2-17}$$

$$C: 4Fe_3O_4 + O_2 \xrightarrow{T} 6Fe_2O_3 \quad \text{2-18}$$

$$D: 6FeCr_2O_4 + O_2 \xrightarrow{T} 2Fe_3O_4 + 6Cr_2O_3 \quad \text{2-19}$$

$$E: 4FeCr_2O_4 + O_2 \xrightarrow{T} 2Fe_2O_3 + 4Cr_2O_3 \quad \text{2-20}$$

$$F: 6FeAl_2O_4 + O_2 \xrightarrow{T} 2Fe_3O_4 + 6Al_2O_3 \quad \text{2-21}$$

$$G: 4FeAl_2O_4 + O_2 \xrightarrow{T} 2Fe_2O_3 + 4Al_2O_3 \quad \text{2-22}$$

Figure 2-31: A plot of Gibbs free energy change for oxidation reactions (indicated below the chart and labelled A-G) of Fe^{2+} spinels and oxides against temperature (Tathavakar *et al.*, 2005)

2.6 Altering the Cr/Fe ratio of chromite ore

The utilisation of chromite ores which are currently classified as low grade, attributable to the large amount of contained Fe, has been the subject of numerous investigations. These have been comprehensively summarised in reviews by Nafziger (1982); Murthy *et al.* (2011) and studies by Dowes and Morgan (1951); Udy (1956); Sen and Chatterjee (1957); Biermann and Heinrichs (1960); Yousef *et al.* (1970); Sundar Murti and Seshadri (1979); Barnes *et al.* (1983); Gu and Wills (1988); Sharma (1990); Amer (1992); Vardar *et al.* (1994); Amer and Ibrahim (1996); Kanari *et al.* (2000); Geveci *et al.* (2002); Maulik and Bhattacharyya (2005); Agacayak *et al.* (2007); Bhatti *et al.* (2008); Shen *et al.* (2009a); Shen *et al.* (2009b); Kumar Tripathy *et al.* (2012) and Tripathy *et al.* (2015).

2.6.1 Physical separation methods

Conventional methods of beneficiation, such as gravity concentration, magnetic separation and flotation are unlikely to increase the Cr/Fe ratio of chromite ore, since both the Fe and Cr are part of the same mineral phase, i.e. the spinel (Nafziger, 1982; Shen *et al.*, 2009a; Shen *et al.*, 2009b). Obviously, the exception to this generalisation, i.e. that Fe cannot be removed from run-of-the-mine chromite ore by conventional separation methods, would be ores that also contain Fe in a separate mineral phase, i.e. gangue materials. In certain Indian chromite ore reserves, a significant amount of the Fe is contained in the gangue material in the form of Fe silicates and Fe minerals, which is frequently beneficiated using wet shaking tables and induced roll magnetic separators (Murthy *et al.*, 2011; Kumar Tripathy *et al.*, 2012; Tripathy *et al.*, 2015). Therefore, in order to increase the Cr/Fe ratio of the chromite spinel, Fe must be selectively extracted by means that facilitates the structural dissociation of the spinel (Nafziger, 1982). Some chemical techniques such as hydrometallurgical methods, roasting and alkali leaching, acid leaching, smelting and chlorination are required for this purpose (Shen *et al.*, 2009a; Shen *et al.*, 2009b).

2.6.2 Roasting and alkali leaching

Roasting and alkali leaching accomplishes decomposition of the chromite spinel by oxidation of the trivalent Cr in the chromite spinel to the hexavalent form. In traditional roasting, chromite ore is oxidised with the addition of sodium carbonate, limestone and dolomite at about 1100-1200 °C in a kiln or rotary furnace. However, disadvantages associated with roasting as currently applied include low Cr yields and environmental pollution by hexavalent chromium-containing residue. Alkali leaching or liquid-phase oxidation of chromite ore is an alternate approach for chromate production in which chromite ore is oxidised in the liquid medium, such as molten NaOH or KOH. High alkali-to-ore ratios, highly concentrated alkali aqueous solutions, disposal of by-products like sodium nitrite, operating pressures higher than 1 atm and high recycling amounts of NaOH or

KOH limit industrial application. Although affecting chromite spinel dissociation, roasting and alkali leaching are directed towards the selective extraction and production of chromate from chromite ore for the manufacture of chromium chemicals. This method will therefore not facilitate an increase in a chromite ores Cr/Fe ratio and is not explored further (Xu *et al.*, 2005; Sun *et al.*, 2007a; Sun *et al.*, 2007b; Zhang *et al.*, 2010a; Zhang *et al.*, 2010b).

2.6.3 Chlorination of chromite

The process of carbochlorination primarily involves three steps, i.e. i) production of chlorine gas (Cl_2) by electrolysing a NaCl solution, ii) carbochlorination of the chromite ore by using a Cl_2-CO gas mixture in the presence of NaCl, iii) treatment of the $FeCl_3$ by-product and unreacted Cl_2-CO gas mixture (Bergeron & Richer-Lafleche, 2004). In this context, the term carbochlorination refers to chlorination in the presence of CO.

Hussein and El-Barawi (1971) and Hussein *et al.* (1974) studied the carbochlorination of Egyptian chromite ores by using Cl_2 gas and carbon between 600 and 1000 °C. The results showed that the chlorination rate of Fe was higher than that of Cr. They also found that the chlorination rate of both Fe and Cr decreased at temperatures over 800 °C. They proposed that the carbochlorination of chromite could be carried out at temperatures of 600 °C or lower to produce residue with Cr/Fe ratios suitable for FeCr production.

Kanari *et al.* (1999) studied the carbochlorination of Albanian chromite in the presence of Cl_2 and CO (without additional additives) and found that 60% of the iron could be extracted at 600 °C after two hours, with a Cr extraction of less than 5%. As a result, the Cr/Fe ratio doubled from the initial value of 3.2.

Kanari *et al.* (2000) studied the chlorination of Albanian chromite in the presence of three different environments, i.e. i) Cl_2 and N_2, ii) Cl_2 and $AlCl_3$, and iii) $AlCl_3$, CO and N_2. However, in contrast to their earlier promising results with carbochlorination (Kanari *et al.*, 1999), i.e. 60% Fe extraction and 95% Cr recovery after treatment for two hours at 600 °C, it appeared as if the chlorination process only started at temperatures of approximately 600 °C in the Cl_2 and N_2 environment. Figure 2-32, reconstructed from Kanari *et al.* (2000), indicates the percentage weight loss of the chromite ore and Fe extraction as a function of temperature exposed for 2 hours to Cl_2 and N_2 gas. It is evident that only ~4% weight loss occurred at 600 °C in this environment. Unfortunately, Kanari *et al.* (2000) did not quantify the loss of Cr in this environment as a function of temperature. Chromium extraction quantification was only done at 1000 °C, where 13 to 50% of the Cr was extracted, depending on the duration of exposure. Based on the results presented in Figure 2-32, Kanari *et al.* (2000) suggested that 800 °C could be the most appropriate temperature, however the authors did not provide definite reasons for this recommendation.

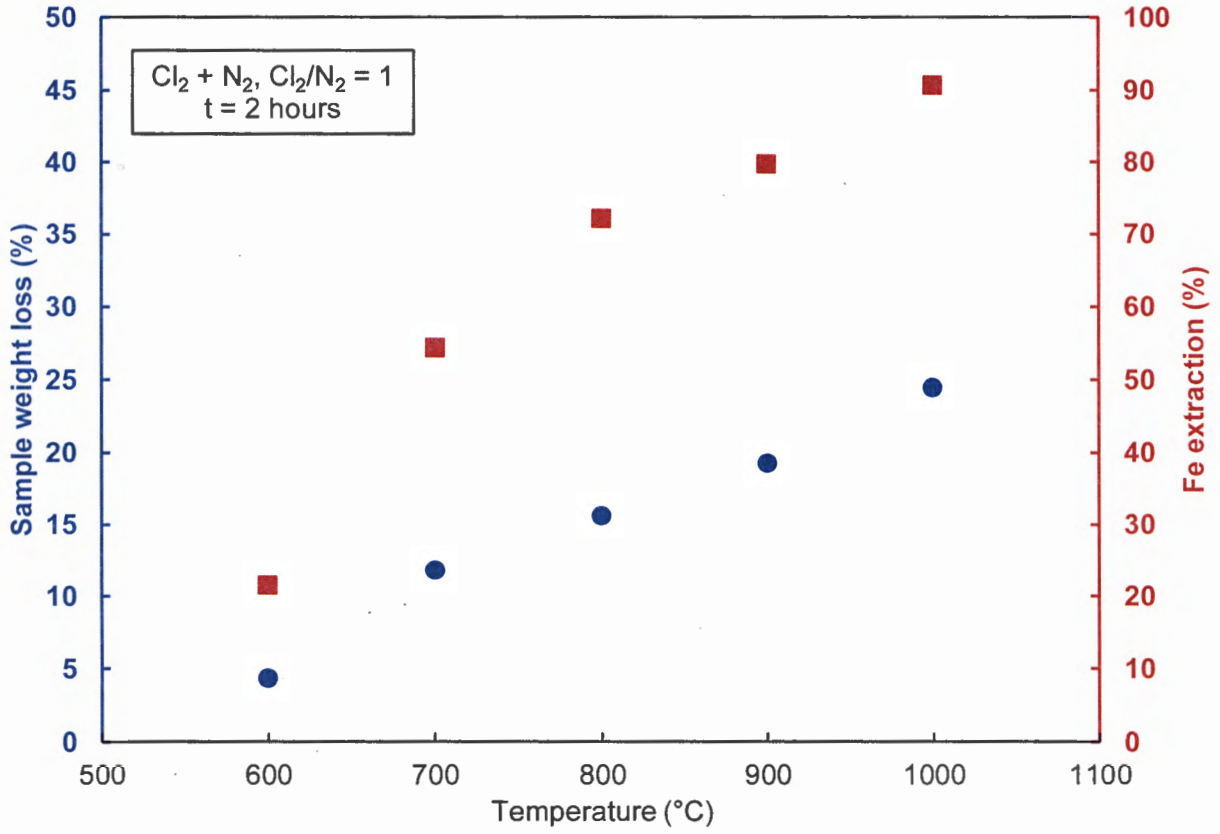

Figure 2-32: Weight loss (%) of chromite (blue) and Fe extraction (%, red) as a function of temperature in a Cl_2 and N_2 atmosphere (Kanari *et al.*, 2000)

The Cl_2 and $AlCl_3$ chlorinating environment investigated by Kanari *et al.* (2000) revealed that the addition of $AlCl_3$ had no beneficial advantages over pure Cl_2 chlorination. Better results were obtained by $AlCl_3$, CO and N_2 chlorination, specifically at 800 °C. Although the most Fe was extracted under these conditions, the Cr recovery was only 60%.

The selective removal of Fe from chromite ores by carbochlorination using Cl_2 and CO gas or Cl_2 gas and petroleum coke was studied and used by Shen *et al.* (2009a). Results indicated that Fe removal efficiency increased with increasing temperature, with significantly low efficiencies being observed at temperatures lower than 500 °C. At temperatures higher than 800 °C, part of the Cr in the chromite spinel were also chlorinated and lost to the vapour phase, while some Cr chlorides produced were soluble in water and consequently lost in the later leaching stage. Similar phenomena were also observed by Pokorny (1957). NaCl is the lowest-cost chlorine containing salt and commercially available in huge quantity, therefore Shen *et al.* (2009a) added NaCl to chromite ores prior to carbochlorination in order to study the effect of NaCl on Fe removal from chromite during carbochlorination. Shen *et al.* (2009b) suggested four possible reactions involved in the carbochlorination of FeO and Cr_2O_3 in chromite, shown in Equations 2-23 to 2-26.

(a) carbochlorination of FeO

$$\frac{2}{3}FeO.Cr_2O_3 + Cl_2(g) + \frac{2}{3}CO(g) = \frac{2}{3}FeCl_3 + \frac{2}{3}CO_2(g) + \frac{2}{3}Cr_2O_3 \quad 2\text{-}23$$

$$\frac{2}{3}FeO.Cr_2O_3 + Cl_2(g) + \frac{2}{3}CO(g) = \frac{1}{3}Fe_2Cl_6(g) + \frac{2}{3}CO_2(g) + \frac{2}{3}Cr_2O_3 \quad 2\text{-}24$$

(b) carbochlorination of Cr_2O_3

$$\frac{1}{3}FeO.Cr_2O_3 + Cl_2(g) + CO(g) = \frac{2}{3}CrCl_3(s) + CO_2(g) + \frac{1}{3}FeO \quad 2\text{-}25$$

(c) carbochlorination of FeO and Cr_2O_3

$$\frac{2}{9}FeO.Cr_2O_3 + Cl_2(g) + \frac{8}{9}CO(g) = \frac{2}{9}FeCl_3 + \frac{8}{9}CO_2(g) + \frac{4}{9}CrCl_3(s) \quad 2\text{-}26$$

Based on thermodynamic calculations done with the HSC Chemistry 2.03 (thermochemical software), Shen *et al.* (2009a) concluded that all the above-mentioned reactions (Equations 2-23 to 2-26) have Gibbs free energies of less than -50kJ/mol between 25 and 1000 °C. This implies that all these reactions are likely to take place. However, due to the fact that the Gibbs free energies of these reactions were so similar, it was impossible to state with certainty which reaction(s) would take place preferentially based on thermodynamic calculations alone. Experimental results obtained by Shen *et al.* (2009b), at temperatures between 606 and 720 °C, showed that up to 80% Fe extraction was obtained with very high corresponding Cr/Fe ratios of ~15, while it was claimed that no significant Cr extraction took place up to 720 °C, since the percentage Fe removal had a linear relationship with the total weight loss. Shen *et al.* (2009a) also found that chlorination of powdered un-agglomerated material was much more effective than chlorination of pelletised material, e.g. at 660 °C after two hours of exposure under carbochlorinating conditions with 5% NaCl (by weight) added, the pelletised material had a Cr/Fe ratio of approximately 20% below that of powdered material. It is evident from the work conducted by Shen *et al.* (2009a) and Shen *et al.* (2009b) that the presence of NaCl significantly enhanced the selective removal of Fe in chromite by carbochlorination, however the mechanisms involved in this phenomenon are not clear. The authors proposed that, i) the added NaCl(s) reacted with the chlorinated product $FeCl_3$(s) to form liquid eutectic films on the top and inner surfaces of the chromite particles due to the formation of the low melting point compound $NaFeCl_4$, ii) the formation of the liquid eutectic films increased the fluidity of the solid product $FeCl_3$(s), iii) part of

the formed $FeCl_3$ was probably volatised in the form of $NaFeCl_4$ vapour, iv) the formation of the liquid and the gaseous eutectic compound $NaFeCl_4$ reduced the pore blockage and increased the mass transfer rates of $Cl_2(g)$, $CO(g)$, $FeCl_3(s)$ at the deeper cores of the chlorinated chromite particles, v) NaCl–$FeCl_3$ eutectic is a good solid solvent for $FeCl_2(s)$, which is formed from the dissociation of $FeCl_3$, vi) $Cl_2(g)$ reacted with the $FeCl_2$ dissolved in the liquid eutectic films more rapidly than with solid $FeCl_2$ and thus increased the adsorption rate of chlorine, vii) NaCl indirectly increased the diffusion rate of $Cl_2(g)$, $CO(g)$, $FeCl_3(s)$ and $FeCl_2(s)$ inside the pore channels of chromite particles and reduced their diffusion activation energies. It is noteworthy that an 80 kJ/mol difference in activation energies between studies in the presence of NaCl and without NaCl was observed. This suggests that NaCl probably acted as a catalyst for carbochlorination of Fe oxides from chromites.

Shen *et al.* (2009a) also proposed two possible process options (Process A and B, Figure 2-33) for the beneficiation of chromite by carbochlorination in the presence of NaCl, with Process A being similar to the process developed by Bergeron and Richer-Lafleche (2004). Of these two options (Figure 2-33), Process A is probably a more economically feasible option, since it does not require additional leaching, filtration, neutralisation, precipitation and drying steps. Furthermore, Shen *et al.* (2009a) did not mention in their process flow diagram whether the carbochlorination was conducted with milled chromite ore. Materials handling of fine constituents (e.g. 90% of the particles <75 µm) always increases capital and operational costs. Apart from the above-mentioned obvious economic considerations, Cl_2, as well as CO, are both considered as toxic. CO concentrations as low as 667ppm may cause up to 50% of the body's haemoglobin to convert to carboxyhemoglobin. Exposure to 30 ppm Cl_2 may result in coughing and vomiting, while lung damage can occur at 60 ppm. Cl_2 is also an extremely strong oxidising agent and thus very corrosive. These health and environmental aspects will also have additional negative capital and operational impacts, making the application of this type of technology even less likely (Mobley, 2001; Snow, 2013; Hauptmanns, 2014). It is the opinion of the candidate that both the above-mentioned processes (Bergeron & Richer-Lafleche, 2004; Shen *et al.*, 2009a) are currently not economically viable for the upgrading of chromite prior to FeCr production. Ferrochrome is a relatively large volume, low profit commodity and the additional costs associated specifically with carbochlorination would not make it a viable option. The author is also not aware of any current application of such processes for FeCr production.

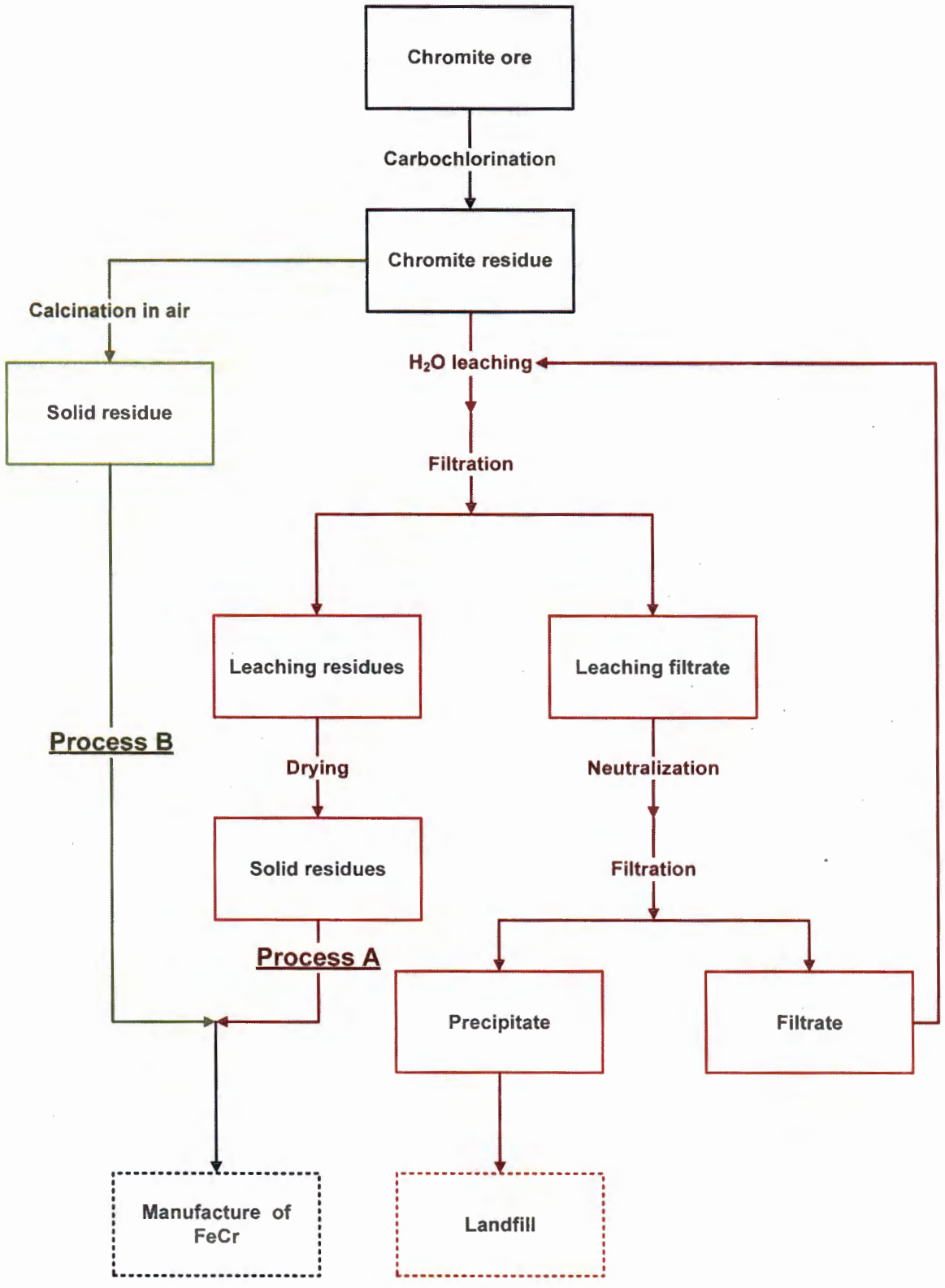

Figure 2-33: Chlorination process suggested by (Shen *et al.*, 2009a) for beneficiation of chromite ores in the presence of NaCl

2.6.4 Hydrometallurgical treatment of chromite ore

In the reviews and studies mentioned earlier, methods based on sulphuric acid leaching of chromite feature prominently. However, these methods are for the most part focused on developing new and cleaner processes for manufacturing of Cr compounds for the chemical industry as opposed to increasing the Cr/Fe ratio for application in the metallurgical industry which is the primary market for chromite (Paragraph 2.1.3, Figure 2-2). Chromite spinel has a stable and compact spinel lattice structure at room temperature and atmospheric pressure that is hardly soluble in a sulphuric acid solution.

Zhang *et al.* (2016) investigated the leaching thermodynamics of chromite in a sulphuric acid solution theoretically, during which a potential E-pH diagram for the Fe-Cr-H_2O system based on the principle of simultaneous equilibrium was developed using Factsage 6.4 (thermochemical software) (Bale *et al.*, 2002). A reconstruction of the diagram using HSC Chemistry 7 (thermochemical software) is shown in Figure 2-34. Cr is soluble as either Cr^{3+} or $Cr_2O_7^{2-}$ in the areas labelled A, B, C, D and E. It is important from a health and environmental perspective to recognise that in the area labelled A and D, Cr soluble as $Cr_2O_7^{2-}$ occurs in the 6+ oxidation state. Cr(VI) is considered a carcinogen, especially through inhalation. The possible negative effects associated with Cr(VI) exposure by way of ingestion are still being debated within the scientific community. Dermal contact is another exposure pathway. Exposure to high concentration levels through dermal contact can lead to so-called Cr ulcers (IETEG, 2005). Although Cr is soluble as Cr^{3+} in the area labelled C, the valence of Fe is the same as it's valency in the chromite spinel. Consequently the structure of the spinel is difficult to disrupt, since no oxidation reaction can occur. Thus, only in the regions labelled B and E is Cr in the chromite spinel dissolved to Cr^{3+} by the oxidation of Fe(II) to Fe(III). It is evident from Figure 2-34 that a low pH value with the appropriate oxidation potential are necessary for the decomposition of chromite spinel and, specially, the oxidation potential plays a key role in limiting Cr(VI) formation.

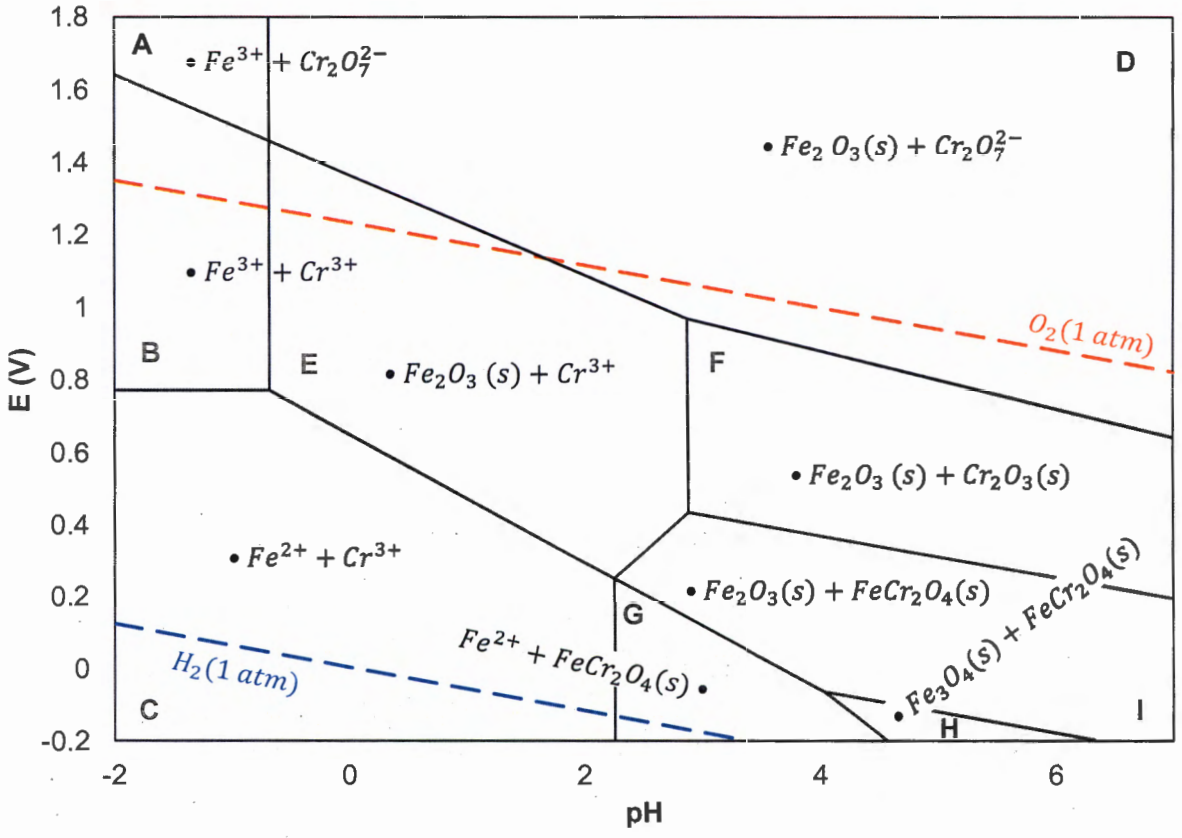

Figure 2-34: E-pH diagram of the Cr-Fe-H_2O system (Zhang *et al.*, 2016)

Biermann and Heinrichs (1960) studied the attack of a low grade chromite concentrate by sulphuric acid of various concentrations with the aim of formulating a more adequate description, or mechanism, of the process. They identified that the first step involves the attack of protons on the chromite lattice, transporting the metallic constituents into solution in a similar ratio as that in the lattice. The second step is the precipitation of polynuclear products that can slow down the attack on the chromite. Therefore, the dissolution of Cr (in its oxidation state as it occurs in the chromite spinel) by sulphuric acid leaching is limited without an oxidant (Zhang *et al.*, 2016).

Geveci *et al.* (2002) used perchloric acid as a catalyst in order to improve the leaching behaviour of chromite in a sulphuric acid solution at atmospheric pressure and achieved Cr extraction of 83%. Vardar *et al.* (1994) studied the effect of temperature, sulphuric acid concentration and perchloric acid addition on the rate of dissolution of Cr from chromite and determined that the activation energy for the leaching of chromite in 82 wt.% sulphuric acid at atmospheric pressure in the temperature range 140–210 °C is 77 kJ·mol^{-1}. Sodium bichromate was utilised as an oxidant by Shi and Liu (2002) in a leaching process at 110–170 °C and atmospheric pressure, attaining Cr dissolution of 82%. None of the abovementioned investigations reported that Cr(VI) formed during sulphuric acid leaching.

Zhao et al. (2014; 2015) and Jiang *et al.* (2014) investigated the sulphuric acid leaching behaviour of South African chromite in the presence of an oxidant and illustrated a sulphuric acid leaching mechanism shown in Figure 2-35. Four types of spinel, labelled I, II, III, and IV in Figure 2-35, representing different states at specific stages of the leaching process were identified. Spinel I demonstrates the shrinking in particle size as leaching of the chromite progresses over time. Three decomposition or corrosion depths, labelled $D_{b(p)}$, $D_{b(g)}$, and D_g, show that the phase boundary ($D_{b(p)}$) is the most inclined to corrosion followed by the grain boundary ($D_{b(g)}$), while the grain surface (D_g) is comparatively stable. Smaller spinel particles break free or react to completion, resulting in the formation of cavities or holes in the silicon-rich phase (Spinel II, Figure 2-35). The precipitation of sulphate may occur inside the formed cavities if the temperature is too high. Some of the inner spinel phase exposed with the formation of the primary cavities (Spinel II, Figure 2-35) may react when the solution flushes the solid layer and is in direct contact with the spinel (Spinel III, Figure 2-35) resulting in the formation of secondary cavities; however, other deeper spinel phases cannot be leached over short times (Spinel IV, Figure 2-35), as the silicon-rich phase acts as a barrier. The model developed by Zhao *et al.* (2014; 2015) and Jiang *et al.* (2014) is based on experimental results obtained by leaching chromite ore with a size distribution of 80 wt.% in the range of 20-100 µm and, therefore, Zhang *et al.* (2016) suggested that the effect of particle size should be explored further.

Sahoo (1988) conducted some preliminary tests on sulphuric acid leaching of chromite ore with the aim of increasing the Cr/Fe ratio, but the leaching time was not sufficient to remove a sufficient amount of Fe. Sharma (1990) conducted physical beneficiation tests followed by sulphuric acid leaching in the temperature range of 30–60 °C on two different ores from Boula Mines of Orissa (India). The Cr/Fe ratio was improved and, in some cases, the levels reached were ~2.8, however it is unclear form the publication if the increase in the Cr/Fe ratio is as a result of the physical beneficiation, sulphuric acid leaching or the combination of both methods.

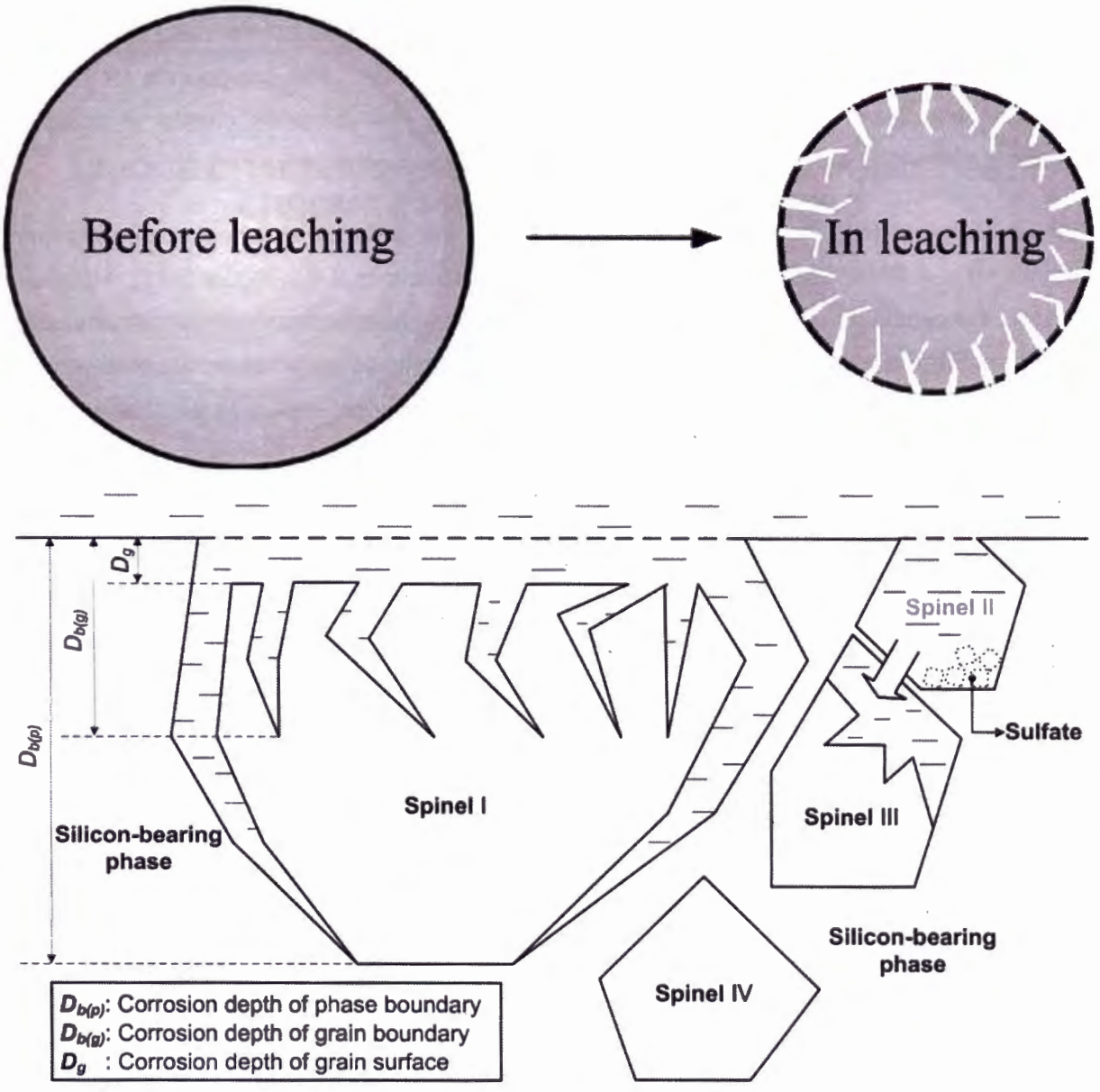

Figure 2-35: Modified shrinking particle model with crack development and leaching mechanism of chromite with sulphuric acid (Zhang *et al.*, 2016)

2.7 Concluding summary

The important of South Africa's FeCr industry, both national and globally, was highlighted in Section 2.2. The main FeCr production processes were presented (Section 2.3.2), while chromite pre-reduction was discussed in more detail (Section 2.4). It was evident from the literature that the chromite pre-reduction process has a significant energy saving advantage. The effect of numerous additives, e.g. Al_2O_3, B_2O_3, CaB_4O_7, $CaCl_2$, $CaCO_3$, CaF_2, CaO, Cr, Fe, KCl, K_2O, K_2O_3, MgO, $Na_2B_4O_7$, NaCl, Na_2CO_3, NaF, NaF-CaF_2, Na_2O_2, SiO_2, on the pre-reduction of chromite has been investigated in various studies which found that the use of these additives either

promoted or decreased the rate of pre-reduction (Section 2.4.4.2). However, the effect of secondary raw materials, i.e. clay binders and carbonaceous reductants, used in the pelletised pre-reduction process, has not been investigated previously. The compounds (or ions of the elements in these compounds) that these secondary raw materials consist of could either enhance or inhibit pre-reduction by effecting the reaction mechanism.

From literature (Section 2.5), it was also clear that the oxidation/sintering of chromite prior to smelting in a SAF holds significant SEC advantages (Sections 2.4.2, Figure 2-21). However, as far as the candidate could assess, pre-oxidation prior to pre-reduction has not been investigated before. For this reason, pre-oxidation of chromite will be investigated as an alternative option to improve the extent of pre-reduction in the pelletised chromite pre-reduction process.

Finally, it was substantiated by the literature that the majority of the chromite ore resources are low grade (Section 2.2.1). It would thus be beneficial to upgrade the lower grade ores. From literature it was revealed that conventional physical methods of beneficiation, such as gravity concentration, magnetic separation and flotation are unlikely to increase the Cr/Fe ratio of chromite ore. Methods based on sulphuric acid leaching of chromite featured prominently in the literature (Section 2.6.4). However, these methods were for the most part ineffective, since the chromite spinel has a stable and compact spinel lattice structure at room temperature and atmospheric pressure that is hardly soluble in a sulphuric acid solution. Methods resulting in the structural dissociation of the chromite spinel are therefore required. It is evident for the literature presented that both pre-reduction (Section 2.4) and oxidation (Section 2.5) alter the chromite spinel structure. Therefore, it would be sensible to investigate a method combining chromite pre-reduction, oxidation and sulphuric acid leaching.

UNIQUE CHALLENGES OF CLAY BINDERS IN A PELLETISED CHROMITE PRE-REDUCTION PROCESS

3.1 Authors list, contributions and consent

Authors list

E.L.J. Kleynhans[a], J.P. Beukes[a], P.G. Van Zyl[a], P.H.I. Kestens[b] and J.M. Langa[b]

[a] Chemical Resource Beneficiation, North-West University, Potchefstroom Campus, Private Bag X6001, Potchefstroom 2520, South Africa

[b] Xstrata Alloys Lydenburg Works, 1 Carrington Drive, Ohrigstad Road, Lydenburg 1120, South Africa

Contributions

Contributions of the various co-authors were as follows:

The bulk of the work, i.e. experimental, data processing and interpretation, research and writing of the scientific paper, was performed by the candidate, ELJ Kleynhans. Prof JP Beukes (supervisor) and Dr PG van Zyl (co-supervisor) assisted in writing the article by sharing conceptual ideas and recommendations with regard to the experimental work, interpretation and results and discussion. PHI Kestens and JM Langa assisted with the pre-reduction analysis. The article resulted from preliminary work conducted during the candidates (ELJ Kleynhans) Master of Science (MSc) in Chemistry degree at the North-West University, Potchefstroom Campus, which was further explored as part of this submitted PhD.

Consent

All the co-authors that contributed to the article presented in this chapter have been informed that the article will form part of the candidates PhD, submitted in article format, and have granted permission that the article may be used for the purpose stated.

3.2 Formatting and current status of the article

The article is presented in Chapter 3 of this thesis as it was published by Minerals Engineering in 2012, Volume 34 (July), pages 55-62 (DOI: http://dx.doi.org/10.1016/j.mineng.2012.03.021, Date of access: 30 November 2016). The journal's details can be found at http://www.journals.elsevier.com/minerals-engineering (Date of access: 30 November 2016).

Minerals Engineering 34 (2012) 55–62

Contents lists available at SciVerse ScienceDirect

Minerals Engineering

journal homepage: www.elsevier.com/locate/mineng

Unique challenges of clay binders in a pelletised chromite pre-reduction process

E.L.J. Kleynhans [a], J.P. Beukes [a,*], P.G. Van Zyl [a], P.H.I. Kestens [b], J.M. Langa [b]

[a] Chemical Resource Beneficiation, North-West University, Potchefstroom Campus, Private Bag X6001, Potchefstroom 2520, South Africa
[b] Xstrata Alloys Lydenburg Works, 1 Carrington Drive, Ohrigstad Road, Lydenburg 1120, South Africa

ARTICLE INFO

Article history:
Received 23 December 2011
Accepted 19 March 2012

Keywords:
Chromite
Pre-reduction
Pelletisation
Clay binder
Bentonite
Attapulgite

ABSTRACT

Ferrochrome producers strive towards lower overall energy consumption due to increases in costs, efficiency and environmental pressures. In South Africa, in particular, higher electricity prices have placed pressure on ferrochrome producers. Pelletised chromite pre-reduction is most likely the ferrochrome production process option with the lowest specific electricity consumption currently applied. In this paper, the unique process considerations of clay binders in this process are highlighted and demonstrated utilising two case study clays. It is demonstrated that the clay binder has to impart high compressive and abrasion resistance strengths to the cured pellets in both oxidising and reducing environments (corresponding to the oxidised outer layer and pre-reduced core of industrially produced pellets), while ensuring adequate hot strength of pellets during the curing process. The possible effects of the clay binder selection and the amount of binder addition on the degree of chromite pre-reduction achieved were also investigated, since it could have substantial efficiency and economic implications. The case study results presented in this paper indicated that it is unlikely that the performance of a specific clay binder in this relatively complex process can be predicted, based only on the chemical, surface-chemical and mineralogical characterisation of the clay.

1. Introduction

Chromite ore mining is the only commercially viable source of new chromium units (Murthy et al., 2011; Beukes et al., 2010; Cramer et al., 2004). South Africa holds approximately 75% of the world's exploitable chromite resources (Basson et al., 2007; Cramer et al., 2004; Riekkola-Vanhanen, 1999), with other smaller but substantial deposits occurring in Kazakhstan, Zimbabwe, India and Finland (Papp, 2009). Approximately 90–95% of mined chromite is consumed by the metallurgical industry for the production of different grades of ferrochrome (FeCr). The stainless steel industry consumes 80–90% of FeCr, primarily as high-carbon or charge grade FeCr (Murthy et al., 2011; ICDA, 2010; Abubakre et al., 2007).

FeCr is produced largely by means of smelting chromite in submerged arc furnaces (SAFs) in the presence of carbonaceous reducing agents. Historically, the use of fine chromite (usually <6 mm) in this process is limited, since fine materials increase the tendency of the surface layer of the SAF to sinter. This traps evolving process gas, which can result in so-called bed turnovers or blowing of the furnace that could have disastrous consequences (Beukes et al., 2010; Riekkola-Vanhanen, 1999). The majority of chromite ore is relatively friable (Beukes et al., 2010; Glastonbury et al., 2010; Cramer et al., 2004; Gu and Wills, 1988); and therefore an agglomeration step is required (e.g. pelletisation), prior to feeding it into the SAF (Beukes et al., 2010; Singh and Rao, 2008).

South Africa is the leading producer of FeCr (ICDA, 2010). There are currently fourteen separate FeCr smelter plants in South Africa, with a combined production capacity of 4.7 million t/y (Beukes et al., accepted for publication; Jones, 2010). The abundant chromite resources and the relatively low historical cost of electricity have contributed to South Africa's dominant position (Basson et al., 2007). However, the electricity demand of South Africa has caught up with its electricity generating capacity. This has led to a dramatic increase in electricity prices that is set to continue in the foreseeable future (Basson et al., 2007). According to statistics from the National Energy Regulator of South Africa (NERSA) the nominal electricity price in South Africa increased steadily at a rate of roughly 0.58 RSA cents/kW h per year, in the period 1980 to 2005 (NERSA, 2009b). However, the nominal price of electricity has increased with 174% from 2007 to 2010 (NERSA, 2009a,b). NERSA has since granted Eskom, South Africa's sole electricity provider, a 3-year rate increase, resulting in electricity costs of 41.57 RSA cents/kW h for 2010/2011, 52.30 RSA cents/kW h for 2011/2012 and 65.85 RSA cents/kW h for 2012/2013 (Eskom, 2011; NERSA, 2009a). Considering that electricity consumption is the single largest cost component in FeCr production (Daavottila et al., 2004), the afore-mentioned cost increases are extremely significant. However, the pressure on South African FeCr producers is not unique, since globally lower specific energy consumption

* Corresponding author. Tel.: +27 82 460 0594; fax: +27 18 299 2350.
E-mail address: paul.beukes@nwu.ac.za (J.P. Beukes).

0892-6875/$ - see front matter © 2012 Elsevier Ltd. All rights reserved.
http://dx.doi.org/10.1016/j.mineng.2012.03.021

(MW h/t FeCr) and a decreased carbon footprint have become driving factors.

Historically, the specific energy consumption of conventional SAFs was 3.9–4.2 MW h/t FeCr (Naiker and Riley, 2006; Weber and Eric, 2006). Several processes have been developed to minimise energy consumption. However, the technology of interest in this study is the pre-reduction of chromite that is applied at two FeCr smelter plants in South Africa (Beukes et al., 2010; McCullough et al., 2010; Naiker, 2007; Naiker and Riley, 2006). In this process fine chromite ore, a clay binder and a carbon reductant are dry milled, pelletised and pre-heated before being fed into a rotary kiln where the chromite is partially pre-reduced. The pre-reduced pellets are then charged hot, immediately after exiting the kiln, into closed SAFs (Beukes et al., 2010; Naiker, 2007). The advantages of pelletised pre-reduction feed are observed in all aspects of operation, i.e. the ability to consume fine chromite; much lower specific energy consumption of approximately 2.4 MW h/t; chromium recoveries in the order of 90%, as well as the ability to produce a low silicon- and sulphur-containing FeCr product (McCullough et al., 2010; Naiker, 2007; Takano et al., 2007; Botha, 2003). It can therefore only be assumed that this process option will become more commonly applied as the pressure on energy consumption and environmental consciousness increases.

In the pelletised chromite pre-reduction process, clay is added to the raw material mixture to act as a binder for green (newly-formed) and cured strengths of the pelletised agglomerates. These functions are not unique, since clay binders also play a similar role in other chromite pelletisation processes. However, due to the unique nature of the pelletised chromite pre-reduction process, there are also aspects other than green and cured strength that should be considered during clay selection. In this paper, these unique process considerations of clay binders in the chromite pre-reduced process are highlighted and demonstrated utilising two clays for this case study.

2. Materials and methods

2.1. Materials

The raw materials utilised in the industrial pelletised chromite pre-reduction process consist of ore, a carbonaceous reducing agent and a clay binder. Raw material used in this study was obtained from a large South African FeCr producer, applying the pelletised chromite pre-reduction process. Samples of metallurgical grade chromite (<1 mm), anthracite breeze and two clays, i.e. attapulgite and bentonite utilised by this FeCr producer, were obtained.

Industrially produced pelletised chromite pre-reduced pellets were also obtained from the same FeCr producer. Industrial Analytical (Pty) Ltd. supplied SARM 8 and SARM 18 that were used as reference materials in the analysis of carbonaceous reductants and chromite containing materials, respectively. All other chemicals used were analytical grade (AR) reagents, obtained from the different suppliers and used without any further purification. Ultra-pure water (resistivity 18.2 MΩ cm^{-1}), produced by a Milli-Q water purification system, was used for all procedures requiring water. Instrument grade synthetic air and nitrogen gas were supplied by Afrox.

2.2. Methods

2.2.1. Chemical and surface analysis

Scanning electron microscopy with energy dispersive X-ray spectroscopy (SEM-EDS) was employed to visually and chemically characterise the surface properties of samples. Two different instruments were utilised, i.e. (i) a FEI QUANTA 200 ESEM, integrated with an OXFORD INCA X-Sight 200 EDS system operating with a 15 kV electron beam at a working distance of 10 mm and (ii) a Zeiss MA 15 SEM incorporating a Bruker AXS XFlash® 5010 Detector X-ray EDS system operating with a 20 kV electron beam at a working distance of 17.4 mm.

Inductively coupled plasma mass spectrometry (ICP-MS) and inductively coupled plasma optical emission spectrometry (ICP-OES) of the bentonite and attapulgite clays were performed. A Perkin Elmer Elan 6100 ICP-MS was utilised to determine minors and trace elements, while a Perkin Elmer Optima 5300 ICP-OES was used to characterise major components. ICP-OES of the metallurgical grade chromite ore, anthracite and the pre-reduced pellets was performed using a SPECTRO CIROS VISION ICP-OES Spectrometer.

Proximate (inherent moisture, ash, volatile matter and fixed carbon) analysis of the anthracite was performed according to the ASTM standard method D3172-07A (ASTM, 2007).

Elemental carbon and sulphur contents of the anthracite samples were determined by means of IR spectrophotometry utilising a LECO CS 244. A 1:1 mixture of tungsten and iron chips was used as the accelerator flux. Elemental carbon and sulphur analyses of the two clays were similarly conducted utilising a LECO CS 230 IR spectrophotometer. Additionally, the water loss and loss on ignition (LOI) of the clays were also determined at 110 and 1000 °C, respectively.

X-ray diffraction (XRD) of the clays was performed according to a back loading preparation method. Semi-quantitative and qualitative XRD analyses of the compounds in the clays were conducted with two different instruments, i.e. (i) a PANalytical X'Pert Pro powder diffractometer with Fe-filtered Co K radiation incorporating an X'Celerator detector and (ii) a Philips X-ray diffractometer (PW 3040/60 X'Pert Pro) with Cu Kα radiation. The measurements were carried out between variable divergence- and fixed receiving slits. The phases were identified using X'Pert Highscore plus software. The relative phase amounts were estimated using the Rietveld method (Autoquan programme).

2.2.2. Sample material preparation

A Wenman Williams & Co. disc mill was utilised to grind the lumpy attapulgite clay and the anthracite to <1 mm. Different mixing ratios of the three components present in the pre-reduced pellets (chromite ore, anthracite and clay) were then made up, according to the objectives of specific experiments. At the time of article preparation 3–4 wt.% clay addition was utilised in the industrial process. It was therefore decided to cover the 2.5–5 wt.% clay addition range. A 10 wt.% clay addition was also included to help identify trends that might be difficult to recognise at low clay additions. The anthracite was kept constant at 20 wt.% (relating to ~15 wt.% fixed carbon) in all experiments. The remainder of the mixtures were made up with the chromite ore.

All raw material mixtures were dry milled to the particle size specifications applied for industrial pre-reduction feed material (90% smaller than 75 μm). A Siebtechnik laboratory disc mill with a tungsten carbide grinding chamber, to avoid possible iron contamination, was used for this purpose. A Malvern Mastersizer 2000 was used to determine the particle size distribution of the pulverised material. A much diluted suspension of milled ore was ultrasonicated for 60 s prior to the particle size measurement, in order to disperse the individual particles without adding a chemical dispersant. It was determined that for a 50 g mixture of raw materials, a milling time of 2 min was required to obtain the desired size specification; therefore, all raw material mixtures were milled similarly.

2.2.3. Pelletising

The milled material was pressed into cylindrical pellets with an LRX Plus strength testing machine (Ametek Lloyd Instruments) equipped with a 5 kN load cell and a Specac PT No. 3000 13 mm die set. Pellets were prepared in batches of 10 each. For each batch 50 g of dry mixed raw material was pre-wetted with 5 g of water and mixed thoroughly. 3.2 g of pre-wetted material was then place in the die set and compressed at a rate of 10 mm/min until a load of 1500 N was reached, where after this load was held for 10 s. Although time consuming (each pellet made individually), this technique was preferred over conventional disc pelletisation, since disc pelletisation on laboratory scale can result in the formation of pellets with different densities, sizes and spherical shapes. The above described procedure ensured consistent density, form and size, which allowed the monovariance investigation of other process parameters.

2.2.4. Pre-reduction and oxidative sintering setup

A ceramic tube furnace (Lenton Elite, UK model TSH15/75/610) with a programmable temperature controller was used to conduct all pre-reduction and oxidative sintering experiments. Ceramic heat shields were inserted at both ends of the tube furnace to improve the tube length in which a stable working temperature could be achieved. These heat shields also protected the stainless steel caps, which were fitted onto both sides of the ceramic tube to seal the ends. The stainless steel caps had a gas inlet on the one side and an outlet on the other side.

The gaseous atmosphere inside the ceramic tube was controlled by either utilising a N_2 flow-rate of 1 NL/min, or a synthetic air-flow rate of 1 NL/min. N_2 was used during pre-reduction experiments, while synthetic air was used during oxidative sintering. An inert (N_2) gaseous atmosphere was preferred for the pre-reduction experiments, since pre-reduction caused by the carbonaceous reductant present in the material mixture was of interest in this study and not pre-reduction due to the presence of an external reducing gas. Before the pre-reduction experiments commenced, the tube furnace already loaded with pellets, was flushed with N_2 for at least 30 min at a flow rate of 1.25 NL/min at room temperature to remove oxidising gases.

Two furnace temperature profiles were used in this experimental study. These profiles were compiled in an attempt to simulate conditions occurring in the industrial pelletised pre-reduction of chromite. Both temperature profiles consisted of three segments, i.e. (i) heating up from room temperature to 900 °C over a period of 30 min, (ii) heating to the final temperature within a 50 min period (and soaking if applicable), and (iii) cooling down while gas flow was maintained. The first segments of both temperature profiles were identical, i.e. heating up to 900 °C in 30 min. In the second segment of the first temperature profile, the temperature was raised from 900 to 1250 °C within a 50 min period and held constant for 20 min, where after cooling down commenced. In the second segment of the second temperature profile, the temperature was raised from 900 to 1300 °C within a 50 min period, where after cooling started without any soaking time.

2.2.5. Compressive strengths testing

The compressive strengths of the pre-reduced or oxidative sintered pellets were tested with an Ametek Lloyd Instruments LRX-plus strength tester. The speed of the compression plates was maintained at 10 mm/min during crushing to apply an increasing force on the pellets. The maximum force applied to incur breakage was recorded for each pellet.

2.2.6. Abrasion resistance testing

The abrasion resistance test apparatus was based on a down-scaled version of the European standard EN 15051 rotating drum. The drum was designed according to specifications provided by Schneider and Jensen (2008). The drum was rotated at 44 rpm, which is faster than the rotating speed used by Schneider and Jensen (2008). This was done to obtain measurable abrasion on the hardest experimentally prepared pellets. A batch (ten pellets) of the pre-reduced or oxidative sintered pellets was abraded for the time periods 1, 2, 4, 8, 16 and 32 min. After every time interval, the material was screened using 9.5 and 1.18 mm screens. The over- and under-sized materials were then weighed and the material returned to the drum for further abrasion, until the final abrasion time was achieved.

2.2.7. Thermo-mechanical analysis (TMA)

Pellets were prepared in the same manner as described in Section 2.2.3, but not pre-reduced or oxidatively sintered as indicated in Section 2.2.4. A single pellet was placed in a Seiko Instruments Inc. TMA/SS 6100 thermo-mechanical analyser, interfaced with SII EXSTAR 6000. With this instrument, the thermal expansion of the pellet could be measured as a function of temperature up to 1300 °C. All TMA experiments were conducted in a N_2 atmosphere (1.67 NL/h), since oxidative corrosion of the internal parts of this specific instrument has been detected when operating under atmospheric gaseous conditions. Since the TMA probe was made of alumina, α-alumina coefficients correction was applied to the data, as specified in the operational manual of the instrument.

2.2.8. Ash fusion temperature analysis

Ash fusion temperature analysis is usually conducted to characterise the melting and sintering behaviours of coal ash (Nel et al., 2011). However, in this investigation it was applied to the two clays utilised as case study materials. The SABS ISO 540:2008 standard method was performed with a Carbolite CAF digital imaging coal ash fusion test furnace. In this test, a moulded cone of each clay was viewed and the following four temperatures recorded: (i) deformation temperature, when the corners of the mould first became rounded; (ii) softening temperature, when the top of the mould took on a spherical shape; (iii) hemisphere temperature, when the entire mould took on a hemisphere shape; and (iv) fluid temperature, when the molten material collapsed to a flattened button on the furnace floor.

2.2.9. Analysis of pre-reduction

The extent of chromite pre-reduction was determined according to the method utilised by laboratories associated with the FeCr smelters in South Africa currently applying the pelletised chromite pre-reduction process. The degree of pellet pre-reduction was determined using the following equation:

$$\%\text{Total Pre-reduction} = \frac{\frac{\%\text{Sol Cr}}{34.67} + \frac{\%\text{Sol Fe}}{55.85}}{0.0121}$$

The % Sol Cr and % Fe were determined by reflux leaching a fixed mass of the sample material with a hot sulphuric/phosphoric acid solution. The % Sol Cr in this aliquot was then established by oxidation of the soluble Cr with potassium permanganate and subsequent volumetric determination with ferrous ammonium sulphate using diphenylamine sulphonate as an indicator. The % Sol Fe in the aliquot (a portion not oxidised with potassium permanganate) was determined by a similar simple volumetric method, using potassium dichromate as the titrant and diphenylamine sulphonate as an indicator.

2.2.10. Statistical handling of data

The results reported were compiled from reiterations for every set of experimental conditions and procedures. Each compressive strength and abrasion resistance strength measurement reported was calculated from 20 and 3 repetitions, respectively. TMA and

pre-reduction analysis results were calculated from six and five reiterations for each set of experimental conditions. The mean and standard deviations were calculated for every dataset, after the elimination of possible outliers that were identified utilising the Q-test with 95% confidence level.

3. Results and discussion

3.1. Raw material characterisation

The chemical characterisation results of the raw materials utilised are indicated in Table 1. From these results, the Cr-to-Fe ratio of the chromite was calculated as 1.57, which is typical of South African deposits (Cramer et al., 2004; Howat, 1986). The anthracite had a fixed carbon content of approximately 75% and a volatile content of 6.87%. The major ash elements in the anthracite were found to be Si, Al, Fe, P, Ca and Mg. As expected, the clays were mainly alumina-silicates. The significance of other elements in the clays will be discussed later. Phosphorous and sulphur contents are usually included in the FeCr specifications (Basson et al., 2007); and therefore, they were also measured, where applicable.

3.2. Characterisation of typical industrial pellets

In order to illustrate the unique process considerations of clay binders in the pelletised chromite pre-reduced process, SEM backscatter micrograph images of an industrially produced pellet are shown in Fig. 1.

Fig. 1A is a partial micrograph of a polished sectional view taken at 45 times magnification of an industrial pre-reduced pellet split in half. It seems that there are two different zones in these pellets, i.e. the core and an outer layer, with a transitional zone in between. These two zones correspond to the different conditions to which the pelletised material is exposed during the industrial pre-reduction process. Initially, the raw material components (chromite, carbon reductant and clay) are homogeneously spread throughout the pellet. However, as the pellet is exposed to the high temperatures inside the rotary kiln, where the pre-reduction process takes place, the carbon in the outer layer is mostly burned off and a partially oxidised outer layer is formed at these high temperatures due to the presence of oxygen. A small amount of iron reduction can occur before all the carbon is consumed in this outer layer, which can be re-oxidised again. Oxygen ingress to the core does not take place, therefore the carbon in the core acts as a reductant resulting in pre-reduction without any oxidation impacting the core. Fig. 1B indicates the transitional area between these two different zones. In the core area (top right of Fig. 1B), small globules of pre-reduced metal can be seen, while the transitional zone (bottom left of Fig. 1B) seems to have a more sintered appearance without any significant metal globules. SEM-EDS analysis of the core and outer layer (not the transitional zone) revealed that the surface chemical carbon content of this specific pellet was approximately 7.1 wt.% in the core and approximately 1 wt.% in the outer layer. The small amount of carbon still present in the outer layer is most likely due to the formation of iron carbides, prior to complete oxidative combustion of free carbon in this layer. The thickness of the outer layer is usually less than 1 mm (approximately 0.5 mm in this

Table 1
Chemical characterisation of the different raw materials utilised with various analytical techniques.

Chromite			
ICP		EDS	
Cr_2O_3	45.37	Cr	27.21
FeO	25.39	Fe	15.33
Al_2O_3	15.21	Al	6.39
MgO	9.83	Mg	6.37
SiO_2	1.72	Si	3.70
CaO	0.22	Ca	0.48
P	<0.01	Ti	0.37
–	–	O	40.16

Anthracite			
ICP		EDS	
SiO_2	10.09	Si	2.53
Al_2O_3	3.13	Al	0.89
FeO	1.62	Fe	1.19
CaO	0.8	Ca	0.18
MgO	0.35	–	–
P	0.011	–	–
S	0.59	S	0.68
–	–	C	76.9
–	–	O	17.63
Proximate analysis			
FC		75.08	
Inherent Moisture		0.26	
Ash		17.79	
Volatiles		6.87	

Attapulgite			
ICP		EDS	
SiO_2	46.91	Si	21.80
Al_2O_3	14.76	Al	8.11
Fe_2O_3	6.72	Fe	5.32
Fe	4.70	–	–
CaO	5.63	Ca	3.14
MgO	5.29	Mg	2.91
TiO_2	0.26	Ti	0.15
–	–	Na	0.12
K_2O	0.21	K	0.09
MnO	0.15	–	–
P	<0.01	–	–
–	–	O	58.36
LECO			
C		1.47	
S		<0.001	
Water loss (110 °C)		8.73	
LOI (1000 °C)		13.04	

Bentonite			
ICP		EDS	
SiO_2	53.53	Si	23.61
Al_2O_3	13.17	Al	7.35
Fe_2O_3	5.33	Fe	5.73
Fe	3.73	–	–
CaO	4.77	Ca	3.37
MgO	2.64	Mg	1.70
TiO_2	0.45	Ti	0.31
–	–	Na	2.15
K_2O	1.14	K	1.10
MnO	0.08	–	–
P	0.02	–	–
–	–	O	54.69
LECO			
C		1.14	
S		<0.001	
Water loss (110 °C)		9.78	
LOI (1000 °C)		7.69	

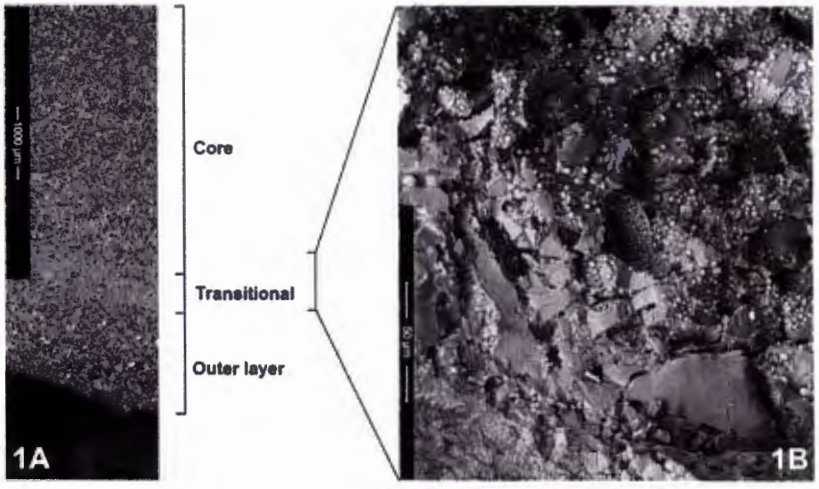

Fig. 1. SEM micrograph (45 times magnification) of a polished section of an industrial pre-reduced pellet split in half (1A), as well as a micrograph of an unpolished section zoomed in on the transitional zone, also showing part of the core area (1B).

case), while the overall diameter of the industrial pellets is usually between 12 and 20 mm.

From the above description, it is evident that the functioning of a clay binder within the pelletised chromite pre-reduced process has to be evaluated within two different environments, i.e. behaviour within an oxidative environment (corresponding to the outer layer of the industrially pre-reduced pellets) and behaviour within a reducing environment (corresponding to the core of the industrially pre-reduced pellets). This is in contrast with other chromite pelletised processes, e.g. the oxidative sintered pelletised process (Beukes et al., 2010) where only one condition prevails. In the paragraphs that follow, clay binder behaviour and characteristics are therefore explored in both environments (reducing and oxidative) in order to completely understand its functioning in the pelletised chromite pre-reduced process. In experiments where the oxidative sintering characteristics were investigated, the carbonaceous reducing agent, i.e. anthracite, was omitted from the raw material mixture to ensure that reducing behaviour did not influence the results.

3.3. Compressive strength

The compressive strength results for the pellets pre-reduced up to 1250 °C for 20 min (containing anthracite and pre-reduced under N_2), as well as oxidative sintered pellets cured at 1250 °C for 20 min (containing no anthracite and sintered in synthetic air) are shown Fig. 2. Fig. 3 shows similar results obtained with the second temperature profile utilised, i.e. maximum temperature of 1300 °C, with no soaking time.

From both these sets of results, several important deductions can be made. The compressive strengths of the oxidative sintered pellets were approximately an order of magnitude higher than that of the pre-reduced pellets. Therefore, although the objective of the industrially-applied pelletised chromite pre-reduced process is to achieve maximum pre-reduction, the compressive strength of pre-reduced chromite pellets is enhanced significantly by the thin oxidised outer layer (Section 3.2).

By comparison of the compressive strengths of the two case study clays, it is clear that the bentonite clay was superior in both pre-reducing and oxidative sintering environments. This is significant, since at the inception of this study, the attapulgite clay was the preferred option at both South African FeCr smelting plants applying the pelletised chromite pre-reduction process.

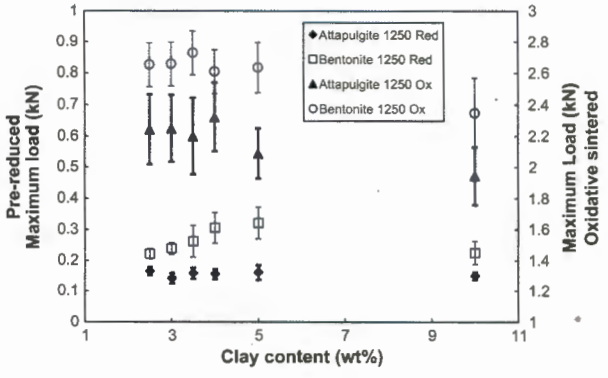

Fig. 2. Compressive strength (kN) of pre-reduced (primary axis) and oxidative sintered (secondary axis) pellets for the temperature profile up to 1250 °C and hold time of 20 min.

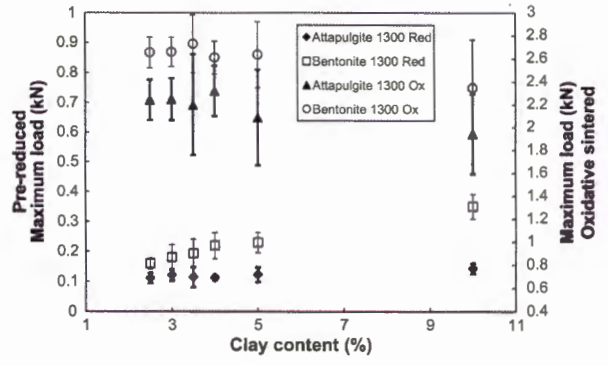

Fig. 3. Compressive strength (kN) of pre-reduced (primary axis) and oxidative sintered (secondary axis) pellets for the temperature profile up to 1300 °C with no hold time.

The compressive strength of the bentonite containing pre-reduced pellets generally improved with increased clay content between 2 and 5 wt.% additions, which is the industrially relevant addition range. Increased attapulgite content, however, did not result in any significant increase in compressive strength of the pre-reduced pellets. Increasing the attapulgite clay content of the

industrial pre-reduced pellets might therefore not result in a stronger pellet core (Section 3.2), although it might aid the green strength, which was not considered in this study.

For both clays used in this case study, larger clay additions resulted in a slight decreasing trend in compressive strengths of the oxidative sintered pellets. This indicates that clay content addition is not such an important parameter in attaining a strong oxidised outer layer (Section 3.2) on the industrially produced pellets.

3.4. Abrasion resistance

The abrasion resistance strength results for both pre-reduced and oxidative sintered pellets cured up to 1300 °C without holding time, for 3.5% and 10% clay contents, are shown in Fig. 4. The results are presented as the percentage weight retained in the size fraction >9.5 mm. Similar to the compressive strength results, the abrasion resistance strength of the oxidative sintered pellets was substantially better than that of the pre-reduced pellets for both clays. This again confirmed the importance of the oxidised outer layer (Section 3.2) in imparting strength to the industrially produced pellets. Furthermore, the bentonite outperformed the attapulgite in pre-reduced, as well as oxidative sintered abrasion resistance strength.

3.5. XRD and ash fusion temperature analysis

In order to explain the better performance of the bentonite compared to the attapulgite in compressive strength and abrasive resistance strength tests, SEM, SEM-EDS, XRD and ash fusion analyses were preformed. Visual inspection with SEM (e.g. observing bridge formations, pore sizes, densities, etc.) and chemical surface analysis with SEM-EDS did not provide any conclusive results and are therefore not discussed further.

Quantitative XRD analysis results of the two clays are presented in Table 2. Amorphous phases, if present, were not taken into account. In addition, mineral names may not reflect the actual compositions of minerals identified, but rather the mineral group. As expected, the smectite clay group minerals were the largest component in both clays. However, the attapulgite clay had considerably higher smectite group content than the bentonite. Considering only these results, the attapulgite clay may be mistakenly regarded as the better binder, due to the higher smectite mineral group content. Limitations of the Rietveld method prevent further breakdown of the smectite group, therefore qualitative XRD analyses were also conducted. Qualitative results indicated that the attapulgite contained palygroskite, which confirms its status as an attapulgite clay. In contrast the bentonite contained montmorillonite, but not palygroskite. It is therefore assumed that the aforementioned quantitative smectite mineral contents of the two clays can be ascribed to mainly palygroskite in the attapulgite and montmorillonite in the bentonite. However, trying to explain why the bentonite seems to be a better binder in the pellets, based only the above-mentioned mineralogical information would be presumptuous. Therefore, ash fusion tests were also conducted to derive parameters that maybe could clarify the previous observations (Sections 3.3 and 3.4). The four ash fusion temperatures recorded for each clay, both in oxidative and reducing conditions, are listed in Table 3.

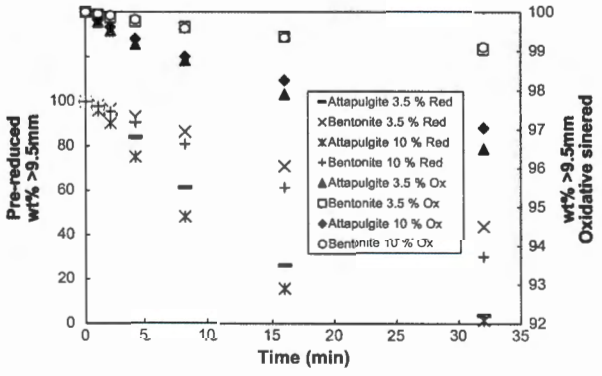

Fig. 4. Abrasion resistance strength indicated in weight percentage remaining above 9.5 mm versus abrasion time (note error bars were removed, since they were smaller than the markers).

Table 2
Quantitative XRD analysis of the attapulgite and bentonite clays utilised.

Attapulgite		Bentonite	
Augite	1.97	Augite	0.64
Calcite	6.66	Calcite	6.34
Kaolinite	2.45	Kaolinite	0.97
Muscovite	2.23	Muscovite	4.93
Orthoclase	1.78	Orthoclase	4.25
Plagioclase	3.86	Plagioclase	5.98
Quartz	4.22	Quartz	14.39
Smectite	76.8	Smectite	62.51

The ash fusion temperatures indicated that the bentonite had lower deformation, softening, hemispherical and fluid temperatures in both oxidising and reducing environments, except for the initial deformation temperature in an oxidising environment. This can possibly give some practical explanation as to why the bentonite performed better in the compressive and abrasion resistance strength tests, for both pre-reduced and oxidative sintered pellets. A lower melting point (construed as incorporating all four measured ash fusion temperatures) implies that bentonite could possibly start forming bridges between the particles at lower temperatures than attapulgite. It is also notable that the fluid temperatures of the attapulgite in both environments were above 1300 °C, implying that that the possibility exists that it was not completely liquefied under the experimental conditions.

3.6. TMA analysis

Cold compressive and abrasion resistance strength tests give an indication of the cured strength of the pelletised materials after being treated in the different environments. However, the question could also be asked what the hot pellet strengths are, since that would influence pellet breakdown in the rotary kiln used in the industrial application. This has relevance to the formation or build-up of dam rings (material sticking to the inside of the rotary kiln). Unfortunately, no instruments that could directly measure high temperature compressive strength or abrasion resistance were available to the authors. A TMA instrument, which measures the thermal expansion of material as a function of temperature, was, however, available. TMA results for the pre-reduced pellets

Table 3
Ash fusion temperatures for the attapulgite and bentonite clays utilised.

Atmosphere	Ash fusion temperature	Attapulgite	Bentonite
Reducing (N_2)	Initial deformation temperature	1216	1170
	Softening temperature	1242	1191
	Hemispherical temperature	1294	1251
	Fluid temperature	1337	1301
Oxidising (O_2)	Initial deformation temperature	1219	1224
	Softening temperature	1256	1255
	Hemispherical temperature	1336	1274
	Fluid temperature	1364	1304

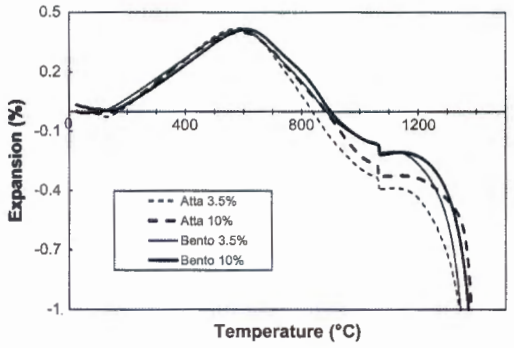

Fig. 5. Average percentage dimensional changes of *in situ* pre-reduction of pellets as a function of temperature for both clays investigated.

are shown in Fig. 5. Oxidative sintering could not be investigated due to instrumental limitation, as explained earlier (Section 2.2.7).

The TMA results of the pellets pre-reduced *in situ* containing either bentonite or attapulgite with the different clay wt.%, all indicate the same initial trends – small shrinkage up to about 120 °C that could probably be ascribed to moisture loss, followed by thermal expansion up to approximately 600 °C. After 700 °C, more significant shrinkage occurred for the attapulgite containing pellets. In the range 900–1200 °C, the attapulgite containing pellets had shrunk significantly more than the bentonite containing pellets did. This additional shrinkage of the attapulgite can possibly be related to the LOI of the attapulgite (13.04%) measured at 1000 °C (Table 1), which was significantly higher than the LOI of bentonite (7.69%). Although thermal expansion and shrinkage cannot be directly related to hot pellet strength, larger variation in thermal dimensional behaviour could possibly indicate weaker hot pellet strength. Therefore, although not quantitatively investigated, there is some indication that the hot strength of the attapulgite pellets could be weaker than the bentonite containing pellets.

3.7. Pellet pre-reduction

The amounts of pre-reduction achieved for the two temperature profiles used, as well as for clay contents from 2.5 to 10 wt.%, are shown in Fig. 6. There are a number of interesting features observed in this data. Firstly, the pre-reduction levels achieved with the 1250 °C temperature profile with holding times of 20 min were significantly higher than that achieved with the 1300 °C temperature profile without any holding time. According to the Ellingham diagram calculations of Niemelä et al. (2004), iron carbon reduction can occur above 710 °C, while chromium reduction is achieved

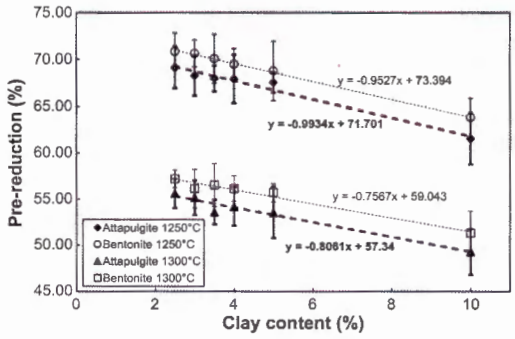

Fig. 6. Percentage pre-reduction achieved as function of clay content, for both case study clays and both temperature profiles utilised.

above 1200 °C. Therefore, the maximum temperature of the 1250 °C temperature profile was above temperatures required for both Fe and Cr reduction to occur and the higher levels of pre-reduction could be ascribed to the 20 min holding time.

From the data in Fig. 6, it is also evident that higher clay contents resulted in lower pre-reduction levels, for both clays and temperature profiles. This is significant within the industrial process, since higher clay contents are on occasion utilised to achieve improved green strength of the uncured pellets. In order to further quantify this observation, trend lines for the amount of pre-reduction with associated equations are given in Fig. 6. In the industrial application of pelletised chromite pre-reduction, clay contents between 3 and 4 wt.% are utilised. Substituting these values into the equations indicates that 0.76–0.99% lower pre-reduction levels can be expected if 4 wt.% instead of 3 wt.% clay addition is made. Not many references exist in the public domain that can be used to translate these lower pre-reduction values into energy and financial losses. Niayesh and Fletcher (1986) published a graph of chromite pre-reduction as a function of specific energy consumption (kW h/t FeCr produced), for different temperatures of pre-reduced feed material. The graph of Niayesh and Fletcher (1986), with the assumption that the material was fed into the furnace at room temperature, was reconstructed and an empirical fit of the data made. Using this fit and assuming 45% pre-reduction as the base case for an industrial plant, it was calculated that 16.7 kW h/t (for the 0.76% lower pre-reduction) to 21.7 kW h/t (for the 0.99% lower pre-reduction) more electricity would be used if 4 wt.% clay is added, instead of the 3 wt.%. This means that for a FeCr smelting plant producing 300 000 t/y, these values relate to 5006 to 6516 MW h/y more electricity, or ZAR2.62 to ZAR3.41 million calculated with the 52.30 RSA cent/kW h price of 2011/2012 (Eskom, 2011; NERSA, 2009c).

The third significant observation from the data in Fig. 6 is that there seems to be a difference between the performances of the two clays used in this case study with regard to pre-reduction levels achieved. Although some overlaps are observed between error bars, it is clear that the average pre-reduction of the bentonite containing pellets was consistently higher than that of the attapulgite containing pellets. Utilising intercept values on the *y*-axis of the trend lines, it was calculated that the bentonite containing pellets had an average of 1.7% higher chromite pre-reduction levels for both temperature profiles. This is significant, since this specific attapulgite clay was at the time of the inception of this study the preferred option at the South African FeCr smelters applying the pre-reduction process – this is primarily attributed to raw material cost considerations. By applying the fitted reconstructed plot of Niayesh and Fletcher (1986) as an indication, the difference in pre-reduction could also be converted to possible electricity and financial losses. For a 300,000 t/y smelter, operating at a specific energy consumption of 2.4 MW h/t, this relates to 9163–10 275 MW h/y more, or ZAR4.79 to ZAR5.37 million calculated with the 52.30 SA cent/kW h price of 2011/2012 (Eskom, 2011; NERSA, 2009c).

The reason for the better performance of the bentonite containing pellets with regard to pre-reduction could be attributed to two possible reasons, i.e. (i) the bentonite had a lower melting point (Section 3.5) than the attapulgite used in this case study, which may imply that the bentonite had already melted during the pre-reduction process, hence serves as a flux that promotes metal reduction, or (ii) the minerals present in the two clays can possibly contain materials that could either catalyse or inhibit the pre-reduction of chromite. Several studies have been published indicating that various substances could have catalytic or inhibiting effects on chromite pre-reduction (e.g. Takano et al., 2007; Weber and Eric, 2006, 1993; Ding and Warner, 1997a,b; Lekatou and Walker, 1997; Nunnington and Barcza, 1989; Van Deventer,

1988; Dawson and Edwards, 1986; Katayama et al., 1986). However, it is beyond the scope of this paper to deal specifically with possible differences in clay fluxing or catalytic and inhibiting clay effects.

4. Conclusions

The case study results presented in the paper proved that the clay binders utilised in the industrially applied pelletised chromite pre-reduction process have some unique process performance requirements that must be fulfilled. The clay binder has to impart high compressive and abrasion resistance strengths to the cured pellets in both oxidising and reducing environments (corresponding to the outer layer and the core of industrially produced pellets – Section 3.2). Without these characteristics, the pelletised material would break down, causing sintering on the surface of the SAF burden material and possible furnace eruptions. The hot pellet strength is equally important, since the breakdown of pellets that are pre-reduced in the rotary kiln results in the build-up of dam rings (material sticking to inside of kiln). While complying with the above-mentioned physical requirements, the clay binder must simultaneously not influence the pre-reduction of chromite negatively, since it could have significant consequences on electricity consumption during the smelting step. Testing of these unique process requirements on two study clays available to South African FeCr smelters applying the pre-reduction process, indicated that the previously preferred attapulgite clay is technically inferior in all aspects measured compared to the bentonite clay that is available as an alternative. Costs of these different clays were not considered in this study, which will obviously also influence the actual selection of clay used in the industry. It was also shown that higher clay content, e.g. to increase pellet green strength, will result in lower chromite pre-reduction. The case study results indicated that it is unlikely that the performance of a specific clay binder in this relatively complex process can be predicted based merely on the chemical, surface chemical and mineralogical characterisation of the clay. Experimental monovariance evaluation of clay performance on the characteristics identified in this study needs to be evaluated in order to distinguish which clay will be best suited for this unique process application.

Acknowledgements

The authors wish to thank Xstrata Alloys SA for financial support. Furthermore, Prof Quentin Campbell and Prof Marthie Coetzee are acknowledged for the use of the particle size analyser and the pulveriser, respectively.

References

Abubakre, O.K., Murian, R.A., Nwokike, P.N., 2007. Characterization and beneficiation of Anka chromite ore using magnetic separation process. Journal of Minerals & Materials Characterization & Engineering 6 (2), 143–150.

ASTM, 2007. D3172-07A Standard Practice for Proximate Analysis of Coal and Coke. In American Society for Testing and Materials (ASTM). Book of Standards v 05.06-Gaseous Fuels; Coal and Coke, West Conshohocken, USA.

Basson, J., Curr, T.R., Gericke, W.A., 2007. South Africa's ferro alloy industry-present status and future outlook. In Proc. of the 11th International Ferro Alloys Conference. New Delhi, India, pp. 3–24.

Beukes, J.P., Dawson, N.F., Van Zyl, P.G., 2010. Theoretical and practical aspects of Cr(VI) in the South African ferrochrome industry. The Journal of the Southern African Institute of Mining and Metallurgy 110 (12), 743–750.

Beukes, J.P., Van Zyl, P.G., Ras, M., accepted for publication. Treatment of Cr(VI) containing wastes in the South African ferrochrome industry – a review of currently applied methods. The Journal of The Southern African Institute of Mining and Metallurgy.

Botha, W., 2003. Ferrochrome production through the SRC process at Xstrata, Lydenburg Works. Journal of the South African Institute of Mining and Metallurgy 103 (6), 373–389.

Cramer, L.A., Basson, J., Nelson, L.R., 2004. The impact of platinum production from UG2 ore on ferrochrome production in South Africa. The Journal of the South African Institute of Mining and Metallurgy 104 (9), 517–527.

Daavottila, J., Honkaniemi, M., Jonkinen, P., 2004. The transformation of ferrochromium smelting technologies during the last decades. The Journal of the South African Institute of Mining and Metallurgy, October, pp. 541–549.

Dawson, N.F., Edwards, R.I., 1986. Factors Affecting the Reduction Rate of Chromite. In Proc of the 4th International Ferro-alloys Congress, Sao Paulo, Brazil, pp. 105–113.

Ding, Y.L., Warner, N.A., 1997a. Catalytic reduction of carbon-chromite composite pellets by lime. Thermochimica Acta 292, 85–94.

Ding, L., Warner, N.A., 1997b. Reduction of carbon-chromite composite pellets with silica flux. Ironmaking and Steelmaking 24 (4), 283–287.

ESKOM. 2011. Eskom retail tariff adjustment for 2011/2012. <http://www.eskom.co.za/content/priceincrease2011.pdf> (accessed 13.10.11.).

Glastonbury, R.A., Van der Merwe, W., Beukes, J.P., Van Zyl, P.G., Lachmann, G., Steenkamp, C.J.H., Dawson, N.F., Stewart, H.M., 2010. Cr(VI) generation during sample preparation of solid samples – a chromite ore case study. Water SA 36 (1), 105–109.

Gu, F., Wills, B.A., 1988. Chromite – Mineralogy and Processing. Minerals Engineering 1 (3), 235–240.

Howat, D.D., 1986. Chromium in South Africa. Journal of the South African Institute of Mining and Metallurgy 86 (2), 37–50.

ICDA (International Chomium Development Association), 2010. Statistical Bulletin 2010 edition. France, Paris.

JONES, R., 2010. Pyrometallurgy in South Africa. <http://www.pyrometallurgy.co.za/PyroSA/index.htm> (accessed 3.03.11.).

Katayama, H.G., Tokuda, M., Ohtani, M., 1986. Promotion of the Carbothermic Reduction of Chromium Ore by the Addition of Borates. The Iron and Steel Institute of Japan 72 (10), 1513–1520.

Lekatou, A., Walker, R.D., 1997. Effect of SiO_2 addition on solid state reduction of chromite concentrates. Ironmaking and Steelmaking 24 (2), 133–143.

McCullough, S., Hockaday, S., Johnson, C., Barza, N.A., 2010. Pre-reduction and smelting characteristics of Kazakhstan ore samples. In: Proc of the 12th International Ferroalloys Congress. Helsinki: Outotec Oyj. pp. 249–262.

Murthy, Y.R., tripathy, S.K., Kumar, C.R., 2011. Chrome ore beneficiation challenges & opportunities – a review. Minerals Engineering 24 (5), 375–380.

Naiker, O., 2007. The development and advantages of Xstrata's Premus Process. In: Proc. of the 11th International Ferroalloys Congress. New Delhi, India. pp. 112–119.

Naiker, O., Riley, T., 2006. Xstrata alloys in profile. In Southern African Pyrometallurgy 2006 Conference. Johannesburg, South Africa: South African Institute of Mining and Metallurgy. pp. 297–306.

Nel, M.V., Sstrydom, C.A., Schobert, H.H., Beukes, J.P., Bunt, J.R., 2011. Comparison of sintering and compressive strength tendencies of a model coal mineral mixture heat-treated in inert and oxidizing atmospheres. Fuel Processing Technology 92 (5), 1042–1051.

NERSA. 2009a. Eskom price increase application 2009. <http://www.nersa.org.za/Admin/Document/Editor/file/Electricity/PricingandTariffs/Eskom%20Current%20Price%202009-10.pdf> (accessed 8.09.11.).

NERSA. 2009b. Historic Eskom Average Selling Price. <http://www.nersa.org.za/Admin/Document/Editor/file/Electricity/PricingandTariffs/Eskom%20Historic%20Prices.pdf> (accessed 8.09.11.).

NERSA. 2009c. Inductive Future Eskom Price Direction. <http://www.nersa.org.za/Admin/Document/Editor/file/Electricity/PricingandTariffs/Eskom%20Future%20Pricepath.pdf> (access 8.09.11.).

Nayeeb, M.J., Fletcher, G.W., 1986. An assessment of Smelting Reduction Processes in the Production of Fe–Cr–C Alloys. In: Proc. of the 4th International Ferro-alloys Congress. Sao Paulo, Brazil. pp. 115–123.

Niemelä, P., Krogerus, H., Oikarinen, P., 2004. Formation, characterization and utilization of CO-gas formed in ferrochrome smelting. In: Proc. of the 12th International Ferroalloys Congress. Cape Town, South, Africa. pp. 68–77.

Nunnington, R.C., Barcza, N.A., 1989. Pre-reduction of fluxed chromite-ore pellets under oxidizing conditions. In: Proc. of the 5th International Ferroalloys Congress. New Orleans, USA. pp. 55–68.

Papp, J.F., 2009. 2009 Minerals Yearbook Chromium [Advance Release]. <http://minerals.usgs.gov/minerals/pubs/commodity/chromium/myb1-2009-chrom.pdf> (accessed 19.10.11.).

Riekkola-Vanhanen, M., 1999. Finnish expert report on best available techniques in ferrochromium production. Helsinki.

Schneider, T., Jensen, K.A., 2008. Combined single-drop and rotating drum dustiness test of fine to nanosize powders. Annals of Occupational Hygiene 52 (1), 23–34.

Singh, V., Rao, S.M., 2008. Study the effect of chromite ore properties on pelletisation process. International Journal of Mineral Processing 88, 13–17.

Takano, C., Zambrano, A.P., Nogueira, A.E.A., Mourao, M.B., Iguchi, Y., 2007. Chromites reduction reaction mechanisms in carbon–chromites composite agglomerates at 1 773 K. Iron and Steel Institute of Japan International 47 (11), 1585–1589.

Van Deventer, J.S.J., 1988. The effect of additives on the reduction of chromite by graphite. Thermochimica Acta 127, 25–35.

Weber, P., Eric, R.H., 1993. The reduction mechanism of chromite in the presence of a silica flux. Metallurgical Transactions B 24B, 987–995.

Weber, P., Eric, R.H., 2006. The reduction of chromite in the presence of silica flux. Minerals Engineering 19, 318–324.

CHAPTER 4: ARTICLE 2

THE EFFECT OF CARBONACEOUS REDUCTANT SELECTION ON CHROMITE PRE-REDUCTION

4.1 Authors list, contributions and consent

Authors list

E.L.J. Kleynhans[a], J.P. Beukes[a], P.G. Van Zyl[a], J.R. Bunt[a], N.S.B. Nkosi[b] and M. Venter[a]

[a] Chemical Resource Beneficiation, North-West University, Potchefstroom Campus, Private Bag X6001, Potchefstroom 2520, South Africa

[b] Pyrometallurgy Division, Mintek, 200 Malibongwe Drive, Private Bag X3015, Randburg, 2125, South Africa.

Contributions

Contributions of the various co-authors were as follows:

The bulk of the work, i.e. experimental, data processing and interpretation, research and writing of the scientific paper, was performed by the candidate, ELJ Kleynhans. Prof JP Beukes (supervisor) and Dr PG van Zyl (co-supervisor) assisted in writing the article by sharing conceptual ideas and recommendations with regard to the experimental work, interpretation and results and discussion. NSB Nkosi determined the reductant CO_2 reactivity, while M Venter assisted in the pre-reduction experiments. JR Bunt provided comments on the drafted article prior to submission to the selected journal.

Consent

All the co-authors that contributed to the article presented in this chapter have been informed that the article will form part of the candidates PhD, submitted in article format, and have granted permission that the article may be used for the purpose stated.

4.2 Formatting and current status of the article

This article was accepted for publication in Metallurgical and Materials Transactions B on the 21st of October 2016. It is presented in Chapter 4 of this thesis as it was accepted by the selected

journal after addressing and implementing the reviewer's comments. The journals details can be found at http://www.springer.com/materials/special+types/journal/11663 (Date of access: 30 November 2016).

The Effect of Carbonaceous Reductant Selection on Chromite Pre-reduction

E.L.J. KLEYNHANS, J.P. BEUKES, P.G. VAN ZYL, J.R. BUNT, N.S.B. NKOSI, and M. VENTER

Ferrochrome (FeCr) production is an energy-intensive process. Currently, the pelletized chromite pre-reduction process, also referred to as solid-state reduction of chromite, is most likely the FeCr production process with the lowest specific electricity consumption, *i.e.*, MWh/t FeCr produced. In this study, the effects of carbonaceous reductant selection on chromite pre-reduction and cured pellet strength were investigated. Multiple linear regression analysis was employed to evaluate the effect of reductant characteristics on the aforementioned two parameters. This yielded mathematical solutions that can be used by FeCr producers to select reductants more optimally in future. Additionally, the results indicated that hydrogen (H)-(24 pct) and volatile content (45.8 pct) were the most significant contributors for predicting variance in pre-reduction and compressive strength, respectively. The role of H within this context is postulated to be linked to the ability of a reductant to release H that can induce reduction. Therefore, contrary to the current operational selection criteria, the authors believe that thermally untreated reductants (*e.g.*, anthracite, as opposed to coke or char), with volatile contents close to the currently applied specification (to ensure pellet strength), would be optimal, since it would maximize H content that would enhance pre-reduction.

DOI: 10.1007/s11663-016-0878-4

I. INTRODUCTION

THE importance of stainless steels to society is obvious, considering the multitude of unique applications thereof and the significant growth in its demand.[1–3] Ferrochrome (FeCr), a crude chromium (Cr)-iron(Fe) alloy, is the only source of new Cr units during stainless steel production.[4,5] According to 2012 data from the International Chromium Development Association (ICDA), 94.53 pct of chromite (the only economically viable Cr-containing ore) was consumed by the metallurgical industry for the production of various FeCr grades, including the most common, *i.e.*, high-carbon (HC) and charge grade (ChG) FeCr. The stainless steel industry consumes the vast majority of HC and ChG FeCr (~70 pct).[6,7]

FeCr is mostly produced by means of pyrometallurgical carbothermic reduction utilizing submerged-arc furnaces (SAFs) and direct current arc furnaces (DCFs).[8–10] FeCr manufacturing is an energy-intensive process consuming not only high quantities of electricity, but also large amounts of carbon-based reductants.[11–13] Typical operational costs of FeCr producers, as presented by Daavittila *et al.*,[14] can be divided into four cost factors, *i.e.*, chromite ore (30 pct), electricity (30 pct), reductant (20 pct), and other production costs (20 pct). A more recent paper focusing on the South African FeCr smelters indicated that the reductant and electricity cost each account for 30 pct of the overall production costs.[15]

Comparing the specific electricity consumption (SEC), *i.e.*, MWh/t FeCr produced, of existing operational FeCr production processes, the pelletised chromite pre-reduction process (also referred to as solid-state reduction of chromite, SRC) has the lowest SEC (~2.4 MWh/t FeCr achieved with approximately 45 pct pre-reduced hot feed). In this process, a carbonaceous reducing agent, chromite ore, and a clay binder are mixed, dry milled, agglomerated by disk pelletisation, and heated in a grate prior to being fed into a counter current rotary kiln, where pre-reduction of the chromite spinel takes place. The pre-reduced pellets are then charged hot into a closed SAF.[10] There have been a number of commercial facilities where the pelletized chromite pre-reduction process has been successfully applied, *i.e.*, in Japan at the Showa Denko K. K. operations at Shunan and Toyama that has since closed down mainly due to the reliance of imported ore, as well as in South Africa at Glencore Alloys' Lydenburg (previously known as CMI smelter) and Lion smelters. The combined production of the latter two operations was recently increased to ~1.13 million tons FeCr per year.[16] FeCr smelters applying this process are also being commissioned in China, but no information regarding these operations is currently available in the peer-reviewed public domain. Internationally, FeCr

E.L.J. KLEYNHANS, J.P. BEUKES, P.G. VAN ZYL, J.R. BUNT and M. VENTER are with the Chemical Resource Beneficiation, North-West University, Potchefstroom Campus, Private Bag X6001, Potchefstroom, 2520, South Africa. Contact e-mail: paul.beukes@nwu.ac.za N.S.B. NKOSI is with the Pyrometallurgy Division, Mintek, 200 Malibongwe Drive, Private Bag X3015, Randburg, 2125, South Africa.

Manuscript submitted June 22, 2016.
Article published online December 27, 2016.

producers are increasingly being pressured to reduce SEC, and it is therefore likely that more FeCr producers will apply chromite pre-reduction in future.

Historically, coke breeze was primarily used as the carbonaceous reductant source included in the pre-reduced pellet mixture.[17,18] Later, char breeze was also introduced as a reductant source due to its lower cost. However, the fixed carbon (FC) content of typical char breeze is lower than that of coke. The result is that more reductant is required, which effectively reduces the chromite capacity of the pre-reduction kiln. Due to increasing cost of coke breeze, the limited availability of coke and char breezes, as well as the need to increase pre-reduction kiln capacity, Xstrata Alloys (now part of Glencore Alloys) introduced anthracite breeze as a reductant in the pre-reduction pellet mixture.[17] The most significant difference in the composition between coke breeze and anthracite breeze is in the volatile content. Generally, anthracite has a higher volatile content than coke. A too high reductant volatile content can result in the pellets bursting in the pre-drying grate, which would also lead to increased formation or build-up (dam rings) inside the pre-reduction kiln.

From the above-mentioned discussion, it is evident that different carbonaceous reductants are being used in the pelletized chromite pre-reduction process, *i.e.*, anthracite, coke, and char. However, these reductants can also originate from different suppliers, geographical locations, and geological seams. As illustrated by Kleynhans *et al.*,[19] the effect of raw material selection on the degree of chromite pre-reduction, as well as the physical properties of the pellets, needs to be assessed. Currently, FeCr producers, applying the pelletized chromite pre-reducing process, select pre-reduction reductants according to specification pertaining only to the FC, ash, volatile and moisture contents, as well as cost of the reductants. However, it is highly likely that other characteristics of the reductants will have a significant effect on the level of achievable pre-reduction, as well as the physical attributes of the pellets. In this paper, results pertaining to the effect of reductant selection on the level of chromite pre-reduction and cured pellet strength are presented. Multi-linear regression (MLR) was used to determine whether chromite pre-reduction and cured pellet strength can be predicted based on the composition of the carbonaceous reducing agents used. These results will help FeCr producers select reductants that provide the highest pre-reduction (correlating with the lowest SEC), while still complying with the physical requirements for the cured pre-reduced pellets.

II. MATERIALS AND METHODS

A. *Materials*

The feed material of the industrial pelletized chromite pre-reduction process comprises fine chromite ore (typically <1 mm), a clay binder, and a carbonaceous reducing agent. Sample materials were obtained from a large South African FeCr producer currently applying the pelletized chromite pre-reduction process. The materials consisted of metallurgical-grade chromite ore, originating from a mine situated on the eastern limb of the Bushveld Igneous Complex (BIC) and activated sodium bentonite clay (binder). Seventeen different fine carbonaceous reducing agents, *i.e.*, ten anthracite, two char, and five coke samples, were also obtained from various suppliers. In order to gain new perspectives on reductant selection for pelletized chromite pre-reduction, reductants that fell within the current selection criteria, as well as reductants outside this specification, were obtained. The selection criteria currently applied by the FeCr producer consist of a maximum volatile content specification of 7.5 pct, a maximum ash content specification of 15.5 pct, and a minimum FC content specification of 75 pct, all reported on an air-dried basis.

All other chemicals used were analytical grade (AR) reagents, obtained from the different suppliers and used without any further purification. Ultra-pure water (resistivity 18.2 MΩ cm^{-1}), produced by a Milli-Q water purification system, was used for all procedures requiring water. Instrument-grade nitrogen gas (N_2), utilized in pre-reduction experiments, was supplied by African Oxygen Ltd. (Afrox).

B. *Raw Material Characterization*

The specific metallurgical-grade chromite ore and clay binder utilized in this study were the same raw materials used by Kleynhans *et al.*,[19] who published a comprehensive chemical and surface analysis of these materials. Therefore, characteristics, as well as methods applied in the characterization of these two materials, are not repeated here.

Each of the 17 reductants was analyzed individually using methods based on ISO and ASTM standard procedures. The analyses, conducted on an air-dried basis, included proximate analysis (*i.e.*, pct inherent moisture, ash, volatiles, and FC), ultimate analysis (pct C, H, N, and O), gross calorific value, elemental sulfur content, CO_2 reactivity, ash composition, and ash fusion temperatures (AFTs) (in reducing and oxidizing atmospheres). The test samples were prepared before analysis using practices according to the ISO 13909-4: 2001 standard.

Proximate analyses were conducted using methods based on ISO11722: 1999, ISO 1171: 2010, and ISO 562: 2010 procedures in order to quantify the moisture, ash, and volatile contents, respectively, while the FC content was determined by difference.

During the ultimate analyses, the carbon and hydrogen contents were determined using a method based on ASTM D5373, nitrogen based on ASTM D3179, and oxygen by difference.

The gross calorific value (CV) (gross heat of combustion) was measured by the bomb calorimeter method, using specified ISO 1928: 2009 procedures. A weighed amount of each of the seventeen carbon reductants was burnt in a closed vessel under specific oxygen pressure (such that all of the water in the products remained in

liquid form), and the amount of heat released was measured.

The ISO 19579:2006 standard method was performed for the determination of elemental sulfur content. The sulfur content was determined by means of infra-red (IR) spectrometry utilizing a LECO CS 244. For the accelerator flux, a 1:1 mixture of tungsten and iron chips was used.

The CO_2 reactivity of the reductants was measured at 1523.15 K (1250 °C) using a vertical tube thermogravimetric (TG) furnace. Prior to TG analysis, all 17 reductants were dry milled for 30 seconds in 50 g batches using a laboratory disk mill with a tungsten carbide grinding chamber. For each TG analysis, 20 g of milled reductant was placed into a 99.8 pct pure aluminum-oxide conical crucible and slowly raised up the tube of the furnace in an inert atmosphere of argon (0.3 NL/minute at STP) until the sample reached the hot zone of the furnace. This was done to prevent thermal shock of the crucible and supporting pedestal. The sample was allowed to devolatilize at this temperature until the mass of the sample had stabilized, typically 15 minute for the specific reductant samples. Once the mass had stabilized, gas was switched from argon to CO_2. The mass loss as a function of time at temperature [1523.15 K (1250 °C)] was recorded to determine the reactivity of the reductant sample. Since reactivity was the fastest at the beginning of the test, data from the first hour of the experiment were evaluated, although tests were allowed to react for 12 hours or longer until the mass of the sample stabilized. The reactivity at any point in the determination was calculated as follows:

$$R_{app} = \frac{1}{w}\frac{dw}{dt}. \quad [1]$$

In the above equation, R_{app} is the apparent reaction rate and w is the mass of the sample on a FC, dry, ash-free basis. R_{app} was expressed as g g^{-1} s^{-1}. The maximum reactivity was taken as the apparent reaction rate during the first hour of the test.

The ash composition was determined by fusion bead X-ray fluorescence (XRF) according to the standard test method for major and minor elements in coal and coke ash, ASTM D4326-13. In instances where samples exhibited a high Cr content, the test methods for the determination of trace elements in coal, coke, and combustion residues from coal utilization processes by inductively coupled plasma mass spectrometry (ICP-MS), ASTM D6357-11, were used.

Prior to fusion temperature analyses, procedures in ISO 1171:2010 were used to ash the reductants. The ISO 540:2008 standard method was performed using a Carbolite CAF digital imaging coal ash fusion test furnace. In this test, a molded cone of each reductant's ash was viewed and the following four temperatures recorded: (i) initial deformation temperature (DT), when the corners of the mold first became rounded; (ii) softening temperature (ST), when the top of the mold took on a spherical shape; (iii) hemisphere temperature (HT), when the entire mold took on a hemisphere shape; and (iv) fluid temperature (FT), when the molten material collapsed to a flattened button on the furnace floor. The ash melting properties were determined under reducing (CO/CO_2) and oxidizing (air) atmospheres up to a maximum temperature of 1823.15 K (1550 °C).

C. *Material Preparation and Pelletization*

Similar to previous studies,[9,19] the FC content (15 wt pct) and bentonite binder (3.5 wt pct) mixing ratios in all pre-reduction mixtures were kept constant, while the remainder of the mixtures was made up with the chromite ore. This mixing ratio corresponded with typical mixing ratios used by FeCr producers applying the pelletized chromite pre-reduction process. All pre-reduction mixtures were made up in 50 g batches that were dry milled in accordance with procedures detailed by Kleynhans *et al.*[19] in order to achieve the particle size specifications applied for industrial pre-reduction feed material (90 pct of the particles, *i.e.*, d_{90}, smaller than 75 μm). Particle size distributions were confirmed with laser diffraction particle sizing (Malvern Mastersizer 2000), as indicated in Table I. The prepared pre-reduction raw material mixtures were pelletized to produce uncured pre-reduction pellets using the same method employed by Kleynhans *et al.*[19] and Neizel *et al.*[9] Therefore, the method is not reiterated in detail here. In essence, this method consisted of cylindrical pellets being pressed with an LRX Plus strength testing machine (Ametek Lloyd Instruments) in a Specac PT No. 3000 10-mm die to ensure that pellet sizes and densities were consistent.

D. *Laboratory Pre-reduction Experiments*

The high-temperature method used to simulate the industrial pelletized chromite pre-reduction process was similar to previously described procedures.[9–19] The high-temperature profile used consisted of three parts, *i.e.*, (i) heating the pellets from room temperature to 1173.15 K (900 °C) over a period of 30 minutes, simulating pellet drying and pre-heating that occur in a grate during the industrial process; (ii) further heating from 1173.15 K to 1573.15 K (900 °C to 1300 °C) over a period of 50 minutes, simulating pre-reduction in the rotary kiln; and (iii) cooling the pellets inside the tube

Table I. Average PSD of the Milled Pellet Material Mixtures

Particle Size (μm)	Milled Material (Wt Pct)
106-125	0.62 ± 0.02
90-106	3.95 ± 0.04
75-90	4.79 ± 0.14
63-75	3.96 ± 0.08
53-63	3.08 ± 0.14
45-53	3.37 ± 0.09
38-45	5.37 ± 0.13
<38	74.86 ± 1.62
Total	100

furnace to room temperature while the inert atmosphere was maintained.

E. *Analysis of Pre-reduction*

The percentage pre-reduction achieved was determined according to the method utilized by laboratories associated with the FeCr smelters in South Africa currently applying the pelletized chromite pre-reduction process.[9,19,20] The percentage pre-reduction was determined using the following equation:

$$\text{Pre-reduction (wt pct)} = \frac{\frac{m_{Cr_{sol}}}{34.664} + \frac{m_{Fe_{sol}}}{55.845}}{\frac{m_{Cr_{Tot}}}{34.664} + \frac{m_{Fe_{Tot}}}{55.845}} \cdot \frac{}{100}. \quad [2]$$

In Eq. [2] $m_{Cr_{sol}}$, $m_{Fe_{sol}}$ represents the mass of Cr and Fe in the metalized state and $m_{Cr_{Tot}}$, $m_{Fe_{Tot}}$ are the total mass of Cr and Fe present, respectively.

F. *Pellet Compressive Strength*

The compressive strengths of the cured pre-reduced pellets were tested with an Ametek Lloyd Instruments LRXplus 5 kN strength tester. NEXYGENPlus material test and data analysis software were used to control and monitor all aspects of the system, as well as capture and process the data generated. The speed of the compression plates was maintained at 10 mm/minutes during crushing to apply an increasing force on the pellets. The maximum load applied to incur fracturing was recorded for each pellet.

G. *Multiple Linear Regression Analysis*

In order to relate reductant characteristics to the ability of the reductants to impart chromite pre-reduction, multiple linear regression analysis (MLR) was applied. MRL is one of the most commonly applied multivariate methods (*e.g.*, du Preez *et al.*,[21] Shoko *et al.*,[22] Compan *et al.*,[23] and Friedel[24]). In MLR, the relationship between two or more independent variables and a dependent variable is modeled by fitting a multi-linear equation to observed data. The regression line for z independent variables, *i.e.*, $x_1, x_2, \ldots, x_z$, is defined to be

$$\hat{y} = B_0 + B_1 x_1 + B_2 x_2 + \cdots + B_z x_z. \quad [3]$$

The correlation line obtained from MLR describes how the predicted dependent variable scores ($\hat{y}$) change with the independent variables (x). The linear equation obtained with MLR can then be used to predict the values of the dependent variable (y).

In order to interpret the MLR equations obtained by different approaches, *i.e.*, β weights, zero-order correlation-, structure-, and commonality coefficients, all possible subset regression and relative importance weights (RIW), as suggested by Nathans *et al.*,[25] were used. IBM® SPSS® Statistics Version 22 together with program syntaxes adapted from Kraha *et al.*[26] and Lorenzo-Seva and Ferrando,[27,28] was utilized to apply these different approaches.

III. RESULTS AND DISCUSSION

A. *Characterization of the Carbonaceous Reductants*

Characterization results of the 17 different carbonaceous reductants tested are presented in Table II. The anthracite samples are denoted as An1-10, the char as Ch1-2, and the coke samples as Co1-5. As previously stated, FeCr producers currently applying the pelletized chromite pre-reduction process use proximate analysis selection criteria, *i.e.*, 7.5 wt pct maximum volatile content, 15.5 wt pct maximum ash content, and 75 wt pct minimum FC content. From the results (Table II), a significant difference between the anthracite, char, and coke samples is observed if only the proximate analyses are considered. On average, the char samples had the lowest FC content and the coke samples the highest, with the anthracite samples in-between. The coke samples had the lowest volatile contents. Although the ash contents varied substantially, the char samples had the highest ash contents.

Several compounds (or ions of the elements in these compounds) indicated in the ash composition characteristics (Table II), *e.g.*, Al^{3+}, Ca^{2+}, Mg^{2+}, and Si^{4+}, could enhance or inhibit pre-reduction by affecting the reaction mechanism, as it is well known that various minerals and substances enhance or inhibit chromite pre-reduction, *e.g.*, Al_2O_3, B_2O_3, CaB_4O_7, $CaCl_2$, $CaCO_3$, CaF_2, CaO, Cr, Fe, KCl, K_2O, K_2O_3, MgO, $Na_2B_4O_7$, NaCl, Na_2CO_3, NaF, NaF-CaF_2, Na_2O_2, and SiO_2.[29–43] By comparing experimental conditions and results of the aforementioned investigations, the conclusion can be made that the enhancement or inhibition of chromite pre-reduction is not only influenced by the presence or addition of the aforementioned minerals and substances, but also by a combination of the following: (i) the specific elements, compounds, minerals or substances present or added, (ii) the specific temperature, (iii) duration of exposure to the specific temperature, (iii) the amount of elements, compounds, minerals, or substances present or added, and (iv) the stage or level of reduction reached. As an example, SiO_2 was employed as a flux in a number of investigations,[31,32,34,35,37,38] to lower the ore mixture smelting point and promote a combination of solid- and liquid-state pre-reductions, since the main components of the gangue consist of the unreducible oxides Al_2O_3 and MgO, which combine as spinel and therefore are difficult to pre-reduce.[29] Lekatou and Walker[44,45] identified that SiO_2, which was present in the gangue of the ore concentrate they used in their investigation, played an active role in the solid-state reduction of chromite and postulated an ion diffusion mechanism recognizing the diffusion of SiO_4^{2-} from the gangue to the spinel in addition to counter diffusion of Al^{3+}. Ding and Warner,[34] and Weber and Eric,[37] investigated SiO_2-fluxed carbon-chromite composite pellets and reached the following conclusions, *i.e.*, (i) at temperatures <1653.15 K (1380 °C), the addition of SiO_2 had no effect on the reduction kinetics of chromite; (ii) above 1653.15 K (1380 °C), the reduction process can be divided into two stages. In the first stage, to reach

Table II. Characterization of the Reductants Used in MLR Determination

Characteristics	Sample Identification									
	An1	An2	An3	An4	An5	An6	An7	An8	An9	An10
Proximate analysis (pct) (air-dried)										
Inherent moisture	3.8	1.9	2.9	2.1	1.4	1.3	3.2	1.2	1.6	3.2
Ash	15.7	20.3	11.8	12.1	15.5	15.9	15.0	16.0	11.7	16.3
Volatiles	5.0	9.7	4.9	4.5	6.5	8.6	4.0	7.6	5.1	5.0
Fixed carbon	75.5	68.1	80.4	81.3	76.6	74.2	77.8	75.2	81.6	75.5
Ultimate Analysis (pct) (air-dried)										
Carbon	74.10	70.6	78.2	79.8	76.0	75.3	76.2	75.7	80.10	73.6
Hydrogen	1.62	2.60	2.12	2.01	2.49	3.06	1.54	2.95	2.29	1.69
Nitrogen	1.63	1.69	1.77	1.41	1.55	1.60	1.60	1.63	1.45	1.64
Oxygen content	2.01	2.14	2.05	1.80	2.15	2.03	1.81	1.86	2.12	2.12
Gross calorific value (MJ/kg)	27.21	27.24	29.49	29.51	29.35	29.59	28.13	29.69	30.49	27.38
Total sulfur (pct)	1.14	0.74	1.07	0.70	0.84	0.81	0.65	0.57	0.74	1.42
Reactivity at 1523.15 K $\times 10^5$ (s^{-1})	2.943	3.692	2.814	2.334	2.458	3.507	3.243	2.636	3.071	3.599
AFT analysis [K (°C)]										
Reducing										
Initial deformation temperature	1591 (1318)	1581 (1308)	1499 (1226)	1690 (1417)	1517 (1244)	1596 (1323)	1501 (1228)	1665 (1392)	1743 (1470)	1479 (1206)
Softening temperature	1602 (1329)	1598 (1325)	1531 (1258)	1711 (1438)	1534 (1261)	1619 (1346)	1510 (1237)	1679 (1406)	1789 (1516)	1527 (1254)
Hemispherical temperature	1607 (1334)	1609 (1336)	1553 (1280)	1739 (1466)	1556 (1283)	1647 (1374)	1519 (1246)	1707 (1434)	>1823 (>1550)	1599 (1326)
Fluid temperature	1698 (1425)	1779 (1506)	1735 (1462)	1809 (1536)	1693 (1420)	1752 (1479)	1617 (1344)	1786 (1513)	>1823 (>1550)	1711 (1438)
Oxidizing										
Initial deformation temperature	1597 (1324)	1591 (1318)	1617 (1344)	1739 (1466)	1543 (1270)	1639 (1366)	1525 (1252)	1675 (1402)	>1823 (>1550)	1665 (1392)
Softening temperature	1611(1338)	1603 (1330)	1671 (1398)	1769 (1496)	1561 (1288)	1659 (1386)	1538 (1265)	1706 (1433)	>1823 (>1550)	1697 (1424)
Hemispherical temperature	1632 (1359)	1617 (1344)	1694 (1421)	1781 (1508)	1587 (1314)	1685 (1412)	1556 (1283)	1724 (1451)	>1823 (>1550)	1712 (1439)
Fluid temperature	1759 (1486)	1795 (1522)	1763 (1490)	1819 (1546)	1705 (1432)	1785 (1512)	1633 (1360)	1803 (1530)	>1823 (>1550)	1759 (486)
Ash Composition (pct)										
Al_2O_3	22.70	19.70	28.59	28.85	17.97	19.25	25.35	21.03	28.58	25.92
CaO	1.22	4.99	2.35	3.08	4.18	1.82	6.29	2.07	2.88	0.97
Cr_2O_3	6.79	16.40	0.38	0.08	1.45	0.06	0.09	0.04	0.09	3.14
Fe_2O_3	21.03	16.20	10.44	4.85	7.28	5.90	5.36	4.15	4.05	13.61
K_2O	1.33	1.00	2.42	2.03	1.69	1.77	1.79	1.64	1.57	1.49
MgO	3.31	5.28	1.30	1.43	1.33	0.87	1.59	0.86	1.29	2.39
MnO	0.11	0.14	0.10	0.07	0.11	0.07	0.10	0.07	0.06	0.07
Na_2O	1.27	1.14	2.37	1.52	0.36	0.70	3.13	1.19	1.11	1.49
P_2O_5	0.08	0.11	0.15	0.08	0.19	0.21	1.83	0.31	0.08	0.08
SiO_2	40.57	29.00	48.52	54.13	61.78	67.04	50.17	67.36	55.60	49.36
TiO_2	1.41	1.09	1.76	1.24	0.96	0.94	1.31	0.84	1.14	1.25
V_2O_5	0.13	0.18	0.15	0.06	0.08	0.06	0.04	0.05	0.06	0.07
ZrO_2	0.07	0.04	0.12	0.07	0.05	0.05	0.06	0.03	0.06	0.06
Ba	0.20	0.16	0.12	0.11	0.14	0.13	0.16	0.13	0.09	0.23
Sr	0.15	0.18	0.33	0.32	0.08	0.07	0.31	0.08	0.29	0.13
SO_3	0.72	4.32	1.77	2.85	3.18	1.50	2.33	1.32	3.89	0.86

Table II. continued

Characteristics	Sample Identification						
	Ch1	Ch2	Co1	Co2	Co3	Co4	Co5
Proximate analysis (pct) (air-dried)							
Inherent moisture	4.4	5.6	1.2	0.2	0.6	0.4	0.4
Ash	34.9	22.1	20.4	7.7	16.5	9.8	12.4
Volatiles	8.4	4.7	1.6	0.6	0.8	0.8	0.9
Fixed carbon	52.3	67.6	76.8	91.5	82.1	89.0	86.3
Ultimate Analysis (pct) (air-dried)							
Carbon	54.68	67.3	75.5	89.1	81.0	87.4	84.7
Hydrogen	0.97	0.45	0.20	0.03	0.01	0.10	0.01
Nitrogen	1.05	1.14	0.87	1.33	0.67	1.02	1.19
Oxygen content	3.59	3.12	1.04	0.80	0.37	0.72	0.48
Gross calorific value (MJ/kg)	19.49	23.45	23.33	29.25	22.76	27.82	27.03
Total sulfur (pct)	0.41	0.25	0.78	0.80	0.82	0.51	0.78
Reactivity at 1523.15 K × 10^5 (s^{-1})	2.597	2.807	2.674	3.439	2.472	2.560	2.215
AFT analysis [K (°C)]							
Reducing							
Initial deformation temperature	1515 (1242)	1717 (1444)	1547 (1274)	1463 (1190)	1607 (1334)	1498 (1225)	1409 (1136)
Softening temperature	1565 (1292)	1729 (1456)	1593 (1320)	1491 (1218)	1642 (1369)	1517 (1244)	1415 (1142)
Hemispherical temperature	1599 (1326)	1767 (1494)	1611 (1338)	1536 (1263)	1675 (1402)	1597 (1324)	1465 (1192)
Fluid temperature	1793 (1520)	1793 (1520)	1765 (1492)	1707 (1434)	1765 (1492)	1784 (1511)	1763 (1490)
Oxidizing							
Initial deformation temperature	1582 (1309)	1729 (1456)	1621 (1348)	1638 (1365)	1652 (1379)	1539 (1266)	1505 (1232)
Softening temperature	1595 (1322)	1737 (1464)	1645 (1372)	1651 (1378)	1670 (1397)	1561 (1288)	1541 (1268)
Hemispherical temperature	1617 (1344)	1771 (1498)	1654 (1381)	1667 (1394)	1703 (1430)	1651 (1378)	1581 (1308)
Fluid temperature	1803 (1530)	1817 (1544)	1793 (1520)	1731 (1458)	1777 (1504)	1795 (1522)	1787 (1514)
Ash Composition (pct)							
Al_2O_3	19.80	28.77	17.41	24.88	19.77	24.89	22.42
CaO	2.65	2.66	1.69	1.78	1.55	5.32	3.74
Cr_2O_3	26.20	6.53	5.64	1.79	0.88	2.20	4.57
Fe_2O_3	17.50	6.94	12.16	17.00	9.01	15.09	14.87
K_2O	0.33	0.45	0.95	1.95	1.16	1.72	2.25
MgO	6.25	3.52	1.93	1.09	0.78	3.03	2.30
MnO	0.17	0.09	0.16	0.12	0.12	0.20	0.13
Na_2O	0.08	0.04	0.09	0.92	0.11	1.37	1.25
P_2O_5	0.08	0.07	0.17	0.33	0.21	1.11	0.29
SiO_2	23.70	48.94	57.45	48.34	63.35	40.21	46.15
TiO_2	0.86	1.25	1.43	1.25	1.69	1.00	0.93
V_2O_5	0.21	0.10	0.16	0.11	0.14	0.10	0.11
ZrO_2	0.03	0.05	0.14	0.04	0.17	0.04	0.04
Ba	0.04	0.07	0.08	0.12	0.12	0.31	0.19
Sr	0.05	0.05	0.04	0.11	0.06	0.19	0.11
SO_3	2.31	1.20	1.02	0.68	0.90	2.72	1.32

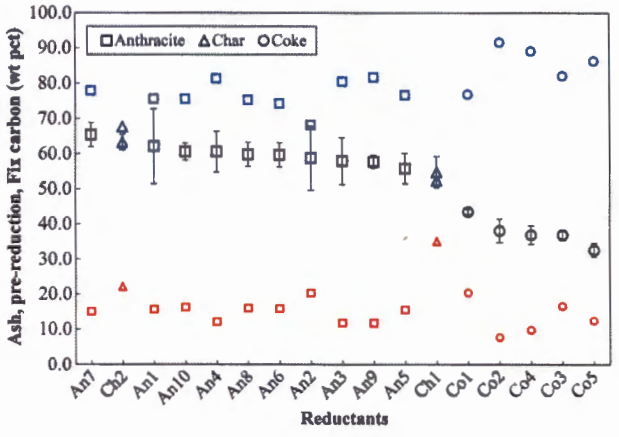

Fig. 1—The effect of different carbonaceous reductants (*i.e.*, anthracite, char, and coke) on the extent of pre-reduction (indicated in black) for the specified temperature profile (Section II–D). Error bars indicate the standard deviations from three repetitions. Also shown are the FC and ash contents of the corresponding reductants, indicated in blue and red, respectively.

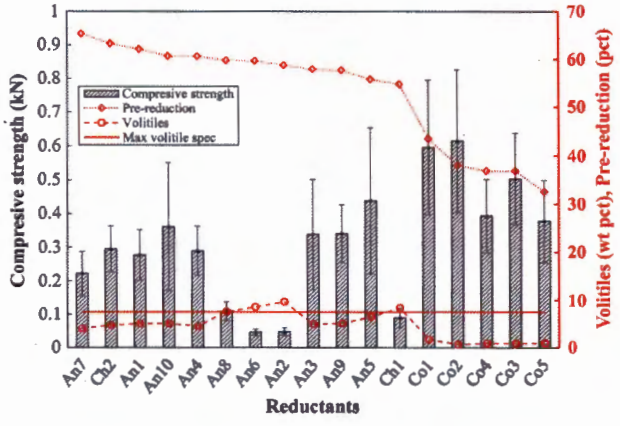

Fig. 2—The effect of different carbonaceous reductants (x axis) on the compressive strength (primary y axis) of pre-reduced pellets (indicated by gray bars) for the specified temperature profile (Section II–D). Error bars indicate the standard deviation from ten experimental repetitions. Also shown on the secondary y axis are the pre-reduction levels achieved and volatile contents of the corresponding reductants, while the industrially applied maximum volatile content specification (7.5 wt pct) is indicated as a solid red line.

pre-reduction levels of up to 30 to 40 pct, the reduction is primarily confined to iron reduction with little to no chromium reduction taking place. SiO_2 addition had no effect on the reduction kinetics in this stage. The second stage is primarily confined to chromium reduction, since most of the iron has already reduced. As a result of the lowering the melting point in the concentrate and the formation of combined solid–liquid states, chromite pre-reduction is enhanced through the dissolution of chromium into the slag and subsequent reduction at the slag–graphite and/or slag–metal interface. However, Lekatou and Walker[35] identified that the SiO_2 content had a critical value related to the carbon content and MgO/Al_2O_3 ratio. Exceeding this critical value hindered chromite pre-reduction due to decreased contact between the chromite and carbon.

Although the above-mentioned studies indicate that various substances could have catalytic or inhibiting effects on chromite pre-reduction, the combined effect of these substances and/or other compounds pertaining to reductant performance in chromite pre-reduction has never been assessed. Furthermore, the effect of other characteristics presented in Table II, such as CO_2 reactivity, gross calorific value, AFTs *etc.*, has not yet been considered in the peer-reviewed literature, nor by FeCr producers applying the pelletized chromite pre-reduction process and is therefore worthwhile to investigate.

B. *Effect of Reductant Selection on Chromite Pre-reduction*

The levels of pre-reduction (indicated in black) achieved with the different carbonaceous reducing agents (x axis), under the specified experimental condition employed (Section II–D), are presented in Figure 1. In order to compare the level of pre-reduction achieved with current reductant selection criteria, the FC and ash contents (indicated in blue and red, respectively) of the different reductants are also presented. The volatile content of the reductants is, however, excluded from this comparison, since it will be discussed in Section III–C.

Several interesting deductions can be made from the results presented in Figure 1. It is evident that substantial fluctuation (~33 pct in absolute terms) in the level of pre-reduction occurred due to the use of the different reductants. This proves that reductant selection could have a significant effect on the pre-reduction process, be it positive or negative. Previous authors,[9,19,46] have indicated how pre-reduction directly influences SEC and lumpy reductant consumption (used in the smelting furnace), which are regarded as two of the three highest cost components in FeCr production.[14,15] In order to further explore trends, the results presented in Figure 1 are arranged according to pre-reduction level achieved (*i.e.*, highest to lowest). From these arranged results, it is apparent that pellets containing anthracite and char, which have lower FC contents than coke (indicated in Section III–A), consistently achieved higher pre-reduction levels than the pellets containing coke as a reductant. According to the material preparation procedure (Section II–C), the FC contributions in all the pellets were kept constant at 15 wt pct.

From the above-mentioned results, it is obvious that there is no correlation between the performance of a specific reductant during pre-reduction and the current FC and ash criteria applied by industry. Higher FC and lower ash content reductants that are currently preferred by industry did not result in higher pre-reduction. On the contrary, reductants with lower FC content seem to correlate somewhat with higher pre-reduction. However, the relatively low R^2 value (~−0.5) of the fitted linear regression between FC content and pre-reduction (which is not shown) indicates that FC content alone cannot be used as a good indicator of pre-reduction that can be achieved. Although there seemed to be no

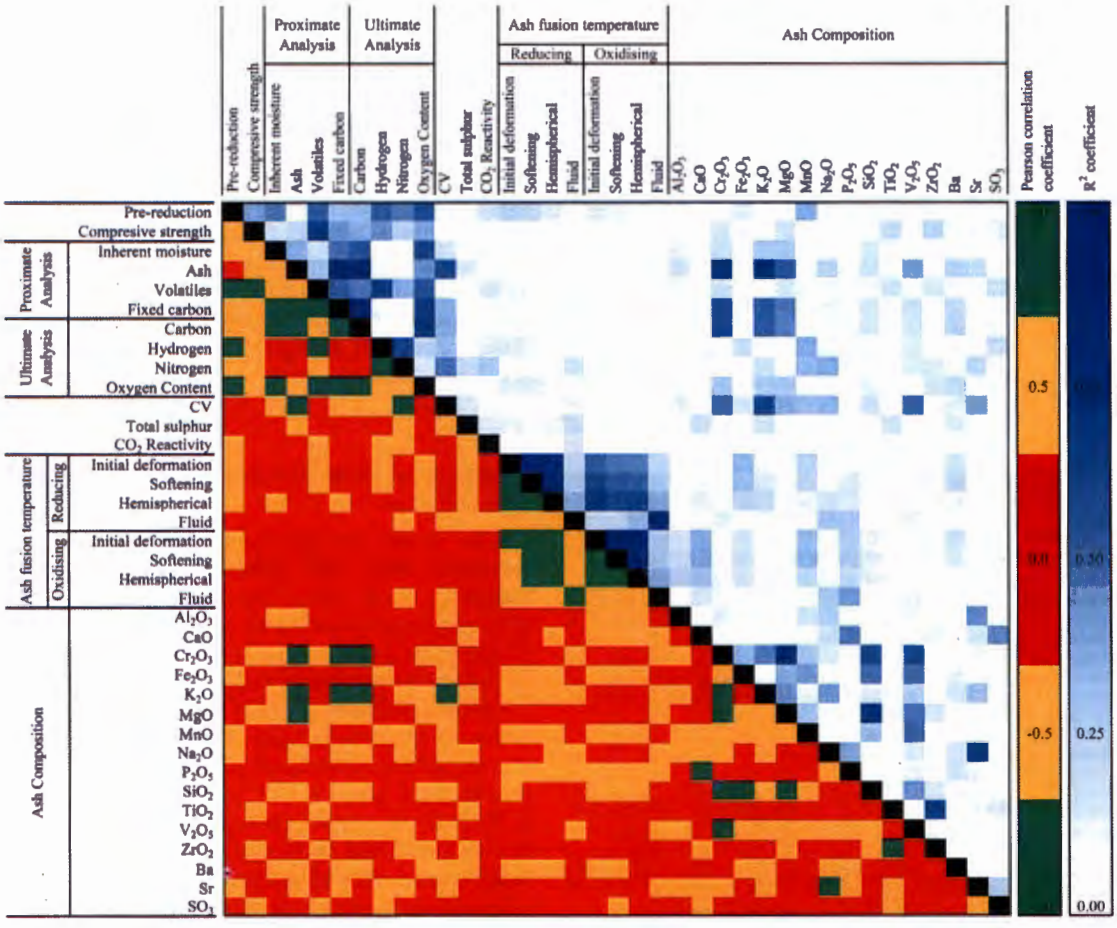

Fig. 3—Correlation matrix for the characteristics (Table II) of the reductants utilized, pre-reduction levels, and compressive strengths. The bottom left triangle shows the Pearson correlation coefficients (r) and the top right triangle shows the linear least squares regression (R^2) coefficients. For r, the guidelines, similar to Jaars *et al.*[48] and Sheskin,[49] were employed to designate the significance of a correlation coefficient, *i.e.*, (i) if $|r| \geq 0.7$, a correlation is considered to be strong/significant; (ii) if $0.3 \leq |r| < 0.7$, a correlation is considered to be moderate/less significant; and (iii) if $|r| < 0.3$, a correlation is considered to be weak/insignificant.

correlation between the ash content and the pre-reduction level, there could be a correlation between some of the individual ash constituents and the extent of pre-reduction achieved. This is explored further in Section III–D.

C. *Compressive Strengths*

Fine materials in the pre-reduction rotary kiln will lead to increased material build-up (dam rings) inside the kiln and result in ensuing operational difficulties. The introduction of fine material into the SAF also needs to be limited, since fine materials increase the tendency of the surface layer of the furnace to sinter. Impermeability of the furnace bed traps evolving process gas, which can lead to the so-called bed turnovers or blowing of the furnace that could have disastrous consequences.[10,47] It was therefore important to determine the influence of the different reducing agents on the cured compressive strength of pelletized chromite pre-reduced pellets, which is indicated in Figure 2 (on the primary y axis). The pre-reduction levels achieved with these reductants, as well as their volatile contents, are also indicated with the maximum volatile content specification (on the secondary y axis).

From the results presented in Figure 2, it is apparent that variations in the compressive strength of the pre-reduced pellets occurred with the use of different reductants. By comparing the compressive strengths of pellets containing anthracite, char, and coke, it is observed that pellets containing coke as a reducing agent had significantly higher compressive strengths than pellets produced with anthracite and char as reductants. This is important, since a reductant, preferred on account of its ability to attain high pre-reduction levels, might be technically inferior in terms of the physical attributes required, when compared to other reductants that achieved lower pre-reduction levels. However, Kleynhans *et al.*[19] proved that a thin outer oxidative sintered layer that is characteristic of industrially produced pre-reduced pellets contributed significantly to cured pre-reduced pellet strength and that the selection of an optimally performing clay binder can also significantly enhance pre-reduced pellet strength.

Therefore, it might be possible to improve the average compressive strengths exhibited by some of the reductants to still capitalize on their ability to impart higher pre-reduction levels. However, the aforementioned aspects were not considered in the current study.

By comparing the compressive strength results with the volatile contents of the reductants, it appears that a higher volatile content caused a decrease in pellet compressive strength. Furthermore, it is apparent that in every instance where the maximum volatile content specification of 7.5 wt pct was exceeded, a dramatic decrease in the pellet compressive strength was observed. These results therefore confirmed the reasoning behind, as well as the importance of the maximum volatile content specification currently applied by FeCr producers applying the pelletized chromite pre-reduction process.

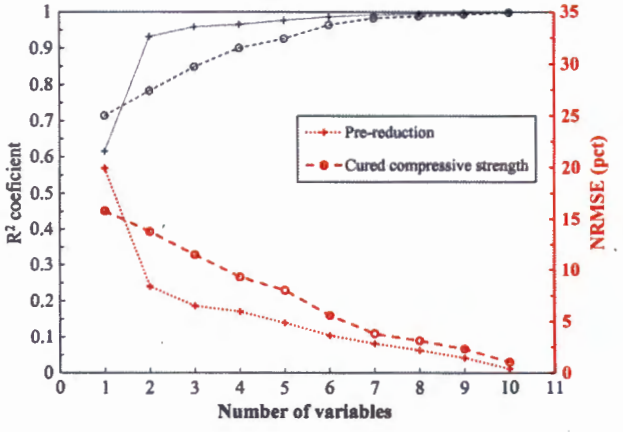

Fig. 4—Linear least squares regression coefficients (R^2) (primary y axis) and the normalized root mean square error (NRMSE) (secondary y axis) difference between calculated and experimentally determined pre-reduction and compressive strengths as a function of the number of independent variables (x axis) included in the optimum MLR solution.

D. *Correlation Analyses*

In order to start investigating the dependence between multiple variables (Table II), a correlation matrix, indicating correlation coefficients between reductant characteristics, pre-reduction, and compressive strength, is presented in Figure 3.

In general, when interpreting correlation coefficients, the use of the terms strong/significant, moderate/less significant, and weak/insignificant in relation to specific values of Pearson correlation coefficients (r) is somewhat arbitrary. Therefore, for the purpose of this discussion, the following guidelines, similar to Jaars *et al.*[48] and Sheskin,[49] will be employed to designate the significance of a correlation coefficient, *i.e.*, (i) if $|r| \geq 0.7$, a correlation is considered to be strong/significant; (ii) if $0.3 \leq |r| < 0.7$, a correlation is considered to be moderate/less significant; and (iii) if $|r| < 0.3$, a correlation is considered to be weak/insignificant. Sheskin,[49] in fact, pointed out that most statistically significant correlations in scientific literature are in the weak to moderate range, and although such correlations are not always considered of practical and/or theoretical meaning, there are many instances where they are indeed of importance. Furthermore, it is important to take note of the distinction between related and unrelated characteristics. With regard to related characteristics, an

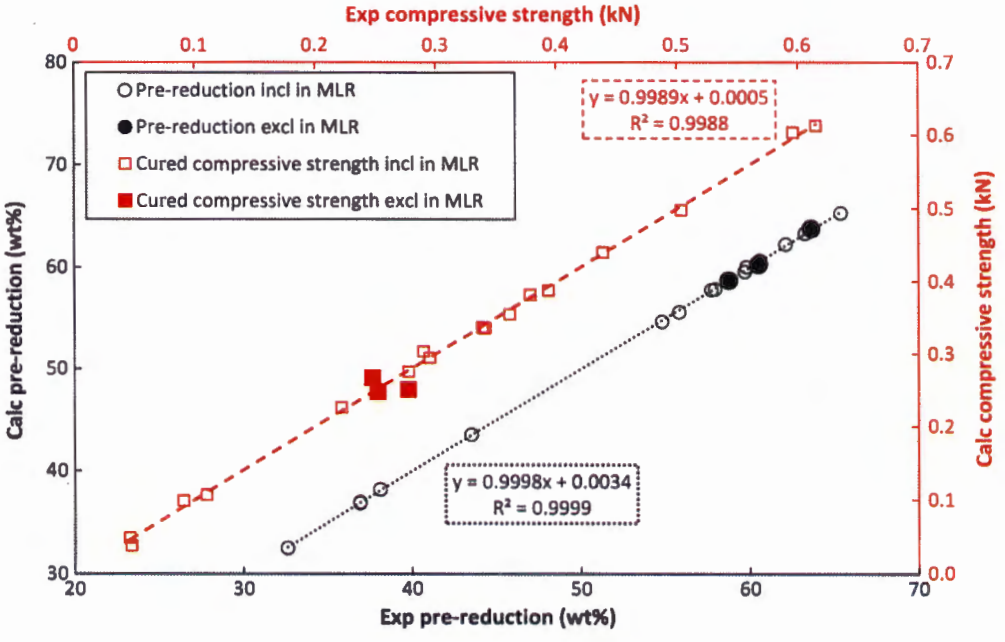

Fig. 5—Correlation between the calculated dependent variable, *i.e.*, pre-reduction and cured compressive strength, using the optimum MLR equation (Eqs. [4] and [5]) and the experimentally determined pre-reduced (Fig. 1) and cured compressive strength (Fig. 2). The solid red and black markers indicate results for reductants that were not included in the determinations of Eqs. [4] and [5].

Table III. Characterization of the Reductants Used to Test the Accuracy of the MLR Equations

Characteristics	Sample Identification		
	An11	An12	An13
Proximate analysis (pct) (air-dried)			
Inherent moisture	2.6	4.8	3.5
Ash	13.0	10.9	15.3
Volatiles	5.6	4.9	4.5
Fixed carbon	78.8	79.4	76.7
Ultimate Analysis (Pct)			
Carbon	77.86	78.48	75.15
Hydrogen	2.30	1.80	1.58
Nitrogen	1.31	1.47	1.62
Oxygen content	2.36	1.97	1.91
Gross calorific value (MJ/kg)	28.61	27.92	27.67
Total sulfur (pct)	0.62	0.64	0.89
Reactivity at 1523.15 K (s^{-1})	1.015×10^{-04}	2.206×10^{-04}	3.093×10^{-05}
AFT analysis (K (°C))			
Reducing			
Initial deformation temperature	1692 (1419)	1533 (1260)	1546 (1273)
Softening temperature	1719 (1446)	1582 (1309)	1556 (1283)
Hemispherical temperature	1739 (1466)	1637 (1364)	1563 (1290)
Fluid temperature	1781 (1508)	1693 (1420)	1658 (1385)
Oxidizing			
Initial deformation temperature	1736 (1463)	1639 (1366)	1561 (1288)
Softening temperature	1756 (1483)	1661 (1388)	1575 (1302)
Hemispherical temperature	1781 (1508)	1684 (1411)	1594 (1321)
Fluid temperature	1808 (1535)	1734 (1461)	1696 (1423)
Ash composition (pct)			
Al_2O_3	27.56	27.03	24.02
CaO	3.67	3.80	3.75
Cr_2O_3	0.47	1.10	3.44
Fe_2O_3	4.52	10.09	13.20
K_2O	1.62	1.00	1.56
MgO	1.64	2.07	2.45
MnO	0.05	0.10	0.10
Na_2O	1.66	0.45	2.20
P_2O_5	0.10	1.06	0.96
SiO_2	53.99	49.58	45.37
TiO_2	1.33	1.45	1.36
V_2O_5	0.05	0.05	0.09
ZrO_2	0.08	0.09	0.06
Ba	0.08	0.06	0.18
Sr	0.27	0.14	0.23
SO_3	2.00	1.41	1.53

underlying relationship exists between the characteristics involved. Examples of related characteristics would be FC content determined through proximate analysis and elemental carbon determined by ultimate analysis.

Considering the results (Figure 3), pre-reduction exhibited strong positive correlations with the reductant volatile content ($r = 0.74$), as well as with H ($r = 0.74$) and O ($r = 0.79$). Correlations with compressive strength, reductant inherent moisture content, FC, C, N, CO_2 reactivity, reducing AFTs (except fluid temperature), oxidizing initial deformation and softening temperatures, Fe_2O_3, MnO, Na_2O and Sr were less significant ($r = |0.3|$ to $|0.7|$). Compressive strength showed a strong negative correlation ($r = -0.845$) with the volatile content of the reductants. This again confirms the importance of the industrially applied maximum volatile content specification. Moderate positive correlations were observed with FC, C, TiO_2 and ZrO_2 ($r = 0.3$ to 0.7), as well as moderate negative correlations with pre-reduction, inherent moisture, ash, H, N, O, Cr_2O_3, MgO and SO_3 ($r = -0.3$ to -0.7). The remaining characteristics exhibited insignificant correlations ($r < |0.3|$).

As is evident from the correlation results presented in Figure 3, it is unlikely that the performance of a reductant, in terms of its effect on pre-reduction level and cured pellet strength, can be forecasted by considering only a single parameter. In an effort to relate the various carbonaceous reductant characteristics (Table II) to the performance of a reductant in the chromite pre-reduction process, MLR analysis was conducted. In Figure 4, the relationships between the number of independent variables included in the optimum MLR analysis equation (x axis) and the R^2

coefficients (primary y axis), as well as the normalized root mean square error (NRMSE, secondary y axis) difference between the calculated (using the MLR optimum equation) and experimentally determined pre-reduction levels and compressive strengths, are presented.

As is evident from Figure 4, an increase in the number of independent variables results in a higher R^2 coefficient and lower NRMSE. The optimum solutions for both pre-reduction and cure compressive strength were attained when the number of independent variables included in the MLR equation were 10, causing the R^2 coefficient to approach 1 and the NRMSE to approach 0. From the aforementioned MLR analyses, the optimal equations containing 10 independent variables were determined as follows:

$$\begin{aligned}\text{Pre-red (pct)} = {} & 13.65+(-156400 \times \text{Reactivity}) \\ & +(8.18 \times H)+(8.59 \times N) \\ & +(8.32 \times \text{MgO})+(139.9 \times \text{MnO}) \\ & +(-1.75 \times \text{Na}_2\text{O})+(31.85 \times \text{TiO}_2) \\ & +(-309.9 \times \text{V}_2\text{O}_5)+(-81.9 \times \text{Ba}) \\ & +(-2.806 \times \text{SO}_3)\end{aligned} \quad [4]$$

$$\begin{aligned}\text{Comp strength (kN)} = {} & 4.903+(-3.413E-2 \times \text{Volatiles}) \\ & +(2.544E-3 \times \text{Red initial deformation temp(°C)}) \\ & +(-4.88E-3 \times \text{Red softening temp (°C)}) \\ & +(-0.719 \times \text{K}_2\text{O})+(-0.2463 \times \text{MgO}) \\ & +(3.427 \times \text{MnO})+(-0.482 \times \text{P}_2\text{O}_5) \\ & +(-0.88 \times \text{V}_2\text{O}_5)+(-2.46 \times \text{ZrO}_2)+(2.548 \times \text{Sr}).\end{aligned} \quad [5]$$

In order to illustrate the accuracy of the determined optimum MLR equations, the experimental pre-reduction (Figure 1) and compressive strength (Figure 2) data are presented as a linear correlation with the calculated results, using equations Eqs. [4] and [5], respectively, in Figure 5. In this figure, pre-reduction and compressive strength results of three addition carbonaceous reductants (indicated in Table III) that were not used to derive the MLR Eqs. [4] and [5] are included. As is evident from Figure 5, the pre-reduction and compressive strength values of these additional samples were on, or close to, the correlation lines, implying that equations Eqs. [4] and [5] can be used to calculate pre-reduction and compressive pellet strength accurately.

An interesting observation with regard to the optimum MLR solutions (Eqs. [4] and [5]) is that the majority of the independent variables were ash components. As mentioned in Section III–A, the individual ash components can possibly either catalyze or inhibit the pre-reduction of chromite. The ash components will also affect the AFT of the reductants. A lower AFT implies that the ash could melt during the pre-reduction process and serve as a glue to increase cured pellet strength. These results prove that the ash composition plays a significant role in the performance of a reductant in the pre-reduction process.

In order to gain a further understanding of the importance of the individual predictors (independent variables) included in the optimum MLR solutions (Eqs. [4] and [5]), several methods (Section II–G) were employed. The results pertaining to these methods are presented in Table IV.

Beta weights (β) are generally used to determine the independent variable contribution to the regression effect, as applied to dependent variable scores that have been standardized (z) in the linear regression equation. Therefore, for an independent variable, β depicts the projected increase or decrease in the dependent variable, in standard deviation units, given a one standard deviation increase in independent variable with all other independent variables held constant.[26] The value of β in Table IV indicates the amount of credit each independent variable is receiving in calculating ($\hat{y}$), and is therefore interpreted by many as an indication of the importance of an independent variable.[26,50] V_2O_5 and the reducing softening temperature obtained the largest β weights in estimating the degree of pre-reduction (Eq. [4]) and pellet compressive strength (Eq. [5]), respectively. According to Kraha *et al.*[26] and Nathans *et al.*,[25] the interpretation of β weights in isolation, without considering additional evaluation criteria, is troublesome and β weights should rather be utilized as a preliminary or exploratory tool. β weights are heavily affected by the covariances/multicollinearity (*i.e.*, high correlation of two or more independent variables) of the variables in question, because they must account for all relationships among all the variables.[26] β weights are partial in their ability to detect and interpret suppression in a regression equation, and they may also receive the credit for explained variance that it shares with one or more independent variables.

The structure coefficients (r_s) are simply the Pearson correlations between the predicted $\hat{y}$ and each independent variable included in the regression equation. The R^2 for both pre-reduction and compressive strength between y and $\hat{y}$ is nearly 1, as shown in Figure 5. Therefore, $r_s \cong r$ (Pearson correlations between the dependent variable y and each independent variable, Section III–D) and $(r_s)^2 \cong R^2_{yx_z}$ (the subset regression between y and each independent variable included in the regression equation). The r_s values make it clear that the β weights are not a direct measure of relationship in this specific case, since in certain instances the β and r_s values differ in sign. This dissimilarity in sign is the first indication that multicollinearity is present within the data.[26] The squared r_s, r_s^2 yielded the proportion of variance in the predicted $\hat{y}$ scores that can be accounted for solely by the specific independent variable, irrespective of multicollinearity with other independent variables. Considering this, H (0.552) and volatiles (0.716) had the largest $(r_s)^2$ values related to Eqs. [4] and [5], respectively. This implies that, for pre-reductions, for which the R^2 was 0.9999 that indicates that 99.99 pct of the variance was explained (Figure 5), H can account for 55.2 pct of the explained variance by itself. Similarly,

Table IV. Summary of Statistically Determined Independent Variable Contributions to Regression Effects

Variable	β	$r_s \cong r$	$(r_s)^2 \cong R^2_{yx_z}$	Unique	Common	RIW Pct
Pre-reduction						
H	0.833	0.743	0.552	0.109	0.444	24.0
N	0.256	0.688	0.473	0.007	0.466	15.1
MgO	1.208	0.124	0.015	0.339	−0.324	15.9
MnO	0.528	−0.602	0.362	0.029	0.334	11.6
Na_2O	−0.135	0.300	0.090	0.005	0.086	3.7
TiO_2	0.793	−0.025	0.001	0.162	−0.162	4.0
V_2O_5	−1.424	−0.293	0.086	0.174	−0.088	12.4
Ba	−0.488	−0.231	0.053	0.093	−0.040	7.1
SO_3	−0.292	0.245	0.060	0.041	0.019	2.5
Reactivity	−0.067	0.381	0.145	0.003	0.142	3.8
Compressive strength						
Volatiles	−0.574	−0.846	0.716	0.132	0.583	45.8
Red init def temp	1.392	−0.277	0.077	0.020	0.056	3.9
Red soft temp	−2.711	−0.237	0.056	0.050	0.006	4.2
K_2O	−2.390	0.192	0.037	0.159	−0.122	5.4
MgO	−2.237	−0.422	0.178	0.156	0.021	15.3
MnO	0.810	0.228	0.052	0.074	−0.022	6.6
P_2O_5	−1.281	−0.012	0.000	0.167	−0.167	5.4
V_2O_5	−0.253	0.038	0.001	0.005	−0.004	4.0
ZrO_2	−0.563	0.491	0.241	0.048	0.193	8.5
Sr	1.514	−0.093	0.009	0.143	−0.134	0.8

volatiles can explain 71.6 pct of the calculated compressive strength. Kraha *et al.*[26] indicated that suppression is apparent when an independent variable has a β weight that is questionably large (consequently getting predictive credit) relative to a low r_s (thereby indicating no relationship with the $\hat{y}$ scores). Comparing the β and r_s values in Table IV, the deduction can be made that suppression is present in the data.

The 'unique' coefficient indicates the proportion of variance explained uniquely by the independent variable, while the 'common' coefficient indicates the proportion of variance explained by the independent variable that is also explained by one or more of the other independent variables.[25,26] Concerning Eq. [4] (estimation of the pre-reduction level), the unique coefficient for MgO (0.339) indicates that it uniquely explains 33.9 pct of the variance of the dependent variable. Kraha *et al.*[26] stated that the common coefficient, representing the proportion of criterion variable variance that can be jointly explained by two or more independent variables, explicitly addresses the issue of multicollinearity with an estimate of each part of the dependent variable that can be explained by more than one independent variable. Negative common coefficients are generally indicative of suppression. Therefore, as a result of its negative common coefficients, MgO serves as a suppressor variable, yielding a unique effect greater than its total contribution to the regression effect $\left(r^2 = R^2_{yx_z}\right) = \text{unique} + \text{common}$. Similarly, for Eq. [5] (predicting pellet compressive strength), P_2O_5 not only has the largest unique coefficient, but also has a suppressor effect. N and volatiles, in conjunction with other independent variables, account for 46.6 and 58.4 pct of pre-reduction (99.99 pct) and compressive strength (99.88 pct) regression effects, respectively.

Relative important weights (RIW) indicate the proportionate contribution from each independent variable to R^2 (Figure 5), after correcting for the effects of intercorrelations among independent variables. This method is used to examine the relative contribution that each independent variable makes to the dependent variable without concern for specific unique and commonly explained portions of the outcome. The RIW offers additional representation of the individual effect of each independent variable, while simultaneously also considering the combination of independent variable. The sum of the RIW is equal to R^2 (Figure 5). This method ranks independent variables in order of importance. However, suppression effects are not identified by this method, which can aid in explaining rank.[25,26] Instead of RIW, RIW pct (RIW × 100) is indicated in Table IV.

Considering the RIW pct values in Table IV, H makes the most significant contribution to the variance (24 pct) in predicting pre-reduction, while several other independent variables make less but still significant contributions, *i.e.*, MgO (15.9 pct), N (15.1 pct), V_2O_5 (12.4 pct), and MnO (11.6 pct). The exact role of H content within this context is currently not clear. However, it is possibly linked to the ability of a reductant to release H that can induce reduction. It is well known that coal gasification in the Fischer–Tropsch process leads to synthetic gas that mainly consists of CO and H_2.[51] In a similar manner, it is believed that the carbonaceous reductants used during FeCr pre-reduction can also form H_2, although in lower concentrations. However, the formation of H_2 in this process has up to now been suppressed due to the use of reductants that had been subjected to higher carburization temperatures (*e.g.*, coke production) that lead to the loss of H in the off-gas of the carburization process.[52,53] Therefore, if a

reductant undergoes a high-temperature pre-treatment process (*e.g.*, coking or charring), it essentially decreases its ability to induce chromite pre-reduction. Therefore, contrary to the current operational selection criteria, the authors believe that thermally untreated (*e.g.*, anthracite) reductants would be the best, since it would maximize H content that would enhance pre-reduction. However, the volatile content of such reductant should be ≤7.5 pct to ensure appropriate compressive pellet strength. Read *et al.*[54] and Ostrovski *et al.*[55] proved that H_2 exerts a catalytic effect on the pre-reduction of chromite. Additionally, these authors indicated that the reduction reactions occurred from 373.15 K to 423.15 K (100 °C to 150 °C) lower in H_2 than when CO or an inert atmosphere is used.

The relative RIW pct importance of MgO, V_2O_5, and MnO in Table IV again reconfirms the importance of ash compounds to catalyze or inhibit chromite pre-production. Since the impacts of V_2O_5 and MnO have not yet been experimentally determined, this work highlights the need for such research in future.

Considering the RIW pct values for the prediction cured pellet compressive strength, it is apparent that the volatile content was by far the most significant independent variable (45.8 pct). This reconfirms the earlier, less quantified observations (Section III–C) that reductant volatile content is the most important parameter to consider.

IV. CONCLUSIONS

In order to determine the influence of carbonaceous reductant selection on chromite pre-reduction, it is important to comprehend the unique process performance requirements that have to be met by such a reductant. The reductant has to ensure that its contribution towards attaining the highest degree of chromite pre-reduction is optimal, while simultaneously not compromising the physical strength of the cured pre-reduced pellets.

The use of different reductants resulted in significant fluctuations in the degree of pre-reduction achieved (Figure 1). FeCr producers currently utilizing the pelletized chromite pre-reduction process prefer reductants with the highest possible FC and lowest possible ash and volatile contents. This operational philosophy stems from the reality that Cr throughput through the rotary kilns has to be maximized, as well as the belief that ash throughput has to be minimized and C throughput maximized to attain optimal pre-reduction. However, reductants with higher FC and lower ash contents did not result in higher pre-reduction. The findings indicate that the currently applied pre-reduction reductant selection criteria are not adequate. The results in particular indicated that the H content of reductants must be maximized to optimize chromite pre-reduction. Therefore, it is recommended that more fundamental research is undertaken to determine how the molecular structure of carbonaceous reductants (and H content in particular) influence the ability of the reductants to impart chromite pre-reduction. The pellet compressive strength results confirmed a link between existing reductant volatile content selection criteria set by industry.

Equations [4] and [5] presented in this paper can be used by FeCr producers to select the reductant used in the pelletized chromite pre-reduction process more optimally in future. The observed ability of reductants to induce pre-reduction varied so significantly (33 pct pre-reduction according to Figure 1) that the cost implications, in terms of electricity usage during smelting of the pre-reduced pellets, are likely to be in the order of millions of dollars per year for smelters applying this process. Therefore, the optimal selection of pre-reduction reductant can no longer be ignored.

The MLR equation that was derived to calculate chromite pre-reduction (Eq. [4]) will only be applicable to the chromite pre-reduction process, which is applied at a limited number of FeCr smelters. However, the concept, *i.e.*, that *in situ* H_2 generation will improve chromite pre-reduction, can be applied more broadly. For instance, *in situ* H_2 formation will also positively influence pre-reduction of manganese ore during ferromanganese (FeMn) production.

Finally, costs and availability of different reductants were not considered in this study, which will obviously also influence the actual selection of reductants used in the industry. In order to select the optimal reductant, industry has to find the balance between cost, availability, and optimal contribution to pre-reduction, while still maintaining adequate cured pellet compressive strength.

ACKNOWLEDGMENTS

The financial assistance of the South African National Research Foundation (NRF) towards the studies of ELJ Kleynhans is hereby acknowledged. The South African Research Chairs Initiative of the Department of Science and Technology and the National Research Foundation of South Africa (Coal Research Chair Grant No. 86880) are also acknowledged. Opinions expressed and conclusions arrived at are those of the authors and are not necessarily to be attributed to the NRF. The authors would also like to thank Lion Ferrochrome (Glencore Alloys) for pre-reduction determinations.

REFERENCES

1. ISSF: Stainless steel demand index 2011. International Stainless Steel Forum, 2011. http://www.worldstainless.org/Statistics/Demand+index/. Accessed 20 January 2012.
2. W.-S. Lee and C.-F. Lin: *Mater. Trans.*, 2001, vol. 42, pp. 2080–86.
3. R.A. Lula, J.G. Parr, and A. Hanson: *Stainless Steel*, American Society for Metals, Metals Park, 1986, pp. 60–70.
4. M. Gasik: *Handbook of Ferroalloys—Theory and Technology*, Butterworth-Heinemann, Oxford, 2013.
5. B.B. Lind, A.-M. Fällman, and L.B. Larsson: *Waste Manag.*, 2001, vol. 21, pp. 255–64.
6. ICDA: *Statistical Bulletin 2013 Edition*, International Chromium Development Association, Paris, 2013, p. 2013.

7. ICDA: Ferrochrome. (International Chromium Development Association, 2013). http://www.icdacr.com/market-intelligence/fecr-brch/fecr-brch.pdf. Accessed 1 June 2012.
8. S. Dwarapudi, V. Tathavadkar, B.C. Rao, T.K.S. Kumar, T.K. Ghosh, and M. Denys: *ISIJ Int.*, 2013, vol. 53 (1), pp. 9–17.
9. B.W. Neizel, J.P. Beukes, P.G. van Zyl, and N.F. Dawson: *Miner. Eng.*, 2013, vol. 45, pp. 115–20, DOI:10.1016/j.mineng.2013.02.015.
10. J.P. Beukes, N.F. Dawson, and P.G. van Zyl: *J. S. Afr. Inst. Min. Metall.*, 2010, vol. 110, pp. 743–50.
11. X. Pan: *International Conference on Mining, Mineral Processing and Metallurgical Engineering (ICMMME'2013)*, Johannesburg, South Africa, 2013, pp. 106–10.
12. C. Ugwuegbu: *Innov. Syst. Design Eng.*, 2012, vol. 3, pp. 48–55.
13. L. Holappa: *Proceedings of The Twelfth International Ferroalloys Congress (INFACON XII)*, A. Vartiainen, Outotec Oyj, ed., Helsinki, 2010, pp. 1–10.
14. J. Daavittila, M. Honkaniemi, and P. Jokinen: *J. S. Afr. Inst. Min. Metall.*, 2004, pp. 541–49.
15. W. Biermann, R.D. Cromarty, and N.F. Dawson: *J. S. Afr. Inst. Min. Metall.*, 2012, vol. 112, pp. 301–08.
16. R.T. Jones: Pyrometallurgy in Southern Africa—List of Southern African Smelters, (Pyrometallurgy, 2015), http://www.pyrometallurgy.co.za/PyroSA/index.htm. Accessed 30 October 2015.
17. O. Naiker: *Proceedings of the The Eleventh International Ferroalloys Congress (INFACON XI)*, New Delhi, 2007, pp. 112–18.
18. Y. Otani and K. Ichikawa: *The First International Congress of Ferro-alloys (INFACON 74)*, H. Glen, ed., SAIMM, Johannesburg, 1974, pp 31–37.
19. E.L.J. Kleynhans, J.P. Beukes, P.G. Van Zyl, P.H.I. Kestens, and J.M. Langa: *Miner. Eng.*, 2012, vol. 34, pp. 55–62, DOI:10.1016/j.mineng.2012.03.021.
20. G.T.M. Mohale: *SEM image processing as an alternative method to determine chromite pre-reduction*, MSc Engineering dissertation, Faculty of Engineering, Potchefstroom Campus, North-West University, South Africa. http://dspace.nwu.ac.za/bitstream/handle/10394/15423/Mohale_GTM.pdf?sequence=1&isAllowed=y, 2014. Accessed 2 May 2016.
21. S.P. du Preez, J.P. Beukes, and P.G. van Zyl: *Metall. Mater. Trans. B*, 2015, vol. 46B, pp. 1002–10, DOI:10.1007/s11663-014-0244-3 .
22. L. Shoko, J.P. Beukes, C.A. Strydom, B. Larsen, and L. Lindstad: *Int. J. Miner. Process.*, 2015, vol. 144, pp. 46–49, DOI:10.1016/j.minpro.2015.09.018.
23. G. Compan, E. Pizarro, and A. Videla: *J. S. Afr. Inst. Min. Metall.*, 2015, vol. 115, pp. 549–56.
24. M.J. Friedel: *Appl. Soft Comput.*, 2013, vol. 13, pp. 1016–32.
25. L.L. Nathans, F.L. Oswald, and K. Nimon: *Pract. Assess. Res. Eval.*, 2012, vol. 17, pp. 1–19.
26. A. Kraha, H. Turner, K. Nimon, L.R. Zientek, and R.K. Henson: *Front. Psychol.*, 2012, vol. 3, p. 44.
27. U. Lorenzo-Seva and P. Ferrando: *Behav. Res. Methods*, 2011, vol. 43, pp. 1–7.
28. U. Lorenzo-Seva, P. Ferrando, and E. Chico: *Behav. Res. Methods*, 2010, vol. 42, pp. 29–35.
29. Y. Wang, L. Wang, and K.C. Chou: *J. Min. Metall. Sect. B-Metall.*, 2015, vol. 51, pp. 15–21, DOI: 10.2298/JMMB130125008W.
30. C. Takano, A.P. Zambrano, A.E.A. Nogueira, M.B. Mourao, and Y. Iguchi: *ISIJ Int.*, 2007, vol. 47, pp. 1585–89.
31. P. Weber and R.H. Eric: *Miner. Eng.*, 2006, vol. 19, pp. 318–24.
32. H.V. Duong and R.F. Johnston: *Ironmak. Steelmak.*, 2000, vol. 27, pp. 202–06.
33. Y.L. Ding and N.A. Warner: *Thermochim. Acta*, 1997, vol. 292, pp. 85–94.
34. Y.L. Ding and N.A. Warner: *Ironmak. Steelmak.*, 1997, vol. 24, pp. 283–87.
35. A. Lekatou and R.D. Walker: *Ironmak. Steelmak.*, 1997, vol. 24, pp. 133–43.
36. D. Neuschiitz, P. JanBen, G. Friedrich and A. Wiechowski: *Proceedings of The Seventh International Ferroalloys Congress*, Trondheim, 1995, pp. 371–81.
37. P. Weber and R.H. Eric: *Metall. Mater. Trans. B*, 1993, vol. 24B, pp. 987–95.
38. P. Weber and R.H. Eric: *Proceedings of The Sixth International Ferroalloys Congress*, SAIMM, Cape Town, 1992, pp. 71–77.
39. R.C. Nunnington and N.A. Barcza: *Proceedings of The Fifth International Ferroalloys Congress*, New Orleans, 1989, pp. 55–68.
40. J.S.J. Van Deventer: *Thermochim. Acta*, 1988, vol. 127, pp. 25–35.
41. H.G. Katayama, M. Tokuda, and M. Ohtani: *ISIJ Int.*, 1986, vol. 72, pp. 1513–20.
42. N.F. Dawson and R.I. Edwards: *Proceedings of The Fourth International Ferroalloys Congress*, Sao Paulo, 1986, pp. 105–113.
43. N.S. Sundar Murti, V.L. Shah, V.L. Gadgeel, and V. Seshadri: *Trans. Inst. Min. Metall. C*, 1983, vol. 98C, pp. C172–74.
44. A. Lekatou and R.D. Walker: *Ironmak. Steelmak.*, 1995, vol. 22, pp. 378–92.
45. A. Lekatou and R.D. Walker: *Ironmak. Steelmak.*, 1995, vol. 22, pp. 393–404.
46. E.L.J. Kleynhans, B.W. Neizel, J.P. Beukes, and P.G. Van Zyl: *Miner. Eng.*, 2016, vol. 92, pp. 114–24, DOI: 10.1016/j.mineng.2016.03.005.
47. M. Riekkola-Vanhanen: *Finnish Expert Report on Best Available Techniques in Ferrochromium Production*, Finnish Environment Institute, Helsinki, 1999.
48. K. Jaars, J.P. Beukes, P.G. van Zyl, A.D. Venter, M. Josipovic, J.J. Pienaar, V. Vakkari, H. Aaltonen, H. Laakso, M. Kulmala, P. Tiitta, A. Guenther, H. Hellén, L. Laakso, and H. Hakola: *Atmos. Chem. Phys.* 2014, vol. 14, pp. 7075–89, DOI:10.5194/acp-14-7075-2014.
49. D.J. Sheskin: *Handbook of Parametric and Nonparametric Statistical Procedures*, 3rd ed., Chapman and Hall/CRC Press, Boca Raton, 2003, p. 1193.
50. G.K. Uyanık and N. Güler: *Proced. Soc. Behav. Sci.*, 2013, vol. 106, pp. 234–40.
51. J.R. Bunt, J.P. Joubert, and F.B. Waanders: *Fuel*, 2008, vol. 87, pp. 2849–55, DOI:10.1016/j.fuel.2008.04.002.
52. B.G. Miller: *Coal Energy Systems*, Elsevier Academic Press, San Diego, 2005, pp. 239–46.
53. C.K. Gupta: *Chemical Metallurgy: Principles and Practice*, Wiley, Weinheim, 2006, pp. 90–100.
54. P.J. Read, D.A. Reeve, J.H. Walsh, and J.E. Rehder: *Can. Metall. Q.*, 1974, vol. 13, pp. 587–95.
55. O. Ostrovski, A. Jacobs, N. Anacleto and G. Mckenzie: *Proceedings of the The Ninth International Ferroalloys Congress (INFACON IX)*, Quebec City, 2001, pp 138–46.

UTILISATION OF PRE-OXIDISED ORE IN THE PELLETISED CHROMITE PRE-REDUCTION PROCESS

5.1 Authors list, contributions and consent

Authors list

E.L.J. Kleynhans[a], B.W. Neizel[a], J.P. Beukes[a] and P.G. Van Zyl[a]

[a] Chemical Resource Beneficiation, North-West University, Potchefstroom Campus, Private Bag X6001, Potchefstroom 2520, South Africa

Contributions

Contributions of the various co-authors were as follows:

Data processing and interpretation, research and writing of the scientific paper, was performed by the candidate, ELJ Kleynhans. BW Neizel conducted some of the experimental work included in the paper as part of his Philosophiae Doctor (PhD) in Chemistry degree at the North-West University, Potchefstroom Campus, which Prof JP Beukes and Dr PG van Zyl also supervised. Prof JP Beukes (supervisor) and Dr PG van Zyl (co-supervisor) assisted in writing the article by sharing conceptual ideas and recommendations with regard to data processing, interpretation and results and discussion.

Consent

All the co-authors that contributed to the article presented in this chapter have been informed that the article will form part of the candidates PhD, submitted in article format, and have granted permission that the article may be used for the purpose stated.

5.2 Formatting and current status of the article

The article is presented in Chapter 5 of this thesis as it was published by Minerals Engineering in 2016, Volume 92 (June), pages 114-124 (DOI http://dx.doi.org/10.1016/j.mineng.2016.03.005, Date of access: 30 November 2016). The journals details can be found at http://www.journals.elsevier.com/minerals-engineering (Date of access: 30 November 2016).

Minerals Engineering 92 (2016) 114–124

Contents lists available at ScienceDirect

Minerals Engineering

journal homepage: www.elsevier.com/locate/mineng

Utilisation of pre-oxidised ore in the pelletised chromite pre-reduction process

E.L.J. Kleynhans, B.W. Neizel, J.P. Beukes *, P.G. van Zyl

Chemical Resource Beneficiation, North-West University, Potchefstroom Campus, Private Bag X6001, Potchefstroom 2520, South Africa

ARTICLE INFO

Article history:
Received 2 September 2015
Revised 15 January 2016
Accepted 2 March 2016

Keywords:
Chromite
Pre-reduction
Solid state reduction
Pre-oxidation
Electricity consumption
Ferrochromium

ABSTRACT

Ferrochromium is a vital alloy mostly used for the production of stainless steel. It is produced from chromite ore, the only economically exploitable natural chromium resource, through carbothermic smelting in submerged arc or direct current furnaces. The pelletised chromite pre-reduction process is currently the industrially applied ferrochromium production process with the lowest specific electricity consumption. Results obtained from this study proved that the pre-oxidation of chromite ore prior to milling, agglomeration and pre-reduction significantly enhances the level of chromite pre-reduction achieved in the pelletised chromite pre-reduction process. The optimum pre-oxidation temperature was established as the temperature where a balance was achieved between maximising iron (Fe) migration to the surface of ore particles that were pre-oxidised, while avoiding the formation of free eskolaite (Cr_2O_3). For the case study metallurgical grade chromite ore considered, the optimum pre-oxidation temperature was found to be 1000 °C. Utilising such pre-oxidised ore could theoretically lead to an improvement of approximately 8.5% in the specific electricity consumption and a 14% decrease in the lumpy carbonaceous material required during submerged arc furnace smelting of pelletised chromite pre-reduced feed.

1. Introduction

Ferrochromium (FeCr) is mostly used for the production of stainless steel, which is vital in various applications (Cramer et al., 2004; Gasik, 2013). Ferrochromium is produced from chromite ore, which is the only economically exploitable natural chromium (Cr) resource (Misra, 2000). At present, global Cr resources are estimated to be between 9 and 12 billion tonnes. South Africa (RSA) holds the vast majority of estimated chromite resources, i.e. ~6.9 billion tonnes (OCC, 2014). In 2012, RSA produced ~10 million tonnes of chromite ore, representing ~41% of the world production. Of the ~10 million tonnes of ore produced, ~55% were exported, which implies that ~28% of ore consumed in the rest of the world in 2012 originated from RSA. RSA is also one of the major producers of FeCr, with production in 2012 accounting for 32% of the total global estimate (ICDA, 2013).

Chromite ore is mainly converted to FeCr through carbothermic smelting in submerged arc furnaces (SAFs) or direct current furnaces (DCFs) (Beukes et al., 2010). The majority of RSA chromite ore is relatively friable (Beukes et al., 2010; Glastonbury et al., 2010). Generally, the use of fine chromite (<6 mm) in SAF smelting is restricted, since fine materials raise the risk of the furnace bed to sinter. Consequently, evolving process gases are trapped, leading to bed turnovers or furnace eruptions that can have devastating consequences (Beukes et al., 2010; Riekkola-Vanhanen, 1999). Therefore, fine ore is agglomerated (e.g. pelletised) before being charged into an SAF.

Ferrochromium production using SAF smelting is a fossil fuel (carbon reductant) and electric energy intensive process. Therefore, production cost depends heavily on energy and raw material prices. International trends to increase energy security in conjunction with increasing energy costs have placed an emphasis on conducting research related to process optimisation, process efficiency and efficient energy utilisation. Holappa (2010) reported the specific electricity consumption (SEC) and carbonaceous reductant consumption of conventional open SAF smelting of lumpy and fine ore (without agglomeration and pre-heating) to be 3.8–4.5 MW h/t FeCr and 0.5–0.7 t reductant/t FeCr, respectively.

A number of processes have been developed to reduce SEC, with the pelletised chromite pre-reduction process considered to be the industrially applied option with the lowest SEC (McCullough et al., 2010; Naiker, 2007; Naiker and Riley, 2006). In the pelletised chromite pre-reduction process, metallurgical grade chromite ore (<1 mm), a clay binder and a carbon reductant are dry milled to

* Corresponding author.
E-mail address: paul.beukes@nwu.ac.za (J.P. Beukes).

http://dx.doi.org/10.1016/j.mineng.2016.03.005
0892-6875/

particle size of 90% < 75 μm, followed by disc pelletisation and pre-heating, before being fed into a rotary kiln where the chromite is pre-reduced (also referred to as solid state reduction). The partially reduced pellets are then fed hot, immediately after exiting the kiln, into closed SAFs (Beukes et al., 2010; Naiker, 2007). Apart from lower SEC, the pelletised chromite pre-reduction process option also holds other significant advantages, which include lower SAF lumpy reductant consumption, exploitation of lower cost fine reductants and energy sources such as anthracite (instead of coke) and oxygen (O_2), 100% agglomerate feed, Cr recoveries in the order of 90% and the ability to produce a low silicon (Si)- and sulphur (S)-containing FeCr product (McCullough et al., 2010; Naiker, 2007; Takano et al., 2007).

Pre-oxidation as a treatment prior to smelting in the SAF is a commercially applied process. In the oxidative sintering process (Outotec, 2015), which has been the most commonly applied process over the last decade in the South African FeCr industry, milled chromite ore is sintered in pelletised form. This sintering process is essentially an oxidative process, during which the small amount of carbon present in the uncured pellets is oxidised to sinter the pellets (Beukes et al., 2010; Niemelä et al., 2004). SEC for SAF FeCr production with oxidative sintered pellets is ⩾3.1 MW h/t FeCr, which is an improvement from the conventional SAF smelting of ores.

Zhao and Hayes (2010) investigated the effects of additional oxidation on the microstructure and reduction (as occurring in the furnace smelting process) of oxidative sintered chromite pellets. They found that pre-heating the pelletised ore at temperatures between 1000 and 1200 °C in air increased the reducibility of the chromite in the smelting furnace. They attributed this increased reducibility to the increase in the effective surface area created due to the shear mechanism generating smaller particles, i.e. the transformation of magnetite (Fe_3O_4) to hematite (Fe_2O_3). The rapid transformation to the Fe_2O_3 phase occurs through a solid state shear mechanism that results in the preferential growth on the planes in the crystals. The strain induced at the Fe_3O_4/Fe_2O_3 phase boundary and the preferential reduction of Fe_2O_3 can result in the mechanical break-up of the crystal grains, thereby increasing the effective surface area for reduction (Zhao and Hayes, 2010).

From the abovementioned, it is evident that the oxidation/sintering of chromite prior to smelting in an SAF can potentially have significant SEC advantages. However, pre-oxidation of chromite ore, prior to being used in the pelletised pre-reduction process, has not been investigated before. In this paper, results are presented that demonstrate how pre-oxidation can improve the extent of pre-reduction, which will further improve the SEC of the pelletised chromite pre-reduction FeCr production process. The objectives were to (i) present the new suggested process, i.e. pre-oxidation of chromite ore prior to pelletised pre-reduction, (ii) assess how to optimise pre-oxidation conditions to maximise the benefit of using pre-oxidised chromite ore, and (3) indicate the possible practical advantages and disadvantages of this process option by considering factors such as SEC, carbonaceous reductant consumption, breaking- and abrasion strengths, as well as the formation of hexavalent chromium, Cr(VI), which is considered a human carcinogen (Beaver et al., 2009; Thomas et al., 2002).

2. Materials and methods

2.1. Materials

The raw materials utilised in the industrially employed pelletised chromite pre-reduction process consist of upgraded fine chromite ore (typically metallurgical grade chromite ore or upgraded UG2 process residue from the Platinum Group Metals industry), a clay binder and a fine carbonaceous reductant. Raw materials used in this study were obtained from a large South African FeCr producer, applying the pelletised chromite pre-reduction process. Metallurgical grade chromite ore (<1 mm), anthracite breeze (reductant) and attapulgite clay (binder) utilised by this FeCr producer were acquired. The same raw material samples were used by Kleynhans et al. (2012), who presented a comprehensive chemical and surface analysis of all these materials, as well as X-ray diffraction (XRD) and ash fusion temperature analyses of the clay binder. Therefore, the material characterisations and methods applied are not repeated here, but only a synopsis of the chemical composition of the three raw materials and the proximate analyses of the anthracite breeze are presented in Table 1.

Ultra-pure water from a Milli-Q water purification system (resistivity18.2 MΩ cm^{-1}) was used to pre-wet materials prior to pelletisation. Instrument grade nitrogen (N_2) gas (Afrox) was utilised in all pre-reduction experiments.

Several Cr(VI) analyses were conducted. Calibration of the analytical instrument was performed using a reference standard (Spectroscan) with a certified concentration of 1009 ± 5 μg/mL chromate (CrO_4^{2-}). Ammonium sulphate ($(NH_4)_2SO_4$) (Merck) and a 25% ammonia (NH_3) solution (Ace) were used to prepare the eluent. The post-column reagent was prepared using 1,5-diphenylcarbazide (Fluka Analytical), 98% sulphuric acid (H_2SO_4) (Rochelle Chemicals) and HPLC grade methanol (Ace). Sodium hydroxide (NaOH) (Promark chemicals) and sodium carbonate (Na_2CO_3) (Minema) were used to prepare a Na_2CO_3–NaOH buffer to extract Cr(VI) from the solid samples.

2.2. Methods

2.2.1. Pre-oxidation of chromite ore

Pre-oxidation of the chromite ore was carried out in an Elite BRF15/5 chamber furnace fitted with a programmable temperature controller. 100 g of metallurgical grade chromite ore (<1 mm) was placed in a ceramic (99.8% Al_2O_3) boat, positioned centrally inside the furnace chamber and heated in a normal gaseous atmosphere (air) during each pre-oxidation test. For each temperature profile, the furnace controller was set to ramp up at its maximum heating rate from room temperature to a desired maximum temperature (i.e. 800–1500 °C) and then to remain constant at the maximum temperature for a further 10 min, after which the furnace was switched off. The furnace door was then opened to aid in rapid cooling to room temperature. These pre-oxidation temperature profiles are graphically presented in Fig. 1.

2.2.2. Material preparation and pelletisation

The preparation of raw materials for pre-reduction was conducted similar to the procedures previously described by

Table 1
Chemical analyses (wt.%) of chromite ore, anthracite breeze (reductant) and attapulgite clay (binder), as well as the proximate analysis of the anthracite breeze (air dry basis) used in this study (from Kleynhans et al., 2012).

	Chromite ore	Anthracite breeze	Attapulgite clay
Cr_2O_3	45.4	–	–
FeO	25.4	1.6	6.0
Al_2O_3	15.2	3.1	14.7
MgO	9.8	0.4	5.3
SiO_2	1.7	10.0	46.9
CaO	0.2	0.8	5.6
P	<0.01	0.01	<0.01
S	<0.01	0.6	<0.01
Fixed carbon	–	75.1	–
Inherent moisture	–	0.3	–
Ash	–	17.8	–
Volatiles	–	6.9	–

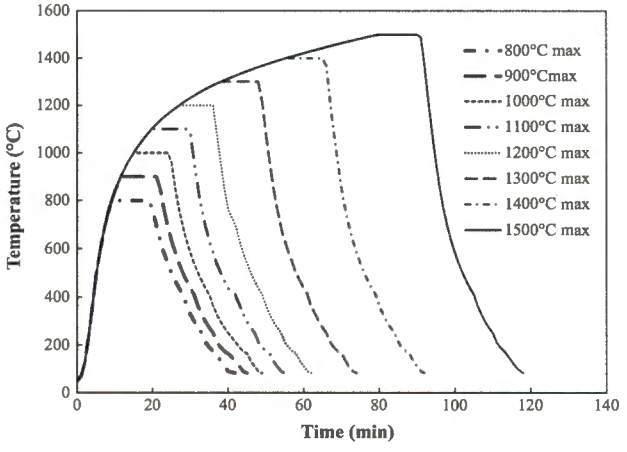

Fig. 1. Experimental temperature profiles used to generate pre-oxidised chromite ore for subsequent use in pre-reduction experiments.

Kleynhans et al. (2012) and Neizel et al. (2013). The primary components of the uncured pre-reduced pellets were mixed in a ratio of 3.5 wt.% attapulgite clay, 20 wt.% anthracite (ensuring 15 wt.% fixed carbon (FC) content in the uncured pellets) and the remaining 76.5 wt.% consisted of normal metallurgical grade chromite ore, or pre-oxidised metallurgical grade chromite ore. The aforementioned mixing ratio is consistent with mixing ratios used in the industrial pelletised chromite pre-reduction process (Kleynhans et al., 2012). Fifty gram batches of the aforementioned dry material mixture was then milled for two minutes with a Siebtechnik laboratory disc mill to ensure that the components were homogeneously mixed and that the particle size distribution of the mixture was similar to the milled material utilised in the industrially applied process, i.e. 90% of the particles smaller than 75 μm. Particle size distribution was confirmed with laser diffraction particle sizing (Malvern Mastersizer 2000), as described by Glastonbury et al. (2015). In order to prevent possible iron (Fe) contamination, a tungsten carbide grinding chamber was used. The same method employed by Kleynhans et al. (2012) and Neizel et al. (2013) to pelletise the milled raw material mixture to produce uncured pellets for pre-reduction was used in this study and is therefore not discussed in detail. In essence, the pelletisation method consisted of cylindrical pellets being pressed with an LRX Plus strength testing machine (Ametek Lloyd Instruments) in a Specac PT No. 3000 10 mm die. Although this pelletisation method was slower than disk or drum pelletisation, it ensured that pellet sizes and densities were consistent, which further ensured that process controlling parameters could be investigated under monovariant conditions.

2.2.3. Pellet pre-reduction

The method used to simulate industrial pelletised chromite pre-reduction on laboratory scale was similar to the procedure described by Kleynhans et al. (2012) and Neizel et al. (2013). A batch of 10 uncured pellets (Section 2.2.2) were placed on a Coorstek AD-998 (99.8% Al_2O_3) plate, which were subsequently positioned in the centre inside a tube furnace (Lenton Elite, UK model TSH15/75/6 10) fitted with a Shunk recrystallised alumina tube. Ceramic heat shields were inserted at both ends of the tube furnace to improve the effective tube length in which a stable working temperature could be achieved. These heat shields also protected the stainless steel caps, which were fitted onto both sides of the ceramic tube to seal off the ends and prevent air ingression. The stainless steel caps had a gas inlet and an outlet on the two opposing sides.

The gaseous atmosphere inside the furnace was controlled by a constant N_2 flow of 1 NL/min through the furnace tube, which ensured an inert gaseous atmosphere. An inert gaseous atmosphere prevented reduction or oxidation due to the presence of an external reducing or oxidising gaseous atmosphere, since the aim of this study was to determine pre-reduction as a result of chromite interaction with the carbonaceous reductant present in the material mixture. Prior to each pre-reduction experiment, the tube furnace, already loaded with uncured pellets, was flushed with N_2 at a flow rate of 1.25 NL/min for at least 5 min at room temperature to displace air inside the tube. Each batch was then treated according to a pre-programmed high temperature profile.

The temperature profile utilised in this investigation was compiled after numerous different profiles were tested to simulate the temperature profile employed during the industrial pelletised pre-reduction process. A base case pre-reduction with a pellet mixture utilising untreated received ore (un-oxidised) was performed to standardise the temperature profile. The specific profile selected for this study obtained a chromite pre-reduction level of 46.5% for the base case pre-reduction, which was considered to be the most appropriate, since it correlated well with the average pre-reduction level achieved at one of the large FeCr smelters applying the pelletised chromite pre-reduction process. The profile consisted of three segments, i.e. (i) heating the pellets from room temperature to 900 °C over a period of 30 min simulating pellet drying and preheating (which take place in a grate in the industrial process), (ii) further heating from 900 to 1300 °C over a period of 50 min simulating pre-reduction (which takes place in a counter current rotary kiln in the industrial process), and (iii) cooling the pellets inside the tube furnace to room temperature while the inert atmosphere was maintained.

2.2.4. Analysis of pre-reduction

Similar to previous studies (Kleynhans et al., 2012; Neizel et al., 2013), the level of chromite pre-reduction was determined according to the method utilised by laboratories at the FeCr smelters in RSA that apply the pelletised chromite pre-reduction process. The degree of pellet pre-reduction was determined using the following equation:

$$\%\ \text{Total pre-reduction} = \frac{\frac{\text{Sol.Cr\%}}{34.67} + \frac{\text{Sol.Fe\%}}{55.85}}{0.0121} \quad (1)$$

The percentages soluble Cr and soluble Fe in Eq. (1) were determined with reflux leaching of a pre-determined mass of the pre-reduced material with a hot sulphuric/phosphoric acid solution. The percentage (%) soluble Cr in this aliquot was then established by means of the oxidation of the soluble Cr with potassium permanganate ($KMnO_4$) and subsequent volumetric titration with ferrous ammonium sulphate ($(NH_4)_2SO_4$) using diphenylamine sulphonate as an indicator. The % soluble Fe in the untreated aliquot was determined by means of a similar method with the only difference being that potassium dichromate ($K_2Cr_2O_7$) was used as the titrant. In this analytical method, the percentages soluble Cr and Fe represent these metals in the metallised state, i.e. the zero oxidation state (Kleynhans et al., 2012; Neizel et al., 2013). However, the level of Cr and Fe metallisation is not directly related to the total pre-reduction, since pre-reduction is more commonly related to the removal of oxygen (Barnes, 1983). Therefore, a constant of 34.67 was calculated by dividing the molar mass of Cr divided by 1.5 and the constant 55.85 for Fe was determined by dividing the molar mass of Fe by 1. These constant factors were derived from the stoichiometrically-balanced chemical reaction equations, wherein 1.5 mol of CO (containing 1 mol of oxygen removed from the oxide) forms in the metallisation reaction for 1 mol of Cr, and 1 mol of CO forms in the metallisation reaction for 1 mol Fe (Barnes, 1983). Lastly, the constant 0.0121 is a

chromite reduction value for typical South African metallurgical grade chromite ore, which is calculated from (total Cr/34.67 + total Fe/55.85)/100. Although this value was indicated as a constant in Eq. (1), this constant was actually calculated for each analysis to compensate for altering chromite compositions.

2.2.5. Pellet compressive and abrasion strength

The compressive strengths of the pre-reduced pellets were tested with an Ametek Lloyd Instruments LRXplus 5 kN strength tester. NEXYGENPlus material test and data analysis software were used to control and monitor all aspects of the system, as well as capture and process the data generated. The speed of the compress plates was maintained at 10 mm/min during crushing to apply an increasing force on the pellets. The maximum load applied to incur fracturing was recorded for each pellet.

The abrasion resistance test apparatus utilised was based on a downscaled version of the European standard EN15051 rotating drum. The drum was designed according to specifications provided by Schneider and Jensen (2008). A batch of 10 pre-reduced pellets was placed inside the drum and rotated at a constant rate of 40 rpm. Each batch of pellets was abraded and checked after specific time intervals, i.e. 1, 2, 4, 8, 16 and 32 min. After each time interval, the material was screened using 9.5, 6.7 and 1.18 mm screens. The over- and under-sized materials were then weighed and all the material returned to the drum for further abrasion, until the final abrasion time (i.e. 32 min) was reached.

2.2.6. Surface analysis

Scanning electron microscopy (SEM) and SEM coupled to energy dispersive spectroscopy (SEM-EDS) were employed to visually characterise the surface properties of samples. A Zeiss MA 15 SEM incorporating a Bruker AXS XFlash® 5010 Detector X-ray EDS system operating with a 20 kV electron beam at various working distances was used. Backscattered electrons combined with EDS were used to determine the elemental composition in different areas of the samples. The same instrument was also used to obtain X-ray mapping, which provided information of elemental spatial distributions on the surface of a sample. Polished and unpolished samples were considered.

2.2.7. X-ray diffraction

X-ray diffraction of the un-oxidised and pre-oxidised chromite ore was performed according to a back-loading preparation method. Semi-quantitative and qualitative XRD analyses of the compounds in the ore were conducted with a PANalytical X'Pert Pro powder diffractometer with Fe-filtered Co-K radiation incorporating an X'Celerator detector. The measurements were carried out between variable divergence- and fixed receiving slits. The phases were identified using X'Pert Highscore plus software. The relative phase amounts were estimated using the Rietveld method (Autoquan program).

2.2.8. Thermomechanical analysis

A single uncured pellet, prepared as described in Section 2.2.2, using a 10 mm die set, was placed in a Seiko Instruments Inc. TMA/SS 6100 thermo-mechanical analyser (TMA), interfaced with SII EXSTAR 6000. The thermal expansion and/or contraction of the pellet were then measured during in situ pre-reduction as a function of temperature up to 1300 °C. All TMA experiments were conducted under inert atmospheric conditions (N_2), similar to the conditions applied during pre-reduction experiments conducted in the tube furnace (Section 2.2.3). Since the TMA probe was made of alumina, α-alumina coefficients correction was applied to the data, as specified in the operational manual of the instrument.

2.2.9. Hexavalent chromium analysis

Hexavalent chromium compounds were leached from the pre-oxidised ore (Section 2.2.1) using an alkaline leaching method described by Abubakre et al. (2007), and Pettine and Capri (2005). The leaching solution utilised consisted of $NaCO_3$ (30 g) and NaOH (20 g) that were made up to 1 L with Milli-Q water. A half gram of the pre-oxidised ore was leached with the aforementioned solution for 60 min at ~65 °C under an N_2 atmosphere. The solution was then filtered and analysed for Cr(VI).

Hexavalent chromium analyses were conducted with ion chromatography (IC). The analytical method was adapted from DIONEX Application updates 144 and 179 (Dionex Corporation, 2003, 2011), and Thomas et al. (2002), as previously described (du Preez et al., 2015; Loock-Hattingh et al., 2015; Loock et al., 2014). A Thermo Scientific Dionex ICS-3000 was used, with a Dionex IonPac AG7 4 × 50 mm guard column and a Dionex IonPac AS7 4 × 250 mm analytical column. The injection loop was 1000 µl and two 375 µl knitted reaction coils were fitted in series. An eluent flow rate of 1.00 ml/min was utilised, while the post-column colorant reagent (diphenylcarbazide) was delivered at a flow rate of 0.5 ml/min.

2.2.10. Thermochemical calculations

HSC Chemistry 7.0 (Roine, 2009) was used to conduct thermochemical calculations in order to assist in the interpretation of the results obtained.

3. Results and discussion

3.1. Effect of pre-oxidation temperature on pre-reduction

The effect of pre-oxidation of the metallurgical grade chromite ore, prior to being milled, pelletised and pre-reduced, on the level of chromite pre-reduction achieved under the specific experimental conditions employed (Section 2.2.1), is illustrated in Fig. 2. The base case in Fig. 2 (indicated by the horizontal dotted line) was determined by utilising untreated received ore (un-oxidised), as mentioned in Section 2.2.3. From these results, it is evident that pre-oxidation between 800 and 1100 °C, prior to milling, agglomeration and pre-reduction, improved the level of achievable chromite pre-reduction. Pre-oxidation at 1000 °C was the optimum pre-oxidation temperature for the specific case study ore utilised. Pre-oxidation temperatures above 1100 °C resulted in lower levels

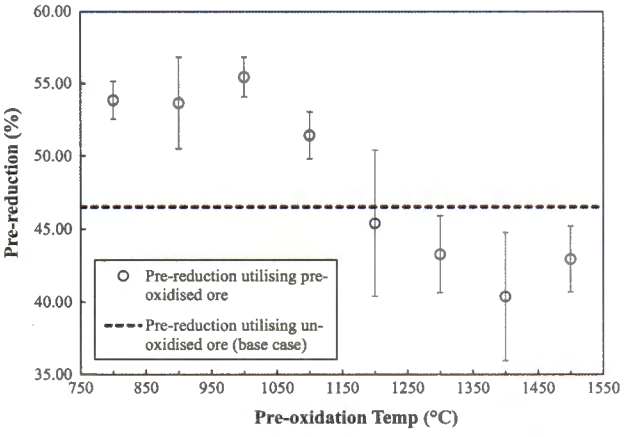

Fig. 2. The effect of pre-oxidation temperature of metallurgical grade chromite ore, prior to milling, agglomeration and pre-reduction, on the extent of chromite pre-reduction. The bars indicate the range of results obtained for three experimental repetitions.

of pre-reduction. At pre-oxidation temperatures higher than 1200 °C, the pre-reduction levels achieved were even lower than the base case utilising un-oxidised ore.

The observation that the highest pre-oxidation temperatures did not result in the highest pre-reduction levels (Fig. 2) seemed somewhat unexpected, if the previous work of Zhao and Hayes (2010) is considered, wherein it was proved that increased oxidation of sintered chromite pellets altered the chromite microstructure, which enhanced the smelting reducibility of these pellets. Therefore, it might have been expected that higher pre-oxidation temperatures would result in a more significant alteration of the very stable chromite spinel, which could result in higher pre-reduction levels. Since this was not observed, it was important to understand the experimental trend observed. In the subsequent sections (Sections 3.2–3.4), results from various experimental techniques are presented in order to explain the observations presented in Fig. 2.

From an operational FeCr production perspective, the results presented in Fig. 2 are very promising. Firstly, the SEC and lumpy carbonaceous materials required for smelting in the SAF will be lower with improved pre-reduction. This aspect will be explored further in Section 3.5. Secondly, the highest pre-oxidation temperatures did not correlate with the best pre-reduction levels. The afore-mentioned observation is encouraging from a production cost perspective, since lower pre-oxidation temperatures imply lower operational costs. The effect of pre-oxidation on the pellet strength, an important operational parameter, will also be discussed (Section 3.6). Both pellet compressive and abrasion strengths are important, since excessive formation of fines in the furnace feed materials could have disastrous consequences (Beukes et al., 2010; Riekkola-Vanhanen, 1999; Visser, 2005).

3.2. Scanning electron microscopy analysis

In order to explore the possible surface chemical effects caused by pre-oxidation, SEM back-scatter micrographs and X-ray map images (Section 2.2.6) of ore particles mounted on carbon tape, as well as of ore particles mounted in resin followed by subsequent cutting and polishing, were obtained. Specifically, the un-oxidised ore, as well as pre-oxidised ore at 1000 °C and 1400 °C, were considered, for which the results are presented in Fig. 3. In addition to the un-oxidised ore (base case), the two pre-oxidation temperatures selected represented the best and worst case pre-reduction scenarios (Fig. 2).

Fig. 3A and B show a SEM micrograph and an X-ray map of the un-treated ore, respectively. From the SEM micrograph (Fig. 3A), it is evident that the chromite ore particles had relatively clean surfaces with relatively sharp edges. The X-ray map of the polished

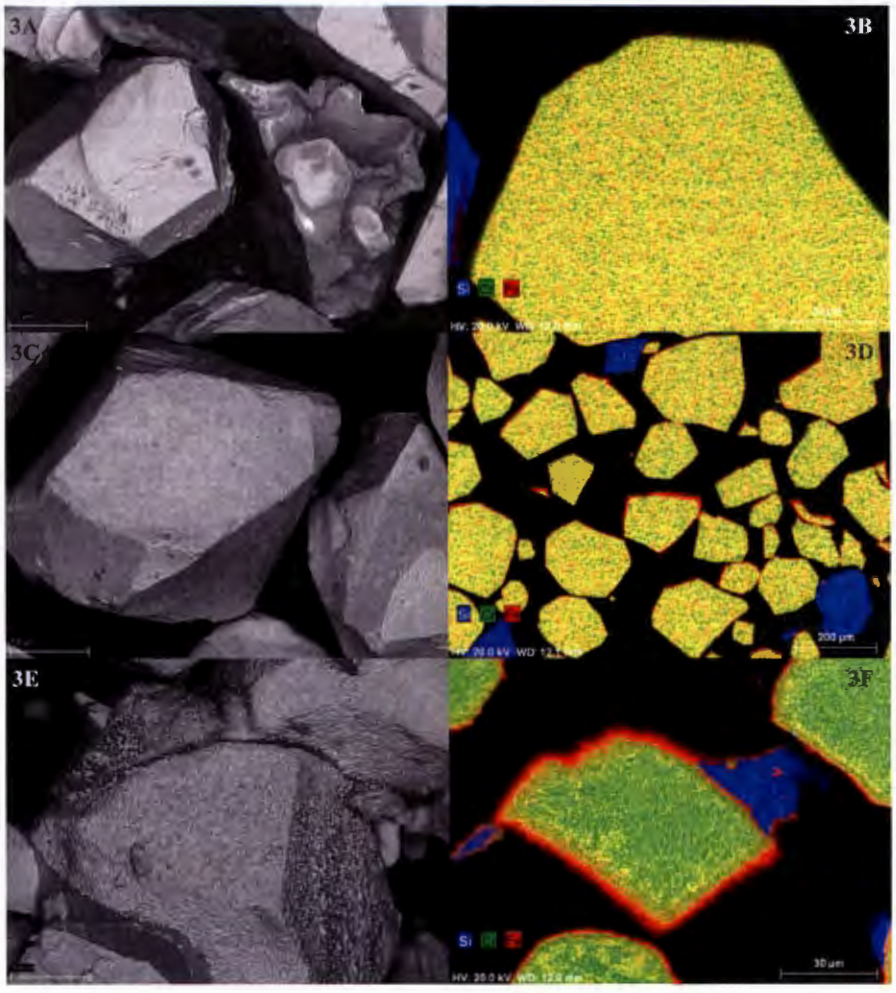

Fig. 3. SEM micrograph images taken at 350 times magnification and X-ray maps taken at 1200 or 150 times magnification of the un-oxidised ore (3A and 3B), ore pre-oxidised at 1000 °C (3C and 3D) and ore pre-oxidised at 1400 °C (3E and 3F).

ore particles (Fig. 3B) indicated that all elements (e.g. Cr, Fe, Si, etc.) were homogeneously spread throughout the chromite particles with no enrichment zones.

In Fig. 3C and D, a SEM micrograph and X-ray map of the chromite ore pre-oxidised at 1000 °C are presented, respectively. The SEM micrograph (Fig. 3C) indicated that a crust formed on the surface of the chromite ore particles. It can also be seen in the accompanying X-ray map (Fig. 3D) that some Fe (depicted with the colour red) enrichment on the surface of the ore particles had occurred. From these results, it seems that Fe migration to the surface of the ore particles had occurred to a small extent, due to pre-oxidation of the ore at 1000 °C.

It was expected that the abovementioned Fe migration associated with pre-oxidation would be further enhanced at higher pre-oxidation temperatures. Increased Fe migration is evident from Fig. 3E and F, which show a SEM micrograph and X-ray map of the chromite ore pre-oxidised at 1400 °C, respectively. From Fig. 3E, it is apparent that the crust formed on the outside of the chromite ore particles due to pre-oxidation had become more significant. The accompanying X-ray map (Fig. 3F) also illustrates a very clear Fe-enriched area on the surface of the chromite particles. Additionally, the silica (Si indicated in blue in Fig. 3F) in the gangue minerals seems to have melted at this higher pre-oxidation temperature. However, this observation is not relevant to this discussion and will not be elaborated on further.

From the results presented in Fig. 3A–F, it is evident that at higher chromite ore pre-oxidation temperatures, Fe migration to the surface of the ore particles increased. According to the Ellingham diagram presented by Niemelä et al. (2004), it is evident that, thermodynamically, solid carbon (C) can reduce higher oxidation states of Fe, i.e. Fe_2O_3 and Fe_3O_4, to FeO at relatively low temperatures, while FeO is reduced to the metal state (Fe^0) above ~710 °C. In contrast, Cr_2O_3 reduction requires much higher temperatures, i.e. ⩾1250 °C. If the SEM and X-ray map results are therefore considered in isolation, chromite pre-reduction levels should have improved with increasing pre-oxidation temperatures, due to enhanced Fe-oxide migration from the spinel to the ore particle surface at higher pre-oxidation temperatures. However, chromite pre-reduction did not necessarily improve with increasing pre-oxidation temperatures (Fig. 2), and therefore further investigation was required. X-ray diffraction analysis on the same samples (un-oxidised ore, as well as ore pre-oxidised at 1000 and 1400 °C) was performed in order to find possible explanations for the observed decrease in pre-reduction of ores pre-oxidised at 1400 °C. The XRD analysis provides information on the crystalline content of samples, which could remain undetected with SEM and X-ray map analyses.

3.3. X-ray diffraction

In Fig. 4A–C, XRD spectra of un-oxidised chromite ore, as well as chromite ore pre-oxidised at 1000 °C and 1400 °C are presented, respectively. Fig. 4D presents the peak list providing information used to identify compounds in these XRD spectra.

From Fig. 4A and B, it is clear that the XRD patterns of the un-oxidised chromite ore and chromite ore pre-oxidised at 1000 °C are the same, notwithstanding the small amount of Fe that migrated to the surface of the chromite particles, as indicated in Fig. 3, by means of X-ray map analysis. The similarity in XRD patterns can be attributed to Fe oxides being particularly difficult to detect with XRD analysis at low concentrations, due to their poor crystallinity (small crystal size and structural disorder) and unspecific particle shape, which requires Fe-specific methods, such as Mössbauer spectroscopy (Schwertmann, 2008). It was therefore not surprising that the XRD spectra of the un-oxidised chromite ore and chromite ore pre-oxidised at 1000 °C were the same. However, for the chromite ore pre-oxidised at 1400 °C (Fig. 4C), it is evident that additional peaks had formed in the XRD spectrum. According to the XRD peak list of standard materials (Fig. 4D), these additional peaks correlated with eskolaite or chromium oxide (Cr_2O_3), which indicates that at pre-oxidation temperatures >1000 °C (e.g. 1400 °C presented in Fig. 4) free Cr_2O_3 formed. Quantitative XRD analyses of chromite ore pre-oxidised at maximum temperatures of 1000, 1100, 1200, 1300 and 1400 °C, according to the temperature profiles presented in Fig. 1, indicated Cr_2O_3 contents of 0%, 15%, 26.6%, 34.5% and 39.4%, respectively.

3.4. Thermochemical perspective

From the SEM and X-ray map results (Section 3.2), it was evident that higher pre-oxidation temperatures resulted in more Fe migration to the surface of the ore particles. The XRD analyses (Section 3.3) indicated that chromite ore pre-oxidised at temperatures >1000 °C contained free Cr_2O_3. In order to contextualise this information, these results are further explored with regard to their effect on the level of pre-reduction by means of relevant thermochemical calculations. An Ellingham diagram constructed with the HSC thermo-chemical software package (Section 2.2.10) indicating the change in ΔG of the reduction of the relevant metal oxides with C and carbon monoxide (CO) is presented in Fig. 5.

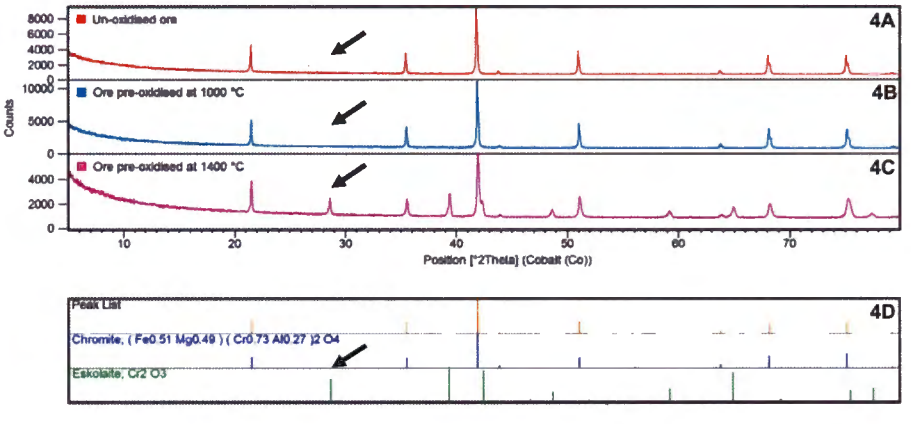

Fig. 4. XRD spectra of un-oxidised chromite ore (4A), chromite ore pre-oxidised at 1000 °C (4B) and chromite ore pre-oxidised at 1400 °C (4C). (4D) presents the peak list providing information used to identify peaks observed in the above-mentioned XRD spectra. The arrows indicate one of the peaks used as an indicator of the absence/presence of eskolaite (Cr_2O_3) in the materials.

Although thermodynamic explanations of reactions ignore any kinetic effects, it is a useful tool. This Ellingham diagram is very similar to the diagram published by Niemelä et al. (2004).

Considering the thermo-chemical data presented in Fig. 5, the following important deductions can be made:

(I) Iron oxide reduction takes place from the highest to the lowest oxidation state, i.e. hematite (Fe_2O_3) to magnetite (Fe_3O_4) to wüstite (FeO) to metallic Fe.
(II) Carbon monoxide can only serve as a reducing agent for FeO (the most reduced oxide state) to metallic Fe at temperatures >710 °C. Although it is not shown in this figure, a high CO/CO_2 ratio would also be required for such reduction to take place.
(III) Reduction of chromium-containing oxides is not possible with CO (gas).
(IV) Solid C can reduce FeO to metallic Fe at temperatures >750 °C.
(V) Cr_2O_3 is reduced by solid C at temperatures >1250 °C.
(VI) Synthetic chromite Cr_2FeO_4 (Niemelä et al., 2004) is reduced at lower temperatures than Cr_2O_3, i.e. 1200 °C. In addition, eskolaite forms a sesquioxide solid solution with α-Al_2O_3, which significantly stabilises the Cr_2O_3 against reduction. Al_2O_3 and Cr_2O_3 are sesquioxides, having the same corundum crystal structure (approximately hexagonal close-packed oxide ions with the Al^{3+} and Cr^{3+} ions occupying two thirds of the available octahedral interstitial sites), which, through reaction at high temperatures (>1000 °C), could form ranges of substitutional corundum–eskolaite, α-$(Al^{3+}, Cr^{3+})_2O_3$ solid (Bondioli et al., 2000).

The last three deductions, in particular, in conjunction with the SEM, X-ray map (Section 3.2) and XRD results (Section 3.3) can be used to explain the experimentally observed pre-reduction levels associated with increased pre-oxidation temperatures (Fig. 2). Since all Fe oxides can be reduced at temperatures >750 °C, Fe migration to the surface of ore particles, as indicated by SEM and X-ray map data, will enhance chromite pre-reduction levels. The aforementioned discussion provides a plausible explanation for the improved pre-reduction levels associated with an increase in the pre-oxidation temperature of the ore up to 1000 °C. However, XRD results indicated that free Cr_2O_3 is formed at pre-oxidation temperatures >1000 °C, which counteracts the positive effect of Fe migration to the surface of the particle, which can be ascribed to Cr_2O_3 being more difficult to reduce than chromite. Therefore, the observed decrease in chromite pre-reduction levels at pre-oxidation temperatures >1000 °C is understandable. The effect of formation of Cr_2O_3 at higher pre-oxidation temperatures was so significant that pre-reduction levels were lower than that of un-oxidised ore (base case) at pre-oxidation temperatures ⩾1200 °C.

Considering the data presented thus far, it can be stated that chromite pre-reduction can be improved by means of utilising pre-oxidised chromite ore. The optimum pre-oxidation temperature would be the temperature at which a balance is obtained between maximising Fe migration to the surface of the ore particles and minimising the formation of free Cr_2O_3. For the specific metallurgical grade chromite ore utilised in this study, the optimum pre-oxidation temperature was determined to be 1000 °C. Although the oxidation state of the Fe that migrated to the surface of the chromite ore particles was not assessed in this study, Zhao and Hayes (2010) indicated that Fe_2O_3 enhanced reduction the most during SAF smelting compared to the other oxides of Fe.

3.5. Energy implications of pre-reduction alterations

Niayesh and Fletcher (1986) published data indicating an improvement in SEC as a result of increasing chromite pre-reduction and feed material temperature. Similar to Neizel et al. (2013), reconstruction of this data and empirical fitting allowed the evaluation of the effect of the level of pre-reduction achieved by using pre-oxidised ore on the SEC as presented in Fig. 6 (primary y-axis).

The effect of improved pre-reduction achieved by utilising pre-oxidised ore on the amount of FC (in the form of lumpy carbonaceous reductant) required to effect complete reduction of the pre-reduced pellets inside the SAF, is also indicated in Fig. 6 (secondary y-axis). The FC requirements were determined using the following equations:

$$\text{wt FC for chromium oxide reduction} = ((\text{T.Cr\%}) - (\text{Sol.Cr\%})) \times \frac{3\,\text{mol} \times 12.011\,\text{g mol}^{-1}}{2\,\text{mol} \times 51.996\,\text{g mol}^{-1}} \times \frac{1000\,\text{kg}}{100\%} \quad (2)$$

$$\text{wt FC for iron oxide reduction} = ((\text{T.Fe\%}) - (\text{Sol.Fe\%})) \times \frac{1\,\text{mol} \times 12.011\,\text{g/mol}^{-1}}{1\,\text{mol} \times 55.845\,\text{g/mol}^{-1}} \times \frac{1000\,\text{kg}}{100\%} \quad (3)$$

$$\text{wt FC equivalent for Si and C in metal produced} = (\text{T.Cr\%}) \times 1.684 \quad (4)$$

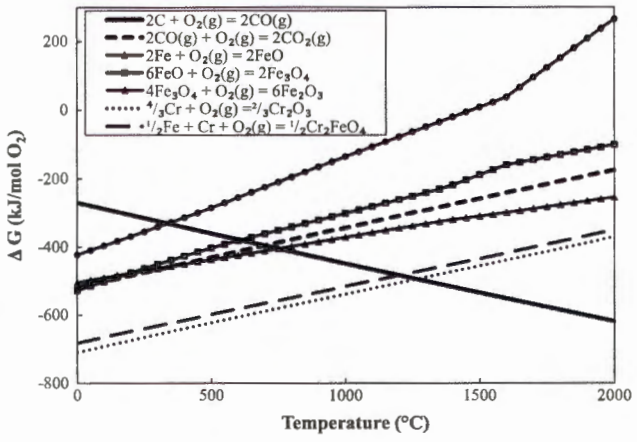

Fig. 5. Ellingham diagram (ΔG as a function of temperature) indicating standard ΔG (Gibbs free energy) of the reduction of metal oxides with solid C and CO, constructed with HSC thermo-chemical software (Roine, 2009).

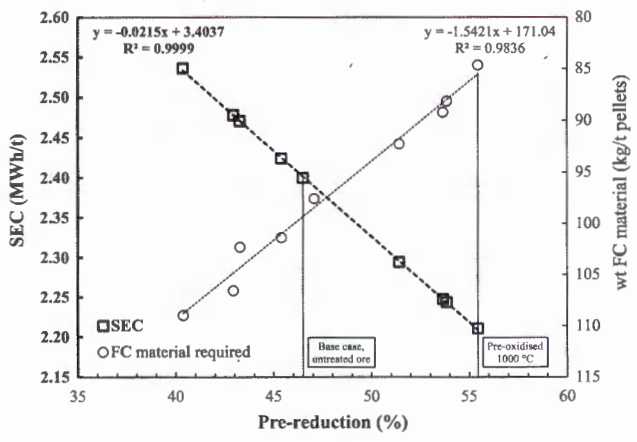

Fig. 6. The effect of enhanced pre-reduction by utilising pre-oxidised ore (x-axis) on the SEC (primary y-axis), as well as on the wt FC required per ton pre-reduced pellets (kg/t pellets) (secondary y-axis).

$$\text{wt FC required} = (\text{Total FC} = (2)+(3)+(4)) - (\text{Residual C} = \frac{\text{T.C\%}}{100\%} \times 1000\ \text{kg}) \quad (5)$$

In the above equations, the Sol.Cr% and Sol.Fe% represent these metals in the metallised state in the pre-reduced pellets, while the T.Cr% and T.Fe% represent the totals of these metals in the pre-reduced pellets. Residual C is the C remaining in the pre-reduced pellets that were not consumed during the pre-reduction process and is calculated using T.C%, i.e. the percentage total C in the pre-reduced pellets. The constant 1.684 is a typical value for South African FeCr alloys produced using the pre-reduction process and represents the C equivalent to the reduced Si and C contained in the metal produced.

From the data presented in Fig. 6, it is evident that an increase in the level of pre-reduction as a result of using pre-oxidised ore, could lead to significant improvements (decrease) in the SEC and lumpy carbonaceous material required in FeCr production, specifically at the pre-oxidation temperature of 1000 °C, where the SEC and FC required are at their lowest.

3.6. Pellet strength

As previously stated, excessive fines present in SAF feed material could have disastrous consequences. It was therefore important to determine the effect of pre-oxidation of chromite ore, prior to milling, agglomeration and pre-reduction, on the cured pre-reduced pellet compressive and abrasion strengths.

3.6.1. Compressive strength

In Fig. 7A, the compressive strengths of pre-reduced pellets produced from chromite ore that were pre-oxidised at different temperatures are compared with the breaking strength of pre-reduced pellets made from un-oxidised chromite ore (base case, indicated with dotted line). It is evident from the results that the pre-reduced pellets made from pre-oxidised ore were significantly weaker. As stated previously, pre-oxidation at 1000 °C resulted in the optimum pre-reduction level (Section 3.1). Compared with un-oxidised ore, pre-reduced pellets made from ore pre-oxidised at 1000 °C lost ~42% of its cured compressive strength (Fig. 7A). It is difficult to contextualise these breaking strength results, since most of the previous studies focusing on improved chromite pre-reduction did not report pellet strength (Ding and Warner, 1997a,b; Sundar Murti et al., 1983; Van Deventer, 1988). However, Neizel et al. (2013) proved that $CaCO_3$ addition, prior to milling, agglomeration and pre-reduction, leads to pre-reduced pellets losing more than 66% of their breaking strength. Therefore, pre-reduced pellets made from ore pre-oxidised at 1000 °C performed noticeably better.

It is important to note that all the aforementioned experiments were conducted in an inert atmosphere (N_2 gas) (Section 2.2.3). However, Kleynhans et al. (2012) demonstrated that industrially produced pre-reduced pellets are not uniformly pre-reduced. The atmosphere outside the pellet is usually partially oxidising, which leads to the formation of a thin oxidised outer layer, a transitional zone and a pre-reduced core. Kleynhans et al. (2012) also indicated that this thin outer oxidised layer contributed significantly to the strength of the pre-reduced pellets. In order to assess whether the presence of such a thin oxidised outer layer will significantly improve the pre-reduced pellet strength, pre-reduced pellets made from chromite ore that were pre-oxidised at 1000 °C were subsequently exposed to oxidative conditions. These pre-reduced pellets were placed in a tube furnace (Section 2.2.3) and the temperature ramped up from room temperature to the maximum desired temperature (700–1300 °C) under normal atmospheric gaseous conditions. When the desired maximum temperature was reached, N_2 gas was passed through the furnace to stop further oxidation. The pellets were then allowed to cool down within the furnace, where after compressive strength tests were conducted. These compressive strength test results are presented in Fig. 7B. It is evident from these results that a considerable improvement in the pellet breaking strength was observed, which demonstrated that the presence of a thin oxidised outer layer will significantly increase the pellet strength and mitigate the decrease in compressive strength of pre-reduced pellets made from pre-oxidised ore (Fig. 7A). Additionally, Kleynhans et al. (2012) also proved that pre-reduced pellet strength can be further significantly improved by selecting the optimum clay binder.

3.6.2. Abrasion strength

In order to assess the effect of pre-oxidation of chromite ore on the abrasion strength of the pre-reduced pellets, the abrasion strength of pellets prepared from pre-oxidised ore at 1000 °C was compared to pellets made from un-oxidised ore. These results are presented in Fig. 8.

Similar to the abovementioned compressive strength results, the abrasion strength of pre-reduced pellets made from chromite ore pre-oxidised at 1000 °C (the optimum temperature) lost some abrasion strength. However, this loss was lower than what was reported by Neizel et al. (2013) for $CaCO_3$-containing pre-reduced pellets. In addition, the abrasion strength of the industrially produced pre-reduced pellets will likely be enhanced by the presence of a thin oxidised layer, as derived from the results published by Kleynhans et al. (2012).

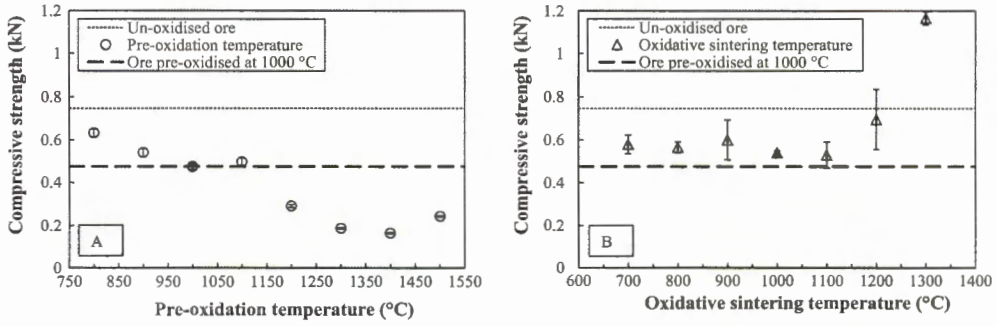

Fig. 7. Fig. 7A: The effect of pre-oxidation of metallurgical grade ore at different temperatures (*x*-axis) on the compressive strength of pre-reduced pellets (*y*-axis). Fig. 7B: The compressive strength of pre-reduced pellets (*y*-axis), prepared from metallurgical grade chromite ore pre-oxidised at 1000 °C that were subsequently oxidatively sintered at different temperatures (*x*-axis) in a normal atmosphere. The bars indicate the standard deviations of results obtained from ten experimental repetitions.

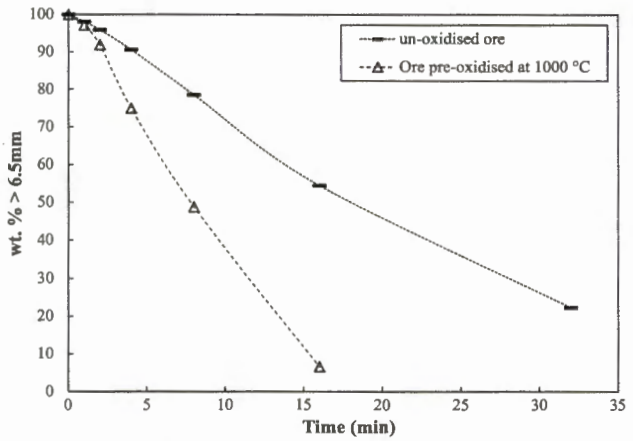

Fig. 8. The effect of the pre-oxidation of metallurgical grade ore at 1000 °C on the abrasion strength of pre-reduced pellets indicated in weight percentage (wt.%) greater than 6.5 mm (*y*-axis) against abrasion time (*x*-axis).

3.7. Thermomechanical analysis

In Fig. 9, data on the primary *y*-axis represents the dimensional changes of pellets prepared from un-oxidised chromite ore and ore pre-oxidised at three different temperatures (800, 1000 and 1400 °C), which were pre-reduced in situ in the TMA. From these results it is evident that all the pellets had similar thermal dimensional change characteristics up to approximately 750 °C. However, at temperatures >750 °C, the pellets made from chromite ore that were pre-oxidised at 1400 °C indicated significant expansion, whereas the pellets made from ore pre-oxidised ⩽1000 °C shrunk.

X-ray diffraction analysis indicated the formation of free Cr_2O_3 in chromite ore pre-oxidised at ⩾1100 °C (Section 3.3). It was therefore proposed that the presence of Cr_2O_3 in the ore pre-oxidised at higher temperatures is responsible for the above-mentioned different behaviours observed for these pellets. In order to verify this proposal, pure Cr_2O_3 was added to un-oxidised ore prior to TMA analysis. From Fig. 9, it is evident that the TMA curve of un-oxidised ore containing 10 wt.% Cr_2O_3 started behaving a bit more similar to the pellets made from ore pre-oxidised at 1400 °C, at temperatures >750 °C during in situ pre-reduction in the TMA.

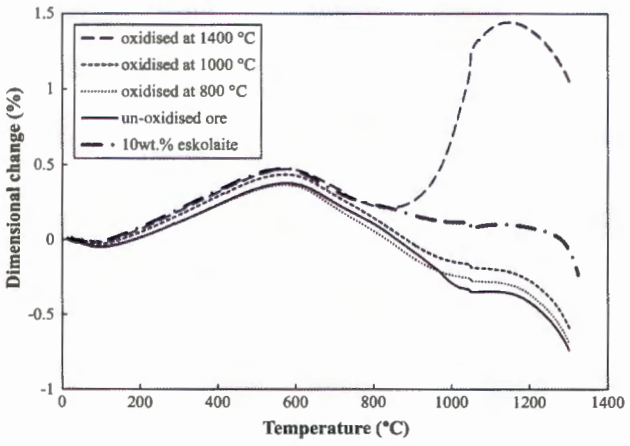

Fig. 9. The average dimensional changes of pellets made from pre-oxidised ore (800 °C, 1000 °C and 1400 °C), which were pre-reduced in situ (primary *y*-axis), as well as the average dimensional change of pellets that contained 10 wt.% pure Cr_2O_3 (eskolaite), pre-reduced in situ (secondary *y*-axis).

The curve of pellets made from the un-oxidised ore containing 10 wt.% Cr_2O_3 and the curve of pellets made from pre-oxidised ore at 1400 °C were not a perfect match, most likely since the matrices of the two pellet types were different from one another, i.e. un-oxidised ore containing Cr_2O_3 in the one pellet type, while the other pellet type contained pre-oxidised ore. However, the tendency of Cr_2O_3 to reduce the shrinkage during in situ pre-reduction at temperatures >750 °C at least provided some preliminary evidence that the presence of Cr_2O_3 caused the pellets to expand at temperatures >750 °C. The afore-mentioned postulation must still be proven in future and should be regarded as an important future perspective.

3.8. Potential Cr(VI) formation

Ferrochromium production from chromite ores occurs at high temperatures under a reducing environment. However, it is impossible to completely exclude oxygen from all high temperature process steps and, although completely unintended, the possibility arises for the formation of small amounts of Cr(VI) species. Certain Cr(VI) species are regarded as carcinogenic, with specifically airborne exposure to these Cr(VI) species being associated with cancer of the respiratory system (Beaver et al., 2009; Thomas et al., 2002). It is therefore important to quantify the amount of Cr(VI) that could be formed if chromite ore is pre-oxidised prior to pre-reduction. For this purpose, several samples of metallurgical grade chromite ore were pre-oxidised in the temperature range 800–1400 °C. The results indicated that 0.4–1 μg Cr(VI) per gram pre-oxidised ore (μg/g or g/metric ton) is formed during pre-oxidation. These Cr(VI) levels are substantially lower than the Cr(VI) content reported for typical semi-closed SAF FeCr furnace off-gas, which varies between 5 and 7000 μg/g (g/metric ton) (Gericke, 1995). The substantially lower Cr(VI) levels in this pre-oxidised ore, than that reported in furnace off-gas, can most likely be attributed to metallurgical grade chromite ore not being milled prior to pre-oxidation, which limited the surface area exposed to oxidation. Milling prior to pre-oxidation would increase the risk of the Cr(VI) becoming airborne, which increases the risk of inhalation.

4. Conclusions

The results presented prove that the pre-oxidation of chromite ore prior to milling, agglomeration and pre-reduction will significantly enhance the level of chromite pre-reduction achieved in the pelletised chromite pre-reduction process. Enhanced pre-reduction could have a corresponding positive effect on the SEC and lumpy carbonaceous material required for smelting in the SAF during FeCr production. By pre-oxidising the case study chromite ore in the temperature range of 800–1100 °C, the level of achievable chromite pre-reduction was improved, with pre-oxidation at 1000 °C established as being the optimum temperature. Theoretically, the improvement in pre-reduction correlates with an 8.5% improvement in the SEC (from ~2.4 to ~2.2 MW h/t) and a 14% decrease (from ~99.5 to ~85.5 kg/t pellets) in the amount of lumpy carbonaceous material required during SAF smelting. However, pre-oxidation temperatures above 1100 °C resulted in decreased levels of pre-reduction with pre-oxidation temperatures higher than 1200 °C resulting in pre-reduction levels even lower than the pre-reduction level obtained by utilising un-oxidised ore. Scanning electron microscopy and X-ray map images indicated that by pre-oxidising the chromite ore, Fe from the spinel migrated to the surfaces of the ore particles, which will enhance the pre-reduction of chromite, since iron oxides reduce at relatively low temperatures. X-ray diffraction analyses provided

evidence of the formation of free Cr_2O_3 (eskolaite) at pre-oxidation temperatures exceeding 1100 °C. According to thermo-chemical calculations, the reduction of Cr_2O_3 by solid C requires a higher temperature compared to chromite, and therefore the decreased pre-reduction if the ore is pre-oxidised >1100 °C.

Pre-oxidation of the chromite ore decreases the pellet compressive and abrasion strengths noticeably, which could result in the generation of fines, which is negative for SAF FeCr production. However, the decreased pellet strength will be significantly mitigated by the presence of a thin oxidative outer layer on the industrially produced pre-reduced pellets, which can further be mitigated if an optimum clay binder is selected.

Small amounts of Cr(VI) can form during the pre-oxidation of the chromite ore; however, these levels were well below that of current fine FeCr waste materials. If this process is implemented on an industrial scale, appropriate preventative measures need to be taken to prevent the negative health effects of Cr(VI).

The effect of varying chromite ore composition was not investigated as part of this work. However, since it is well known that varying ore composition and various additives can affect chromite pre-reduction, it can be expected that the responses reported in this paper could differ if ores with different compositions are considered. Therefore, an investigation to assess the effect of varying ore composition should be regarded as an important future perspective. However, the basic mechanism reported here, i.e. optimisation of pre-oxidation conditions to maximise Fe migration from the spinel to the surfaces of the ore particles and minimisation of the formation of free Cr_2O_3 (eskolaite), should remain constant to achieve maximum chromite pre-reduction.

The possible financial benefit of the alternative FeCr production process described in this paper can only be determined by means of a comprehensive techno-economic feasibility investigation, which should be considered as an important future perspective.

Intellectual property

The work presented in the paper is based on a PCT international patent application (application number PCT/IB2013/056313), with priority date 1 August 2013.

Acknowledgements

The financial assistance of the South African National Research Foundation (NRF) towards the studies of E.L.J. Kleynhans is hereby acknowledged. Opinions expressed and conclusions arrived at are those of the authors and are not necessarily to be attributed to the NRF. The authors also thank Glencore Alloys South Africa for partial support of the research.

References

Abubakre, O.K., Murian, R.A., Nwokike, P.N., 2007. Characterization and beneficiation of Anka chromite ore using magnetic separation process. J. Miner. Mater. Charact. Eng. 6, 143–150. http://dx.doi.org/10.4236/jmmce.2007.62012.

Barnes, A.R., Finn, C.W.P., Algie, S.H., 1983. The prereduction and smelting of chromite concentrate of low chromium-to-iron ratio. J. Southern Afric. Inst. Min. Metall., 49–54

Beaver, L.M., Stemmy, E.J., Constant, S.L., Schwartz, A., Little, L.G., Gigley, J.P., Chun, G., Sugden, K.D., Ceryak, S.M., Patierno, S.R., 2009. Lung injury, inflammation and Akt signaling following inhalation of particulate hexavalent chromium. Toxicol. Appl. Pharmacol. 235, 47–56. http://dx.doi.org/10.1016/j.taap.2008.11.018.

Beukes, J.P., Dawson, N.F., van Zyl, P.G., 2010. Theoretical and practical aspects of Cr (VI) in the South African ferrochrome industry. J. Southern Afric. Inst. Mining Metall. 110, 743–750.

Bondioli, F., Ferrari, A.M., Leonelli, C., Manfredini, T., Linati, L., Mustarelli, P., 2000. Reaction mechanism in alumina/chromia (Al2O3–Cr2O3) solid solutions obtained by coprecipitation. J. Am. Ceram. Soc. 83, 2036–2040. http://dx.doi.org/10.1111/j.1151-2916.2000.tb01508.x.

Cramer, L.A., Basson, J., Nelson, L.R., 2004. The impact of platinum production from UG2 ore on ferrochrome production in South Africa. J. South Afric. Inst. Mining Metall. 104, 517–527.

Ding, Y.L., Warner, N.A., 1997a. Catalytic reduction of carbon-chromite composite pellets by lime. Thermochim. Acta 292, 85–94.

Ding, Y.L., Warner, N.A., 1997b. Reduction of carbon–chromite composite pellets with silica flux. Ironmaking Steelmaking 24, 283–287.

Dionex Corporation, 2003. Determination of Hexavalent Chromium in Drinking Water Using Ion Chromatography. Application Update 144, LPN 1495. Corporation, D., Sunnyvale, California, USA.

Dionex Corporation, 2011. Sensitive Determination of Hexavalent Chromium in Drinking Water. Application Update 179, LPN 2772. Corporation, D., Sunnyvale, California, USA.

Du Preez, S.P., Beukes, J.P., van Zyl, P.G., 2015. Cr(VI) generation during flaring of CO-rich off-gas from closed ferrochromium submerged arc furnaces. Metall. Mater. Trans. B 46B, 1002–1010. http://dx.doi.org/10.1007/s11663-014-0244-3.

Gasik, M., 2013. Handbook of Ferroalloys – Theory and Technology. Butterworth-Heinemann, Oxford. http://dx.doi.org/10.1016/B978-0-08-097753-9.01001-7, p. 520.

Gericke, W.A., 1995. Environmental aspects of ferrochrome production., The Seventh International Ferroalloys Congress (INFACON VII). Trondheim, Norway, pp. 131–140.

Glastonbury, R.I., Beukes, J.P., Van Zyl, P.G., Sadiki, L.N., Jordaan, A., Campbell, H.M., Stewart, H.M., Dawson, N.F., 2015. Comparison of physical properties of oxidative sintered pellets produced with UG2 or metallurgicalgrade South African chromite: a case study. J. Southern Afric. Inst. Mining Metall. 115, 699–706. http://dx.doi.org/10.17159/2411-9717/2015/v115n8a6.

Glastonbury, R.I., van der Merwe, W., Beukes, J.P., van Zyl, P.G., Lachmann, G., Steenkamp, C.J.H., Dawson, N.F., Stewart, H.M., 2010. Cr(VI) generation during sample preparation of solid samples – a chromite ore case study. Water SA 36, 105–110.

Holappa, L., 2010. Towards sustainability in ferroalloys production. In: Vartiainen, A. (Ed.), The Twelfth International Ferroalloys Congress (INFACON XII). Outotec Oyj, Helsinki, Finland, pp. 1–10.

ICDA, 2013. Statistical Bulletin 2013, Paris, France.

Kleynhans, E.L.J., Beukes, J.P., Van Zyl, P.G., Kestens, P.H.I., Langa, J.M., 2012. Unique challenges of clay binders in a pelletised chromite pre-reduction process. Miner. Eng. 34, 55–62. http://dx.doi.org/10.1016/j.mineng.2012.03.021.

Loock-Hattingh, M.M., Beukes, J.P., van Zyl, P.G., Tiedt, L.R., 2015. Cr(VI) and conductivity as indicators of surface water pollution from ferrochrome production in South Africa: four case studies. Metall. Mater. Trans. B 46B, 2315–2325. http://dx.doi.org/10.1007/s11663-015-0395-.

Loock, M.M., Beukes, J.P., van Zyl, P.G., 2014. A survey of Cr(VI) contamination of surface water in the proximity of ferrochromium smelters in South Africa. Water SA 40, 709–716. http://dx.doi.org/10.4314/wsa.v40i4.16.

McCullough, S., Hockaday, S., Johnson, C., Barza, N.A., 2010. Pre-reduction and smelting characteristics of Kazakhstan ore samples. In: Vartiainen, A. (Ed.), The Twelfth International Ferroalloys Congress (INFACON XII). Outotec Oyj, Helsinki, Finland, pp. 249–262.

Misra, K.C., 2000. Chromite Deposits, Understanding Mineral Deposits. Springer, Netherlands. http://dx.doi.org/10.1007/978-94-011-3925-0_5, pp. 238-272.

Naiker, O., 2007. The development and advantages of Xstrata's Premus Process, The Eleventh International Ferroalloys Congress (INFACON XI), New Delhi, India, pp. 112–118.

Naiker, O., Riley, T., 2006. Xstrata alloys in the profile. In: Jones, R.T. (Ed.), South African Pyrometallurgy 2006. SAIMM, Johannesburg, South Africa, pp. 297–306.

Neizel, B.W., Beukes, J.P., van Zyl, P.G., Dawson, N.F., 2013. Why is CaCO3 not used as anadditive in the pelletised chromite pre-reduction process? Miner. Eng. 45, 115–120. http://dx.doi.org/10.1016/j.mineng.2013.02.015.

Niayesh, M.J., Fletcher, G.W., 1986. An assessment of smelting reduction processes in the production of Fe-Cr-C alloys, The Fourth International Ferroalloys Congress (INFACON IV), Sao Paulo, Brazil, pp. 115–123.

Niemelä, P., Krogerus, H., Oikarinen, P., 2004. Formation, characterisation and utilisation of CO-gas formed inferrochrome smelting. The Tenth International Ferroalloys Congress (INFACON X). SAIMM, Cape Town, South Africa, pp. 68–77.

OCC, 2014. Beneath the Surface – Uncovering the Economic Potential of Ontario's Ring of Fire. Commerce, O.C.o., Ontario, Canada.

Outotec, 2015. Ferrochrome. <http://www.outotec.com/en/Products-services/Ferrous-metals-and-ferroalloys-processing/Ferrochrome/>, (accessed 06.07.15).

Pettine, M., Capri, S., 2005. Digestion treatments and risks of Cr(III)-Cr(VI) interconversions during Cr(VI) determination in soils and sediments – a review. Anal. Chim. Acta 540, 231–238. http://dx.doi.org/10.1016/j.aca.2005.03.040.

Riekkola-Vanhanen, M., 1999. Finnish expert report on best available techniques in ferrochromium production, Helsinki, Finland.

Roine, A., 2009. HSC Chemistry 7.0 User's Guide: Chemical reaction and Equilibrium Modules.

Schneider, T., Jensen, K.A., 2008. Combined single-drop and rotating drum dustiness test of fine to nanosize powders using a small drum. Annals Occup. Hygiene 52, 23–34. http://dx.doi.org/10.1093/annhyg/mem059.

Schwertmann, U., 2008. Iron oxides. In: Chesworth, W. (Ed.), Encyclopedia of Earth Sciences Series. Springer, Dordrecht, Netherlands, p. 898.

Sundar Murti, N.S., Shah, V.L., Gadgeel, V.L., Seshadri, V., 1983. Effect of lime addition on rate of reduction of chromite by graphite. Institution of Mining and Metallurgy (Great Britain) Transactions. Section C, Miner. Process. Extract. Metall. 98C, C172–C174.

Takano, C., Zambrano, A.P., Nogueira, A.E.A., Mourao, M.B., Iguchi, Y., 2007. Chromites reduction reaction mechanisms in carbon-chromites composite agglomerates at 1 773 K. ISIJ Int. 47, 1585–1589.

Thomas, D.H., Rohrer, J.S., Jackson, P.E., Pak, T., Scott, J.N., 2002. Determination of hexavalent chromium at the level of the California Public Health Goal by ion chromatography. J. Chromatogr. A 956, 255–259. http://dx.doi.org/10.1016/S0021-9673(01)01506-0.

Van Deventer, J.S.J., 1988. The effect of additives on the reduction of chromite by graphite. Thermochim. Acta 127, 25–35.

Visser, H., 2005. Status of, and challenges in, ferrochrome production. Mine Metallurgical Managers' Association of South Africa Circular No. 1/2005, pp. 47–72.

Zhao, B., Hayes, P.C., 2010. Effects of oxidation on the microstructure and reduction of chromite pellets. In: Vartiainen, A. (Ed.), The Twelfth International Ferroalloys Congress (INFACON XII). Outotec Oyj, Helsinki, Finland, pp. 263–273.

CHAPTER 6: ARTICLE 4

TECHNO-ECONOMIC FEASIBILITY OF A PRE-OXIDATION PROCESS TO ENHANCE PRE-REDUCTION OF CHROMITE

6.1 Authors list, contributions and consent

Authors list

E.L.J. Kleynhans[a,b], J.P. Beukes[a], P.G. Van Zyl[a] and J.I.J. Fick[b]

[a] Chemical Resource Beneficiation, North-West University, Potchefstroom Campus, Private Bag X6001, Potchefstroom 2520, South Africa

[b] Centre for Research and Continued Engineering Development – CRCED Vaal, Faculty of Engineering, Vaal Triangle Campus, North-West University, P.O. Box 3184, Vanderbijlpark, 1900, South Africa

Contributions

Contributions of the various co-authors were as follows:

The bulk of the work, i.e. the development of the necessary procedures and experimental/numerical models, execution of the empirical and numerical investigation to address the research problem, relevant data processing and interpretation, research and writing of the scientific paper, was performed by the candidate, ELJ Kleynhans. Prof JP Beukes (supervisor), Dr PG van Zyl (co-supervisor) and Prof JIJ Fick assisted in writing the article by sharing conceptual ideas and recommendations with regard to the procedures and experimental/numerical model development, data processing, interpretation and results and discussion. The article resulted from preliminary work conducted during the candidates (ELJ Kleynhans) Master of Engineering (MEng) in Development and Management Engineering degree at the North-West University, Potchefstroom Campus of which Prof JIJ Fick and Prof JP Beukes were supervisor and co-supervisor, respectively.

Consent

All the co-authors that contributed to the article presented in this chapter have been informed that the article will form part of the candidates PhD, submitted in article format, and have granted permission that the article may be used for the purpose stated.

6.2 Formatting and current status of the article

This article was accepted for publication in the Journal of the South African Institute of Mining and Metallurgy on the 12th of July 2016. It is presented in Chapter 6 of this thesis as it was accepted by the selected journal after addressing and implementing the reviewer's comments. The journals details can be found at http://www.saimm.co.za/publications/journal-papers (Date of access: 30 November 2016).

Techno-economic feasibility of a pre-oxidation process to enhance pre-reduction of chromite

E.L.J. Kleynhans[a,b], J.P. Beukes[a,*], P.G. van Zyl[a], J.I.J. Fick[b]

[a] *Chemical Resource Beneficiation, North-West University, Potchefstroom Campus, Private Bag X6001, Potchefstroom, 2520, South Africa*

[b] *Centre for Research and Continued Engineering Development – CRCED Vaal, Faculty of Engineering, Vaal Triangle Campus, North-West University, P.O. Box 3184, Vanderbijlpark, 1900, South Africa*

* Corresponding author. Tel.: +27 82 460 0594; fax: +27 18 299 2350.
E-mail address: paul.beukes@nwu.ac.za (J.P. Beukes)

Synopsis

Ferrochrome (FeCr) is vital to the production of stainless and high-alloy ferritic steels, since it is the only source of new Cr units. FeCr production is an energy intensive process. The pelletised chromite pre- reduction process is most likely the FeCr production process with the lowest specific electricity consumption (SEC), i.e. MWh/ton, currently in operation. However, due to increases in costs, efficiency and environmental pressures, FeCr producers applying the afore-mentioned process are still attempting to achieve even lower overall energy consumption. Recently, it was proven that pre-oxidation of chromite ore, prior to pelletised pre-reduction, significantly decreases both the SEC and lumpy carbonaceous reductants required for furnace smelting. This paper presents the first attempt at conceptualising the techno-economic feasibility of integrating chromite pre-oxidation into the pre-reduction process. Financial modelling yielded a net present value (NPV) at a 10% discount rate of

~ZAR 900 million and an internal rate of return (IRR) of ~30.5% after tax, suggesting that the implementation of pre-oxidation prior to pelletised pre-reduction may be viable from a financial standpoint. Sensitivity analysis indicated that the parameter with the greatest influence on project NPV and IRR is the level of pre-reduction achieved. This indicated that the relationship between maintaining the optimum pre-oxidation temperature and the degree of pre-reduction achieved is critical to maximise process efficiency.

Keywords: Chromite pre-reduction, solid-state reduction of chromite (SRC), pre-oxidation of chromite, discounted cash flow (DCF) model, techno-economic feasibility

Introduction

Stainless steel is a crucial alloy in modern society. Virgin chromium (Cr) units used in the manufacturing of stainless steel are obtained from ferrochrome (FeCr) – a relatively crude alloy consisting predominantly of Cr and iron (Fe) (Murthy et al., 2011, Beukes et al., 2012). FeCr is mainly produced during the pyrometallurgical carbo-thermic reduction of chromite ore, mainly in submerged arc furnaces (SAFs) and direct current arc furnaces (DCFs) (Neizel et al., 2013, Beukes et al., 2010, Dwarapudi et al., 2013). In the afore-mentioned processes, electricity supplies the energy required to heat, smelt and reduce the chromite ore to the metallised state (Pan, 2013). FeCr production is an energy intensive process, with specific electricity consumption (SEC), i.e. MWh/ton FeCr produced, varying from 2.4 to more than 4.0 MWh/ton FeCr produced, depending on the process applied (Pan, 2013, Neizel et al., 2013). Daavittila et al. (2004) stated that the typical operational costs of FeCr smelters can be divided into four cost categories, i.e. chromite ore (30%), carbonaceous reductant (20%), electricity (30%) and other production costs (20%). This makes electricity consumption the joint largest factor that influences operational costs in FeCr production. Beukes et al. (2010) presented an overview of processes utilised for FeCr production, referring specifically to the South African FeCr industry. However, similar processes are also applied internationally. According to this review (Beukes et al., 2010), FeCr is produced via (i) conventional semi-closed/open submerged arc furnace (SAF) operation, with bag filter off-gas treatment; (ii) closed SAF operation that usually utilises oxidised sintered pelletised feed, with venturi scrubbing of off-gas; (iii) closed SAF operation consuming pre-reduced pelletised feed, with venturi scrubbing of off-gas; and (iv) closed direct current (DC) arc furnace operation, with venturi scrubbing of off-gas. Until now, these processing options have allowed for economical FeCr production, particularly in

countries with local chromite resources (Daavittila et al., 2004). Although equipment has been technologically advanced and modern automation systems implemented, there still are some significant technological limitations in the smelting of chromite, i.e. (i) the efficient use of energy (i.e. electricity and chemical energy in the form of reductants) and the utilisation of secondary energy produced (e.g. CO-rich off-gas, radiation heat), (ii) increased use of lower cost raw materials through advanced beneficiation and agglomeration, or corresponding technologies, (iii) enlarged production units in order to benefit from the large-scale economies, and (iv) higher degrees of automation to improve operation (Daavittila et al., 2004). These limitations, coupled with the fact that SAF and DC smelting operations can be regarded as having reached the 'mature' phase of its evolutionary development, indicate that FeCr producers and their main customers, the stainless steel producers, should consider more cost and quality effective production of Cr units (Slatter, 1995, Holappa, 2010). FeCr producers face significant challenges that will require innovative advances in FeCr production process technologies (Ugwuegbu, 2012), e.g. a downward trend in FeCr prices, increasing awareness of environmental impacts and working conditions, increasing electricity costs (and availability thereof in some countries) and carbon footprint reduction requirements (Daavittila et al., 2004).

In the past, various measures to improve FeCr production with the SAF process have been investigated (Kapure et al., 2010, Daavittila et al., 2004, Slatter, 1995, Goel, 1997, Ugwuegbu, 2012). These developments mainly included pre-reduction and preheating methods in order to improve Cr recoveries and minimise smelting costs. The pelletised chromite pre-reduction process (commercially known as the Premus process), applied by two Glencore Alloys FeCr smelters in South Africa (RSA) (with six large smelting SAFs), is considered to be the FeCr production process option with the lowest

SEC currently in operation (Kleynhans et al., 2012). Similar smelters are being commissioned in China, but no information regarding these operations is currently available in the peer-reviewed public domain. The SEC of the pelletised chromite pre-reduction process is approximately 20% lower than that of its nearest rival, i.e. the SAF smelting process with oxidised sintered pellets as furnace feed (commercially referred to as the Outotec technology) (Neizel et al., 2013). The pelletised chromite pre-reduction process also has some disadvantages, as indicated by Mohale (2014), i.e. the higher capital cost and the extensive operational control that are required due to the variation in pre-reduction levels and carbon contents of the pre-reduced pelletised furnace feed material.

In view of the previously mentioned challenges faced by FeCr producers and regardless of the lower SEC of the pelletised chromite pre-reduction process, it is apparent that smelters applying the afore-mentioned process would benefit from a process improvement capable of achieving even lower SEC. Beukes et al. (2015) developed a new process during which chromite ore is subjected to oxidation before it is used as feed material for pre-reduction that was patented, while Kleynhans et al. (2015) reported on this patent in the peer-reviewed public domain. In principle, the afore-mentioned authors found that pre-oxidation enhanced the susceptibility of the chromite spinel to be pre-reduced, mainly by Fe liberation and preventing the release of chromium(III)oxide (Cr_2O_3) from the spinel (Beukes et al., 2015, Kleynhans et al., 2015). As indicated by Niayesh and Fletcher (1986), an increase in the level of pre-reduction will result in a decrease in SEC. It is claimed by Beukes et al. (2015) and Kleynhans et al. (2015) that a reduction in SEC of ~8.5% can be achieved by the afore-mentioned patented process. Therefore, the aim of this paper was to investigate the economic feasibility of the patented pre-oxidation process applied as a pre-treatment to

the pelletised chromite pre-reduction process and to evaluate the extent of the impact of integration of this process on the economics of a typical FeCr smelter applying pelletised chromite pre-reduction. Through an analysis of cost efficiency for various cost model parameter options, as well as their subsequent development within a comprehensive cost model and discounted cash flow (DCF) model, the long-term feasibility of integrating such a pre-oxidation process with an existing smelter applying the pelletised chromite pre-reduction is evaluated.

Feasibility study backdrop

RSA holds the majority of global chromite reserves (Beukes et al., 2012, Merafe-Resources, 2012, Creamer, 2013). The majority of RSA's chromite ore is relatively friable. It is therefore common to only recover 10 to 15% lumpy ore (15 mm < typical size range < 150 mm) and 8 to 12% chip/pebble ores (6 mm < typical size range < 15 mm) during the beneficiation process employed after chromite mining. The remaining ore would typically be in the < 6 mm fraction, which would usually be crushed and/or milled to < 1 mm and then upgraded utilising gravity separation techniques (e.g. spiral concentrators) to ~45% Cr_2O_3 content. This upgraded < 1 mm ore is commonly known as metallurgical grade chromite ore (Glastonbury et al., 2010). Additionally, upgraded fine (< 1mm) UG2 process residue from the platinum group metals (PGMs) industry is also available as chromite feed material for the South African FeCr industry (Cramer et al., 2004).

Effective SAF smelting operation desires a permeable burden to ensure uniform flow of reduction gases and smooth furnace operation (Dwarapudi et al., 2013). The use of fine chromite ore in SAFs is limited, since fine materials increase the tendency of the surface layer of the SAF burden to sinter. This traps evolving process gas, which

can result in so-called bed turnovers or blowing of the furnace that could result in damage to equipment or injury to personnel. A process that can accommodate fine ore is therefore required, typically one where an agglomeration step (e.g. pelletisation) prior to feeding into the SAF is employed (Kleynhans et al., 2012, Beukes et al., 2010).

RSA, at present, has 14 separate FeCr production facilities with a combined production capacity in the region of ~5.2 million t/a (Beukes et al., 2012, Jones, 2015). The abundant chromite resources and comparatively low historic cost of electricity have contributed to RSA maintaining the dominant position in the international FeCr industry, contributing on average 44.5% to the global FeCr production in the period 2000 to 2011. However, in 2012, it produced only 32% of the world's output, as production decreased by 30% from 2007, with China becoming the largest FeCr producer (ICDA, 2013b). A number of factors led to this major downturn in the RSA FeCr industry. Firstly, RSA is facing several internal challenges that have negatively impacted the manufacturing ability and production cost of FeCr producers. Historically, the country benefited from favourable, inexpensive logistics and relatively cheap labour. In the present day, this is no longer the case, since RSA is experiencing energy and labour problems. By the end of 2007, the electricity demand of RSA caught up with its electricity generating capacity. In order to avoid destabilisation of the national electricity grid, rolling blackouts were implemented. Erosion of surplus generation capacity led to a dramatic increase in the nominal price of electricity, increasing by ~245% from 2007 to 2013 (Eskom, 2012). In 2012, Eskom, the country's state-controlled energy supplier, realised that it would not be able to support total electricity demand and agreed to reimburse FeCr smelters to not use already contracted electricity supply and to temporarily shut down their furnaces. This lack of energy-generation capacity is the result of years of underinvestment in the electricity sector. FeCr

smelters, facing low prices for the alloy, welcomed the proposition and started to shut down their furnaces. Anecdotal evidence indicated that it was more profitable for them to sell energy back to Eskom than to produce FeCr. In addition, in order to deal with this major energy crisis, Eskom announced in early 2013 that it needed ZAR50 billion (approximately US$5 billion) more than planned to meet funding needs in the next five years until 2018. This was in addition to the ZAR225 billion shortfall in revenue due to higher coal prices and increased capex expenses. Eskom needed to invest immensely in new capacity, but the National Electricity Regulator of RSA (NERSA) refused the price increase of 16% per year requested by Eskom for the multiyear price determination period of 2013 to 2018. Instead, NERSA granted Eskom permission to raise the energy tariff by 8% per annum for the next five years, to finance investments in new electricity capacity. Furthermore, Eskom struggles to find the coal it requires. Coal production has to rise from the current 254 million t/a to more than 320 million t/a by 2020 to satisfy the state-owned power utility's demand. Finally, as a result of the first factor, RSA's main FeCr buyer, i.e. China, had increased domestic FeCr production and reduced imports thereof, taking advantage of the increasing demand for FeCr and filling the gap in the market. Lower shipping costs, brought about by the slowdown in the world economy, made geographical positioning of smelters less relevant. Therefore, at present, RSA ships less FeCr to China, which now imports more chromite ore from RSA, with China smelting it locally and supplying most of its own FeCr to its own stainless steel industries (ICDA, 2013a, ICDA, 2013b).

Considering the above-mentioned background, the South African FeCr industry is an ideal economic environment to serve as the backdrop for this feasibility study, i.e. i) RSA holds the majority of the world's chromite resources, ii) the ore is friable which

necessitates an agglomeration process step and iii) the energy situation also justifies exploring new FeCr production technologies to reduce SEC.

Process options

Although the pre-oxidation process prior to pre-reduction has been patented (Beukes et al., 2015), the pre-oxidation process prior to pre-reduction has not yet been applied on an industrial scale. The process therefore needs to be matched with appropriate equipment. Equipment used in currently applied and previously attempted pre-treatment options could be considered to serve for this purpose, i.e.:

I) Outotec's steel belt sintering process is the only commercially applied FeCr process where oxidation as a pre-treatment method prior to smelting in the SAF is utilised. The pre-oxidation of un-agglomerated chromite ore prior to pre-reduction (solid state reduction of chromite) must not be confused with oxidation prior to smelting. Furthermore, reduction, as taking place during smelting in an SAF when the ore is completely reduced to the zero oxidation or metal state, must not be confused with pre-reduction where the ore is only partially reduced. Molten or liquid materials are formed during the smelting reduction process in contrast to the absence of molten or liquid phases being formed during the pre-reduction process, hence the alternative name "solid state reduction of chromite". The primary raw materials in the Outotec steel belt sintering process, which has been the most commonly applied process over the last decade in the South African FeCr industry, are ore fines, a refined clay binder, and fine coke. The ore and coke are wet-milled in a ball mill up to ~90% of the particles smaller (d_{90}) than 108 μm (Glastonbury et al., 2015) and de-watered in capillary-type ceramic filters. The de-watered material is mixed with a clay binder and pelletised in a drum pelletiser before finally being sintered in the steel belt sintering furnace. The fixed

carbon (FC) content (from coke fines) added in the steel belt sintering feed mixture is low (~1-2%) compared to the FC content of the feed mixture for pre-reduction (~12.5-15%). The sintering process is basically an oxidative process, during which the carbon present in the pellets is oxidised to sinter the pellets (Beukes et al., 2010, Glastonbury et al., 2015).

II) In rotary hearth furnace technology, normally applied as a preliminary heating or reduction step prior to smelting, ore, reductants, and fluxes are milled to less than typically 100 μm before being blended, mixed, and fed into a pelletising plant. The green pellets are dried using exhaust gas from the rotary hearth furnace. The furnace operates continuously and the pellets are sintered, reduced, and cooled in controlled zones with a maximum zone temperature of 1450 °C (Slatter, 1995). The reduction occurs in stages in different zones of the furnace. Additional hot air is introduced into the rotary hearth furnace to control the temperature and the composition of the atmosphere in order to provide conditions conducive to the optimal reduction of chromite and minimisation of re-oxidation. Once the material has passed through the rotary hearth furnace, it is discharged and can be cooled using various methods. Energy for the sintering and pre-reduction zones can be provided by the oxidation of the CO gas obtained from the exhaust gas of SAFs (Slatter, 1995). By operating this furnace with an oxidising atmosphere, it could be applied as a pre-oxidation process.

III) Fluidised beds are ideally suited for the processing of finely sized raw materials (Luckos et al., 2007). Since the fluidised bed can be used as a pre-heater for chromite, it can also be considered as a means to pre-oxidise ore prior to pre-reduction. Laboratory-scale pre-heating tests with chromite ores and coals were carried out in a fluidised bed facility at Lurgi Metallurgie, which was followed by a pilot-scale test in a four-stage flash preheater at Polysius AG. These tests confirmed that chromite ores and

fluxes can be thermally treated up to a gas temperature of 1 150°C without succumbing to the forces of attrition and producing fines, or forming low-melting point phases and agglomerating. Denton et al. (2004) stated that the best option from an economic point of view is to use CO-rich furnace off-gas to pre-heat the chromite and fluxes to 1 200°C.

IV) The rotary kiln serves as the process unit for a number of pre-heating and pre-reduction process technologies. In principle, rotary kilns can be effectively used for preheating charge by making use of CO-rich furnace off-gas. The use of a rotary kiln for pre-reduction of chromite ore was developed and applied on an industrial scale by three companies, i.e. Outokumpu, Showa Denko and Krupp/MS&A (McCullough et al., 2010, Ugwuegbu, 2012). Outokumpu used a rotary kiln for preheating pellets up to 1 000 °C before continuously feeding the pre-heated pellets to a closed SAF. Outokumpu studied its process for approximately ten years on laboratory and pilot scale, as well as for two years in a commercial-scale operation. The process consisted of a rotary kiln with a length of 55 m and an inner diameter of 2.3 m (Daavittila et al., 2004). The process involved grinding and pelletising of ore fines, followed by sintering of green pellets that were pre-reduced before smelting. The ore and coke fines used by Outokumpu were wet-ground to approximately d35 of 37 µm and then pelletised up to approximately 15 mm diameter. The bulk of the fuel for sintering and pre-reduction of the pellets was provided by CO off-gas from closed SAFs (Goel, 1997). Showa Denko's process that pre-reduces pellets is currently still in use. It was installed by Consolidated Metallurgical Industries in RSA in the mid-1970s. This was the first commercial pre-reduction process for chromite. In this process, chromite ore fines are milled to d_{90} <75µm, pelletised with coke as reductant, and fired in a rotary kiln to approximately 1 400 °C. The kiln is heated by a pulverised coal burner. The pellets with approximately 40 to 60% metallisation of Cr and Fe are discharged into an SAF for

final smelting (Naiker, 2007, Naiker and Riley, 2006). To address some of the apparent weaknesses of the Showa Denko K.K. (SDK) process, Krupp commenced development of a rotary kiln pre-reduction process in 1984, based upon their CODIR process. In this process, chromite ore and coal fines react in a rotary kiln at temperatures approaching 1 450°C to produce a semi-solid product consisting of highly metallised FeCr, slag, gangue and char. High temperature and intimate contact between the chromite grains and carbon are necessary over the entire residence time in the kiln in order to achieve a high degree of metallisation (>90%). For this purpose, the burden is transformed into a semi-solid state with a combination of molten and solid phases, to allow for only a small portion of the surface of the metallised phase to be exposed to air without macroscopic phase separation occurring (McCullough et al., 2010). The Premus process, currently applied by Glencore Alloys, was developed from the SDK/CMI process. In this process, anthracite or char is used as a reductant instead of coke. Similar to the SDK/CMI process, the raw materials are dry milled, pelletised, pre-heated and fed into a rotary kiln. Pure oxygen and a pulverised carbon fuel (PF) are used to fire the kiln (Basson et al., 2007, Naiker, 2007, Naiker and Riley, 2006, Ugwuegbu, 2012). Kleynhans et al. (2012) indicated that while the pellets are exposed to the high temperatures inside the rotary kiln, the carbon in the outer layer of the pellets is mostly burned off and a partially oxidised outer layer is formed. A small amount of Fe reduction can occur before all the carbon is consumed in this outer layer, which can be re-oxidised again. Oxygen ingress to the core does not take place, since CO gas formed from the carbon inside the pellets produces a positive partial pressure. This positive CO pressure is therefore necessary to prevent re-oxidation of the pellets. If chromite ore is fed into the kiln without a carbon reductant to generate CO, natural oxidation would consequently occur as required for the pre-oxidation process.

The disadvantage of Option I, the Outotec steel belt sintering process, is that the raw materials used, including the ore, are milled and pelletised before being sintered in an oxidising environment. In order to use the oxidised pellets in the pre-reduction process, these pellets would have to be pulverised. The energy and raw materials used to initially pelletise the ore for pre-oxidation would therefore be wasted. The rotary hearth furnace and fluidised-bed processes, Options II and III, offer an interesting alternative; however, although tested on pilot scale, these processes have not yet progressed to successful large-scale operation within the FeCr industry and further development is required. Considering the above-mentioned four options, the one most likely to be implemented by FeCr producers already utilising the pre-reduction process is the option employing a rotary kiln. FeCr producers using chromite pre-reduction are accustomed to kiln operation and would prefer this route as it fits within their current pre-reduction operations culture. It also has an advantage from a maintenance perspective, i.e. employing a kiln with the same diameter for pre-oxidation as the kiln used for pre-reduction. This standardisation of equipment components would reduce spare parts required, thereby lowering capital that is tied up.

Process descriptions

Since it is expected that a counter current rotary kiln will be used if the pre-oxidation process is implemented at a smelter already applying the pelletised chromite pre-reduction process (see discussion in preceding the section), a hypothetical process flow diagram was developed consisting of a rotary kiln and axillary equipment. This flow diagram, together with the flow diagram of the current industrially applied pre-reduction process, is presented in Figures 1A and B, respectively. In the chromite pre-oxidation process (Figure 1A), fine chromite ore is fed into holding silos. The ore is then fed with weigh feeders onto a conveyer and that enters the kiln. The oxidation of the ore in the

rotary kiln is achieved with thermal energy supplied by pulverised coal and/or furnace off-gas at the discharge end of the kilns. A gas fan at the feed end pulls air through the kiln that is sent to a cyclone to remove coarse particles (<1 mm), where after it passes through a bag house to remove finer particles (<30 μm) before being released into the atmosphere (Pšunder, 2012). The pre-oxidised fine chromite ore (OC) is then discharged into a bunker and transported to the pre-reduction raw material storage heaps. The oxidising temperature inside the kiln is controlled by measuring the ore discharge temperature with an optical sensor. The pre-oxidised fine chromite ore is then fed as raw material into the pre-reduction process (Figure 1B), instead of normal chromite ore. The pre-reduction and smelting process flow (Figure 1B) is not discussed here, since various publications have presented detailed discussions (Ugwuegbu, 2012, Naiker, 2007, Naiker and Riley, 2006, Botha, 2003). The off-gas produced during SAF smelting is cleaned through a venturi water scrubbing system and recycled, specifically to the chromite pre-oxidation process, to serve as an energy fuel source.

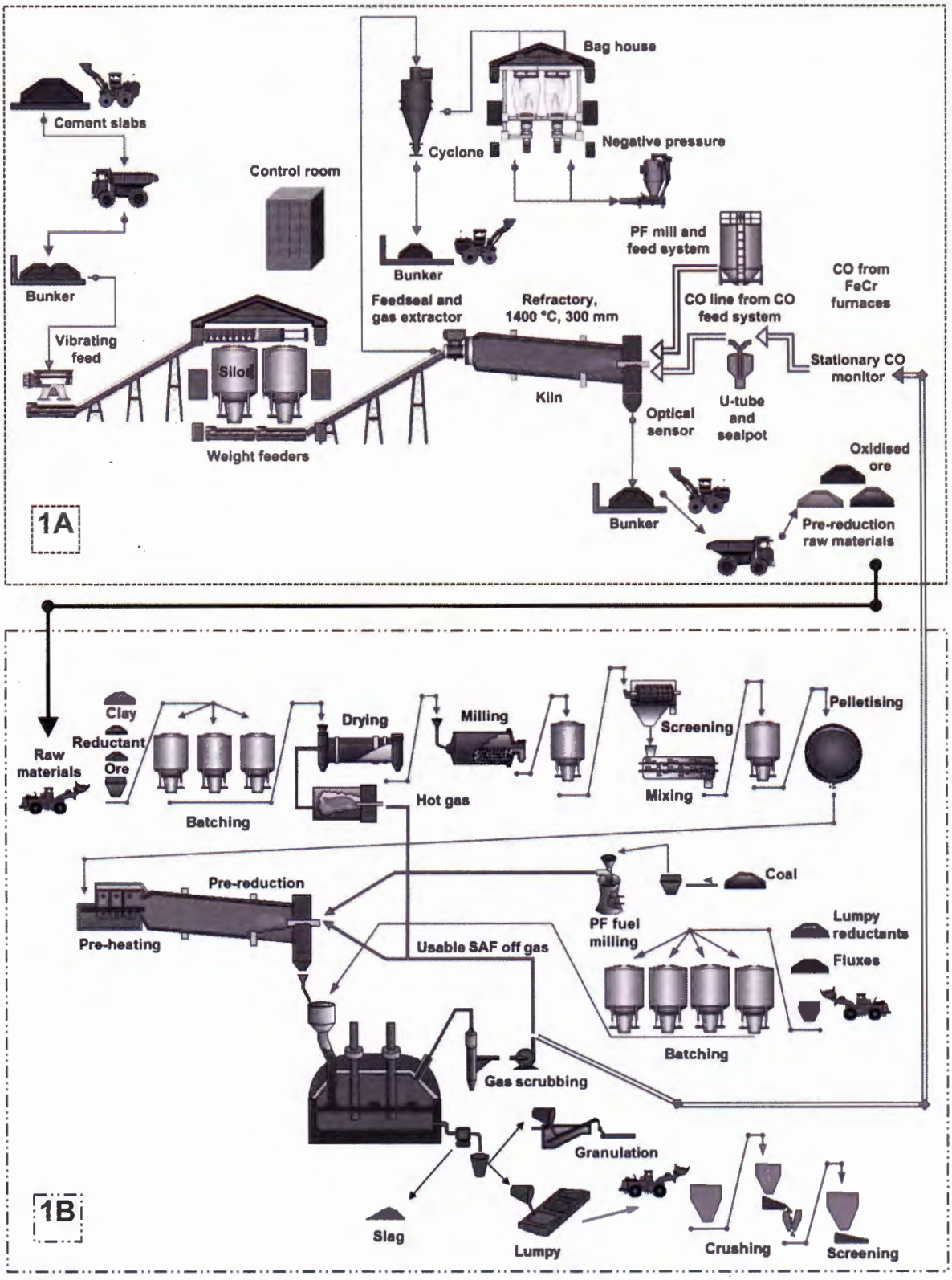

Figure 1-(A) Pre-oxidation process, (B) Pre-reduction process

Methodology

Quantification of process benefits associated with chromite pre-oxidation

From experimental results presented by Kleynhans et al. (2015), it is evident that the level of pre-reduction could be considerably enhanced through the pre-oxidation of chromite ore prior to pre-reduction. The advantages of improved pre-reduction can be observed in several aspects of operation. However, the two main advantages include the decrease in SEC and lumpy carbonaceous reductants required for SAF operation. Niayesh and Fletcher (1986) published a graph of chromite pre-reduction as a function of SEC, for different temperatures of pre-reduced feed material. Kleynhans et al. (2015) reconstructed and empirically fitted the data published by Niayesh and Fletcher (1986) to estimate the improvement in SEC. Furthermore, Kleynhans et al. (2015) also used the fundamental carbon-based metallisation and reduction reactions for chromite presented by Barnes et al. (1983) to calculate the decrease in FC content associated with the lumpy reductants fed into the SAF. If it is assumed that pre-oxidation of the chromite takes place at 1 000°C, the improvements in both the afore-mentioned parameters, i.e. SEC and FC requirement, due to pre-oxidation are presented in Figure 2.

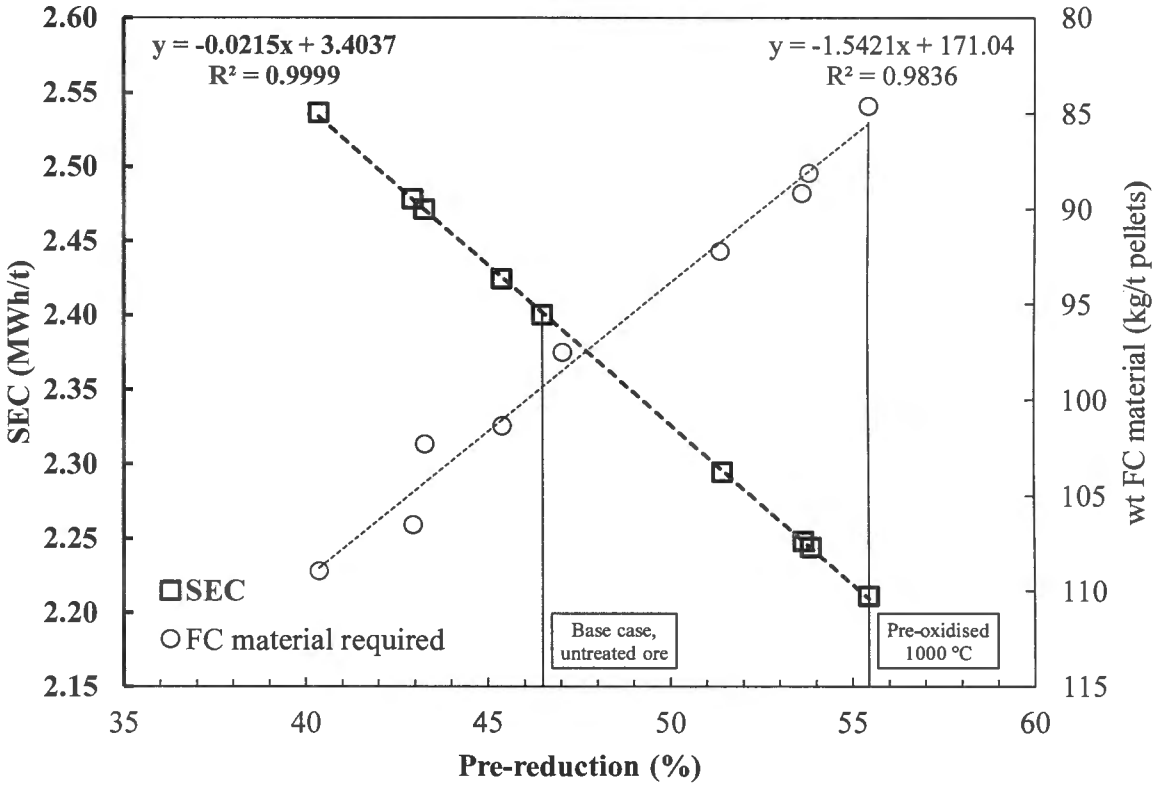

Figure 2-The effect of enhanced pre-reduction by utilising pre-oxidised fine chromite ore (x-axis) on the SEC (primary y-axis), as well as on the weight (wt) FC required per ton pre-reduced pellets (kg/t pellets) (secondary y-axis) (Kleynhans et al., 2015)

From Figure 2 it is evident that less FC is required for smelting in the furnaces with an increase in pre-reduction. Although one could directly calculate the electric energy financial gain from the improved SEC, annual FeCr production capacity and the current price of electricity, this is not a true reflection of the financial advantage that can be achieved. An electric arc furnace is designed according to a specific apparent power (S). However, only a fraction of this power, called the power factor (K_p), is available as electrical energy for smelting. This total available electrical energy, called the active power (P), is a constant and cannot be changed. The production capacity of an

operation is determined by dividing the active power by the SEC. Therefore, since the total energy available cannot be changed, the benefit of improved or lower SEC is observed as an increase in the operation's production capacity. This implies that, as a result of an increase in pre-reduction levels, for the same total available electrical energy, FeCr production is increased.

Cost distribution

The typical cost factors for the FeCr industry in European conditions were presented by Daavittila et al. (2004). According to Biermann et al. (2012), the cost factors for South African FeCr smelters vary to some extent; with chromite ore, reductants and electricity each accounting for 30% of the production costs, while factors such as maintenance, labour and waste disposal account for the remaining 10%. An analysis of South African FeCr input costs conducted by Cartman (2008) differed from Biermann et al. (2012), with chromite ore accounting for 38%, electricity for 18%, reductants and other raw materials for 24% and maintenance, overheads and labour for 20%. The difficulty in interpreting these cost distributions is that in none of these references were/was the process(es) to which the cost distribution was linked, mentioned. Therefore, it can be any of the process combinations mentioned in the 'Introduction' section (Beukes et al., 2010) and cost distribution for different process combinations will certainly vary. In order to conduct the financial modelling, it was important to consider lifecycle costs associated with the implementation of the chromite pre-oxidation process and the cost distribution of the chromite pre-reduction smelting operation. Since previously cited FeCr costs estimates (Daavittila et al., 2004, Biermann et al., 2012, Cartman, 2008) did not focus specifically on the pre-reduction process, a lifecycle cost factor breakdown of the chromite pre-oxidation process in combination with the pre-reduction process was developed, as illustrated in Figure 3.

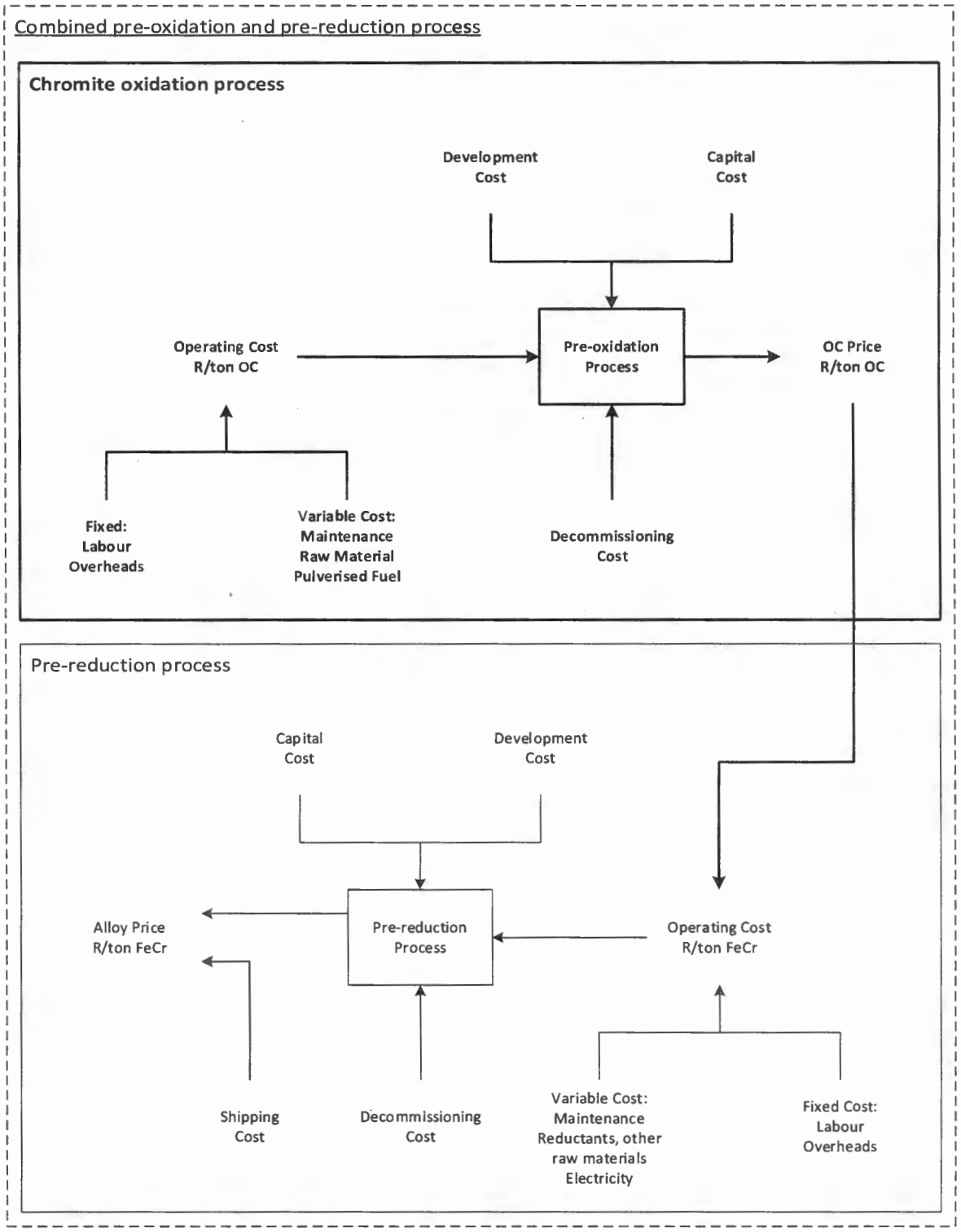

Figure 3-Life cycle cost factor breakdown of the chromite pre-oxidation process and in combination with the pre-reduction process

The lifecycle costs for both the chromite pre-oxidation process and pre-reduction process were divided into initial development costs (e.g. environmental impact assessment, design), capital costs, operating costs and decommissioning costs, with the operating costs for both processes being sub-divided into fixed and variable costs. As mentioned in the previous section, the effect of increasing the pre-reduction level results in a decrease in the reductant content required for smelting in the furnace, as well as an increase in production capacity with the same total active power. Therefore, from a cost distribution perspective, both the electricity and reductant cost factors (R\t FeCr) are lowered for the pre-reduction process, while production capacity is increased (refer to previous section). The nett result is a decrease in other cost factors, e.g. maintenance, labour, waste disposal and overheads, due to the dilution of fixed costs and ultimately a decrease in the pre-reduction process overall production cost (R/t FeCr).

Discounted cash flow (DCF) analysis

DCF analysis methods are capable of producing a good approximation of the value of a project in order to aid in the feasibility evaluation process. According to Hitch and Dipple (2012), it is fairly simple to appraise a project in terms of revenue versus cost; however, it is imperative to consider the time value of money and the influence that substantial up-front capital costs may have. Pšunder (2012) pointed out in a recent literature overview that the use of DCF methods for engineering project evaluation has increased significantly in the last decades. In appraising potential investments for its ability to quantify the added value to shareholders, financial analysis through DCF modelling is currently the most commonly used methodology (Hitch and Dipple, 2012). Pšunder and Ferlan (2007) further indicated that net present value (NPV), net present value index (NPVI), internal rate of return (IRR) and modified internal rate of return (MIRR) were some of the most commonly used DCF methods, but that the most

frequently applied were the NPV and IRR methods. The employment of the IRR method is justifiable since it is easy to understand, due to the result being expressed in a percentage rate of return. Simultaneously, results can easily be compared between various projects and different forms of investments. The regular use of the NPV method can be justified by the simplicity of the calculation (Pšunder, 2012).

Assumptions

As indicated in the 'Process options' section, it is likely that current FeCr producers utilising the pre-reduction process would employ a rotary kiln for chromite pre-oxidation. The operation input parameters for the combined pre-oxidation and pre-reduction process (Figure 1) were obtained through personal communications with individuals from a large South African FeCr producer, applying the pelletised chromite pre-reduction process and from one of the co-authors' personal experience in the FeCr industry, i.e. JP Beukes, who has held various senior positions in the FeCr industry in RSA. Capital costs were estimated by the general works project manager responsible for the first- and second-phase development of the largest single-phase FeCr expansion in the world, with both phases employing the pre-reduction process (Henrico, 2014). The base case input parameters used in this study, based on costs estimated in 2015, are presented in Tables I, II and III.

In the cost modelling, the chromite pre-oxidation process (Figure 1A) and pre-reduction process (Figure 1B) were kept as separate business units. Figure 4 presents a conceptual flow diagram of the financial model of the combined pre-oxidation and pre-reduction process (Figure 4A), indicating the effect of chromite pre-oxidation on SEC, lumpy carbonaceous reductants required for furnace smelting and FeCr production (additional FeCr produced), compared to the pre-reduction process (Figure 4B). Revenue generated by the chromite pre-oxidation operation was divided into two

income streams (Figure 4), I) pre-oxidised chromite sales and II) FeCr production increase revenue (returns as a result of the increase in FeCr production capacity). The pre-oxidised chromite sales price is determined from the cost distribution of the pre-reduction process (Figure 4). The furnace reductant and electricity cost factors per ton FeCr are reduced by utilising pre-oxidised chromite. The assumption was then made to keep the pre-reduction process production cost constant at R10 000/t FeCr, which is the same as before exploiting oxidised ore. Therefore, the pre-reduction process chromite ore cost factor is increased, which sets the pre-oxidised chromite sale price. Using pre-oxidised chromite also results in an increased production capacity. The profit generated by the additional FeCr produced served as the second income stream for the chromite pre-oxidation process.

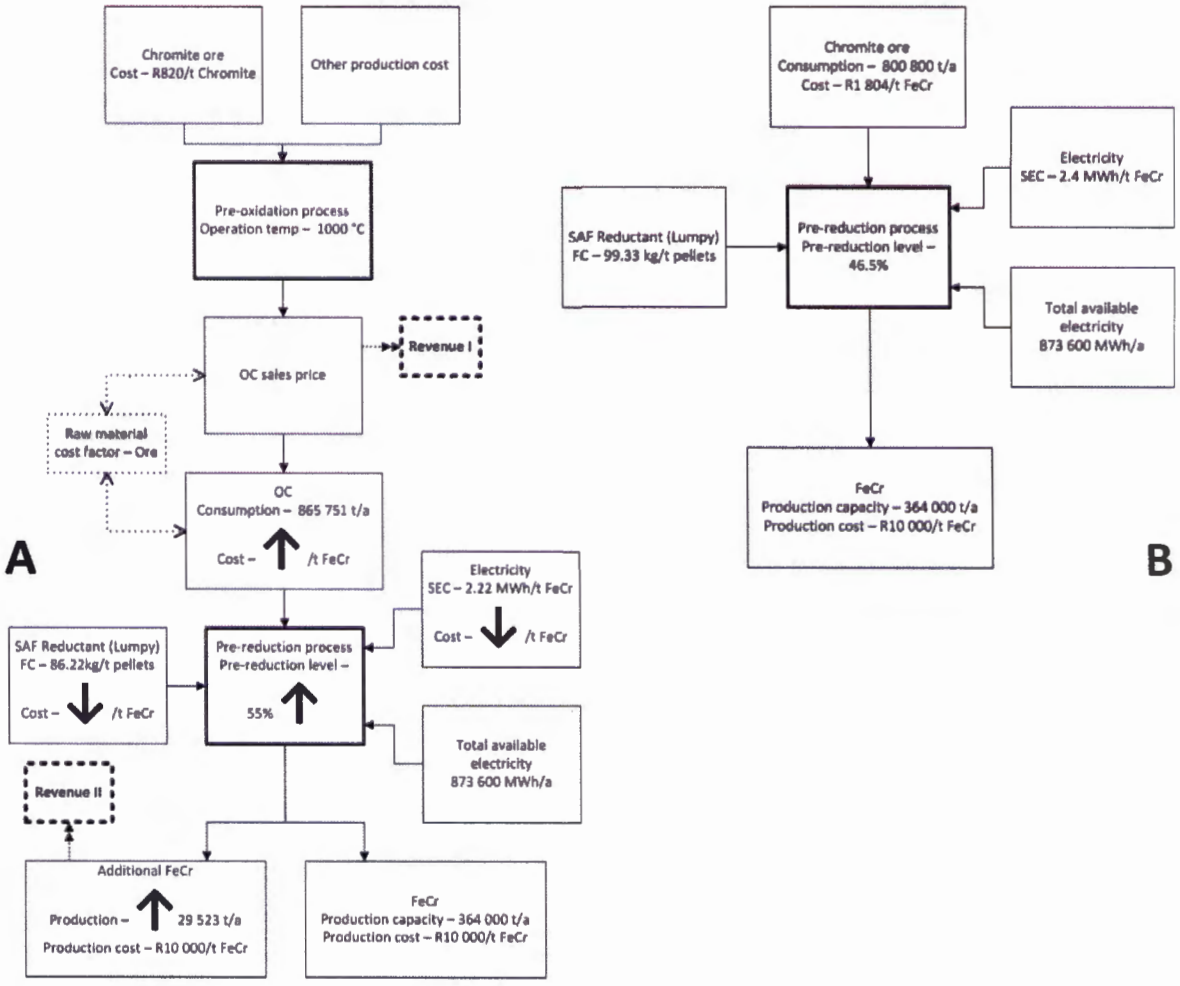

Figure 4-Conceptual flow diagram of the financial model for the combined pre-oxidation and pre-reduction process (A), indicating the influence of chromite pre-oxidation on SEC, lumpy carbonaceous reductants required for furnace smelting and FeCr production (additional FeCr produced), the determination of the OC sales price and the pre-oxidation process revenue streams (I and II), compared to the pre-reduction process (B)

Table I

Base case model input parameters (based on costs estimated in 2015)

Input parameters	Value	Unit
Process availability	90	%/a
Available hours	7 884	h
Furnace capacity	63	MVA
Furnaces	2	-
Power factor	0.879	-
Total available electricity	873 600 000	kWh/a
Electricity price	0.74	R/kWh
ZAR/US$ exchange rate	10.95	ZAR/US$
Freight cost* (Wellmer et al., 2008)	25	US$/t FeCr
FeCr price (Merafe-Resources, 2014)	1.19	US$/lb Cr contained
Cr content in FeCr produced	50	%
Coke price (Biermann et al., 2012)	4 000	ZAR/t
Anthracite price (Biermann et al., 2012)	1 100	ZAR/t
Char price (Biermann et al., 2012)	900	ZAR/t
**Shipping distance of ~8 300 nmi*		
Furnace reductant mixture composition:		
Furnace reductant FC content	77.8	wt.%
Coke	30	%
Anthracite	20	%
Char	50	%
Pre-reduction pellet composition:		
Chromite/OC	76.5	wt.%
Reductant	20.0	wt.%
Reductant FC content	75.0	wt.%
Clay binder	3.50	wt.%
Pre-reduction process (with un-oxidised chromite):		
FeCr production capacity	364 000	t FeCr/a
Chromite consumption	2.2	t Chromite/t FeCr
Pre-reduction process pellet consumption	2.876	t Pellets/t FeCr
Pre-reduction level	46.50	%
Production cost	10 000.00	R/t FeCr
Combined pre-oxidation & pre-reduction process:		
Pre-reduction increase	8.50	%
SEC	2 220	kWh/t FeCr
Kiln burner fuel composition	100	% PF
OC kiln PF consumption	0.0627	t PF/t OC
FeCr production capacity	393 523	t FeCr/a
Chromite required	865 751	t Chromite/a
OC production	1.014	t OC/t chromite
OC consumption	2.231	t OC/t FeCr
OC produced	877 872	t OC/a
OC Pre-reduction pellet consumption	2.916	t OC Pellets/t FeCr
OC Pre-reduction pellets required	1 147 545	t OC Pellets/a

Table II

Base case pre-oxidised chromite ore production costs (based on costs estimated in 2015)

Fixed costs	**Quantity**	**Unit cost**	**Cost/t OC produced**
Operators	4	R 240 000.00	R 1.09
Maintenance personnel	2	R 540 000.00	R 1.23
PPE	6	R 250.00	R 0.0017
Total			R 2.33
Variable costs	**Value**	**Unit**	**Cost/t OC produced**
Internal transport (Moving)	700.00	R/h	R 6.29
Internal transport (Loading)	400.00	R/h	R 3.59
Maintenance	5.70	R/t OC	R 5.70
Refractory	0.10	R/t OC	R 0.10
PF	1 038.00	R/t PF	R 65.08
Auxiliary power	0.68	R/t OC	R 0.68
Provident fund for large replacements	0.57	R/t OC	R 0.57
Chromite ore	820.00	R/t Chromite	R 808.68
Total			R 890.69
Grand total			R 893.01

Table III

Base case DCF model input parameters (based on costs estimated in 2015)

Input parameters	**Value**	**Unit**
Development phase duration	1	years
Development cost	5	% of total capital cost
Construction phase duration	2	years
Total capital cost:	383 627 322	R
Civils	71 232 000.00	R
Structural	25 446 400.00	R
Plate work	14 660 800.00	R
Mechanical	188 182 400.00	R
Electrical	32 947 376.00	R
Geotechnical studies	1 120 000.00	R
Project contingencies	15	% of capital cost
Plant Life	20	years
Depreciation	5	year MACRS
Decommissioning phase duration	2	years
Decommissioning cost	15	% of total capital cost
Cost escalation factor (inflation rate)	6	%
Benefit escalation factor (FeCr price increase)	6	%
Income tax rate	28	%
Discount rate	10	%

Sensitivity analysis

Although it is important to correctly approximate the operation and cost parameters of the combined pre-oxidation and pre-reduction process, changes to these values will invariably take place due to economic fluctuation and advances in research and development. Therefore, sensitivity analysis is essential in determining the overall feasibility. A more comprehensive understanding of the project economics and viability can only be achieved by evaluating the ranges between extreme levels for the various input parameters. Similar to Hitch and Dipple (2012), sensitivity analysis was first performed on the pre-oxidation process production cost model input parameters, since the pre-oxidation process production cost is subsequently required as a DCF input parameter. This allowed for the examination of deviations from the base case to assess the impact of the various input parameters. The sensitivity of each of these input parameters allowed for a more accurate appraisal of project value and return, as determined through DCF modelling and its corresponding sensitivity analysis.

Financial modelling results and discussion

Base case results

The base case results, consisting of the pre-oxidised chromite cost margins, the cost distributions of the pre-reduction process with and without pre-oxidised chromite, and the DCF model outputs are listed in Table IV. In order to keep the production cost of the pre-reduction process constant at R10 000/t FeCr, as explained in the 'Assumptions' section, the pre-oxidised chromite sales price was determined at R905.28/t OC. By employing the pre-oxidation process and utilising pre-oxidised chromite the cost distributions of furnace electricity and reductants were reduced from 17.76% and 6.87%, to 16.43% and 6.04%, respectively. By applying the method used

by Kleynhans et al. (2012) to convert electrical energy improvements to financial gains, the reduction in the furnace electricity cost distribution translated to ~ R48.5 million/a for the 364 000 t/a pre-reduction process. The financial gain associated with the decrease of the furnace reductant cost distribution by using Figure 2 translates to ~ R30 million/a for the 364 000 t/a pre-reduction process. It is therefore evident that applying this process has financial advantages.

Table IV
Base case results

Parameter	**Value**	**Unit**		
Oxidised chromite production				
Oxidised chromite production cost	893.01	R/t OC		
Oxidised chromite price	905.28	R/t OC		
FeCr production increase	29 523	t FeCr/a		
Cost distribution				
Production cost (PR process)	10 000.00	R/t FeCr		
PR process using chromite			*% of production cost*	
Chromite ore	1 804.00	R/t FeCr	18.04	
Electricity	1 776.00	R/t FeCr	17.76	
Furnace reductants	686.62	R/t FeCr	6.87	
Other production costs	5 733.38	R/t FeCr	57.33	
PR process using OC			*% of production cost*	
OC ore	2 019.50	R/t FeCr	20.20	↑
Electricity	1 642.76	R/t FeCr	16.43	↓
Furnace reductants	604.35	R/t FeCr	6.04	↓
Other production costs	5 733.38	R/t FeCr	57.33	-
NPV (after tax)	R 894 489 279.24			
IRR (after tax)	30.5%			
Profitability index (after tax)	2.88			
Simple payback	3 years 0 months 16 days			
Discounted payback	4 years 0 months 11 days			

Although not investigated in this study, another cost benefit resulting from employing the pre-oxidation process is the dilution of fixed costs. The large increase in production capacity effectively ensures a reduced impact of fixed cost with the fixed

cost only increasing slightly. For a pre-oxidised chromite production cost of R893.01/t OC and a FeCr production increase of 29 523 t FeCr/a, the DCF model yielded an NPV of ~R895 million with an IRR of 30.5% and a profitability index (PI) of 2.88 after tax. This significantly positive base case NPV, the IRR approximately three times greater than the 10% discount rate and PI approximately three times higher than one suggests that integrating the pre-oxidation process and utilising pre-oxidised ore may be a potentially feasible development option from a project economics standpoint. In order to put these results into perspective, it would be beneficial to compare the NPV and IRR to other reasonable values within the industry. However, economic feasibility results of smaller expansion or process improvement projects are not readily available in the peer-reviewed scientific domain, since the publication of such results could potentially erode the strategic advantage of the developing company. Development of The Ring of Fire, a large mineral resource-rich area of approximately 5 120 km^2 located in Canada's Northern Ontario region can be considered as a recent example. Based on current projections, the chromite deposit is significant enough to sustain North American activity for a century (OCC, 2014). KWG Resources of Montreal, Canada released the preliminary economic assessment (PEA) study for the Big Daddy chromite deposit in the Ring of Fire in 2011. The PEA examined an open-pit mine, crushing plant, site infrastructure as well as development of a railway and power line to the site. Pre-production capital expenses were estimated to be around $784 million, which included half of the $900 million cost of the railway to establish an 8 000 t/d operation over a 16-year life cycle. At a 2011 exchange rate of ~7 ZAR/US$, capital cost to develop the Big Daddy chromite deposit amounts to ~ZAR 5.5 billion. The Big Daddy project's undiscounted gross revenue was appraised at ~$12.6 billion. The after-tax evaluation estimated the NPV to be ~$1.6 billion at an 8% discount rate or ~$1.25 billion at a 10%

discount rate. The after-tax internal rate of return calculated to ~31.8%, resulting in a pre-tax payback period of 2.5 years (CMJ, 2011; KWG Resources, 2011).

Although the NPV and IRR look promising and show comparisons with the PEA study for the Big Daddy chromite deposit, it is necessary to keep in mind that this investigation is conceptual in nature and that an inherent uncertainty surrounding some model input parameters exists to a certain extent. Intrinsically, sensitivity analysis allowed for a more in-depth investigation into the influences of some uncertainties on the overall project appraisal, which are discussed in the following sections.

Cost sensitivity of the pre-oxidation process in isolation

The overall sensitivity of the pre-oxidation process' pre-oxidised chromite production cost parameters, consisting of a spider plot diagram showing parameter sensitivity and a table ranking these parameters from most to least sensitive, is presented in Figure 5. The spider plot offers a comparative representation of the sensitivity of the pre-oxidised chromite production cost model elements. Input elements with the sharpest gradients represent the parameters with the greatest impact per unit of change from the base case, as denoted by the x-axis with the base case value set at 0%.

The most sensitive parameter defined through sensitivity analysis, if the pre-oxidised chromite process' production cost was considered in isolation, was chromite ore cost. This is easily explained since (i) the pre-oxidation process section was considered as a separate economic component in the financial cost model to determine the oxidised chromite production cost and selling price, and (ii) ~90.5% of the total pre-oxidised chromite production cost is allocated to the cost of obtaining chromite ore. PF cost and PF composition were jointly the second most sensitive parameters. The cost of PF account for ~7.3% of the total pre-oxidised chromite production cost.

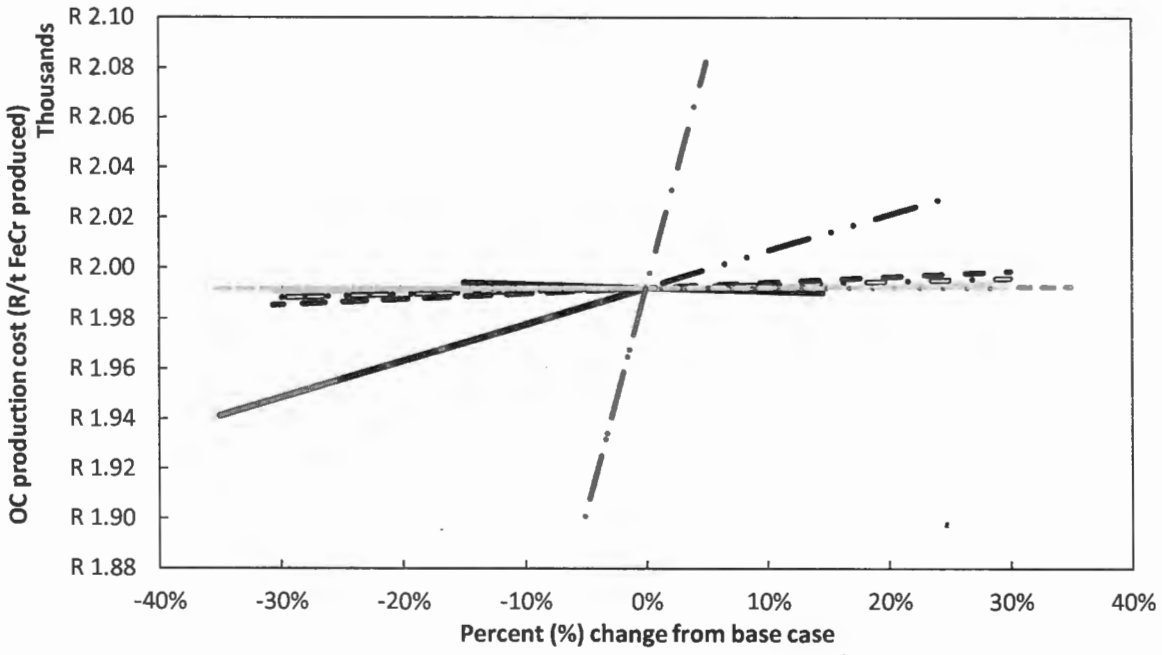

Parameter		Rank
— · —	Chromite cost	1
— · · —	PF Cost	2
———	PF composition	2
- - - -	Internal transport	3
———	Pre-reduction level	4
▭ · ▭ · ▭	Maintenance	5
———	Labour	6
- - - - - - -	Auxiliary power	7
.....	Refractory	8

Figure 5-Overall sensitivity of pre-oxidised chromite production cost parameters

The percentage change from the base case for the PF composition in Figure 5 is only indicated as a negative change, which can be attributed to the kiln being operated only on PF in the base case scenario. The cost contribution of the PF to the total chromite pre-oxidising production cost can, however, be significantly reduced if a mixture of PF and CO off-gas, or exclusively CO from the closed SAF, can be used. The use of CO off-gas in the pre-reduction kiln is not completely effective, since temperatures higher than 1 250 °C are required. Although the adiabatic flame temperature of CO gas is high enough (du Preez et al., 2015, Niemelä et al., 2004), it

has been found in practice that PF fuel has a deeper penetrating flame. Pre-reduction kilns are also long (60-80 m) to ensure the required retention time of ~3 hours for effective pre-reduction. Consequently, the fuel utilised needs to be able to penetrate deep into the kiln for effective heat transfer and to maximise the area with a temperature distribution higher than 1 250 °C. It will, however, be possible to use CO off-gas in the chromite pre-oxidation process since a lower temperature (1000 °C) and shorter retention time (1 hour) are required, which implies a shorter kiln. The remaining pre-oxidised chromite production cost parameters account for less than 2.2% of the total production cost, and therefore, in terms of sensitivity, these parameters had minimal impact.

The pre-reduction level was also considered since it has an impact on the pre-oxidised chromite required for the pre-reduction process. If the pre-reduction level decreases from the base case, the FeCr production capacity also decreases, resulting in a decrease of pre-oxidised chromite required. This will result in an increase in the production cost per ton of pre-oxidised chromite produced. The opposite would occur if the pre-reduction level increases. However, the sensitivity of the pre-reduction level was minimal, since it is approximately a 130 times less sensitive than chromite cost.

Cost sensitivity of the pre-oxidation process integrated with the pelletised pre-reduction process

Spider plot diagrams showing parameter sensitivity relating to the NPV and IRR with these parameters being ranked from most to least sensitive in a table are presented in Figure 6 in order to illustrate the overall sensitivity of the DCF model designed for the integrated pre-oxidation and pre-reduction process.

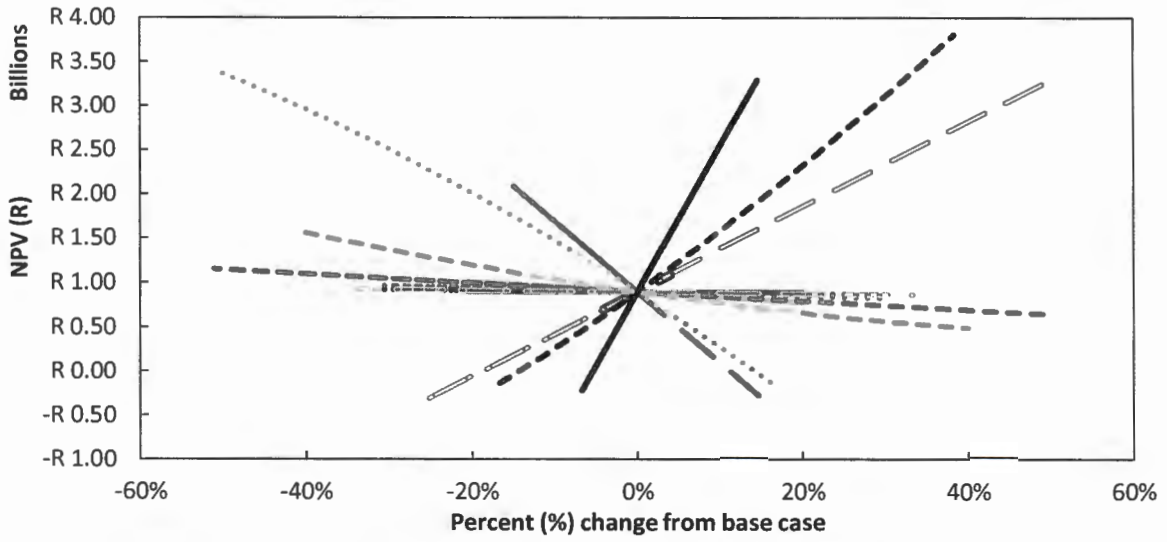

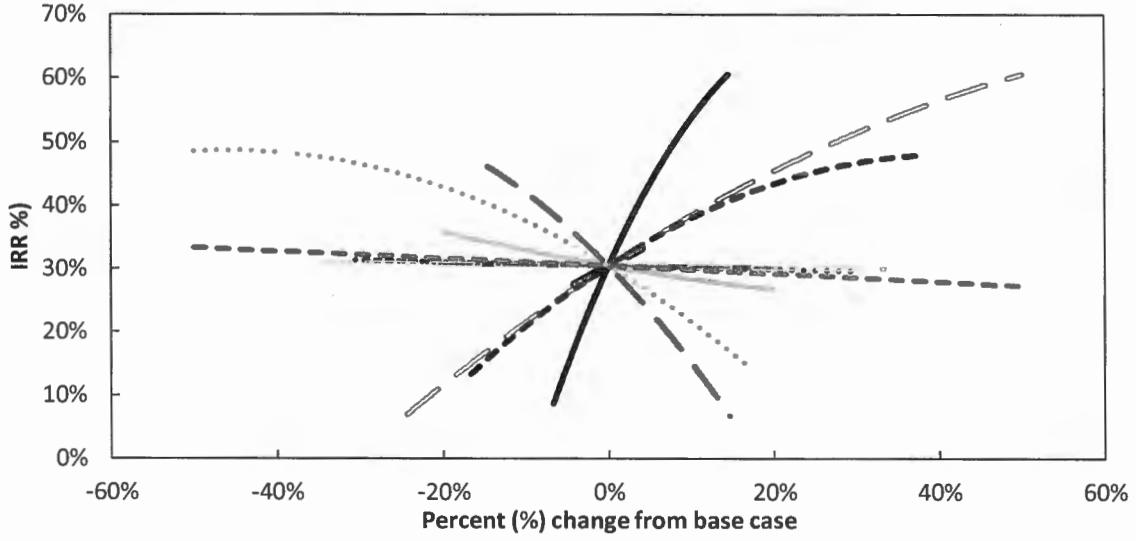

Parameter		Rank		Overall DCF sensitivity (%)
		NPV	IRR	
———	Pre-reduction level	1	1	34.86
— — —	Chromite cost	2	2	18.33
- - - - -	Benefit escalation factor	3	5	11.90
═══	FeCr Cr content	6	3	10.26
═ ═ ═	FeCr price	5	4	10.21
.....	Cost escalation factor	4	6	8.90
———	Total capital cost	8	7	2.33
- - - - -	Discount rate	7	-	1.35
- - - - -	Income tax rate	9	8	0.97
.....	Project contingencies	12	9	0.31
.....	Decommissioning cost	10	-	0.23
═ ═ ═	Freight cost	11	11	0.20
———	Development cost	13	10	0.14

Figure 6-Overall sensitivity of the DCF model

Although the level of pre-reduction was relatively insensitive with regard to the pre-oxidation process' production cost, it was found to be the most sensitive parameter in determining both the NPV and IRR. The level of pre-reduction, accounting for ~34.9% of the overall DCF sensitivity, is approximately two times more sensitive than the parameter ranked second for both the NPV and IRR. The level of pre-reduction primarily affects the FeCr production capacity, which, in turn, has an effect on the pre-oxidised chromite required. As a result, the level of pre-reduction has an effect on both the chromite pre-oxidation process' revenue streams (Figure 4) and consequently affects the operation's cash flow. Chromite cost, the second most sensitive parameter, accounted for ~18.3% of the overall DCF sensitivity. Four parameters, more specifically the benefit escalation factor, FeCr Cr content, FeCr price and cost escalation factor, could be grouped together for each, accounting for between ~9 and 12% of the overall DCF sensitivity. An interesting observation is that the order of importance for these four parameters was dissimilar for the NPV and IRR. Nevertheless, these cost or price parameters have significant implications for overall project feasibility by directly controlling the total available revenue from the two income streams. Specifically, significant increases in the cost of chromite and parameters negatively influencing the FeCr price and income thereof will imply that there will not be an adequate source of revenue in order to offset the associated costs. It is interesting to note that the total capital cost is the seventh most sensitive parameter for the IRR and the eighth most sensitive for NPV. It was originally assumed that the capital cost would have a bigger influence on project appraisal as a result of the front-loaded nature of the cash flows. However, it does not have a considerable impact on project valuation. The capital cost necessary for funding may have a more dramatic impact on the ability to secure project financing, either through debt or equity. Although this does not necessarily affect

project valuation, it may have an impact on project feasibility in determining the ability to generate funding for project construction. Factors of less significant influence include the discount rate, income tax rate, project contingencies, decommissioning cost, as well as freight- and development cost. The significance and contribution of each of the individual parameters investigated through this research cannot be ignored. However, their ranking in terms of sensitivity has provided a means by which further research can be prioritised and efforts can be focused on parameters that will result in the greatest influence on project valuation.

Conclusions

It was recently proven that pre-oxidation of fine chromite ore, prior to pelletised pre-reduction, significantly decreases the SEC and lumpy carbonaceous reductants required for furnace smelting. In this paper, an analysis of the techno-economic feasibility of integrating chromite pre-oxidation into the currently applied pelletised pre-reduction process as a pre-treatment method was presented. RSA's FeCr industry provided the ideal backdrop conditions within which the techno-economic feasibility of implementing such a chromite pre-oxidation process could be evaluated. Through the conceptualisation of the pre-oxidation process route, it became evident that FeCr producers currently utilising the pre-reduction process would most likely opt to employ an operation with a rotary kiln at its core to conduct chromite pre-oxidation. Chromite pre-oxidation at the optimum temperature of 1 000 °C translated to an ~8.5% increase in the level of achievable chromite pre-reduction (from ~46.5% to ~55.5%), an ~8.3% improvement in the SEC (from ~2.4 to ~2.2 MWh/t) and a ~14% decrease (from ~99.5 to ~85.5 kg/t pellets) in the amount of lumpy carbonaceous material required during SAF smelting. In order to more accurately approximate input costs for further lifecycle financial modelling, a comprehensive estimate of the costs associated with pre-oxidising

the fine chromite ore was determined. The lifecycle financial model, which was built on a DCF approach, generated a base case NPV of ~R895 million and an IRR of ~30.5% after tax. This strongly indicates that integration of the chromite pre-oxidation process into the currently applied pre-reduction process may be viable from a financial perspective. Sensitivity analysis of the pre-oxidation process in isolation indicated that the most influential parameter was chromite ore cost, whereas the most influential parameter was found to be the level of pre-reduction if the pre-oxidation process was integrated with the pelletised pre-reduction process. The level of achievable pre-reduction is interrelated with the pre-oxidation temperature, which implies that the capability of maintaining the optimum pre-oxidation temperature is of critical importance.

Acknowledgements

The authors would like to thank Glencore Alloys for technical assistance.

References

BARNES, A.R., FINN, C.W.P. and ALGIE, S.H. 1983. The prereduction and smelting of chromite concentrate of low chromium-to-iron ratio. Journal of the South African Institute of Mining and Metallurgy, no. March. pp. 49-54.

BASSON, J., CURR, T.R. and GERICKE, W.A. 2007. South Africa's ferro alloys industry – present status and future outlook. Proceedings of the 11th International Ferro Alloys Conference (INFACON XI). Das, R.K. and Sundaresan, T.S. (eds.). New Delhi, India, The Indian Ferro Alloys Producers Association. pp. 3-24.

BEUKES, J.P., DAWSON, N.F. and VAN ZYL, P.G. 2010. Theoretical and practical aspects of Cr(VI) in the South African ferrochrome industry. The Journal of The Southern African Institute of Mining and Metallurgy, vol. 110, no. December. pp. 743-750.

BEUKES, J.P., VAN ZYL, P.G. and NEIZEL, B.W. 2015. North-West University. Process for enhanced pre-reduction of chromite. PCT/IB2013/056313.

BEUKES, J.P., VAN ZYL, P.G. and RAS, M. 2012. Treatment of Cr(VI)-containing wastes in the South African ferrochrome industry - a review of currently applied

methods. The Journal of The Southern African Institute of Mining and Metallurgy, vol. 112, no. May. pp. 347-352.

BIERMANN, W., CROMARTY, R.D. and DAWSON, N.F. 2012. Economic modelling of a ferrochrome furnace. The Journal of The Southern African Institute of Mining and Metallurgy, vol. 112, no. April. pp. 301-308.

BOTHA, W. 2003. Ferrochrome production through the SRC process at Xstrata, Lydenburg Works. Journal of the South African Institute of Mining and Metallurgy, vol. 103, no. 6. pp. 373-389.

CARTMAN, A. 2008. An analysis of ferrochrome input costs, Metal Bulletin Special and Stainless Steel Summit [Online]. Hatch Beddows. Available: http://hatch.ca/Mining_Metals/Iron_Steel/Articles/documents/analysis_ferrochrome_input_costs.pdf [Accessed 30 Jan. 2015].

CMJ. 2011. CHROMITE STUDY: Big Daddy headed for feasibility [Online]. http://www.canadianminingjournal.com/news/chromite-study-big-daddy-headed-for-feasibility/ [Accessed 22 Nov. 2015].

CRAMER, L.A., BASSON, J. and NELSON, L.R. 2004. The impact of platinum production from UG2 ore on ferrochrome production in South Africa. The Journal of The South African Institute of Mining and Metallurgy, vol. 104, no. 9. pp. 517-527.

CREAMER, M. 2013. South Africa's raw chrome exports soar as ferrochrome edge is lost [Online]. Mining Weekly. Available: http://www.miningweekly.com/article/south-africas-raw-chrome-exports-soar-as-ferrochrome-edge-is-lost-2013-09-20 [Accessed 15 Jan. 2014].

DAAVITTILA, J., HONKANIEMI, M. and JOKINEN, P. 2004. The transformation of ferrochromium smelting technologies during the last decades. The Journal of The South African Institute of Mining and Metallurgy, no. October. pp. 541-549.

DENTON, G.M., BENNIE, J.P.W. and DE JONG, A. 2004. An improved DC-arc process for chromite smelting. Proceedings of the 10th International Ferroalloys Congress (INFACON X). Johannesburg, South Africa, The South African Institute of Mining and Metallurgy. pp. 60-67.

DU PREEZ, S.P., BEUKES, J.P. and VAN ZYL, P.G. 2015. Cr(VI) Generation During Flaring of CO-Rich Off-Gas from Closed Ferrochromium Submerged Arc Furnaces. Metallurgical and Materials Transactions B, vol. 46B, no. April. pp. 1002-1010. DOI: 10.1007/s11663-014-0244-3

DWARAPUDI, S., TATHAVADKAR, V., RAO, B.C., KUMAR, T.K.S., GHOSH, T.K. and DENYS, M. 2013. Development of Cold Bonded Chromite Pellets for Ferrochrome Production in Submerged Arc Furnace. ISIJ International, vol. 53, no. 1. pp. 9-17. DOI: 10.2355/isijinternational.53.9

ESKOM. 2012. Eskom retail tariff adjustment for 2012/2013 [Online]. Available: http://www.eskom.co.za/c/article/816/home/ [Accessed 7 Oct. 2012].

GLASTONBURY, R.I., BEUKES, J.P., VAN ZYL, P.G., SADIKI, L.N., JORDAAN, A., CAMPBELL, H.M., STEWART, H.M. and DAWSON, N.F. 2015. Comparison of physical properties of oxidative sintered pellets produced with UG2 or metallurgical grade South African chromite: a case study. The Journal of The Southern African Institute of Mining and Metallurgy, vol. 115, no. August. pp. 1-8. DOI: 10.17159/2411-9717/2015/v115n8a6

GLASTONBURY, R.I., VAN DER MERWE, W., BEUKES, J.P., VAN ZYL, P.G., LACHMANN, G., STEENKAMP, C.J.H., DAWSON, N.F. and STEWART, H.M. 2010. Cr(VI) generation during sample preparation of solid samples – A chromite ore case study. Water SA, vol. 36, no. 1. pp. 105-110. DOI: 10.4314/wsa.v36i1.50913

GOEL, R.P. 1997. Smelting Technologies for Ferrochromium Production - Recent Trends. In: Ferro Alloy Industries in the Liberalised Economy. Vaish, A.K., Singh, S.D., Goswami, N.G. and Ramachandrarao, P. (eds.). Jamshedpur, India, National Metallurgical Laboratory (NML), India.

HENRICO, M. 2014. Glencore Alloys. RE: De Oude Werf Personal Communication, 25 September 2014. Middelburg, Mpumalanga, South Africa.

HITCH, M. and DIPPLE, G.M. 2012. Economic feasibility and sensitivity analysis of integrating industrial-scale mineral carbonation into mining operations. Minerals Engineering, vol. 39. pp. 268-275. DOI: 10.1016/j.mineng.2012.07.007

HOLAPPA, L. 2010. Towards sustainability in ferroalloys production. Proceedings of the 12th International Ferroalloys Congress (INFACON XII). Vartiainen, A. (ed.). Helsinki, Finland, Outotec Oyj. pp. 1-10.

ICDA. 2013a. Energy Update - November 2013. International Chromium Development Association [Online]. Available: http://dev.icdacr.com/index.php?option=com_content&view=article&id=617&Itemid=590&lang=en [Accessed 14 Sept. 2015].

ICDA. 2013b. Statistical Bulletin 2013. Paris, France: International Chromium Development Association.

JONES, R.T. 2015. Pyrometallurgy in Southern Africa - List of Southern African Smelters [Online]. Available: http://www.pyrometallurgy.co.za/PyroSA/index.htm [Accessed 14 Sept. 2015].

KAPURE, G., TATHAVADKAR, V., RAO, C.B., RAO, S.M. and RAJU, K.S. 2010. Coal based direct reduction of preoxidezed chromite ore at high temperature. Proceedings of the 12th International Ferroalloys Congress (INFACON XII). Vartiainen, A. (ed.). Helsinki, Finland, Outotec Oyj. pp. 293-301.

KLEYNHANS, E.L.J., BEUKES, J.P., VAN ZYL, P.G., KESTENS, P.H.I. and LANGA, J.M. 2012. Unique challenges of clay binders in a pelletised chromite pre-reduction process. Minerals Engineering, vol. 34. pp. 55-62. DOI: 10.1016/j.mineng.2012.03.021

KLEYNHANS, E.L.J., NEIZEL, B.W., BEUKES, J.P. and VAN ZYL, P.G. 2015. Utilisation of pre-oxidised ore in the pelletised chromite pre-reduction process. Minerals Engineering, vol. 92. pp. 114-124. DOI: 10.1016/j.mineng.2016.03.005

KWG RESOURCES. 2011. Daddy chromite deposits [Online]. http://www.kwgresources.com/_resources/corp_presentations/corporate_presentation.pdf [Accessed 22 Nov. 2015].

LUCKOS, A., DENTON, G. and DEN HOED, P. 2007. Current and potential applications of fluid-bed technology in the ferroalloy industry. Proceedings of the 11th International Ferroalloys Congress (INFACON XI). Das, R.K. and Sundaresan, T.S. (eds.). New Delhi, India, The Indian Ferro Alloys Producers Association. pp. 123-132.

MCCULLOUGH, S., HOCKADAY, S., JOHNSON, C. and BARZA, N.A. 2010. Pre-reduction and smelting characteristics of Kazakhstan ore samples. Proceedings of the 12th International Ferroalloys Congress (INFACON XII). Vartiainen, A. (ed.). Helsinki, Finland, Outotec Oyj. pp. 249-262.

MERAFE-RESOURCES. 2012. Maximising South Africa's chrome ore endowment to create jobs and drive sustainable [Online]. Available: http://www.meraferesources.co.za/pdf/presentations/2012/chrome_ore_brochure.pdf [Accessed 14 Jan. 2014].

MERAFE-RESOURCES. 2014. Third quarter 2014 ferrochrome price announcement [Online]. Sandton, South Africa: Overend. Available: http://www.overend.co.za/download/third_quarter_2014_30072014.pdf [Accessed 3 Mar 2016].

MOHALE, G.T.M. 2014. SEM image processing as an alternative method to determine chromite pre-reduction. MSc Chemical Engineering dissertation, North-West University, South Africa.

MURTHY, Y.R., TRIPATHY, S.K. and KUMAR, C.R. 2011. Chrome ore beneficiation challenges & opportunities – A review. Minerals Engineering, vol. 24, no. 5. pp. 375-380. DOI: 10.1016/j.mineng.2010.12.001

NAIKER, O. 2007. The development and advantages of Xstrata's Premus Process. Proceedings of the 11th International Ferroalloys Congress (INFACON XI). Das, R.K. and Sundaresan, T.S. (eds.). New Delhi, India, The Indian Ferro Alloys Producers Association. pp. 112-119.

NAIKER, O. and RILEY, T. Xstrata alloys in the profile. In: South African Pyrometallurgy 2006. Johannesburg, South Africa, SAIMM. pp. 297-306.

NEIZEL, B.W., BEUKES, J.P., VAN ZYL, P.G. and DAWSON, N.F. 2013. Why is CaCO3 not used as an additive in the pelletised chromite pre-reduction process? Minerals Engineering, vol. 45. pp. 115–120. DOI: 10.1016/j.mineng.2013.02.015

NIAYESH, M.J. and FLETCHER, G.W. An assessment of smelting reduction processes in the production of Fe-Cr-C alloys. Proceedings of the 4th International Ferroalloys Congress (INFACON IV). Sao Paulo, Brazil. pp. 115-123.

NIEMELÄ, P., KROGERUS, H. and OIKARINEN, P. 2004. Formation, characterisation and utilisation of CO-gas formed in ferrochrome smelting. Proceedings of the 10th International Ferroalloys Congress (INFACON X). Johannesburg, South Africa, The South African Institute of Mining and Metallurgy. pp. 68-77.

OCC. 2014. Beneath the Surface - Uncovering the Economic Potential of Ontario's Ring of Fire. Ontario, Canada: Commerce, O.C.O.

PAN, X. 2013. Effect of South Africa Chrome Ores on Ferrochrome Production. International Conference on Mining, Mineral Processing and Metallurgical Engineering. Johannesburg, South Africa.

PŠUNDER, I. 2012. Use of Discounted Cash Flow Methods for Evaluation of Engineering Projects. In: Mechanical Engineering. Gokcek, M. (ed.). Rijeka, Croatia, InTech.

PŠUNDER, I. and FERLAN, N. 2007. Analysis of the knowledge and the use of investment project evaluation methods in the field of mechanical engineering. Journal of Mechanical Engineering, vol. 53, no. 9. pp. 569-581.

SLATTER, D.D. 1995. Technological trends in chromium unit production and supply. Proceedings of the 7th International Ferroalloys Congress (INFACON VII). Tveit, H., Tuset, J.K. and Page, I.G. (eds.). Trondheim, Norway, The Norwegian Ferroalloy Producers Research Organization (FFF). pp. 249-262.

UGWUEGBU, C. 2012. Technology Innovations in the Smelting of Chromite Ore. Innovative Systems Design and Engineering, vol. 3, no. 12. pp. 48-55.

WELLMER, F.-W., DALHEIMER, M. & WAGNER, M. 2008. Calculation of Cost Data. Economic Evaluations in Exploration. Berlin, Heidelberg: Springer Berlin Heidelberg. p. 249.

CHEMICAL BENEFICIATION OF CHROMITE ORE TO IMPROVE THE CHROMIUM-TO-IRON RATIO FOR FERROCHROME PRODUCTION

7.1 Authors list, contributions and consent

Authors list

E.L.J. Kleynhans[a], J.P. Beukes[a], P.G. Van Zyl[a] and S.P. du Preez[a]

[a] Chemical Resource Beneficiation, North-West University, Potchefstroom Campus, Private Bag X6001, Potchefstroom 2520, South Africa

Contributions

Contributions of the various co-authors were as follows:

The bulk of the work, i.e. experimental, data processing and interpretation, research and writing of the scientific paper, was performed by the candidate, ELJ Kleynhans. Prof JP Beukes (supervisor) and Dr PG van Zyl (co-supervisor) assisted in writing the article by sharing conceptual ideas and recommendations with regard to the experimental work, interpretation and results and discussion. SP du Preez assisted with the pre-reduction analysis.

Consent

All the co-authors that contributed to the article presented in this chapter have been informed that the article will form part of the candidates PhD, submitted in article format, and have granted permission that the article may be used for the purpose stated.

7.2 Formatting and current status of the article

The article was formatted in accordance with journal specifications to which it will be submitted, i.e. Minerals Engineering. The journals details, as well as the author's guide that was followed in preparation of the article, is available at: http://www.journals.elsevier.com/minerals-engineering (Date of access: 30 November 2016). **It is the opinion of the candidate and the supervisors that the article may contain information that is of value to the North-West University (NWU). The thesis was therefore classified as confidential by the NWU Senate to give effect to the**

General Academic Rules rule A.5.4.12 (NWU, 2015). At the time when this PhD was submitted for examination, there were ongoing negotiation with a company regarding the intellectual property and possibly patenting this technology. Consequently, this paper has not yet been submitted for review to a journal.

Chemical beneficiation of chromite ore to improve the chromium-to-iron ratio for ferrochrome production

E.L.J. Kleynhans[a], J.P. Beukes[a,*], P.G. van Zyl[a] and S.P. du Preez[a]

[a] Chemical Resource Beneficiation, North-West University, Potchefstroom Campus, Private Bag X6001, Potchefstroom, 2520, South Africa

* Corresponding author. E-mail address: paul.beukes@nwu.ac.za;
Telephone: +27 82 460 0594; Fax: +27 18 299 2350

ABSTRACT

Ferrochrome (FeCr), a relatively crude alloy comprised primarily of iron (Fe) and chromium (Cr), is vital for the production of stainless steel. FeCr is produced from chromite ore, the most important source of virgin Cr units. FeCr producers are only paid per mass unit of Cr content in the FeCr, i.e. in US¢/lb contained Cr, according to the current global FeCr markets pricing structure. Consequently, FeCr producers transport a large fraction of their product weight, i.e. the Fe content of the FeCr, without any benefit. The Fe content in the FeCr produced depend on the chromite spinel Cr/Fe ratio. Therefore, the selective removal of Fe from the chromite spinel using different combinations of chromite pre-oxidation, pre-reduction and sulphuric acid leaching were investigated. The Cr/Fe ratio of the case study ores could be increased from 1.57 up to ~23.4. However Cr recovery decreased significantly under experimental conditions to achieve such high Cr/Fe ratios. More desirable Cr/Fe ratios of >2 up to ~4.28 were achieved, while maintaining Cr recoveries of >90%.

Keywords: Chromite, ferrochrome or ferrochromium, chromium-to-iron ratio, pre-reduction, pre-oxidation, sulphuric acid leaching

1. Introduction

The international market for chromite ore (synthetic formula – $FeO.Cr_2O_3$), the only commercially viable source of new chromium (Cr) units, is predominantly driven by the global demand for ferrochrome (FeCr), with secondary markets comprising of the Cr chemicals-, abrasives-, refractories- and foundry sand industries. The vast majority of FeCr, a crude Cr-iron (Fe) alloy that is mainly produced through pyrometallurgical carbo-thermic reduction, is utilised in the manufacturing of stainless steel (ICDA, 2013a, b, c; Murthy et al., 2011). The worldwide demand for stainless steel continues to grow steadily despite occasional slumps in the global economy. Typical long-term growth rates of 5–6% per annum are estimated for the foreseeable future with no evidence of a mature market developing and the consequent slowing of growth (Fowkes, 2014; ISSF, 2016a, b; Yuksel, 2013).

Currently, chromite ore resources around the globe is estimated to be between 9 and 12 billion tonnes (Kogel et al., 2006; OCC, 2014; USGS, 2015). Geologically the world's commercially viable chromite ore resources occur primarily in two forms, i.e. podiform- or stratiform-type deposits. Podiform deposits are relatively small in comparison with stratiform deposits and occur in irregular shapes, like pods or lenses. The deposit distribution within a mineralised zone is erratic and unpredictable, making exploration and exploitation costly. Nevertheless, these type of deposits are generally richer in Cr than the stratiform deposits and have higher chromium-to-iron (Cr/Fe) ratios. Podiform-type ores tends to be hard, which results in the production of mostly lumpy ore (15 mm < typical size range <150 mm), as opposed to the softer, more friable ores from the stratiform deposits that results in mainly fine ore (<6 mm) being produced. Therefore, Podiform-type ores were initially preferred, as the best source of metallurgical grade chromite for high-carbon FeCr production. Economic podiform deposits are located in Kazakhstan, Turkey and Albania.

Stratiform chromite deposits occur as parallel, often multiple, seams in large, basin-like layered igneous rock intrusions. The layering is regular through repeated igneous injections and there is large lateral continuity. The largest and best known example of a stratiform deposit is South Africa's Bushveld Complex (BC). This complex contains most of the world's chromite resources, with smaller such deposits being exploited in Finland and Zimbabwe. Deformed and faulted stratiform deposits are exploited in India, but at exploration and mining costs comparable to the podiform deposits (Cramer et al., 2004; Murthy et al., 2011).

Historically, South Africa produced chromite ore predominantly for its own requirements, being the main FeCr producer globally. However, in 2012 South Africa relinquished its position as the world's leading FeCr producer to China. This shift was largely driven by a deterioration of historical cost competitiveness and recent electricity supply constraints in South Africa which in turn sparked a surge in chromite ore exports to supply the demand of a rapid growing Chinese FeCr industry (Oberholzer and Daly, 2014). In 2012, South Africa produced the majority of the world's chromite ore, accounting for ~41% of the global production. However, ~55% of the ~10 million tonnes of chromite ore South Africa produced in 2012 were exported, implying that ~28% of ore consumed in the rest of the world in 2012 originated from South Africa (ICDA, 2013c).

Although South Africa is the largest supplier of chromite, the majority of these chromite ores have relatively low Cr/Fe ratios. Supply of South Africa's chromite ores have also shifted over the last half century from the relatively high-grade deposits to lower grade deposits, as demand volumes increased. Historically, ore with a relatively high Cr/Fe ratio in the basic chromite mineral, exploited from thick chromite seams (~2 metres) to optimise unit mining costs, was sought after in order to reduce the cost of producing FeCr. The deposits located in the surrounding areas of South Africa's Zeerust and Potgietersrus districts, where

the resources are limited, have Cr/Fe ratios of 2 to 2.9. Following the introduction of the argon oxygen decarburisation process, that allowed charge grade FeCr alloys (typically 50–52% Cr) to be converted to stainless steel, the exploitation of chromite reserves with Cr/Fe ratios <2 became the norm in South Africa. The major deposits in the western and eastern BC, where resources are vast, currently serve as the typical smelter feeds with Cr/Fe ratios of 1.5 to 1.6. However, with customers lowering specification requirements even further, chromite ores with even lower Cr/Fe ratios are also processed, resulting in alloy grades with Cr contents <50% (with concomitantly increased Fe credits). Consequently significant volumes of Upper Group 2 (UG2) chromite, a process residue by-product from the platinum group metals (PGM) industry in South Africa, is exported and/or consumed by local FeCr producers. UG2 chromite ores usually has Cr/Fe ratios of 1.3 to 1.4 (Cramer et al., 2004; Howat, 1986).

The current pricing structure in the global FeCr market dictates that FeCr producers are paid per mass unit of Cr content in the FeCr, i.e. in US¢/lb contained Cr (Cramer et al., 2004). This implies that the Fe content has a negative effect on the FeCr price. Yet, considering the thermodynamics behind the pyrometallurgical carbo-thermic reduction of chromite to produce FeCr, the Fe oxides in the chromite spinel are preferentially reduced at temperatures >710 °C, as opposed to the Cr oxides that are reduced at >1250 °C (Kleynhans et al., 2016; Niemelä et al., 2004). As a result, almost all the Fe present in the chromite ore ends up in the FeCr, therefore the Cr content in the FeCr strongly depends on the Cr/Fe ratio in the chromite ore. With the Cr/Fe ratio being the primary determining factor of the Cr grade in the FeCr product, the low Cr/Fe ratios of the South African chromite deposits imply that the FeCr produced from these deposits usually has a Cr content of less than 52% and, subsequently, contains 35-39% Fe. Although the use of lower grade FeCr (<52%) has become readily accepted by the stainless steel industry, there will always be a large drive for

the use of higher grade (Cr/Fe ratio) ores so as to maximise the output from any particular capital investment and hence the revenue flows (Shen et al., 2009a; Shen et al., 2009b). Furthermore, South Africa was only the 13th largest stainless steel producer globally in 2014, accounting for ~1.13% of production. Therefore most of the locally produced FeCr is exported to stainless steel producers in Europe, Asia and America (ISSF, 2016a, b). This implies that South African FeCr producers export 35-39% of their product weight, i.e. the Fe content of the FeCr, without any benefit.

In order to further enhance the growth and profitability of the South African chromite and FeCr industry, as well as other international producers mining/consuming lower grade chromite, possible improvement of chromite ore by selectively removing Fe from chromite concentrates need to be investigated with the aim of increasing the Cr/Fe ratio. Conventional methods of beneficiation such as gravity concentration, magnetic separation and flotation cannot effectively increase the Cr/Fe ratio in a chromite ore, unless the Fe occurs in the gangue materials (Murthy et al., 2011; Nafziger, 1982), since the Fe content mainly depends on the spinel composition. Therefore, to increase the Cr/Fe ratio, the spinel has to be structurally dissociated in order for the Fe to be extracted. This requires either a hydrometallurgical method, pyrometallurgical method or a combination of both. Selective chlorination of Fe have received some attention (Nafziger, 1982; Shen et al., 2009a; Shen et al., 2009b). However, considering the health and safety risks associated with chlorine (Cl_2) gas used for chromite chlorination, it is unlikely that this option will be implemented on an industrial scale (Kanari et al., 2000; Shen et al., 2009a; Shen et al., 2009b). Therefore, the objectives of this investigation were firstly, to exploit the preferential reduction of Fe with a solid carbonaceous reducing agent in order to selectively segregate it from the Cr contained in the chromite spinel. Secondly, leaching of the metallised Fe with a sulphuric acid mixture. Sulphuric acid is well established as a leaching agent and has been frequently used to treat

different ores in previous investigations, indicating that Fe present in the ore can be readily stripped under certain conditions (Amer, 1992; Amer and Ibrahim, 1996; Biermann and Heinrichs, 1960; Geveci et al., 2002; Kumar Tripathy et al., 2012; Ledgerwood and van der Westhuyzen, 2011; Sen and Chatterjee, 1957; Sharma, 1990; Sundar Murti and Seshadri, 1979; Vardar et al., 1994). The pelletised chromite pre-reduction process will be used as the base for this investigation, as it is currently the only industrially applied solid-state reduction process for chromite. However, in practice, this would mean that the ore is pelletised before being pre-reduced. The pre-reduced pellets would then need to be broken down before being leached. Thus, alternatively, a process where the ore is first pre-oxidised to encourage Fe migration and enrichment on the surface of the chromite ore particles (Kleynhans et al., 2016) and subsequent pre-reduction without precursory milling and agglomeration would be considered as the third objective.

2. Materials and methods

2.1. Materials

Samples of raw materials were obtained from a large South African FeCr producer operating the pelletised chromite pre-reduction process (Beukes et al., 2010; Kleynhans et al., 2012; Kleynhans et al., 2016) at two of their smelters. The sample materials, utilised on an industrial scale during the pelletised chromite pre-reduction process, consist of metallurgical grade chromite ore (<1 mm), bentonite clay (binder) and anthracite (carbonaceous reductant). The same raw material samples as used by Kleynhans et al. (2012), who presented a comprehensive chemical and surface analysis of all these materials, were used in this investigation. Therefore, the material characterisations and methods applied are not repeated in detail here. However, a summary of the chemical composition of the three raw materials and the proximate analyses of the anthracite breeze are presented in Table 1.

Table 1
Chemical analyses (wt.%) of chromite ore, anthracite breeze (reductant) and bentonite clay (binder), their particle size distribution (PSD, μm, wt.%) and the proximate analysis (wt.%) of the anthracite breeze (air dry basis) used in this study (from Kleynhans et al., 2012).

		Anthracite	Chromite		Bentonite
ICP	Al_2O_3	3.13	15.21		13.17
	CaO	0.8	0.22		4.77
	Cr_2O_3	-	45.37		-
	FeO	1.62	25.39		-
	Fe_2O_3	-	-		5.33
	K_2O	-	-		1.14
	MgO	0.35	9.83		2.64
	MnO	-	-		0.08
	P	0.011	<0.01		0.02
	S	0.59	-		-
	SiO_2	10.09	1.72		53.53
	TiO_2	-	-		0.45
	Cr/Fe ratio (calc.)		*1.57*		
Proximate analysis	Fixed carbon	75.08	LECO	C	1.14
	Inherent moisture	0.26		S	<0.001
	Ash	17.79		H_2O loss (110 °C)	9.78
	Volatiles	6.87		LOI (1000 °C)	7.69
Particle size distribution	μm	wt.%			
	>4000	0.27	-		-
	2000-4000	16.77	-		-
	500-2000	64.69	18.63		-
	300-500	3.56	63.30		-
	150-300	4.46	12.75		-
	75-150	4.22	3.70		5.34
	45-75	2.06	1.04		8.31
	<45	3.98	0.59		86.35
	Total	100	100		100

Ultra-pure water from a Milli-Q water purification system (resistivity18.2 MΩ cm^{-1}) was used in all instances that required water. Instrument grade nitrogen (N_2) gas (Afrox Ltd.) was utilised in all pre-reduction experiments. Industrial Analytical (Pty) Ltd. supplied SARM 8 that was used as a reference standard in the analysis of chromite containing materials. Sulphuric- (H_2SO_4, 98%) and ortophosphoric acid (H_3PO_4, 85%) supplied by Rochelle Chemicals & Lab Equipment CC were used in the leaching experiments, as well as in the determination of the soluble Cr and Fe to calculate the pre-reduction levels achieved. Sodium peroxide (Na_2O_2), sodium carbonate (Na_2CO_3), hydrochloric- (HCl, 32%) and nitric acid (HNO_3, 55%) obtained from Associated Chemical Enterprises (Pty) Ltd. were used during the determination of the total Cr and Fe content in chromite and pre-reduced samples prepared by Na_2O_2 fusion. Ultraspec aqueous single and multi-element certified reference material standards (De Bruyn Spectroscopic Solutions) were used for calibration during inductively coupled plasma optical emission spectrometry (ICP-OES) and inductively coupled plasma mass spectrometry ICP-MS analysis. All other chemicals used were analytical grade (AR) reagents and used without any further purification.

2.2. Methods

2.2.1. Pre-oxidation of chromite ore

Pre-oxidation of the as-received chromite ore (<1 mm) was performed in a Lenton Elite model BRF15/5 chamber furnace fitted with a programmable temperature controller. 100 g of the metallurgical grade chromite ore was placed in a CoorsTek Inc. AD-998 ceramic (99.8% Al_2O_3) 340 mL rectangular tray, positioned centrally inside the furnace chamber and heated in a normal gaseous atmosphere (air) during each pre-oxidation test (Kleynhans et al., 2016). For each temperature profile, the furnace controller was set to ramp up from room temperature to a desired maximum temperature, i.e. 800, 1000 and 1200 °C, over time periods of 10, 20 and 40 min, respectively. The controller was then programmed to remain

constant at the specific maximum pre-oxidation temperature for the desired pre-oxidation retention times, i.e. 30, 60, 120 and 240 min, after which the furnace was set to automatically switch off and left to naturally cool to room temperature. The durations it took for the furnace to cool from 800, 1000 and 1200 °C to 500 °C were approximately 65, 82 and 90 min, respectively.

2.2.2. Raw material preparation

The preparation of raw materials was conducted similarly to the procedures previously described by Kleynhans et al. (2016), Neizel et al. (2013) and Kleynhans et al. (2012). A Retsch GmbH BB 100 jaw crusher, set at a minimum plate width of <4 mm, and a Wenman Williams & Co. disc mill was utilised to crush and grind the as-received lumpy anthracite to <4 mm fragments (PSD, Table 2). The three primary components of the uncured pellets for pelletised pre-reduction experiments were mixed in a ratio of 3 wt.% bentonite, 15 wt.% anthracite (ensuring ~11.3 wt.% fixed carbon content in the pellets) and the remaining 82 wt.% comprised of metallurgical grade chromite ore. The afore-mentioned dry material mixture was then milled in 50 g batches for 2 min to ensure that the components were well mixed and that the particle size distribution (PSD) of the milled mixture was similar to the sizing requirement applied in the industrially applied pre-reduction process, i.e. 90% smaller than 75 µm (d_{90} = 75 µm) (Kleynhans et al., 2012). A Siebtechnik vibratory disc mill and grinding jar (250 mL sample volume), commonly used to mill solid samples prior to chemical analysis, were used for this purpose. All parts of the grinding jar, which made contact with the sample, were made of tungsten carbide. This prevented possible Fe contamination of the milled sample, which could influence pre-reduction levels. The PSD (d_{90} = 75 µm specification) of the milled material was verified with a Malvern Mastersizer 2000 and the average PSD presented in Table 2.

Table 2
Average PSD of the milled pellet material mixtures for pelletised pre-reduction experiments (Section 2.2.2).

		Milled material (wt.%) (d_{90} = 75 µm specification)
Particle size (µm)	106-125	0.62
	90-106	3.95
	75-90	4.79
	63-75	3.96
	53-63	3.08
	45-53	3.37
	38-45	5.37
	<38	74.86
	Total	100

For the un-agglomerated pre-reduction experiments the two components, i.e. un-milled pre-oxidised metallurgical grade ore (<1 mm, Table 2) and fragmented anthracite reductant (<4 mm, Table 2), were mixed by hand in a ratio of ~79 wt.% ore (40 g) and ~21 wt.% reductant (10.383 g), in order to have a 0% fixed carbon excess according to the reaction stoichiometry of Eq. (1).

$$FeO.Cr_2O_3 + 4C \rightarrow Fe + 2Cr + 4CO \quad (1)$$

In the base case un-agglomerated pre-reduction experiment untreated, un-milled metallurgical grade ore (<1 mm), that was not subjected to pre-oxidation, was used.

2.2.3. Pelletised pre-reduction pellet preparation

Pellet preparation methods similar to that presented by Neizel et al. (2013) and Kleynhans et al. (2012) were applied. The milled (d_{90} = 75 µm) ore-reductant-clay material mixture, used in the pelletised pre-reduction experiments, was pressed into cylindrical pellets with an LRX Plus strength testing machine (Ametek Lloyd Instruments) equipped with a

5 kN load cell and a Specac PT No. 3000 13 mm die set. Pellets were prepared in batches of 10 each. For each batch 50 g of dry mixed raw material was pre-wetted with 5 g of water and mixed thoroughly. 3.2 g of pre-wetted material was then place in the die set and compressed at a rate of 10 mm/min until a load of 1500 N was reached, where after this load was held for 10 s. Although time consuming (each pellet made individually), this technique was preferred over conventional disc pelletisation, since disc pelletisation on laboratory scale can result in the formation of pellets with different densities, sizes and spherical shapes. The above described procedure ensured consistent density, form and size, which allowed the monovariance investigation of other process parameters.

2.2.4. Pelletised and un-agglomerated pre-reduction tests

Two ceramic tube furnaces, namely the Lenton Elite models TSH 15/75/610 and LTF 18/75/300, with built-in programmable temperature controllers capable of 1500 and 1800 °C maximum temperatures, respectively, was used to conduct all pre-reduction experiments. Ceramic heat insulation plugs were inserted at both ends of the furnaces tubes to enhance the effective zone inside the tube in which a stable working temperature could be achieved. These heat insulation plugs also shielded stainless steel caps, which were fitted onto both sides of the ceramic tubes to seal the ends and prevent air ingression. The stainless steel caps was equipped with a gas inlet and an outlet on opposing sides of the tubes. The gaseous atmosphere inside the furnace was controlled by a constant N_2 flow of 1 NL/min through the furnace tube, which ensured an inert gaseous environment inside the tubes, preventing reduction or oxidation due to ingress of an external reducing or oxidising gas. Before the pre-reduction experiments commenced the tube furnace, already loaded with pellets (batch of 10 pellets) or the un-agglomerated mixture (50.383 g batch), depending on the specific test, was flushed with N_2 for 15-30 min at a flow rate of 1.25 NL/min at room temperature to remove oxidising gases.

For the pelletised pre-reduction experiments eight maximum temperatures was investigated. For each temperature profile, the furnace controller was set to ramp up from room temperature to the desired maximum pre-reduction temperature over specific time periods, i.e. 750°C (20 min), 825 °C (20 min), 900 °C (20 min), 975 °C (40 min), 1050 °C (40 min), 1125 °C (40 min) and 1200 °C (40 min). The controller was then programmed to remain constant at the specific maximum pre-reduction temperature for the desired pre-reduction retention times, i.e. 30, 60, 120 and 240 min, after which the furnace was set to automatically switch off and left to naturally cool to room temperature while the gas flow was maintained. The tube furnace capable of 1500 °C was used for tests with a maximum pre-reduction temperature of 750, 825 and 900 °C, while the furnace capable of 1800 °C was used for the remaining pelletised pre-reduction tests.

For the un-agglomerated pre-reduction tests only one temperature profile was used which consisted of three segments, i.e. (i) heating up from room temperature to the maximum temperature of 1300 °C over a period of 30 min, (ii) keeping the furnace temperature constant at 1300 °C for 150 min, (iii) ending the temperature profile by shutting down the furnace controller and naturally cooling the furnace to room temperature while maintaining the N_2 gas atmosphere. The Lenton Elite model LTF 18/75/300 capable of 1800 °C was used for the un-agglomerated pre-reduction tests.

The two furnaces with different power outputs and maximum temperatures was used in order to reach the desired maximum pre-reduction temperature within the specific time periods identified during the ramp up segment of the temperature profiles. The durations it took for the furnaces to cool from 750, 825, 900, 975, 1050, 1125, 1200 and 1300 °C to 500 °C was approximately 56, 65, 73, 79, 83, 86, 88 and 90 min, respectively.

2.2.5. Analysis of pre-reduction levels achieved

The percentage pre-reduction achieved was determined, similar to previous studies by Kleynhans et al. (2016), Mohale (2014), Neizel et al. (2013) and Kleynhans et al. (2012), according to the method utilised by laboratories associated with FeCr smelters in South Africa currently applying the pelletised chromite pre-reduction process. The percentage pre-reduction was determined using the following equation:

$$Pre-reduction\ (\text{wt.}\%) = \frac{\frac{m_{Cr_{sol}}}{34.664} + \frac{m_{Fe_{sol}}}{55.845}}{\frac{m_{Cr_{Tot}}}{34.664} + \frac{m_{Fe_{Tot}}}{55.845}} \over 100 \quad (2)$$

In Eq. (2) $m_{Cr_{sol}}$, $m_{Fe_{sol}}$ represents the mass of Cr and Fe in the metallised state and $m_{Cr_{Tot}}$, $m_{Fe_{Tot}}$ are the total mass of Cr and Fe present, respectively. However, the level of Fe and Cr metallisation is not directly related to the total pre-reduction, which is most commonly related to the removal of oxygen (Barnes et al., 1983). Therefore, the constant 34.67 was calculated from the molar mass of Cr divided by1.5 and the constant 55.85 for Fe was calculated from the molar mass of Fe divided by 1. These factors, i.e. 1.5 for Cr and 1 for Fe, were derived from the balanced reaction equations, wherein 1.5 mol of CO form in the metallisation reaction for Cr and 1 mol of CO form in the metallisation reaction for Cr (Barnes et al., 1983). The $m_{Cr_{sol}}$ and $m_{Fe_{sol}}$ were determined by digesting a fixed mass of the sample material with a hot sulphuric-phosphoric acid solution. The $m_{Cr_{sol}}$ in this aliquot was then established by oxidation of the soluble Cr with potassium permanganate and subsequent volumetric determination with ferrous ammonium sulphate using diphenylamine sulphonate as an indicator. The $m_{Fe_{sol}}$ in the aliquot (a portion not oxidised with potassium permanganate) was determined by a similar volumetric method, using potassium dichromate as the titrant and diphenylamine sulphonate as an indicator. The $m_{Cr_{Tot}}$ and $m_{Fe_{Tot}}$ were determined by Na_2O_2 fusion. Precisely 0.2 g of finely ground sample (d_{90} = 75 µm) was

fused with 3 g of Na_2O_2 and 0.5 g of Na_2CO_3 in a zirconium crucible. The fused solid mixture was transferred into a 250 mL volumetric flask containing a 20% acid mixture of 1:1 HCl and HNO_3 and left to dissolve completely. The total Cr and Fe content was determined by a Spectro Ciros Vision ICP-OES Spectrometer.

2.2.6. Acid leaching setup and procedure

Batch-leaching equipment consisted of a FMH electronics CC model STR-MH hot plate (up to 420 °C) with magnetic stirrer (60-2000 rpm), 250 mL Erlenmeyer flask, magnetic stirrer bar (ø 8 mm × 40 mm), Claisen adapter, thermometer adapter with O-ring, thermometer (up to 250 °C) and a 300 mm (H) Liebig medium-capacity condenser. All glassware fitted together with ST/NS 14/20 joints.

Prior to specific leaching tests the pre-reduced material, both pelletised and un-agglomerated were pulverised to the d_{90} = 75 µm specification, if indicated that milled material were leached. The same Siebtechnik vibratory disc mill and grinding jar indicated in Section 2.2.2, was used for this purpose. Batches consisting of 10 pre-reduced pellets (<32 g after pre-reduction, Section 2.2.2) and un-agglomerated mixtures (<50.383 g after pre-reduction, Section 2.2.2) were milled for 0.25 and 2 min, respectively. The PSD was verified with the Malvern Mastersizer 2000 (Section 2.2.2) and the average PSD for the milled pre-reduced pellet and un-agglomerated material was practically identical to the PSD reported in Table 2 (Section 2.2.2), i.e. d_{90} = 75 µm.

The acid leaching mixture was made up of 40 wt.% H_2SO_4 (98%) and 10 wt.% H_3PO_4 (85%), with the remaining balance (50 wt.%) consisting of ultra-pure Milli-Q water. At the beginning of each test 50 mL (vol.) of the acid mixture was pipetted into the 250 mL Erlenmeyer flask and the stirrer set to ~500 rpm (using ø 8 mm × 40 mm magnetic stirrer bar). The acid mixture was heated to 120 °C, and, when the leaching liquid reached the

desired temperature, 2.5 g (wt.) of milled pre-reduced material was added, resulting in a slurry concentration of 5% wt./vol. In leaching tests of the un-milled un-agglomerated pre-reduced ore, 5 g of material was added to the 50 mL acid mixture, giving a slurry concentration of 10% wt./vol. The slurry was leached for 1 h in all leaching tests, where after the hot plate was switched off, leaving the slurry to cool down to room temperature while stirring continued. The cooled slurry was filtered, washed with water and dried, where after the total Cr and total Fe contents were determined (Section 2.2.5) and the Cr/Fe ratio was calculated.

2.2.7. Surface topography and surface elemental analysis

Scanning electron microscopy (SEM) and SEM coupled to energy dispersive spectroscopy (SEM-EDS) were employed to characterise the surface properties of samples. A Zeiss MA 15 SEM incorporating a Bruker AXS XFlash® 5010 Detector X-ray EDS system operating with a 20 kV electron beam at various working distances was used. Backscattered electrons combined with EDS were used to determine the elemental composition in different areas of the samples. The same instrument was also used to obtain X-ray mapping, which provided information of elemental spatial distributions on the surface of a sample. Polished and unpolished samples were considered.

3. Results and discussion

During this investigation, two process options were considered as potential approaches to selectively remove Fe from the chromite spinel and consequently increase the ores Cr/Fe ratio. The different process options will therefore be discussed in different sub-sections, i.e. Section 3.1 and 3.2. When considering a systems engineering approach to development, the life cycle of a process or project usually starts with a concept and exploration phase, of which system requirements and conceptual design forms an integral

part (INCOSE, 2015). However, this step is often ignored when either improvements to an existing process or a new process is researched and reported on in the peer reviewed public domain. Therefore, before going into the technical aspects of this investigation, is important to firstly conceptualise the process steps, illustrated in the form of elementary process flow diagrams (Section 3.1.1 and 3.2.1), that would be required for the different process alternatives proposed in this investigation.

3.1. Pelletised pre-reduction prior to leaching

3.1.1. Proposed process flow

A process flow diagram indicating the likely process steps to be utilised when combining pelletised carbo-thermic pre-reduction, with the aim of selectively separating Fe from the chromite spinel, with subsequent acid leaching to extract the Fe and improve the ores Cr/Fe ratio, is shown in Fig. 1. In this general process flow diagram (Fig. 1), process steps 1-5 are based on the currently applied pelletised chromite pre-reduction process. In these steps, the raw materials (metallurgical grade chromite ore (<1 mm), a clay binder and a carbon reductant) are dry milled to a particle size specification of 90% <75 μm, followed by pelletisation and preheating, before being fed into a rotary kiln where the chromite is partially pre-reduced. In order to maximise the Cr/Fe ratio, the kiln must either be specifically designed and/or operated with the aim to optimise the required conditions favouring Fe reduction, as opposed to Cr reduction. Then, in process step 6, it is proposed that the hot partially reduced pellets (~1000 °C) is purposely quenched in water to prevent re-oxidation of the metallised Fe. This will undoubtedly result in bursting of the hot pellets, which is advantageous since lower energy would be required during subsequent milling (process step 7).

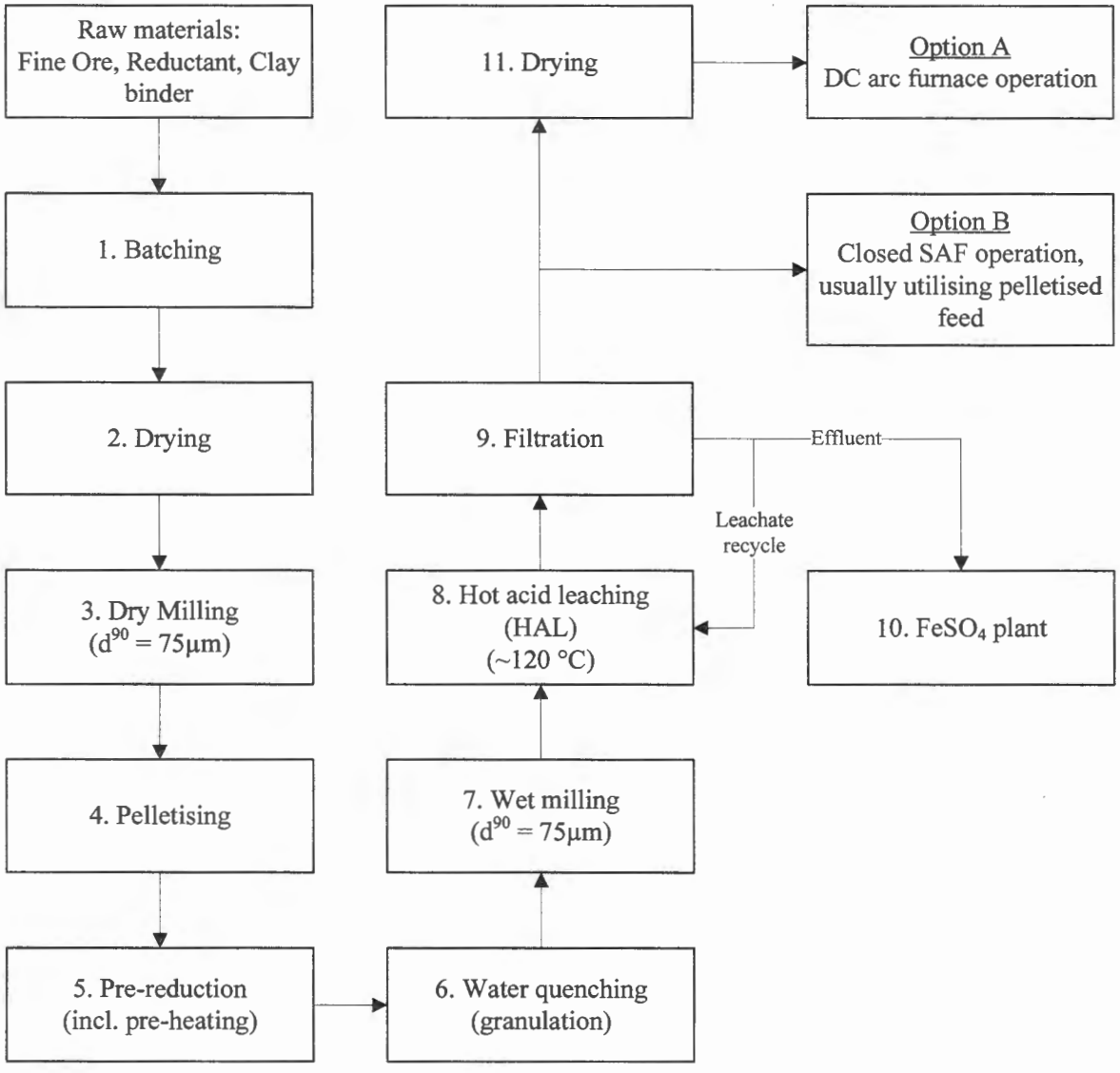

Fig. 1. A process flow diagram indicating the likely process steps to be utilised for pelletised pre-reduction prior to acid leaching to improve the Cr/Fe ratio of chromite.

Wet milling, as opposed to dry milling would be utilised, since both process steps 6 and 8 are hydro (water)-metallurgical process steps. Following acid leaching (process step 8), the leachate is recycled and re-used until saturated, where after the effluent is sent to the $FeSO_4$ plant (process step 10). It is well known that ferrous chemical are used to reduce hexavalent chromium, Cr(VI), in the FeCr industry (Beukes et al., 2012). It is therefore

proposed that the saturated ferrous effluent could be used to treat Cr(VI)-containing wastes, either at the FeCr smelter where the Fe leaching is conducted, or sold as a by-product to other FeCr smelters. After leaching (process step 8) the solid material would be separated from the leach liquid by filtration (process step 9). The upgraded ore would then be fed as raw material to either a closed submerged arc furnace (SAF) operation utilising a pelletised feed, or dried and fed to a direct current (DC) arc furnace. These processes are discussed in some detail by Beukes et al. (2010), as well as in earlier papers (Gasik, 2013; Naiker, 2007; Naiker and Riley, 2006; Ugwuegbu, 2012).

3.1.2. Effect of temperature and retention time on agglomerated pre-reduction

From previous studies it is evident that pre-reduction temperature and retention time are the main parameters that affect the pre-reduction level (Hu et al., 2016; Wang et al., 2014, 2015). Therefore, in order to determine the process conditions to obtain the desired Cr/Fe ratio, the effect of pre-reduction temperature and retention time on the extent of pre-reduction, as well as individual Fe and Cr metallisation were investigated. These results are graphically illustrated in Fig. 2, with the experimental data included in the Supplementary materials (Table S1). It is clear from Fig. 2 and Table S1 that pre-reduction temperatures and retention times up to 1050 °C and 240 min, respectively, did not have a significant effect on the pre-reduction level achieved. The pre-reduction level increased marginally from~4 % to ~8 % over the 750-1050 °C temperature range, while the Cr metallisation remained constant at ~2 %. The Fe metallisation increased to some extent form ~10 to ~22 %.

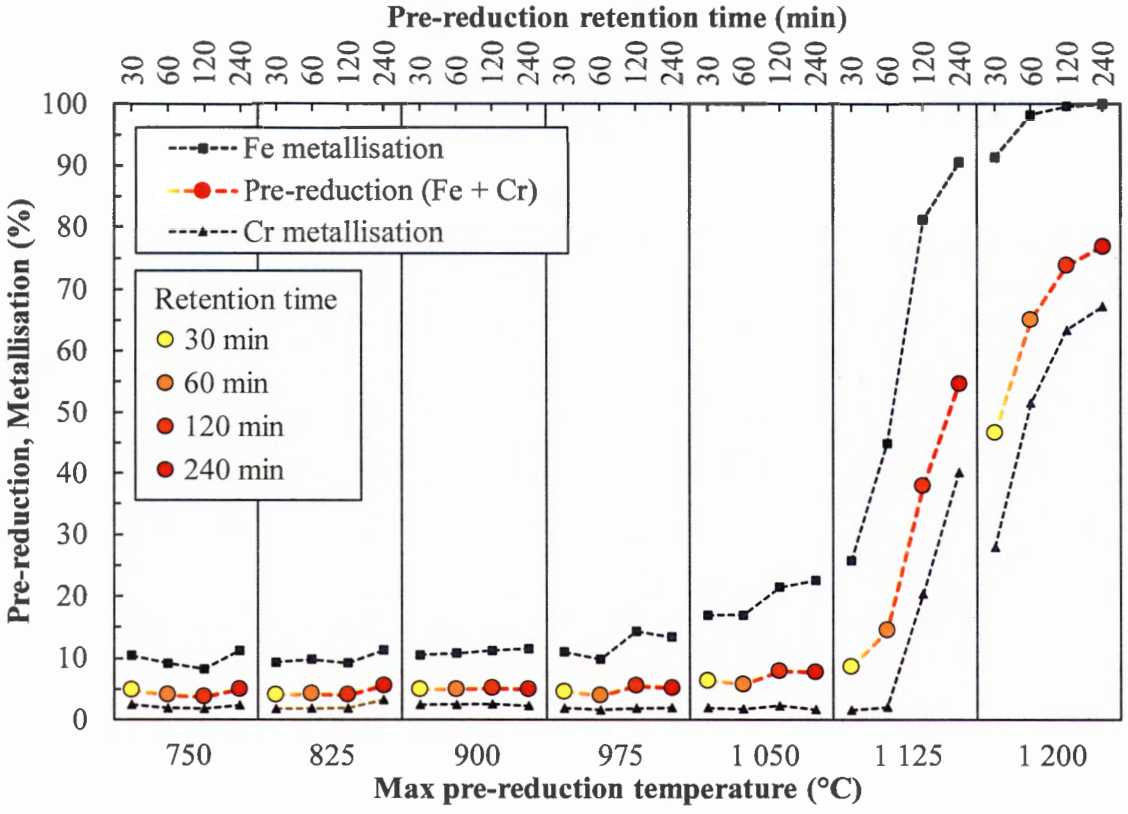

Fig. 2. The effect of pre-reduction temperature (primary x-axis) and retention time (secondary x-axis) on the extent of pre-reduction, as well as individual metallisation of Fe and Cr (primary y-axis)

Considering published thermodynamic data (e.g. Kleynhans et al. (2016); Niemelä et al. (2004)), solid C can reduce Fe oxides to metallic Fe at temperatures >750 °C, with reduction taking place from the highest to the lowest oxidation state, i.e. hematite (Fe_2O_3) to magnetite (Fe_3O_4) to wüstite (FeO) to metallic Fe. However, in thermodynamic calculations the kinetic effects are not taken into account. McCullough et al. (2010) indicated that the reduction rate is temperature dependent, as expected, and that it conform to the Arrhenius equation. Therefore, although thermodynamically Fe metallisation occurs at >750 °C, it is evident that the rate of Fe metallisation and, consequently, pre-reduction is limited at temperatures <1050 °C. At pre-reduction temperatures ≥1125 °C a dramatic increase in the rate of both Fe and Cr metallisation, as well as pre-reduction, is observed in Fig. 2. Here the

results for Cr metallisation is somewhat unexpected since, thermodynamically, Cr_2O_3 is supposed to be reduced by solid C at temperatures >1250 °C (Kleynhans et al., 2016; Niemelä et al., 2004). Although synthetic chromite ($FeO.Cr_2O_3$) is thermodynamically predicted to reduce at lower temperatures than Cr_2O_3, i.e. 1200 °C, it still does not explain the surge in Cr metallisation at ≥1125 °C. Perry et al. (1988) explained the occurrence of various phases that form during chromite pre-reduction (also known as solid-state carbothermic reduction of chromite), using a point-defect ionic diffusion mechanism. In this model each chromite particle was considered to be comprised of concentric layers of spinel unit cells (Fe^{2+} and Mg^{2+} occupy tetrahedral sites, Cr^{3+}, Al^{3+}, and Fe^{3+} occupy octahedral sites). The phases that form are a result of the interchange of cations between unit cells within the particle affected by the presence of carbon monoxide at the surface of the particle. Perry et al. (1988) identified four stages of reduction, i.e. (I) the formation of a slightly Fe-enriched core comprising of distorted spinel unit cells surrounded by a region of normal spinel unit cells, effected by the reduction of Fe^{3+} to Fe^{2+}; (II) the formation of Cr-Al sesquioxide and Mg-Cr-Al spinel phases affected by the metallisation of Fe^{2+} ions and subsequent production of Cr^{2+} ions; (III) reduction of Fe^{2+} interstitials in the spinel core; and (IV) metallisation of Cr ions via the Cr^{2+} intermediate. In order to retain the spinel structure during stage II of the afore-mentioned mechanism, the direct reduction of an Fe^{2+} ion results in two trivalent cations being assigned to interstitial sites that results in the solution of a sesquioxide (itself a solid solution of Cr_2O_3 and Al_2O_3 having the hexagonal close-packed structure) in the spinel unit cell. When Cr reduction takes place, the Cr ions occur in both the oxide phase, the Cr-Al sesquioxide phase and the Mg-Cr-Al spinel phase. Chromite ore in South Africa's BC occurs in 13 layers, i.e. UG1 and 2 (Upper group), MG1-4 (Middle group) and LG1-7 (Lower group) (de Waal and Hiemstra, 1975). Rankin (1979) identified the occurrence of the Cr-Al sesquioxide phase only during the reduction of LG6 chromite at temperatures below 1200 °C,

while the sesquioxide phase still formed in UG2 chromite at 1300 °C. The formation of the Cr-Al sesquioxide phase is an important step in the reduction mechanism and the temperature at which the sesquioxide forms is thus dependent on the chromite composition as indicated by Rankin (1979). The specific chromite ore utilised in this investigation was extracted from the LG6 seam, which therefore explains the Cr metallisation at temperatures below 1200 °C.

3.1.3. Leaching of pelletised pre-reduced material

The effect of the level of pre-reduction achieved at different temperatures and retention times on the Cr/Fe ratio and Cr recovery of pelletised pre-reduced metallurgical grade chromite ore, after milling and hot acid leaching (Section 2.2.6), is presented in Fig. 3 (and Supplementary Table S1). From these results it is apparent that pre-reduction temperatures of 750–1050 °C with related retention times (30-240 min) hand no effect or resulted in only a slight increase, i.e. from 1.57 to ~1.56 and ~1.87, in the Cr/Fe ratio, while the Cr recovery remained at ~98%. At pre-reduction temperatures above 1125 °C, both an increase in temperature and retention time had a substantial effect on the Cr/Fe ratio, rising from ~2.3 to ~23.4. However, these pre-reduction conditions (temperatures >1125 °C) and subsequent leaching, resulted in a drastic decrease in the recoverable Cr, declining from ~98% to ~33%.

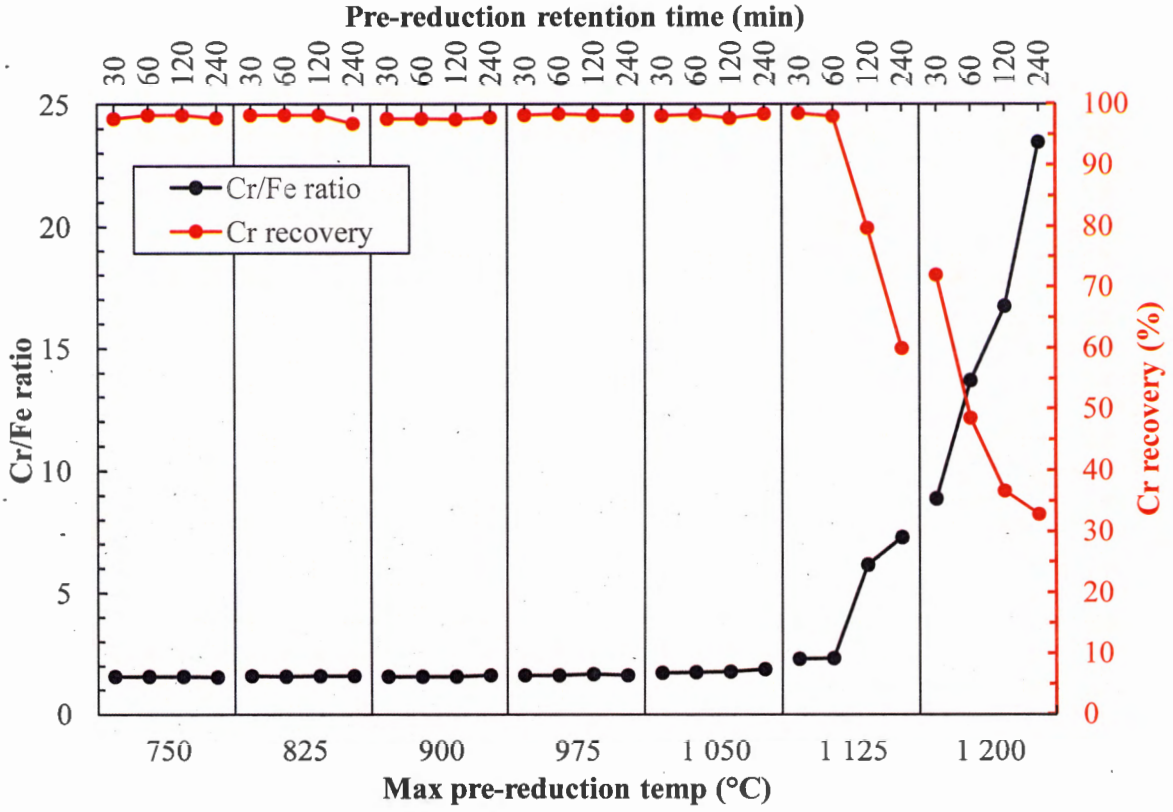

Fig. 3. The effect of pre-reduction temperature (primary x-axis) and retention time (secondary x-axis) on the Cr/Fe ratio (primary y-axis) and Cr recovery (secondary y-axis) of pelletised pre-reduced metallurgical grade chromite ore subjected to milling (d_{90} = 75 µm) and subsequent hot acid leaching (Section 2.2.6).

The Cr/Fe ratio achieved coupled with the corresponding Cr recovery will have a significant influence on the economic feasibility of implementing a process to selectively remove Fe for the chromite ore. Therefore, in order to put the results presented in Fig. 3 (and Table S1) into perspective, the Cr recoveries are compared to that of existing FeCr production processes. The current industrially applied pelletised pre-reduction process recovers ~88-90% of Cr from chromite ore, while the Outotec oxidative sintering process recovers in the order of 80-88%%. The conventional ore fed SAFs process recover 68-75% of Cr from chromite ore, while the DC arc process recovers ~90%. Therefore, hypothetically, chromite ore subjected to the proposed pelletised pre-reduction condition that result in a Cr recovery of 80% or less after leaching, could have an ultimate Cr recovery of 70% or less

after smelting by means of a DC arc process. This would be similar to that of the current conventional processes Cr recovery (68-75%). Another factor would be the potential market for a FeCr produced from an improved Cr/Fe ratio chromite ore. Currently, the main FeCr alloys produced are; I) high-carbon FeCr with Cr contents >60% and C contents typically between 4 and 6%, produced from ores with Cr/Fe ratios >2.0 up to 4, mainly from Kazakhstan, India and Turkey, and II) charge grade FeCr containing 50-55% Cr and 6-8% C, produced from lower grade ores mainly from South Africa, with Cr/Fe ratios ranging from 1.3-1.8 (Gasik, 2013; McCullough et al., 2010). The typical average Cr/Fe ratio of Kazakhstan, Turkey and Indian chromite ore are 3.5, 3.0 and 2.7, respectively. As high-carbon FeCr is currently produced from a >2 to 4 Cr/Fe ratio chromite ore, it makes sense to improve the Cr/Fe to this level in order to sell into the already existing market. Examining Fig. 3 (and Table S1) it is observed that samples pre-reduced at 1125 °C with 30 and 60 min retention times (Samples FW and FX, Table S1) resulted in Cr/Fe ratios of ~2.28 and ~2.32, respectively. This is above the typical minimum Cr/Fe ratio for high-carbon FeCr production, i.e. >2. Furthermore, for both these data points the Cr recovery is ~98%. A Cr/Fe ratio of 3-3.5 and a Cr recovery >95% might also be possible. However, due to the metallisation of Cr at lower temperatures than thermodynamically expected (as explained in Section 3.1.2), it is the opinion of the authors that it would be difficult to manage and maintain the exact optimum conditions necessary, i.e. temperature and retention time, to obtain the desired Cr/Fe ratio and Cr recovery after leaching.

3.1.4. Scanning electron microscopy analysis

In order to visually examine the possible surface and internal chemical effects caused by pre-reduction and subsequent leaching, SEM back-scatter micrographs of the pulverised (d_{90} = 75 μm) pre-reduced pellet material mounted in resin followed by polishing (Fig. 4), as well as of the leached pulverised pre-reduced pellet material mounted on copper tape (Fig. 5),

were attained. SEM-EDS analysis of only the Cr and Fe content (wt.%) for different points or areas indicated in Fig. 4, are presented in Table 3.

Fig. 4–AW and Fig. 4–DW show SEM micrographs taken at 1000 times magnification of pulverised (d_{90} = 75 µm) pre-reduced pellet material that was treated at 750 and 975 °C, respectively, with a retention time of 30 min. In both these images no metal globules of pre-reduced material are observed, despite reaching pre-reduction and Fe metallisation levels of ~4 and ~11 wt.%, respectively. In both images, smaller fragmented particles are observed, which is consistent with the pellets being pulverised after pre-reduction for subsequent leaching.

In Fig. 4–FW_a and Fig. 4–FW_b, SEM micrographs taken at 1000 and 4000 times magnification, respectively, of pulverised (d_{90} = 75 µm) pre-reduced pellet material that was treated at 1125 °C with a retention time of 30 min, are presented. In the 4000 times magnified Fig. 4–FW_b, very small metal globules of pre-reduced material are observed on the outside of the ore particle in the vicinity of marker A and B. SEM-EDS analysis (Table 3) of a metal globules (white particle) marked by A had a high Fe content (94.15 wt.%) compared to Cr (5.85 wt.%). The Cr/Fe ratio on the interior of the particle (grey area) marked by B was 2.33, similarly to what was presented in Fig. 3 and Table S1 for sample FW.

Fig. 4–FY and Fig. 4–GZ show SEM micrographs taken at 1000 times magnification of pulverised (d_{90} = 75 µm) pre-reduced pellet material that was treated at 1125 °C with a retention time of 120 min and 1200 °C with a retention time of 240 min, respectively. The amount and proportion (size) of the pre-reduced metal globules increased with an increase in pre-reduction temperature and retention time. The metal globules are also located near or on the surface of the ore particles. Fragments of small metal globules that broke off during milling for subsequent leaching are also observe. SEM-EDS analysis (Table 3) of metal

globules (white particles) marked A, C and E shows an increase in the Cr content that the metal globules contain, which corresponds to the increase in Cr metallisation observed at ≥1125 °C in Section 3.1.2. The Cr/Fe ratio of the areas marked D and F on the interior of the ore particles (grey areas) was 6.65 and 20.31, similarly to the results presented in Fig. 3 and Table S1 for sample FY and GZ, respectively.

Table 3
SEM-EDS results for different points/areas in Fig. 4.

Point/Area	Cr (wt.%)	Fe (wt.%)	Cr/Fe ratio
A	5.85	94.15	0.06
B	69.93	30.07	2.33
C	20.06	79.94	0.25
D	86.93	13.07	6.65
E	40.21	59.79	0.67
F	95.31	4.69	20.31

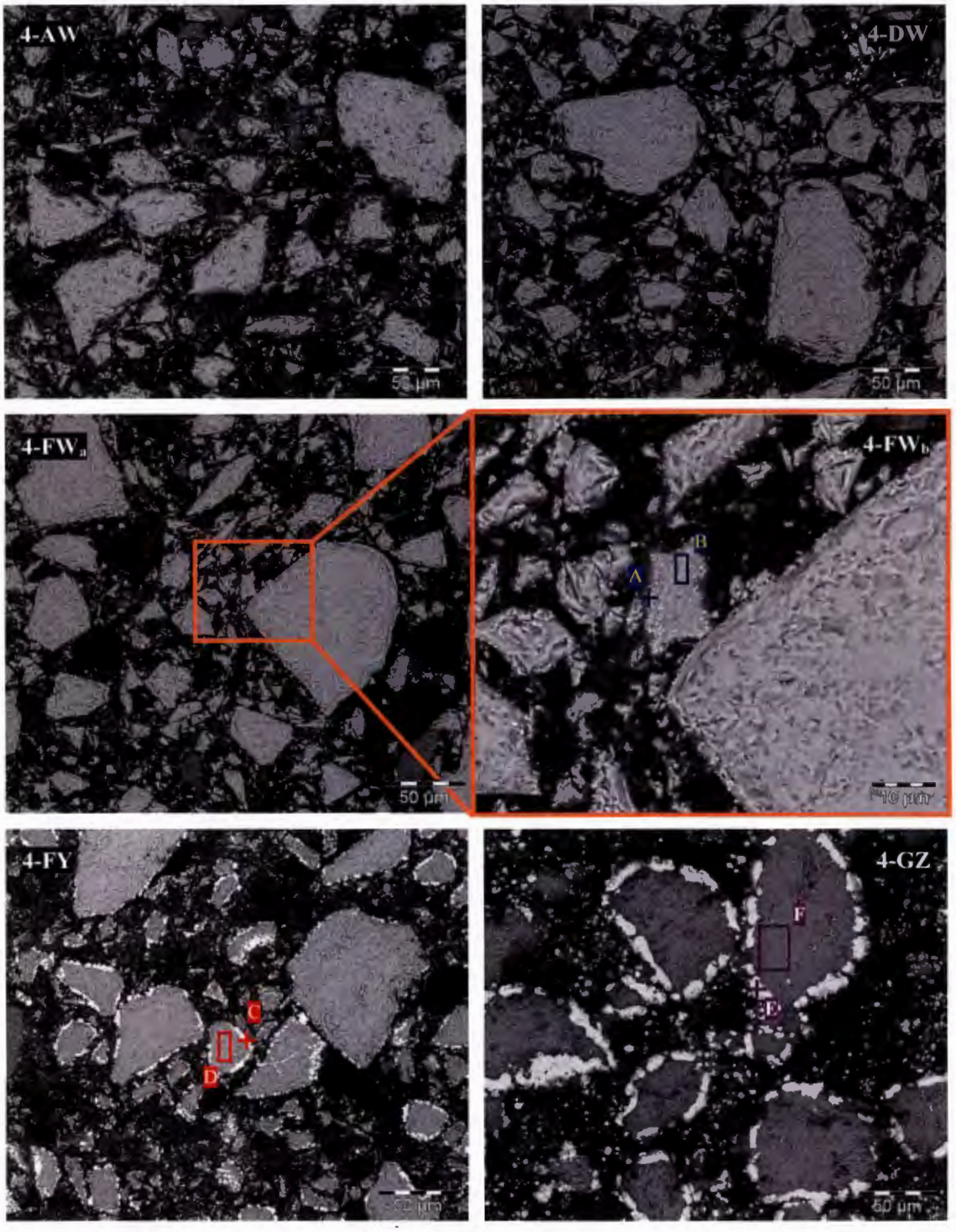

Fig. 4. SEM micrograph images taken at 1000 (50 µm) and 4000 (10 µm) times magnification of pulverised (d_{90} = 75 µm) pre-reduced pellet material mounted in resin. The material was treated at 750 °C, 30 min retention time (AW), 975 °C, 30 min retention time (DW), 1125 °C, 30 min retention time (FW_a, FW_b), 1125 °C, 120 min retention time (FY), 1200 °C, 240 min retention time (GZ).

Fig. 5–A and Fig. 5–B show SEM micrographs taken at 6000 and 28 000 times magnification of pulverised (d_{90} = 75 μm) pre-reduced pellet material that was treated at 1125 °C with a retention times of 60 min (sample FX). It is evident that the chromite ore particle had a relatively smooth surface with finer material present as a result of pulverisation after pre-reduction for subsequent leaching. Fig. 5–AL, Fig. 5–BL and Fig. 5–CL show SEM micrographs taken at 6000, 28 000 and 60 000 time magnification of the pulverised (d_{90} = 75 μm) pre-reduced pellet material treated at 1125 °C with a retention time of 60 min (sample FX) after leaching (Section 2.2.6). Cavities as a result of leaching are clearly observed on the surface of the chromite ore particle.

Considering Fig. 4 and Fig. 5, it seems that the metal globules containing mainly Fe collects near and/or on the surface of the chromite ore particle. SEM-EDS results presented in Table 4 of the areas shown in Fig. 5–A and Fig. 5–B indicates that the Cr/Fe ratio on the surface of the pre-reduced particles, i.e. 1.31 and 1.42, are less than the homogeneously determined 1.57 Cr/Fe ratio of the untreated chromite ore. This is consistent with the observation of the metal globules, consisting mainly of Fe, collecting near and/or on the surface of the chromite ore particle, thus lowering the Cr/Fe ratio. The Cr/Fe ratios on the surface of the pre-reduced ore particle after leaching, calculated from the SEM-EDS analysis of the areas shown in Fig. 5–AL, Fig. 5–BL and Fig. 5–CL, was 3.65, 2.96 and 3.29, respectively. This was higher than the homogeneously determined 2.33 Cr/Fe ratio reported in Table S1 for sample FW after leaching. This is again consistent with Fe collecting at the surface and being stripped from the exterior of the ore particle by leaching. The result is a higher Cr/Fe ratio on the surface of the ore particle when compared to the average homogeneously calculated Cr/Fe ratio.

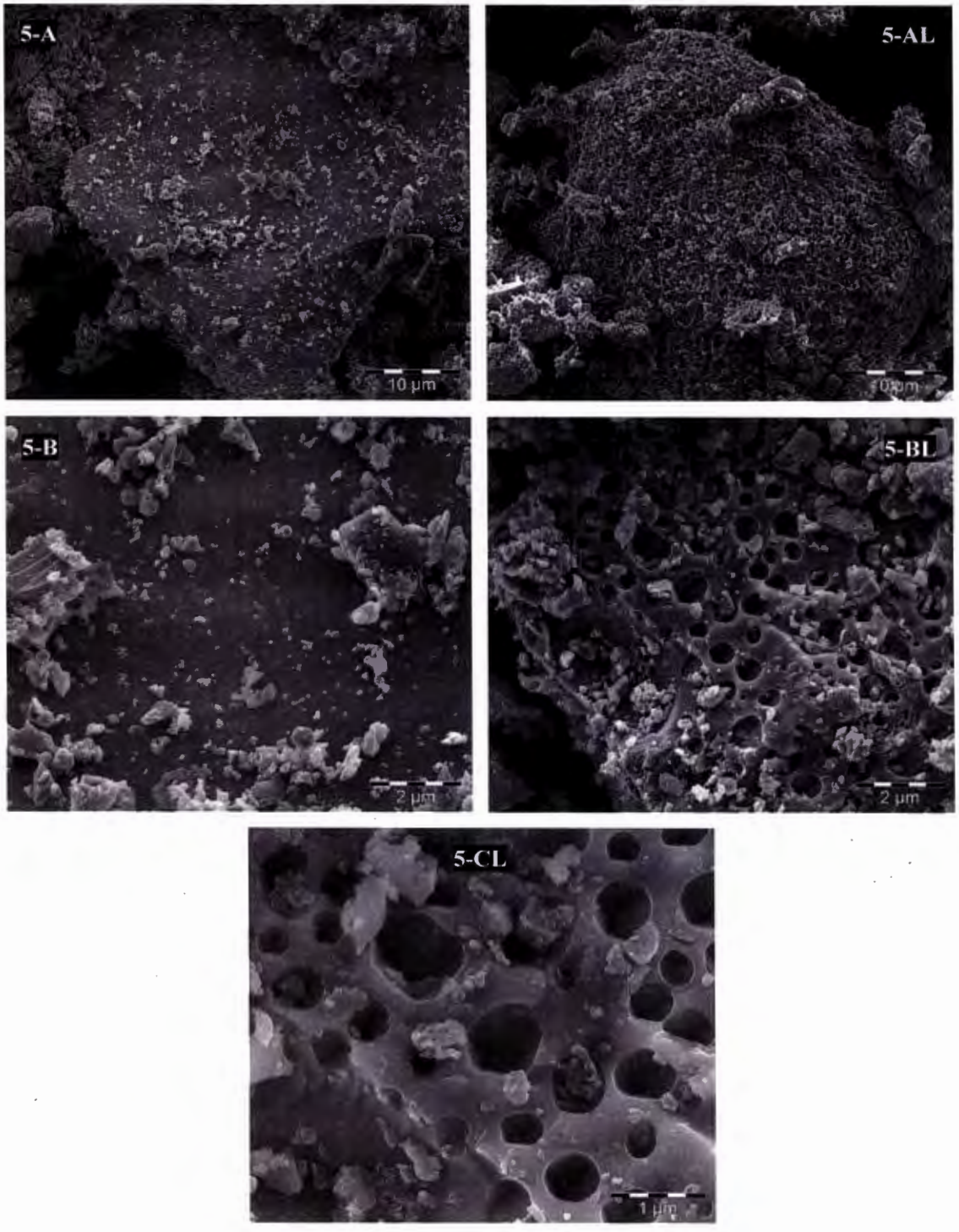

Fig. 5. SEM micrograph images taken at 6000 (10 µm), 28 000 (2 µm) and 60 000 (1 µm) times magnification of pulverised (d_{90} = 75 µm) pre-reduced pellet material, as well as images of the same material after hot acid leaching (HAL), mounted on copper tape. All the images was taken of sample FX, treated at 1125 °C with a 60 min retention time. A and B show the surface of an ore particle after pre-reduction, prior to leaching. AL, BL and CL show the surface of ore particles after leaching.

Table 4
SEM-EDS results for different micrographs in Fig. 5.

Image	C	Mg	Al	Si	Ti	Cr	Fe	O	Cr/Fe ratio
5-A	16.83	1.19	1.96	1.24	0.18	11.95	9.09	57.17	1.31
5-B	10.47	3.11	4.6	0.49	0.24	19.41	13.7	47.98	1.42
5-AL	17.37	1.57	2.39	1.53	0.19	13.87	3.80	58.99	3.65
5-BL	10.44	3.47	4.94	1.92	0.27	22.21	7.50	49.26	2.96
5-CL	10.14	1.93	4.67	2.85	0.32	17.91	5.45	56.72	3.29

3.2. Pre-oxidation with subsequent un-agglomerated pre-reduction prior to leaching

3.2.1. Proposed process flow

A process flow diagram illustrating the possible process steps to be utilised when combining chromite pre-oxidation and un-agglomerated pre-reduction, to selectively metallise Fe in the chromite spinel, with subsequent acid leaching, to extract the Fe and improve the ores Cr/Fe ratio, is shown in Fig. 6. Firstly, the metallurgical grade chromite ore (<1 mm) is pre-oxidised (Fig. 6, process step 1) prior to un-agglomerated pre-reduction (process step 2). Concurrently, a carbonaceous reductant is fed along with the pre-oxidised ore into the un-agglomerated pre-reduction process. The pre-reduced material discharging from the un-agglomerated pre-reduction process is quenched in water to prevent re-oxidation of the metallised Fe (process step 3). The water quenched pre-reduced material could then either be wet-milled (process step 4) to the desired PSD or fed directly to the hot acid leaching (HAL) (process step 5). The subsequent process steps is identical to the steps discussed for the previous process flow diagram presented in Fig. 1 in Section 3.1.1, and are therefore not repeated here.

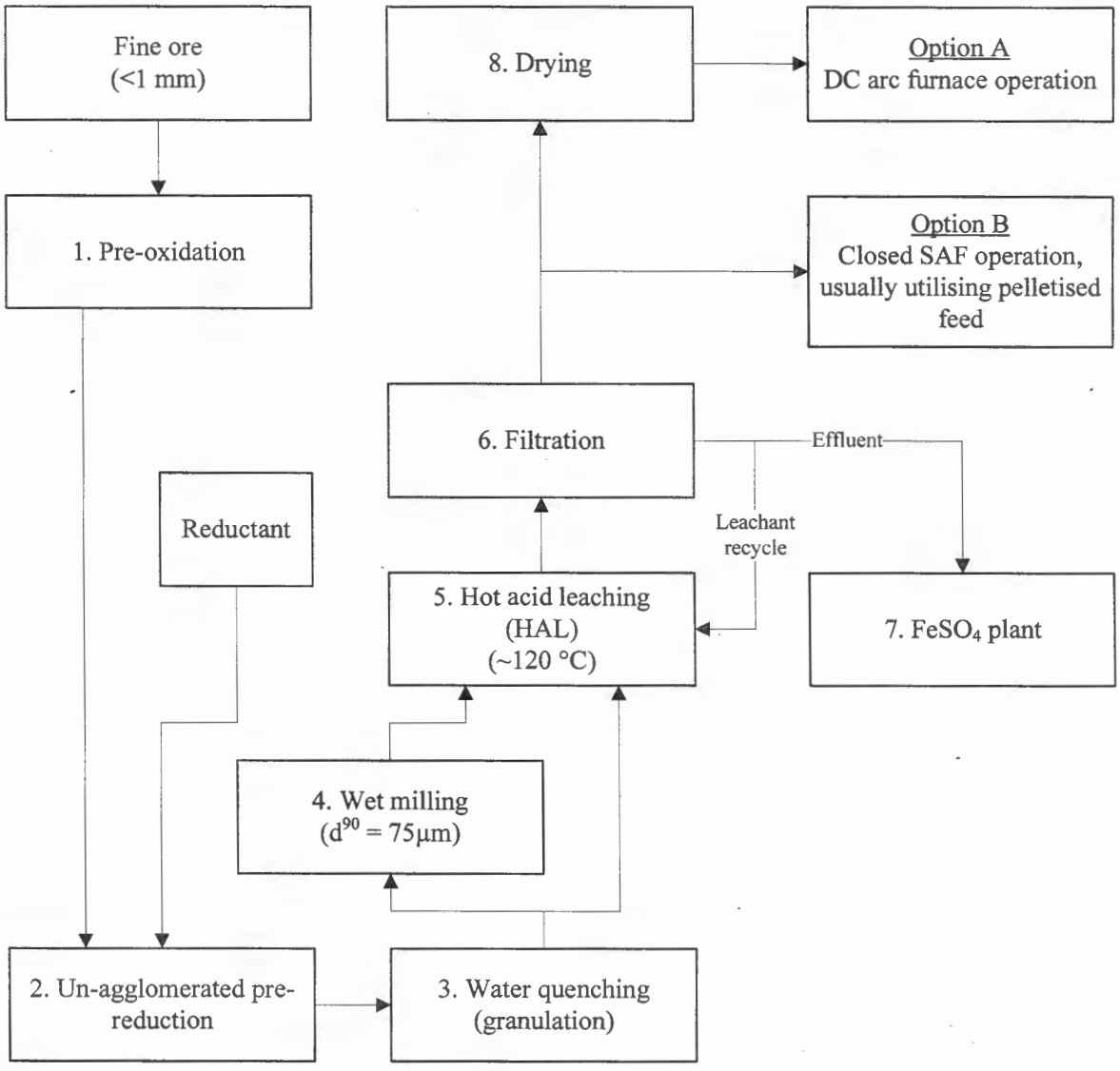

Fig. 6. A flow diagram indicating the likely process steps to be utilised for chromite pre-oxidation combined with un-agglomerated pre-reduction prior to leaching to improve the Cr/Fe ratio of chromite.

3.2.2. Effect of pre-oxidation temperature and retention time on un-agglomerated pre-reduction

The effect of pre-oxidation of the metallurgical grade chromite ore at different temperatures and retention times on the level of un-agglomerated chromite pre-reduction achieved under specific constant un-agglomerated pre-reduction experimental conditions

employed (Section 2.2.4), is illustrated in Fig. 7. The base case in Fig. 7 (indicated at a pre-oxidation temperature and retention time of zero) was determined by utilising untreated ore (un-oxidised) in the un-agglomerated pre-reduction experiment (Section 2.2.4). From these results, it is evident that pre-oxidation temperatures of 800, 1000 and 1200 °C along with an increase in retention time at each temperature, prior to un-agglomerated pre-reduction, improved the level of achievable chromite pre-reduction. For these specific results, the higher the pre-oxidation temperature, up to 1200 °C, and the longer the retention time, up to 240 min, the greater was the improvement in the level of achievable chromite pre-reduction.

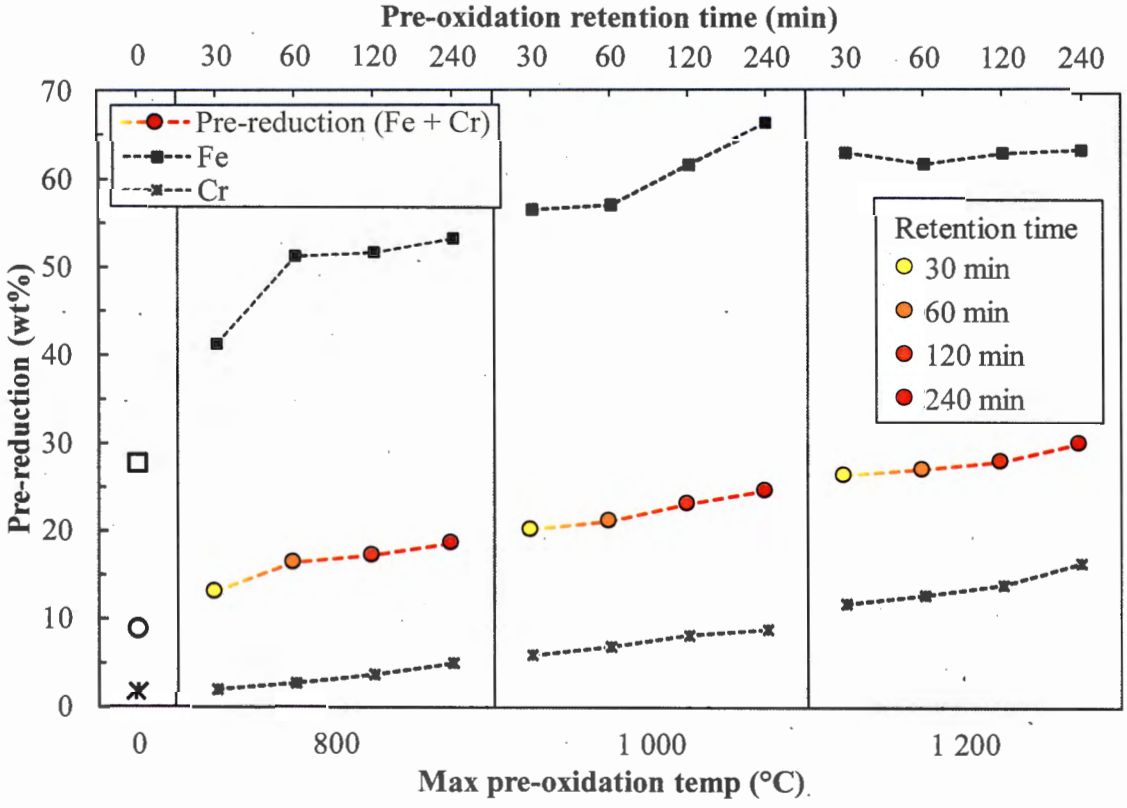

Fig. 7. The effect of pre-oxidation of metallurgical grade chromite ore at different temperatures and retention times, prior to un-agglomerated pre-reduction, on the extent of chromite pre-reduction.

Previous work published by Kleynhans et al. (2016) indicated that pre-oxidation between 800 and 1100 °C with a 10 min retention time, prior to milling (d_{90}) and pelletised

pre-reduction (similar to Section 3.1), improved the level of achievable chromite pre-reduction, with pre-oxidation at 1000 °C being the optimum pre-oxidation temperature for the specific case study chromite ore the authors used. However, Kleynhans et al. (2016) also revealed that pre-oxidation temperatures above 1100 °C resulted in lower levels of pre-reduction, with pre-oxidation temperatures of 1200 °C and higher resulting in even lower pre-reduction levels than the base case utilising un-oxidised ore. XRD analysis conducted by Kleynhans et al. (2016) on the milled (d_{90} = 75 μm) pre-oxidised ore indicated the formation of free eskolaite (Cr_2O_3) at pre-oxidation temperatures >1000 °C. A thermodynamic investigation done by Kleynhans et al. (2016) showed that Cr_2O_3 is reduced by solid C at temperatures >1250 °C, while synthetic chromite Cr_2FeO_4 (Niemelä et al., 2004) is reduced at lower temperatures than Cr_2O_3, i.e. 1200 °C, thus contributing to lower pre-reduction levels. Kleynhans et al. (2016) also showed by SEM and X-ray map images that Fe migration to the surface of ore particles takes place as a result of pre-oxidation with Cr remaining on the interior of the ore particle. In the case of the work conducted by Kleynhans et al. (2016), the pre-oxidised ore was milled and pelletised before pre-reduction, whereas in this investigation the ore is pre-oxidised and subsequently pre-reduced without any milling or pelletisation. This, therefore, might explain why an increase instead of a decrease in pre-reduction levels are observed in Fig. 7 for ore pre-oxidised at 1200 °C. It is proposed that because the ore is not milled and pelletised, no so much Cr_2O_3 forms since the surface contact area is reduced. On the other hand, the higher pre-oxidation temperature (1200 °C) and increased retention time resulted in more Fe migrating to the surface of the ore particle, which are exposed directly to the carbonaceous reductant, resulting in an increase in pre-reduction. It is also important to note that the range of pre-reduction achieved in this investigation was approximately 10–30%, where the pre-reduction levels studied by Kleynhans et al. (2016) were ≤40%. Although Cr reduction is observed in Fig. 7, the Cr

metallisation is still low as the pre-reduction levels are below 30%. The Cr metallisation observed is possibly from the Cr contained in the chromite spinel that has not been transformed to Cr_2O_3. A final observation with regard to Fig. 7, is that Fe metallisation seems to plateau at a pre-oxidation temperature of 1200 °C.

3.2.3. Leaching of pre-oxidised un-agglomerated pre-reduced material

The influence of improved pre-reduction (Section 3.2.2) due to the effect of pre-oxidation temperature and retention time on the Cr/Fe ratio and Cr recovery of un-agglomerated pre-reduced metallurgical grade chromite ore are presented in Fig. 8.

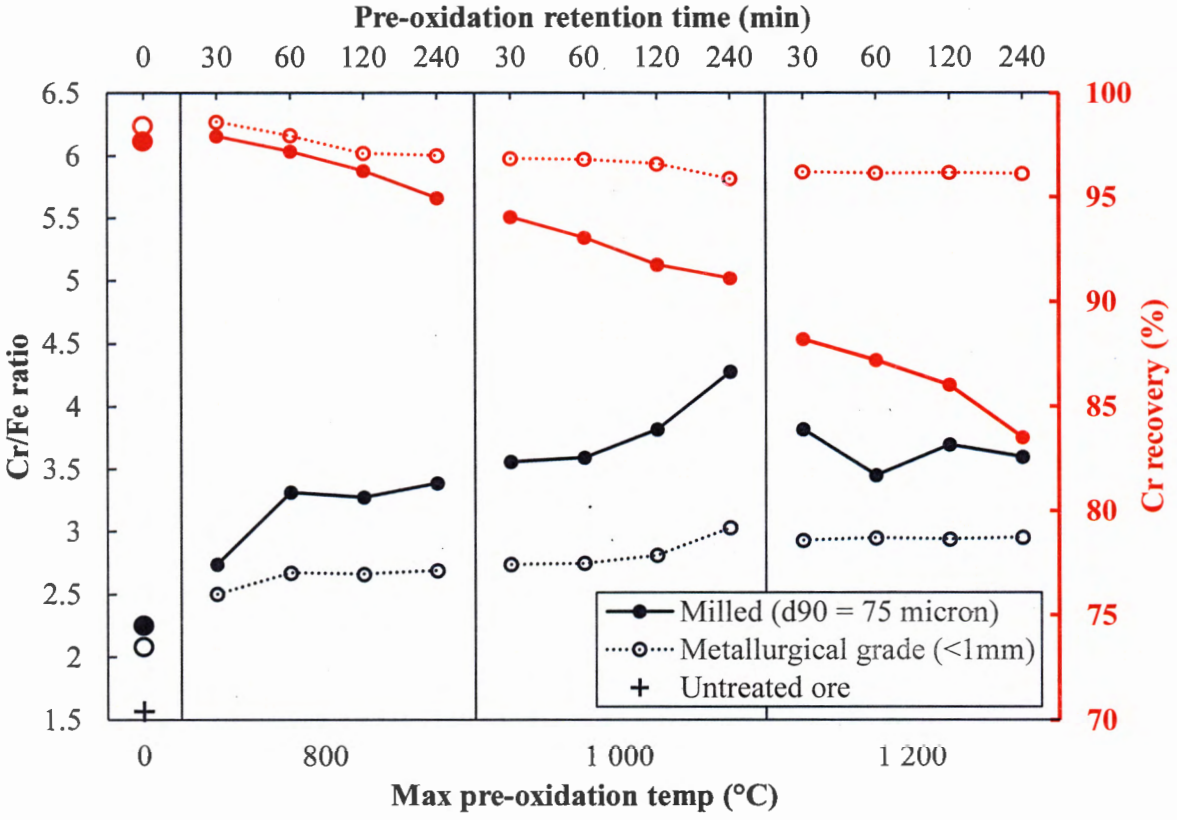

Fig. 8. The influence of improved pre-reduction due to the effect of pre-oxidation temperature (primary x-axis) and retention time (secondary x-axis) on the Cr/Fe ratio (primary y-axis) and Cr recovery (secondary y-axis) of un-agglomerated pre-reduced metallurgical grade chromite ore. The un-agglomerated pre-reduced ore was leached as is, with the results indicated by the dashed lines, as well as pulverised (d_{90} = 75 µm) before HAL with the results indicated by the solid lines (Section 2.2.6). The Cr/Fe ratio of the untreated ore is indicated by a black cross.

The un-agglomerated pre-reduced ore was leached as is (without being pulverised beforehand), with the results indicated by the unfilled markers and dashed lines in Fig. 8. The un-agglomerated pre-reduced ore was then also pulverised (d_{90} = 75 μm) before subsequent HAL, with the results indicated by the solid markers and lines in Fig. 8. The Cr/Fe ratio of the untreated ore is indicated by a black cross as a marker. From Fig. 8 it is observed that the increase in the level of pre-reduction as a result of pre-oxidation at different temperatures and retention times had a positive effect on improving the Cr/Fe ratio of the ore. It was expected that leaching the un-agglomerated pre-reduced ore without pulverising it beforehand would result in less effective extraction of the Fe, however significant increases in the Cr/Fe ratio was still obtained. Pre-oxidation at 1000 °C with a retention time of 240 min resulted in the highest Cr/Fe ration, for both pulverised and un-pulverised leaching test, reaching Cr/Fe ratios of ~4.3 and 3, respectively. However, pre-oxidation at 1000 °C with a retention time of 240 min for the pulverised leaching test resulted in a Cr recovery of ~91%, while leaching the un-pulverised ore only lowered the Cr recovery to ~96%. The optimum option might therefore be pulverised pre-reduced ore initially pre-oxidised at 800 °C with a retention time of 240 min. Leaching this pulverised ore resulted in a Cr/Fe ratio of ~3.4 and a Cr recovery of ~95%, which is close to the ~96% recovery achieved by leaching the un-pulverised ore. Ore pre-oxidised at 1200 °C resulted in lower Cr/Fe ratios and Cr recoveries, although an increase in pre-reduction was observed as shown in Section 3.2.2. This is due to the plateau in Fe reduction, while the Cr reduction still increased with higher temperatures. Although an increase in Cr reduction would be advantageous for un-agglomerated pre-reduction prior to smelting in a furnace, in the contexts of this investigation it is certainly a disadvantage.

3.2.4. Scanning electron microscopy analysis

SEM micrograph images taken at 500, 3200 and 14 500 times magnification of an un-pulverised pre-reduced chromite ore particle, that was pre-oxidised at 1200 °C with a 240 min retention time prior to pre-reduction (A, B, C), as well as images of an un-pulverised chromite ore particle after HAL that were subjected to the identical pre-oxidation and pre-reduction condition mentioned above (AL, BL, CL), are shown in Fig. 9. Fig. 9–A shows cracks in the surface of the ore particle, undoubtedly as a result of either pre-oxidation, pre-reduction or both. In Fig. 9–B and Fig. 9–C, metal accumulation on the surface of the ore particle, consisting mainly of Fe, is observed. SEM-EDS analysis of areas α and β in Fig. 9–C are presented in Table 5.

Table 5
SEM-EDS results for different areas in Fig. 9.

Area		*C*	*O*	*Al*	*Si*	*Cr*	*Fe*
9–C	α	4.98	14.14	2.74	1.41	6.83	69.91
	β	6.47	37.88	21.47	11.16	8.82	14.21

The metal globule at area α consist predominantly of Fe and has low Al and Si contents compared to the chromite spinel indicated by area β. The effects of the HAL on the pre-reduced chromite particle are evident in Fig. 9–AL. The crack that was visible in Fig. 9–A is eroded and no metallisation is observed in Fig. 9–BL and Fig. 9–CL.

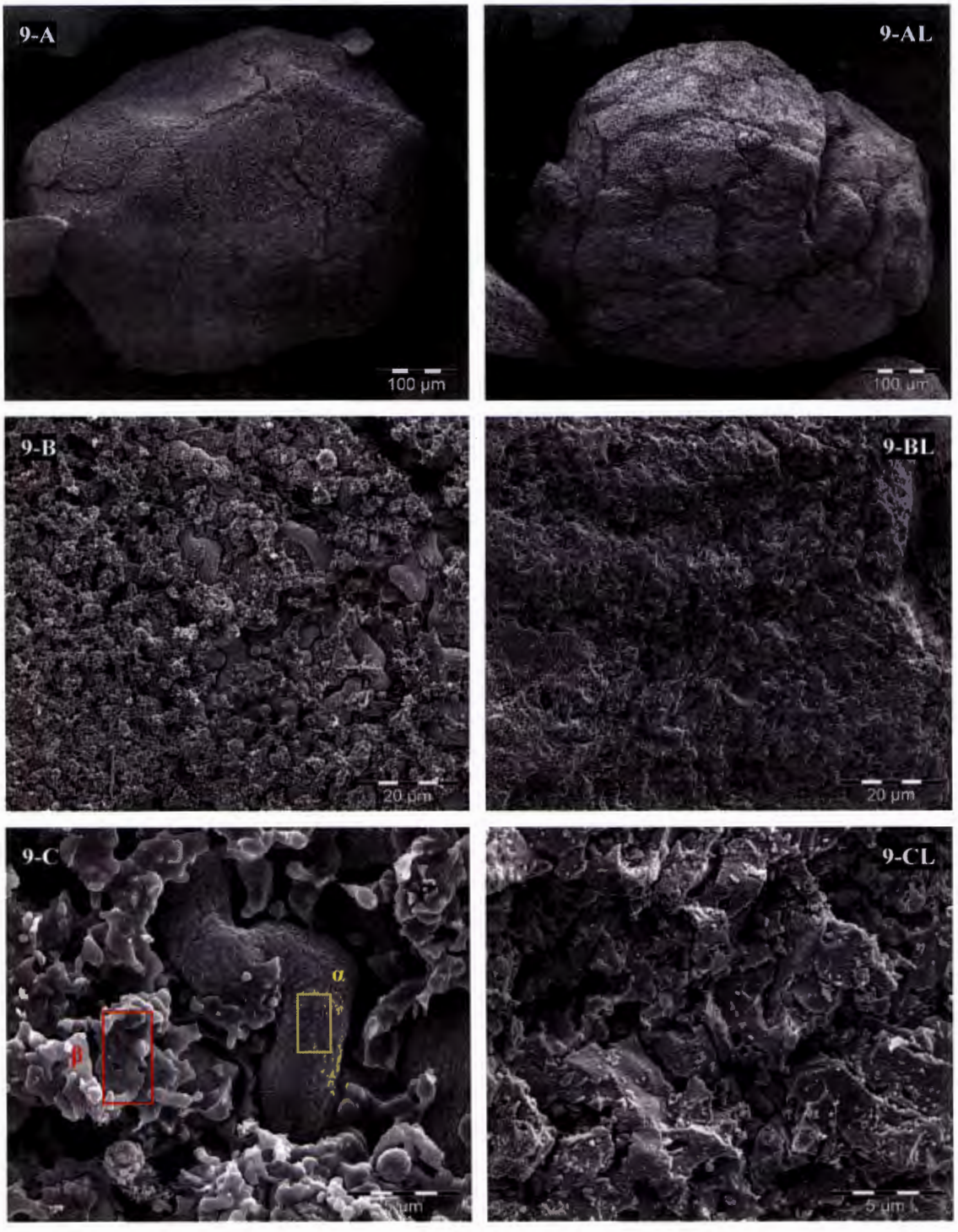

Fig. 9 SEM micrograph images taken at 500, 3200 and 14 500 times magnification of an un-pulverised pre-reduced chromite ore particle that was pre-oxidised at 1200 °C with a 240 min retention time prior to pre-reduction (A, B, C). Images AL, BL and CL shows an un-pulverised chromite ore particle after leaching that were subjected to the identical pre-oxidation and pre-reduction condition of the particle depicted in images A, B and C.

3.3. Leaching effluent as a Cr(VI) reducing agent

In general Cr(VI) is formed in significantly important quantities during FeCr production as an unintended by-product, due to it being impossible to entirely exclude oxygen from all high temperature production processes. Certain Cr(VI) species are commonly regarded as cancer-causing, with specifically Cr(VI) species transmitted via airborne exposure being associated with malignance neoplasm of the respiratory system. In order to treat Cr(VI) containing wastes effectively, Beukes et al. (2012) identified several basic process steps have to be followed, i.e. i) capturing the materials that potentially contain Cr(VI), ii) contacting the potentially Cr(VI) containing materials with water, since the risks associated with airborne Cr(VI) is considerable higher than the risks associated with aqueous Cr(VI), iii) reducing Cr(VI) to Cr(III) (e.g. in the aqueous phase) and iv) containing and storing the treated material. Various reducing agents are available that can be utilised in an aqueous environment to convert Cr(VI) to Cr(III). However, Beukes et al. (2012) reported that aqueous reduction of Cr(VI) with ferrous iron from ferrous chemicals, such as ferrous chloride or ferrous sulphate, was currently the preferred method. Beukes et al. (2012) described in detail why ferrous chemicals have been the reducing agents of choice for South African FeCr producers. However, the main reason was attributed to this treatment route being a proven technology that is well researched, and that the reducing agents (e.g. ferrous chloride or sulphate) are readily available. The intent of this paper was not specifically aimed at investigating possible commercial applications linked to the effluent by-product from the leaching process. It is, however, useful to report what elements were contained in the effluent after leaching, in the event that possible commercial applications are considered in future investigations. Table 6 shows the elements identified in the effluent after leaching pre-reduced pellet material that was treated at 1125 °C with retention times of 30, 60 and 240 min. From the results in Table 6 it is observed that the main element contained in the effluent

is Fe, which is expected. Predictably, in the case where higher Cr metallisation occurred (referring to sample FZ) a significant increase in the Cr content within the effluent is observed. The other elements detected, i.e. Ca, Mg, Na, K, Ti and Mn, occurred in minor quantities. However, compared to these minor elements, the Si and Al contents are noticeably higher. Considering the initial characterisation of the raw material in Table 1, it is observed that Si and Al are present in higher quantities in the raw materials compared to the other elements and therefore would be expected to occur in higher concentrations in the effluent. The results in Table 6 thus support the possibility that the effluent could be used as an aqueous Cr(VI) reducing agent, should Cr metallisation be controlled and restricted in the pre-reduction process, thus consequently limiting the Cr content in the effluent. Additionally, the HAL solution should be re-used, until sufficient Fe saturation of the effluent occurred.

Table 6
Elements present in the effluent after HAL pre-reduced pellet material that was treated at 1125 °C with retention times of 30, 60 and 240 min.

Pelletised pre-reduction			g/L									
Sample	Temp (°C)	Retention time (min)	Fe	Cr	Si	Al	Ca	Mg	Na	K	Ti	Mn
FW	1125	30	2.269	0.222	0.181	0.145	0.073	0.058	0.030	0.012	0.007	0.001
FX		60	4.129	0.288	0.187	0.141	0.084	0.037	0.027	0.009	0.006	0.001
FZ		240	9.464	6.376	0.180	0.257	0.076	0.095	0.023	0.007	0.014	0.001

4. Conclusions

The results presented in this investigation proved that by combining pyrometallurgical and hydrometallurgical methods the Cr/Fe ratio of low grade chromite ores could be successfully increased. The key step in this method is the selective pre-reduction of the Fe contained in the spinel in order to firstly, structurally dissociate the spinel and, secondly, segregate the Fe from the spinel for effective subsequent leaching. The overall pre-reduction level on its own is insufficient as a parameter to determine the process condition required to

obtain the desired Cr/Fe ratio. It is important to recognise that both the level of pre-reduction, Fe- and Cr metallisation and the respective relationship between reduction and metallisation has to be determined in order to identify the optimum process conditions. Limited references are available in the public domain that specifically illustrate overall pre-reduction as a function of Fe- and Cr metallisation. Dawson and Edwards (1986) published a graph, illustrated in Fig. 10, showing the overall pre-reduction level as a function of the extent of Fe- and Cr metallisation of a LG6 chromite ore (data used to reconstruct the graph is presented in Table S3). This ore is from the same layer group than the ore used in this investigation. In order to consolidate, as well as contextualise and substantiate the results obtained in this investigation, data from the pelletised pre-reduction experiments, Section 3.1.2, Fig. 2 (Table S1), and pre-oxidised, un-agglomerated pre-reduction experiments, Section 3.2.2, Fig. 7 (Table S2), was added to the graph from Dawson and Edwards (1986) (Fig. 10). The theoretical Cr recovery and possible Cr/Fe ratio subsequent to leaching was calculated from the metallisation data (Table S3) of Dawson and Edwards (1986). Conclusions with regard to this investigation, with reference to Fig. 10, can henceforth be made.

The optimum pre-reduction range, resulting in a Cr/Fe ratio >2 to ~3.5 and a Cr recovery approximately ≥90%, is concluded to be between 10 to 30% from the collective data presented in Fig. 10. It is apparent that the significant majority of the results produced using the pelletised pre-reduction option (Section 3.1) fall outside the specific pre-reduction range. However, the vast majority of results generated using the pre-oxidised, un-agglomerated pre-reduction option (Section 3.2) fall inside the 10-30% pre-reduction range. It is, however, important to recognise that the pelletised pre-reduction option data was produced by varying pre-reduction peak-temperature and -retention time.

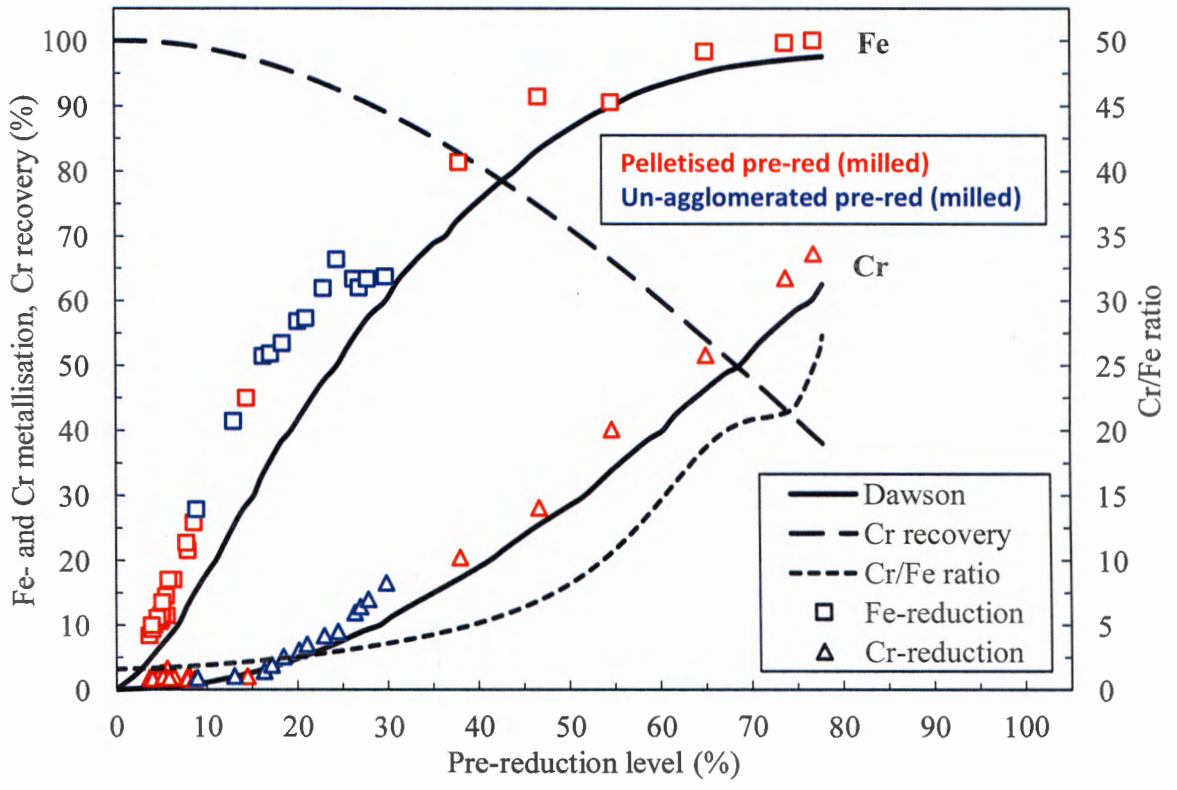

Fig. 10. Extents of Fe- and Cr metallisation as a function of overall pre-reduction reconstructed from data by Dawson and Edwards (1986) (Table S3). The theoretical Cr recovery and possible Cr/Fe ratio subsequent to leaching was calculated from the metallisation data of Dawson and Edwards (1986). Pelletised pre-reduction data, Section 3.1.2, Fig. 2 (Table S1), is indicated in red, while pre-oxidation, un-agglomerated pre-reduction data, Section 3.2.2, Fig. 7 (Table S2), is indicated in blue.

The pre-oxidised, un-agglomerated pre-reduction option data was generated by varying pre-oxidation peak-temperature and -retention time, while the pre-reduction condition were kept constant. The results therefore does not indicate that the pre-oxidised, un-agglomerated pre-reduction option is superior to the pelletised pre-reduction option because the majority of the results fall in the 10 to 30% pre-reduction range. Experimental design, in addition to temperature and retention time parameter interval selection, ultimately gave rise to the data spread seen in Fig. 10. The results does, however, indicate that pre-oxidation significantly enhance Fe metallisation, as well as the level of pre-reduction

achieved in the un-agglomerated pre-reduction process step, which is a benefit pertaining to this specific option.

The metallisation pre-reduction data (Fig. 10) from this investigation follow the same trend as the metallisation pre-reduction curves reconstructed from Dawson and Edwards (1986). However, obvious differences in Fe- and Cr metallisation related to specific pre-reduction levels are observed, despite both ores, from this investigation and from Dawson and Edwards (1986), originating from the same LG6 geological layer. Therefore, the origin and specific characteristic of a chromite ore will have an effect on the ore's metallisation pre-reduction curves. The importance of the temperature at which the Cr-Al sesquioxide phase forms during the chromite reduction mechanism, which is characteristic to a specific chromite ore, was also highlight in Section 3.1.2. From literature (as explained in Section 3.1.2) the Cr-Al sesquioxide phase for LG6 chromite ore forms at temperatures below 1200 °C, while the sesquioxide phase in UG2 chromite forms at higher temperatures up to 1300 °C. The ore used in this investigation was therefore the least ideal, in terms of its reduction and metallisation characteristics, to optimally maximise Fe metallisation while simultaneously minimise Cr metallisation. However, examining the metallisation curves of the ore used by Dawson and Edwards (1986), it is apparent that it has a lower Fe metallisation curve than the ore used in this investigation, which would imply lower Fe/Cr ratios and Cr recoveries.

The appropriate chromite ore raw material should therefore be selected according to high Fe- and low Cr metallisation specifications as a function of pre-reduction. The technology chosen for pre-reduction, e.g. a rotary kiln or rotary heart furnace, should offer controllability in order to appropriately maintain the exact optimum pre-reduction conditions necessary, i.e. temperature and retention time, to operate in the desired pre-reduction range with the aim of obtain the desired Cr/Fe ratio and Cr recoveries.

Acknowledgements

The financial assistance of the South African National Research Foundation (NRF) towards the studies of E.L.J. Kleynhans is hereby acknowledged. Opinions expressed and conclusions arrived at are those of the authors and are not necessarily to be attributed to the NRF. The authors also thank SamancorCr for partial support of the research.

References

Amer, A.M., 1992. Processing of Ras-Shait chromite deposits. Hydrometallurgy 28, 29-43.

Amer, A.M., Ibrahim, I.A., 1996. Leaching of a low grade Egyptian chromite ore. Hydrometallurgy 43, 307-316.

Barnes, A.R., Finn, C.W.P., Algie, S.H., 1983. The prereduction and smelting of chromite concentrate of low chromium-to-iron ratio. Journal of the South African Institute of Mining and Metallurgy, 49-54.

Beukes, J.P., Dawson, N.F., van Zyl, P.G., 2010. Theoretical and practical aspects of Cr(VI) in the South African ferrochrome industry. The Journal of The Southern African Institute of Mining and Metallurgy 110, 743-750.

Beukes, J.P., van Zyl, P.G., Ras, M., 2012. Treatment of Cr(VI)-containing wastes in the South African ferrochrome industry - a review of currently applied methods. The Journal of The Southern African Institute of Mining and Metallurgy 112, 347-352.

Biermann, W.J., Heinrichs, M., 1960. The attack of chromite by sulphuric acid. Canadian Journal of Chemistry 38, 1449-1454.

Cramer, L.A., Basson, J., Nelson, L.R., 2004. The impact of platinum production from UG2 ore on ferrochrome production in South Africa. The Journal of The South African Institute of Mining and Metallurgy 104, 517-527.

Dawson, N.F., Edwards, R.I., 1986. Factors affecting the reduction rate ofchromite, Proceedings of the 4th International Ferro-alloys Congress, Sao Paulo,Brazil, pp. 105-113.

de Waal, S.A., Hiemstra, S.A., 1975. Report No. 1709, Johannesburg, South Africa.

Fowkes, K., 2014. Is there a limit to the market share of South African chrome units?, Metal Bulletin 7th South African Ferroalloys Conference. Metal Bulletin, Johannesburg, South Africa.

Gasik, M., 2013. Handbook of Ferroalloys - Theory and Technology. Butterworth-Heinemann, Oxford, p. 520.

Geveci, A., Topkaya, Y., Ayhan, E., 2002. Sulfuric acid leaching of Turkish chromite concentrate. Minerals Engineering 15, 885-888.

Howat, D.D., 1986. Chromium in South Africa. Journal of The South African Institute of Mining and Metallurgy 86, 37-50.

Hu, X., Yang, Q., Sundqvist Ökvist, L., Björkman, B., 2016. Thermal Analysis Study on the Carbothermic Reduction of Chromite Ore with the Addition of Mill Scale. steel research international 87, 562-570.

ICDA, 2013a. Chrome ore - Global overview of the chrome ore market, Paris, France.

ICDA, 2013b. Ferrochrome. <http://www.icdacr.com/market-intelligence/fecr-brch/fecr-brch.pdf> (accessed 13 January.2014).

ICDA, 2013c. Statistical Bulletin 2013, Paris, France.

INCOSE, 2015. INCOSE Systems Engineering Handbook: A Guide for System Life Cycle Processes and Activities, 4th ed. John Wiley & Sons, New Jersey, USA, p. 304.

ISSF, 2016a. ISSF Stainless Steel in Figures 2016. <http://www.worldstainless.org/Files/issf/non-image-files/PDF/ISSF_Stainless_Steel_in_Figures_2016_English_Public.pdf> (accessed 13 June.2016).

ISSF, 2016b. Stainless Steel Consumption Forecast (SCF). <http://www.worldstainless.org/Files/issf/non-image-files/PDF/statistics/150530_SCF_Public.pdf> (accessed 13 June.2016).

Kanari, N., Gaballah, I., Allain, E., 2000. Use of chlorination for chromite upgrading. Thermochimica Acta 351, 109-117.

Kleynhans, E.L.J., Beukes, J.P., Van Zyl, P.G., Kestens, P.H.I., Langa, J.M., 2012. Unique challenges of clay binders in a pelletised chromite pre-reduction process. Minerals Engineering 34, 55-62.

Kleynhans, E.L.J., Neizel, B.W., Beukes, J.P., Van Zyl, P.G., 2016. Utilisation of pre-oxidised ore in the pelletised chromite pre-reduction process. Minerals Engineering 92, 114-124.

Kogel, J.E., Trivedi, N.C., Barker, J.M., Krukowski, S.T., 2006. Industrial Minerals and Rocks - Commodities, Markets, and Uses (7th Edition). Society for Mining, Metallurgy, and Exploration (SME).

Kumar Tripathy, S., Singh, V., Ramamurthy, Y., 2012. Improvement in Cr:Fe Ratio of Indian Chromite Ore for Ferro Chrome Production. International Journal of Mining Engineering and Mineral Processing 1, 101-106.

Ledgerwood, J., van der Westhuyzen, P., 2011. The use of sulphuric acid in the mineral sands industry as a chemical mechanism for iron removal, 6th Southern African Base Metals Conference. The Southern African Institute of Mining and Metallurgy, Phalaborwa, South Africa, pp. 169-186.

McCullough, S., Hockaday, S., Johnson, C., Barza, N.A., 2010. Pre-reduction and smelting characteristics of Kazakhstan ore samples, in: Vartiainen, A. (Ed.), The Twelfth

International Ferroalloys Congress (INFACON XII). Outotec Oyj, Helsinki, Finland, pp. 249-262.

Mohale, G.T.M., 2014. SEM image processing as an alternative method to determine chromite pre-reduction, Faculty of Engineering. North-West University, South Africa, Potchefstroom Campus.

Murthy, Y.R., Tripathy, S.K., Kumar, C.R., 2011. Chrome ore beneficiation challenges & opportunities – A review. Minerals Engineering 24, 375-380.

Nafziger, R.H., 1982. A review of the deposits and beneficiation of lower-grade chromite. Journal of The South African Institute of Mining and Metallurgy, 205-226.

Naiker, O., 2007. The development and advantages of Xstrata's Premus Process, in: Roy, T.K. (Ed.), Proceedings of The 11th International Ferroalloys Congress. IFAPA, New Delhi, India, pp. 112-118.

Naiker, O., Riley, T., 2006. Xstrata alloys in the profile, in: Jones, R.T. (Ed.), South African Pyrometallurgy 2006. SAIMM, Johannesburg, South Africa, pp. 297-306.

Neizel, B.W., Beukes, J.P., van Zyl, P.G., Dawson, N.F., 2013. Why is CaCO3 not used as anadditive inthe pelletised chromite pre-reduction process? Minerals Engineering 45, 115–120.

Niemelä, P., Krogerus, H., Oikarinen, P., 2004. Formation, characterisation and utilisation of CO-gas formed inferrochrome smelting., The Tenth International Ferroalloys Congress (INFACON X). SAIMM, Cape Town, South Africa, pp. 68-77.

Oberholzer, J., Daly, K., 2014. SA Chrome & Ferrochrome - Tug-of-war with a giant, Johannesburg, South Africa.

OCC, 2014. Beneath the Surface - Uncovering the Economic Potential of Ontario's Ring of Fire. Ontario Chamber of Commerce, Ontario, Canada.

Perry, K.D.P., Finn, C.W.P., King, R.P., 1988. An ionic diffusion mechanism of Chromite Reduction (KPD Perry. Metallurgical Transactions B 19B, 667-684.

Rankin, W., 1979. Si-Mn equilibrium in ferromanganese alloy production. TRANSACTIONS OF THE INSTITUTION OF MINING AND METALLURGY SECTION C-MINERAL PROCESSING AND EXTRACTIVE METALLURGY 88, C167-C174.

Sen, M.C., Chatterjee, A.B., 1957. Chemical Beneficiation of Indian Chromites. Indian Mining Journal, 85-94.

Sharma, T., 1990. The kinetics of iron dissolution from chromite concentrate. Minerals Engineering 3, 599-605.

Shen, S.-B., Bergeron, M., Richer-Laflèche, M., 2009a. Effect of sodium chloride on the selective removal of iron from chromite by carbochlorination. International Journal of Mineral Processing 91, 74-80.

Shen, S.-B., Hao, X.-F., Yang, G.-W., 2009b. Kinetics of selective removal of iron from chromite by carbochlorination in the presence of sodium chloride. Journal of Alloys and Compounds 476, 653-661.

Sundar Murti, N.S., Seshadri, V., 1979. On the improvement in Cr/Fe ratio of Byrapur chromite. Transactions of The Indian Institute of Metals 32, 239-243.

Ugwuegbu, C., 2012. Technology Innovations in the Smelting of Chromite Ore. Innovative Systems Design and Engineering 3, 48-55.

USGS, 2015. Mineral commodity summaries 2015. U.S. Geological Survey, Reston, VA.

Vardar, E., Eric, R.H., Letowski, F.K., 1994. Acid leaching of chromite. Minerals Engineering 7, 605-617.

Wang, Y., Wang, L., Chou, K.C., 2014. Kinetics of carbothermic reduction of synthetic chromite. Journal of Mining and Metallurgy, Section B: Metallurgy 50, 15-21.

Wang, Y., Wang, L., Chou, K.C., 2015. Effects of CaO, MgO, Al2O3 and SiO2 on the carbothermic reduction of synthetic FeCR2O4. Journal of Mining and Metallurgy, Section B: Metallurgy 51, 8pp.

Yuksel, R., 2013. Ferrochrome Market Outlook - Supply & Demand Shifting East, 12th International Stainless & Special Steel Summit. MetalBulletin, London, United Kingdom.

Supplementary materials

Table S1
Pelletised pre-reduction and leaching tests experimental data.

Pre-reduction		Sample number	(wt.%)						Cr/Fe ratio		Cr recovery (wt.%)	
Temperature (°C)	Retention time (min)		Pre-reduction		Fe-reduction		Cr-reduction					
750	30	AW	4.85	(0.79)	10.41	(1.17)	2.47	(0.61)	1.56	(0.011)	97.53	(0.61)
	60	AX	4.08	(0.22)	9.21	(0.26)	1.90	(0.23)	1.55	(0.011)	98.10	(0.23)
	120	AY	3.75	(0.58)	8.26	(1.26)	1.83	(0.42)	1.57	(0.008)	98.17	(0.42)
	240	AZ	5.02	(0.49)	11.27	(0.64)	2.39	(0.44)	1.55	(0.011)	97.61	(0.44)
825	30	BW	4.05	(0.64)	9.39	(1.87)	1.84	(0.11)	1.59	(0.055)	98.16	(0.11)
	60	BX	4.24	(1.28)	9.85	(2.91)	1.87	(0.36)	1.57	(0.010)	98.13	(0.36)
	120	BY	4.06	(0.66)	9.22	(1.50)	1.90	(0.30)	1.58	(0.017)	98.10	(0.30)
	240	BZ	5.65	(0.47)	11.33	(1.02)	3.29	(0.85)	1.59	(0.002)	96.71	(0.85)
900	30	CW	4.95	(0.21)	10.59	(1.09)	2.49	(0.49)	1.58	(0.008)	97.51	(0.49)
	60	CX	4.99	(0.85)	10.84	(1.43)	2.51	(0.65)	1.56	(0.029)	97.49	(0.65)
	120	CY	5.17	(0.27)	11.30	(0.19)	2.59	(0.30)	1.57	(0.002)	97.41	(0.30)
	240	CZ	5.06	(0.55)	11.58	(0.68)	2.27	(0.48)	1.61	(0.014)	97.73	(0.48)
975	30	DW	4.63	(0.37)	11.03	(1.02)	1.91	(0.27)	1.61	(0.000)	98.09	(0.27)
	60	DX	3.97	(0.00)	9.88	(0.46)	1.65	(0.09)	1.62	(0.011)	98.35	(0.09)
	120	DY	5.56	(0.22)	14.34	(0.25)	1.85	(0.20)	1.67	(0.036)	98.15	(0.20)
	240	DZ	5.18	(0.03)	13.44	(0.00)	1.96	(0.24)	1.62	(0.045)	98.04	(0.24)
1050	30	EW	6.39	(0.05)	16.95	(0.20)	1.96	(0.05)	1.72	(0.027)	98.04	(0.05)
	60	EX	5.82	(1.12)	16.95	(0.01)	1.78	(0.67)	1.75	(0.022)	98.22	(0.67)
	120	EY	7.97	(1.37)	21.46	(2.09)	2.34	(1.02)	1.77	(0.005)	97.66	(1.02)
	240	EZ	7.86	(0.31)	22.59	(0.86)	1.69	(0.24)	1.87	(0.038)	98.31	(0.24)
1125	30	FW	8.63	(1.34)	25.75	(1.20)	1.60	(0.13)	2.28	(0.068)	98.40	(0.13)
	60	FX	14.50	(1.02)	44.86	(2.90)	2.05	(0.23)	2.33	(0.654)	97.95	(0.23)
	120	FY	37.97	(0.49)	81.27	(0.83)	20.39	(0.82)	6.16	(0.133)	79.61	(0.82)
	240	FZ	54.69	(2.09)	90.54	(2.50)	40.16	(1.77)	7.29	(3.866)	59.84	(1.77)
1200	30	GW	46.69	(0.73)	91.40	(0.86)	28.02	(0.68)	8.87	(0.285)	71.98	(0.68)
	60	GX	65.12	(0.24)	98.26	(0.94)	51.54	(0.50)	13.69	(3.236)	48.46	(0.50)
	120	GY	73.84	(1.40)	99.59	(2.46)	63.43	(1.11)	16.71	(5.859)	36.57	(1.11)
	240	GZ	76.93	(1.12)	100.00	(1.22)	67.26	(1.20)	23.44	(3.034)	32.74	(1.20)

* Values in brackets indicate the standard deviation.

Table S2
Un-agglomerated pre-reduction and leaching tests experimental data.

Pre-oxidation		Sample number	(wt.%)						Milled		Un-milled	
Temperature (°C)	Retention time (min)		Pre-reduction		Fe-reduction		Cr-reduction		Cr/Fe ratio	Cr recovery (wt.%)	Cr/Fe ratio	Cr recovery (wt.%)
0	0	BC	8.91	(0.99)	27.71	(2.80)	1.75	(0.38)	2.25	97.69	2.08	98.43
800	30	PMW	13.02	(0.75)	41.32	(2.99)	2.05	(0.12)	2.74	97.95	2.50	98.64
	60	PMX	16.35	(1.01)	51.26	(3.81)	2.77	(0.20)	3.31	97.23	2.67	97.98
	120	PMY	17.14	(1.04)	51.68	(3.42)	3.72	(0.31)	3.28	96.28	2.66	97.12
	240	PMZ	18.48	(1.07)	53.27	(3.59)	5.02	(0.41)	3.39	94.98	2.69	97.02
1000	30	QMW	20.13	(0.78)	56.63	(2.42)	5.94	(0.39)	3.56	94.06	2.74	96.87
	60	QMX	21.07	(1.20)	57.18	(3.69)	6.94	(0.54)	3.59	93.06	2.75	96.83
	120	QMY	22.98	(0.91)	61.78	(0.75)	8.25	(0.73)	3.82	91.75	2.81	96.62
	240	QMZ	24.49	(1.74)	66.20	(1.76)	8.86	(1.09)	4.28	91.14	3.03	95.89
1200	30	RMW	26.30	(1.50)	63.18	(2.69)	11.79	(1.18)	3.82	88.21	2.93	96.22
	60	RMX	26.92	(1.87)	61.90	(2.47)	12.79	(1.63)	3.45	87.21	2.95	96.16
	120	RMY	27.80	(1.13)	63.15	(1.63)	13.96	(1.12)	3.70	86.04	2.94	96.19
	240	RMZ	29.79	(1.17)	63.53	(1.72)	16.46	(1.17)	3.60	83.54	2.96	96.14

* Values in brackets indicate the standard deviation.

Table S3
Data extracted from Dawson and Edwards (1986) and used to reconstruct Fig. 10.

Pre-reduction	Cr-metallisation	Fe-metallisation	Total Cr (Cr_2O_3 = 45.37 wt.%)	Total Fe (FeO = 25.39 wt.%)	Cr/Fe ratio	Cr recovery
0	0.00	0.00	31.04	19.74	1.57	100.00
2.5	0.00	2.75	31.04	19.19	1.62	100.00
5	0.19	6.99	30.98	18.36	1.69	99.81
7.5	0.56	12.19	30.87	17.33	1.78	99.44
10	1.10	17.96	30.70	16.19	1.90	98.90
12.5	1.81	23.98	30.48	15.00	2.03	98.19
15	2.67	30.03	30.21	13.81	2.19	97.33
17.5	3.70	35.93	29.89	12.64	2.36	96.30
20	4.87	41.59	29.53	11.53	2.56	95.13
22.5	6.18	46.93	29.12	10.47	2.78	93.82
25	7.64	51.93	28.67	9.49	3.02	92.36
27.5	9.23	56.59	28.18	8.57	3.29	90.77
30	10.94	60.91	27.65	7.72	3.58	89.06
32.5	12.78	64.92	27.08	6.92	3.91	87.22
35	14.74	68.65	26.47	6.19	4.28	85.26
37.5	16.81	72.13	25.83	5.50	4.69	83.19
40	18.99	75.37	25.15	4.86	5.17	81.01
42.5	21.27	78.41	24.44	4.26	5.74	78.73
45	23.66	81.24	23.70	3.70	6.40	76.34
47.5	26.14	83.87	22.93	3.18	7.20	73.86
50	28.71	86.29	22.13	2.71	8.18	71.29
52.5	31.37	88.48	21.30	2.27	9.37	68.63
55	34.11	90.43	20.45	1.89	10.83	65.89
57.5	36.93	92.11	19.58	1.56	12.57	63.07
60	39.82	93.51	18.68	1.28	14.58	60.18
62.5	42.78	94.61	17.76	1.06	16.70	57.22
65	45.79	95.43	16.83	0.90	18.66	54.21
67.5	48.86	96.00	15.88	0.79	20.10	51.14
70	51.97	96.37	14.91	0.72	20.82	48.03
72.5	55.12	96.66	13.93	0.66	21.12	44.88
75	58.29	97.01	12.95	0.59	21.97	41.71
77.5	61.48	97.66	11.96	0.46	25.90	38.52
80	62.00	97.81	11.80	0.43	27.30	38.00

CHAPTER 8: CONCLUSION

The success of a project is mostly determined by the number of aim/objectives successfully achieved. In this chapter, the project is evaluated (Section 8.1) against the general aims and specific objectives set in Chapter 1, Section 1.2. Some future perspectives for continued research are also presented (Section 8.2).

8.1 Project evaluation

The areas within ferrochrome (FeCr) production where each article, presented in the different chapters, made a scientific contribution are indicated in Figure 8-1.

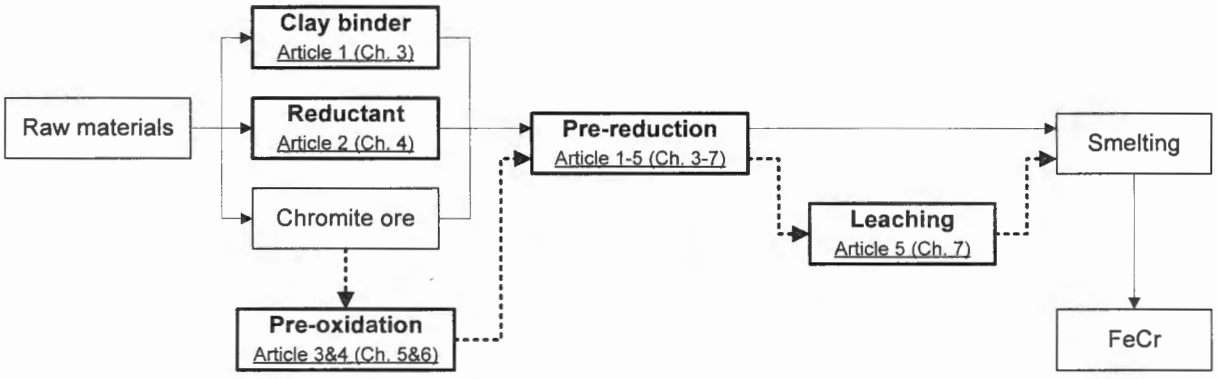

Figure 8-1: The areas within FeCr production where each article chapter made a scientific contribution.

The project was evaluated using the objectives that were set in Chapter 1. The points listed below therefore correlate with the objectives set in Section 1.2. The results were presented in Chapter 3, 4, 5, 6 and 7 in article format. Therefore, conclusions drawn from results were presented in each of the article chapters. These detailed conclusions are not repeated here and only a brief summary is given together with information and knowledge gained by combining results from several chapters.

a) **Objective 1: Investigate the effect of secondary raw materials, i.e. i) the clay binder and ii) carbonaceous reductant, on the unique process requirements of the chromite pre-reduction process to ultimately assist FeCr producers in optimising the selection of their raw materials.**

i) Typical raw materials, including two clay binders, were obtained from a large local FeCr producer currently applying the chromite pelletised pre-reduction process and extensively characterised (Chapter 3, Section 3.1). In order to identify, understand and demonstrate the process considerations of clay binders in the pelletised chromite pre-reduced process, industrially produced chromite pre-reduced pellets were also obtained from the same FeCr producer. It was shown that chromite pre-reduced pellets consist of an oxidised outer layer containing small amounts of carbon and a pre-reduced core containing a substantial amount of carbon (Chapter 3, Section 3.2). Therefore, in order to differentiate between these two zones, the two case study clays performances in oxidative sintered and pre-reduced environment were evaluated with several experiments designed and conducted to test the effect of the two case study clays on the pelletised pre-reduction process requirements that must be achieved (Chapter 3, Section 3.3-3.7). Finally, various industrial relevant recommendations dealing with the selection of clay binder for chromite pre-reduction could be made (Chapter 3, Section 4). The results exemplified that the clay binder use has to impart the necessary high compressive and abrasion resistance strengths to the cured pellets in both oxidising and reducing environments (Chapter 3, Section 3.3-3.4), while, at the same time, not influence the pre-reduction of chromite negatively (Chapter 3, Section 3.7). The hot pellet strength is equally important, since the breakdown of pellets that are pre-reduced in the rotary kiln results in material built-up (Chapter 3, Section 3.6). In conclusion, the study showed that it is unlikely that the performance of a specific clay binder in this relatively complex pelletised chromite pre-reduction process can be predicted based merely on the chemical, surface chemical and mineralogical characterisation of the clay. Experimental monovariance evaluation of clay performance on the characteristics identified in this study needs to be evaluated in order to distinguish which clay will be best suited for this unique process application.

ii) Seventeen different fine carbonaceous reducing agents, i.e. ten anthracite, two char and five coke samples, used by FeCr smelter applying the chromite pre-reduction process were obtained from various suppliers. In order to gain new perspectives on reductant selection for pelletised chromite pre-reduction, reductants that fell within the current selection criteria, as well as reductants that fell outside the industrial specification, were obtained. These seventeen different carbonaceous reductants were extensively characterised by conducting proximate-, ultimate-, gross calorific value-, total sulphur value-, ash fusion temperatures- and ash composition analyses (Chapter 3, Section IIIA). As a testament to the comprehensive range in composition and characteristics of the carbonaceous reductants received, it can be mentioned that the fixed carbon contents of the samples, for example, ranged between ~52 to ~92 wt.%. According to the candidate's knowledge of research data available in the peer-reviewed public domain, this is one of

the most comprehensive sets of carbonaceous reductants data ever considered in a study focusing on chromite pre-reduction. The effect of the different carbonaceous reducing agents on the two most important pelletised chromite pre-reduction process performance indicators, i.e. the extent of pre-reduction achieved and cured compressive strength of pelletised chromite pre-reduced pellets, was determined under specific experimental condition (Chapter 3, Section IIIB and IIIC). The dependence between the multiple variables, i.e. reductant characteristics, level of pre-reduction and compressive strengths was demonstrated by constructing a correlation matrix. The correlation matrix showed that it is implausible to estimate the performance of a reductant, in terms of its effect on pre-reduction level and cured pellet strength, by considering only a single parameter (Chapter 3, Section IIID). Multi-linear regression (MLR) was successfully used to relate the various carbonaceous reductant characteristics (Chapter 3, Section IIIA) to the main performance indicators (Chapter 3, Section IIIB and IIIC) of a reductant in the chromite pre-reduction process (Chapter 3, Section IIID). Optimum solutions to predict both pre-reduction and cure compressive strength were attained, which can be utilised by FeCr producers henceforth to more efficiently select reductants for use in the pelletised chromite pre-reduction process (Chapter 3, Section IIID). Three other carbonaceous reductants not used to derive the MLR equations were used to illustrate the accuracy of the determined optimum MLR equations. The predicted pre-reduction and compressive strength values of these additional samples were on, or close to the actual experimentally determined pre-reduction and compressive strength values, which verified that the determined MRL equations can be used to estimate pre-reduction and compressive pellet strength accurately (Chapter 3, Section IIID). In order to interpret and gain further understanding of the importance of individual predictors (independent variables) included in the optimum MLR solutions, several statistical techniques were successfully employed. By employing these techniques, a novel concept of *situ* H_2 generation to improve chromite pre-reduction emerged (Chapter 3, Section IIID).

b) **Objective 2: Evaluate whether pre-oxidation of chromite ore, prior to being used in the pelletised pre-reduction process, can improve the extent of pre-reduction, which will further improve the specific electricity consumption (SEC) of the submerged arc furnaces (SAF). The specific objectives were to i) present the new suggested process, i.e. pre-oxidation of chromite ore prior to pelletised pre-reduction, ii) assess how to optimise pre-oxidation conditions to maximise the benefit of using pre-oxidised chromite ore iii) indicate the possible practical advantages and disadvantages of this process option by considering factors such as SEC, carbonaceous reductant consumption, breaking- and abrasion strengths, as well as the formation of hexavalent chromium, Cr(VI), which is considered a**

human carcinogen and iv) asses the techno-economic feasibility of implementing the proposed pre-oxidation process prior to the chromite pre-reduction process.

i) Technical aspects surrounding the utilisation of pre-oxidised ore in the pelletised chromite pre-reduction process was presented in Chapter 5, which provided input into the assessment of possible process option (Chapter 6), where after a hypothetical process flow diagram was developed and presented in Chapter 6 detailing implementation of pre-oxidation of chromite ore prior to pelletised pre-reduction.

ii) From the results presented in Chapter 5, Section 3.1, it was evident that by pre-oxidising the chromite ore prior to pre-reduction, the extent of achievable pre-reduction could be increased significantly. The results presented in Chapter 5 indicated that a pre-oxidation temperature of 1000 °C was the optimum pre-oxidation temperature, for the specific case study metallurgical grade chromite ore considered. The highest pre-oxidation temperatures (1100-1500 °C) investigated did not correlate with the highest pre-reduction levels, which from a production cost perspective is beneficial, since lower pre-oxidation temperatures are associated with lower operational costs.

iii) Through the application of several investigative techniques, i.e. SEM, SEM-EDS, X-ray mapping, XRD and thermo-chemical calculation, it was found that pre-reduction could be optimised by enhancing iron (Fe) migration during pre-oxidation with prevention of the formation of free Cr_2O_3. It is therefore believed that this fundamental understanding of the mechanism for enhanced pre-reduction by pre-oxidation will enable this technique to be applied to any chromite ore (Chapter 5, Section 3.2-3.4). It was demonstrate how an increase in the level of pre-reduction as a result of using pre-oxidised ore, could lead to significant improvements (decrease) in the SEC and lumpy carbonaceous material required in FeCr production, specifically at the pre-oxidation temperature of 1000 °C, where the SEC and FC required are at their lowest (Chapter 5, Section 3.5). The effect of pre-oxidation on the cured compressive and abrasion strength of pre-reduced pellets was investigated, which revealed a decreases in pellet compressive and abrasion strengths as a result of utilising pre-oxidised ore (Chapter 5, Section 3.6). However, it is likely that the lower pellet strength could be mitigated by the selection of an optimum clay binder and the presence of a thin oxidised outer layer formed on the exterior of industrially produced pre-reduced pellets. Should this processing option be considered for currently operational FeCr smelters applying the pelletised chromite pre-reduction process, only limited modifications to the current plant operation would be required. In principle, all that would be required is the construction of a furnace/kiln in which the chromite ore could be pre-oxidised. This pre-oxidised ore could then be stockpiled and fed into the currently existing process (Chapter 6). From an occupational health and environmental

perspective, it was identified that small amounts of Cr(VI) could be generated during chromite pre-oxidation (Chapter 5, Section 3.8). The appropriate measures, such as dust extraction, capturing and/or suppression, as well as the necessary compulsory personal protective equipment, will have to be addressed and implemented to limit exposure to dust particles possibly containing Cr(VI).

iv) The techno-economic feasibility of integrating chromite pre-oxidation into the currently applied pelletised pre-reduction process as a pre-treatment method was investigated successfully and the results presented in Chapter 6. A comprehensive estimate of the costs associated with the pre-oxidation of chromite ore was determined, in order to more accurately approximate input costs for further lifecycle financial modelling. The South-African FeCr industry and economy was chosen as the ideal backdrop conditions within which the techno-economic feasibility of implementing such a chromite pre-oxidation process could be evaluated. The lifecycle financial model, built on a discounted cash flow (DCF) approach, strongly indicated that integration of the chromite pre-oxidation process into the currently applied pre-reduction process is feasible from a financial perspective.

c) **Objective 3: Identify an appropriate method/methods to alter the chromite spinel and improve the chromium-to-iron (Cr/Fe) ratio of low grade chromite ore.**

The Cr/Fe ratio of low grade chromite ores was successfully increased by developing a combined pyro- and hydrometallurgical method. Two process options were identified and investigated and the results presented in Chapter 7. The first option involved selective metallisation of Fe in pelletised chromite pre-reduction, where after the metallised Fe was removed by means of hot acid leaching. The second option consisted of chromite pre-oxidation to encourage Fe migration and enrichment on the surface of the chromite ore particles, Fe selective un-agglomerated chromite metallisation by pre-reduction followed by hot acid leaching to strip the metallised Fe from the ore mixture. Sensible Cr/Fe ratios of >2 up to ~4.28 were achieved, with corresponding chromium (Cr) recoveries in the excess of 90%, warranting further considerations for possible pilot scale testing.

8.2 Future perspectives

The significant effect of secondary raw material, i.e. the clay binder and fine carbonaceous reductant, on the pelletised chromite pre-reduction process was demonstrated in this study. It was also mentioned from literature that the origin, geology and physical- and chemical characteristics of chromite ore has an effect on chromite reduction rate. It is therefore suggested that chromite ore as the primary raw material are investigated similarly to the studies presented in Chapter 3 and 4 employing the methods and techniques identified therein. It is also suggested

that the effect of raw materials on the smelting process is investigated. Historically, access to a wide range of chromite ore by FeCr producers was limited due to different entities owning smelting facilities and mines. However, recently, companies within the FeCr industry have become more vertically integrated by owning/accessing various ore sources and smelting operation utilising different smelting technologies. It therefore makes sense to match specific chromite ores with specific smelting technologies, as well as with possible future technologies as suggested in this investigation. Additionally, the current framework relating to the acquisition of raw materials by FeCr producers is predominantly focused on the price of the raw materials. Factors affecting the FeCr operations, which could lead to substantial losses or savings, as illustrated in this investigation, are currently not properly addressed in the procurement management of raw materials. Therefore, a new framework from a management perspective needs to be developed to deal with the procurement of technically optimal raw materials.

Although integration of the chromite pre-oxidation process into the currently applied pre-reduction process shows potential, pre-oxidation could also be considered as a pre-treatment process prior to other FeCr production processes. The process that could greatly benefit from the pre-oxidation of ore would be DCF operations. The DC arc process allows the direct use of chromite fines (<6 mm, 90% <1 mm) without the need for expensive agglomeration techniques (pelletising). Furthermore, non-coking coal can be used as reduction agent, which is low-priced compared to metallurgical coke. The main disadvantage of DCF operations is the relatively high SEC, i.e. ~4.5-4.8 MWh/t FeCr, compared to conventional SAF operations (3.9–4.2 MWh/t FeCr), the oxidative sintered process (>3.1 MWh/t FeCr) and the pre-reduction process (~2.4 MWh/t FeCr). However, in order to assess the techno-economic feasibility of pre-oxidation prior to DC arc smelting, the effect of pre-oxidation on DCF SEC needs to be determined. Another crucial future perspective would be the development of a method to determine the extent of pre-oxidation, similar to determining the level of pre-reduction achieved. This would be important in order to assess the effect of pre-oxidation on DCF SEC. Companies follow different approaches during the lifecycle development of a project. Although the candidate recommends that the project be tested on pilot scale, it is more-likely that FeCr producers would prefer to conduct a campaign study on a commercial scale.

Oxalic has been extensively studied and is commonly used in processes for the purification of industrial minerals, such as quartz sand, feldspars, and kaolins, contaminated by Fe oxides (Taxiarchou *et al.*, 1997; Veglió *et al.*, 1998; Dudeney *et al.*, 1999; Tarasova *et al.*, 2001; Lee *et al.*, 2006; Lee *et al.*, 2007; Li *et al.*, 2016). Oxalic acid reacts with surface Fe ions to form soluble complexes. It was identified in this investigation that during the pre-oxidation of chromite, Fe migration and enrichment on the surface of the chromite ore particles occurs. Therefore, it is suggested that the pre-oxidation of chromite ore, followed by oxalic acid leaching is investigated

in the future to assess if the Cr/Fe ratio of low grade chromite ores cannot be increased. Such a process would be simpler, and possibly more cost effective, than the process options investigated in detail in this study. However, it would have been impossible to identify this research opportunity at the onset of this study, since results from this study gave insight into this new possibility.

BIBLIOGRAPHY

Abubakre, O.K., Murian, R.A. & Nwokike, P.N. 2007. Characterization and beneficiation of Anka chromite ore using magnetic separation process. *Journal of Minerals and Materials Characterization and Engineering*, 6(2):143-150.

Agacayak, T., Zedef, V. & Aydogan, S. 2007. Benefication of low-grade chromite ores of abandoned mine at Topraktepe, Beyşehir, SW Turkey. *Acta Montanistica Slovaca*, 4:323-327.

Amer, A.M. 1992. Processing of Ras-Shait chromite deposits. *Hydrometallurgy*, 28:29-43.

Amer, A.M. & Ibrahim, I.A. 1996. Leaching of a low grade Egyptian chromite ore. *Hydrometallurgy*, 43:307-316.

Antweiler, W. 2016. The University of British Columbia, Sander School of Business, PACIFIC Exchange Rate Service. http://fx.sauder.ubc.ca/data.html. Date of access: 28 October 2016.

Baker, R. 2006. Poor planning. *Business Day*(5). 3 May 2006.

Bale, C.W., Chartrand, P., Degterov, S.A., Eriksson, G., Hack, K., Ben Mahfoud, R., et al. 2002. FactSage thermochemical software and databases. *Calphad*, 26(2):189-228.

Barcza, N.A., Featherstone, R.A. & Finn, C.W.P. 1982. Recent developments in the ferro-alloy field in South Africa. (*In* Glen, H.W., *ed.* Proceedings of the 12th CMMI Congress organised by Johannesburg, South Africa: SAIMM. p. 595-604)

Barnes, A., Muinonen, M. & Lavigne, M.J. 2015. Reducing energy consumption by alternative processing routes to produce ferrochromium alloys from chromite ore. Paper presented at the The Conference of Metallurgists.

Barnes, A.R., Finn, C.W.P. & Algie, S.H. 1983. The prereduction and smelting of chromite concentrate of low chromium-to-iron ratio. *Journal of the South African Institute of Mining and Metallurgy*(March):49-54.

Basson, J., Curr, T.R. & Gericke, W.A. 2007. South Africa's Ferro Alloy Industry-Present Status and Future Outlook. (*In* Roy, T.K., *ed.* Proceedings of The 11th International Ferro Alloys Conference organised by New Delhi, India: Indian Ferro Alloy Producers' Association (IFAPA). p. 3-24)

Bergeron, M. & Richer-Lafleche, M. 2004. A method for increasing the chrome to iron ratio of chromites products. (Patent: Montreal, Canada.

Beukes, J.P., Dawson, N.F. & van Zyl, P.G. 2010. Theoretical and practical aspects of Cr(VI) in the South African ferrochrome industry. *The Journal of The Southern African Institute of Mining and Metallurgy*, 110(December):743-750.

Beukes, J.P., Van Zyl, P.G. & Neizel, B.W. 2015. Process for enhanced pre-reduction of chromite.

Beukes, J.P., van Zyl, P.G. & Ras, M. 2012. Treatment of Cr(VI) containing wastes in the South African ferrochrome industry - A review of currently applied methods. *The Journal of The Southern African Institute of Mining and Metallurgy*, 112(May):347-352.

Bhatti, M.A., Kazmi, K.R. & Anwar, M.S. 2008. High Intensity Magnetic Separation Studies of Low Grade Chromium Ore. *JOURNAL-CHEMICAL SOCIETY OF PAKISTAN*, 30(1):42.

Biermann, W., Cromarty, R.D. & Dawson, N.F. 2012. Economic modelling of a ferrochrome furnace. *The Journal of The Southern African Institute of Mining and Metallurgy*, 112(April):301-308.

Biermann, W.J. & Heinrichs, M. 1960. The attack of chromite by sulphuric acid. *Canadian Journal of Chemistry*, 38:1449-1454.

Bonga, M. 2009. Ferrous mineral commodities produced in the Republic of South Africa 2009. Directorate: Mineral Economics, Department: Minerals and Energy, Republic of South Africa. *Department of Mineral Resources*. http://www.dmr.gov.za/Mineral_Information/New/D8%202009.pdf. Date of access: 5 March 2011.

Botha, W. 2003. Ferrochrome production through the SRC process at Xstrata, Lydenburg Works. *Journal of the South African Institute of Mining and Metallurgy*, 103(6):373–389.

Cramer, L.A. 2001. The Extractive Metallurgy of South Africa's Platinum Ores. *Journal of the Minerals, metals, and Materials Society*, 53(10):14-18.

Cramer, L.A., Basson, J. & Nelson, L.R. 2004. The impact of platinum production from UG2 ore on ferrochrome production in South Africa. *The Journal of The South African Institute of Mining and Metallurgy*, 104(9):517-527.

Creamer, M. 2010. Energy for Xstrata's R4,9bn Lion ferrochrome add-on, plus new R700m mine. http://www.miningweekly.com/article/energy-sure-xstrata-approves-r49-billion-ferrochrome-expansion-new-r700m-mine-2010-10-20 Date of access: 20 October 2010.

CRU. 2010. Ferrochrome cost and market service. Mount Pleasant, London

Curr, T.R. 2009. History of DC arc furnace process development. Paper presented at the Mintek 75 - A celebration of technology, Randburg, South Africa.

Daavittila, J., Honkaniemi, M. & Jokinen, P. 2004. The transformation of ferrochromium smelting technologies during the last decades. *The Journal of The South African Institute of Mining and Metallurgy*(October):541–549.

Dawson, N.F. & Edwards, R.I. 1986. Factors Affecting the Reduction Rate of Chromite. (*In* Finardi, J., Nascimento J.O. & Homem De Melo F.D., *eds*. Proceedings of the 4th International Ferro-alloys Congress organised by Sao Paulo, Brazil: ASSOCIACAO BRASILEIRA DOS PRODUTORES DE FERRO-IIGAS - ABRAFE. p. 105-113)

Denton, G.M., Bennie, J.P.W. & De Jong, A. 2004. An improved DC-arc process for chromite smelting. (*In* Barcza, N.A., *ed.* Proceedings of the Tenth International Ferroalloys Congress (INFACON X) organised by Cape Town, South Africa: SAIMM. p. 60-67)

Ding, Y.L. & Warner, N.A. 1997a. Catalytic reduction of carbon-chromite composite pellets by lime. *Thermochimica Acta*, 292:85-94.

Ding, Y.L. & Warner, N.A. 1997b. Reduction of carbon-chromite composite pellets with silica flux. *Ironmaking and Steelmaking*, 24(4):283-287.

Dos Santos, M. 2010. Meeting the challenges of sustainability through technology development and intergration in ferroalloy submerged arc furnace plant desing. (*In* Vartiainen, A., *ed.* Proceedings of The 12th International Ferroalloys Congress organised by Helsinki, Finland: Outotec Oyj,. p. 71-80)

Dowes, K.W. & Morgan, D.W. 1951. Utilization of low grade domestic chromite. Ontario, Canada: Canada Department of Mines and Technical Surveys, M.B. Canada Department of Mines and Technical Surveys, Mines Branch

Dudeney, A.W.L., Narayanan, A. & Tarasova, I.I. 1999. Removal of iron from silica sand: Integrated effluent treatment by sulphate reduction, photochemical reduction and reverse osmosis. *(In* Amils, R. & Ballester A., *eds.* Process Metallurgy. Elsevier. p. 617-625).

Duong, H.V. & Johnston, R.F. 2000. Kinetics of solid state silica fluxed reduction of chromite with coal. *Ironmaking & Steelmaking*, 27(3):202-206.

Dwarapudi, S., Tathavadkar, V., Rao, B.C., Kumar, T.K.S., Ghosh, T.K. & Denys, M. 2013. Development of Cold Bonded Chromite Pellets for Ferrochrome Production in Submerged Arc Furnace. *ISIJ International*, 53(1):9-17.

Eskom. 2011. Eskom retail tariff adjustment for 2011/2012. http://www.eskom.co.za/content/priceincrease2011.pdf Date of access: 1 December 2011.

Eskom. 2012. Eskom retail tariff adjustment for 2012/2013. http://www.eskom.co.za/c/article/816/home/ Date of access: 7 October 2012.

FAPA. 2016. Impact of the RCA adjustment on MYPD3: Submission from the Ferro Alloy Producers' Association to the National Energy Regulator of South Africa. http://www.nersa.org.za/Admin/Document/Editor/file/Consultations/Electricity/Presentations/FAPA.pdf Date of access: 3 November 2016.

Featherstone, R.A. & Barcza, N.A. 1982. The growth of ferro-alloy production in South Africa. *Mintek*. http://www.mintek.co.za/Pyromet/Files/1982FeatherstoneBarcza.pdf Date of access: 28 October 2016.

Fowkes, K. 2014. Is there a limit to the market share of South African chrome units? (*In*. Metal Bulletin 7th South African Ferroalloys Conference organised by Johannesburg, South Africa: Metal Bulletin. www.alloyconsult.com/files/MB_conf_presentation_-_SA_Sep_2014.pdf Date of access: 28 October 2016.

Gediga, J. & Russ, M. 2007. Life cycle inventory (LCI) update of primary ferrochrome production. Leinfelden – Echterdingen, Germany. PE International GmbH

Geveci, A., Topkaya, Y. & Ayhan, E. 2002. Sulfuric acid leaching of Turkish chromite concentrate. *Minerals Engineering*, 15:885-888.

Glastonbury, R.I., Beukes, J.P., Van Zyl, P.G., Sadiki, L.N., Jordaan, A., Campbell, H.M., et al. 2015. Comparison of physical properties of oxidative sintered pellets produced with UG2 or metallurgicalgrade South African chromite: a case study. *The Journal of The Southern African Institute of Mining and Metallurgy*, 115(August):1-8.

Glastonbury, R.I., van der Merwe, W., Beukes, J.P., van Zyl, P.G., Lachmann, G., Steenkamp, C.J.H., et al. 2010. Cr(VI) generation during sample preparation of solid samples – A chromite ore case study. *Water SA*, 36(1):105-110.

Greyling, F.P., Greyling, W. & De Waal, F.I. 2010. Developments in the design and construction of DC arc smelting furnaces. *The Journal of The South African Institute of Mining and Metallurgy*, 110:711-716.

Gu, F. & Wills, B.A. 1988. Chromite - mineralogy and processing. *Minerals Engineering*, 1(3):235-240.

Hauptmanns, U. 2014. Process and Plant Safety. Berlin, Germany: Springer Berlin Heidelberg.

Hayes, P.C. 2004. Aspects of SAF smelting of Ferrochrome. (*In* Barcza, N.A., *ed.* Proceedings of the 10th International Ferroalloys Congress organised by Cape Town, South Africa: SAIMM. p. 1-14)

Heinz H. Pariser. 2013. Alloy Metals & Steel Market Research. Xanten, Germany: Heinz H. Pariser. Heinz H. Pariser,

Howat, D.D. 1986. Chromium in South Africa. *Journal of the South African Institute of Mining and Metallurgy*, 86(2 (Feb)):37-50.

Hu, X., Yang, Q., Sundqvist Ökvist, L. & Björkman, B. 2016. Thermal Analysis Study on the Carbothermic Reduction of Chromite Ore with the Addition of Mill Scale. *steel research international*, 87(5):562-570.

Hussein, M.K. & El-Barawi, K. 1971. Study of the chlorination and benificiation of Egyptian chromite ores. *Transactions of the Institution of Mining and Metallurgy. Section C. Mineral Processing & Extractive Metallurgy*, 80:C7–C11.

Hussein, M.K., Winterhager, H., Kammel, R. & El-Barawi, K. 1974. Chlorination behaviour of the main oxide components chromite ores. *Transactions of the Institution of Mining and Metallurgy. Section C. Mineral Processing & Extractive Metallurgy*, 83:C154-C160.

ICDA. 2010. Statistical Bulletin 2010. Paris, France. International Chromium Development Accociation

ICDA. 2013a. Chrome ore - Global overview of the chrome ore market. Paris, France. International Chromium Development Association. http://www.icdacr.com/index.php?option=com_phocadownload&view=file&id=133:icda-overview-of-the-chromium-industry-in-2012&lang=en Date of access: 29 October 2016.

ICDA. 2013b. Energy Update - November 2013. International Chromium Development Association

ICDA. 2013c. Ferrochrome. http://www.icdacr.com/market-intelligence/fecr-brch/fecr-brch.pdf Date of access: 13 January 2014.

ICDA. 2013d. Statistical Bulletin 2013. Paris, France. International Chromium Development Association

ICDA. 2016. Chronology of Chrome. http://www.icdacr.com/index.php?option=com_content&view=article&id=135&Itemid=340&lang=en Date of access: 10 November 2016.

Ideas 1st Research. 2010. Ferrochrome March 2010. http://ideasfirst.in/Admin/Downloads/Reports/1720868194_Chrome-Ferrochrome%20-%20Final%20-%2031Mar20101.pdf Date of access: 28 October 2016.

IETEG. 2005. Chromium(VI) Handbook. Boca Raton, USA: CRC Press.

ISSF. 2011. Stainless steel demand index. <http://www.worldstainless.org/Statistics/Demand+index/ Date of access: 14 January 2014.

Jiang, M.F., Zhao, Q., Liu, C.J., Shi, P.Y., Zhang, B., Yang, D.P., et al. 2014. Sulfuric acid leaching of South African chromite. Part 2: Optimization of leaching conditions. *International Journal of Mineral Processing*, 130:102-107.

Jones, R.T. 2010. Pyrometallurgy in South Africa. *Pyrometallurgy*. http://www.pyrometallurgy.co.za/PyroSA/index.htm Date of access: 22 June 2010.

Jones, R.T. 2015. Pyrometallurgy in Southern Africa - List of Southern African Smelters. http://www.pyrometallurgy.co.za/PyroSA/index.htm Date of access: 14 September 2015 2015.

Kanari, N., Gaballah, I. & Allain, E. 1999. A study of chromite carbochlorination kinetics. *Metallurgical and Materials Transactions B*, 30(4):577-587.

Kanari, N., Gaballah, I. & Allain, E. 2000. Use of chlorination for chromite upgrading. *Thermochimica Acta*, 351(1–2):109-117.

Kapure, G., Tathavadkar, V., Rao, C.B., Rao, S.M. & Raju, K.S. 2010. Coal based direct reduction of preoxidezed chromite ore at high temperature. Paper presented at the The Twelfth International Ferroalloys Congress (INFACON XII), Helsinki, Finland, 6-9 June.

Kapure, G., Tathavadkar, V., Rao, C.B., Sen, R., Raju, K.S. & Shastri, D. 2013. A method for direct reduction of oxidized chromite ore fines composite agglomerates in a tunnel kiln using carbonaceous reductant for production of reduced chromite product/ agglomerates applicable in ferrochrome or charge chrome production: Google Patents.

Katayama, H.G., Tokuda, M. & Ohtani, M. 1986. Promotion ofthe carbothermic reduction of chromium ore by the addition of borates. *The Iron and Steel Institute of Japan*, 72(10):1513-1520.

Kleynhans, E.L.J., Beukes, J.P., Van Zyl, P.G., Kestens, P.H.I. & Langa, J.M. 2012. Unique challenges of clay binders in a pelletised chromite pre-reduction process. *Minerals Engineering*, 34:55-62.

Kogel, J.E., Trivedi, N.C., Barker, J.M. & Krukowski, S.T. 2006. Industrial Minerals and Rocks - Commodities, Markets, and Uses (7th Edition): Society for Mining, Metallurgy, and Exploration (SME).

Kumar Tripathy, S., Singh, V. & Ramamurthy, Y. 2012. Improvement in Cr:Fe Ratio of Indian Chromite Ore for Ferro Chrome Production. *International Journal of Mining Engineering and Mineral Processing*, 1(3):101-106.

Lee, S.O., Tran, T., Jung, B.H., Kim, S.J. & Kim, M.J. 2007. Dissolution of iron oxide using oxalic acid. *Hydrometallurgy*, 87(3–4):91-99.

Lee, S.O., Tran, T., Park, Y.Y., Kim, S.J. & Kim, M.J. 2006. Study on the kinetics of iron oxide leaching by oxalic acid. *International Journal of Mineral Processing*, 80(2–4):144-152.

Lekatou, A. & Walker, R.D. 1997. Effect of SiO2 addition on solid state reduction of chromite concentrates. *Ironmaking and Steelmaking*, 24(2):133-143.

Li, X., Li, T., Gao, J., Huang, H., Li, L. & Li, J. 2016. A novel "green" solvent to deeply purify quartz sand with high yields: A case study. *Journal of Industrial and Engineering Chemistry*, 35:383-387.

Lide, D.R. 2009. CRC Handbook of Chemistry and Physics, 89th edition (Internet Version). Boca Raton, USA: CRC Press/Taylor and Francis,.

Loock-Hattingh, M.M., Beukes, J.P., van Zyl, P.G. & Tiedt, L.R. 2015. Cr(VI) and Conductivity as Indicators of Surface Water Pollution from Ferrochrome Production in South Africa: Four Case Studies. *Metallurgical and Materials Transactions B*:1-11.

Loock, M.M., Beukes, J.P. & van Zyl, P.G. 2014. A survey of Cr(VI) contamination of surface water in the proximity of ferrochromium smelters in South Africa. *Water SA*, 40(4):709-716.

Lungu, J. 2010. Mining and the impact of the recession in the southern African development community states. *Sarwatch*. http://www.sarwatch.org/sarwadocs/john_lungu/module1_SARW_Importance_of_mining_in_SADC.pdf Date of access: 31 November 2011.

Makhoba, G. & Hurman Eric, R. 2010. Reductant characterization and selection for ferrochromium production. (*In* Vartiainen, A., *ed.* Proceedings of The 12th International Ferroalloys Congress organised by Helsinki, Finland: Outotec Oyj. p. 359-365)

Maulik, S. & Bhattacharyya, K. 2005. Beneficiation of Low Grade Chromite Ores from Sukinda. (*In* Venugopal, R., Sharma T., Saxena V.K. & Mandre N.R., *eds.* International Seminar on Mineral Processing Technology (Mpt-2005) organised by: The McGraw Hill Companies. p. 146-154)

McCullough, S., Hockaday, S., Johnson, C. & Barcza, N.A. 2010. Pre-reduction and smelting characteristics of Kazakhstan ore samples. (*In* Vartiainen, A., *ed.* Proceedings of The 12th International Ferroalloys Congress organised by Helsinki: Outotec Oyj. p. 249-262)

Merafe-Resources. 2012. Maximising South Africa's chrome ore endowment to create jobs and drive sustainable. http://www.meraferesources.co.za/pdf/presentations/2012/chrome_ore_brochure.pdf Date of access: 14 January 2014.

Mobley, R.K. 2001. Plant Engineer's Handbook. Woburn, USA: Butterworth-Heinemann.

Murthy, Y.R., Tripathy, S.K. & Kumar, C.R. 2011. Chrome ore beneficiation challenges & opportunities – A review. *Minerals Engineering*, 24(5):375-380.

Nafziger, R.H. 1982. A review of the deposits and beneficiation of lower-grade chromite. *Journal of the South African Institute of Mining and Metallurgy*(August):205-226.

Naiker, O. 2007. The development and advantages of Xstrata's Premus Process. (*In* Roy, T.K., *ed.* Proceedings of The 11th International Ferroalloys Congress organised by New Delhi, India: IFAPA. p. 112-118)

Naiker, O. & Riley, T. 2006a. Xstrata Alloys in Profile. (*In* Jones, R.T., *ed.* Southern African Pyrometallurgy organised by Johannesburg, South Africa: South African Institute of Mining and Metallurgy. p. 297-306)

Naiker, O. & Riley, T. 2006b. Xstrata alloys in the profile. (*In* Jones, R.T., *ed.* South African Pyrometallurgy 2006 organised by Johannesburg, South Africa: SAIMM. p. 297-306)

National Academy of Sciences. 1974. Chromium. Medical and Biologic Effects of Environmental Pollutants. Washington D.C., USA: National Academy of Sciences,.

Nedzingahe, L., Managa, M.A. & Ncube, O. 2010. Forecasting energy consumption in the ferrochrome sector. *energize*(April):52-55.

Neizel, B.W. 2010. Alteration of chrome-to-iron ratio in chromite ore by chlorination. Potchefstroom: North-West University (Dissertation - M.Sc.). p. 90).

Neizel, B.W., Beukes, J.P., van Zyl, P.G. & Dawson, N.F. 2013. Why is CaCO3 not used as anadditive inthe pelletised chromite pre-reduction process? *Minerals Engineering*, 45:115–120.

NERSA. 2009a. Eskom price increase application 2009. http://www.nersa.org.za/Admin/Document/Editor/file/Electricity/PricingandTariffs/Eskom%20Current%20Price%202009-10.pdf Date of access: 28 October 2016.

NERSA. 2009b. Historic Eskom Average Selling Price. http://www.nersa.org.za/Admin/Document/Editor/file/Electricity/PricingandTariffs/Eskom%20Historic%20Prices.pdf Date of access: 28 October 2016.

Neuschiitz, D., JanBen, P., Friedrich, G. & Wiechowski, A. 1995. Effect of Flux Additions on the Kinetics of Chromite Ore Reduction with Carbon. (*In*. Proceedings of the 7th International Ferroalloys Congress organised by Trondheim, Norway. p. 371-381)

Niayesh, M.J. & Fletcher, G.W. 1986. An assessment of smelting reduction processes in the production of Fe-Cr-C alloys. (*In*. The Fourth International Ferroalloys Congress (INFACON IV) organised by Sao Paulo, Brazil. p. 115-123)

Niemelä, P., Krogerus, H. & Oikarinen, P. 2004. Formation, characterization and utilization of CO-gas formed in ferrochrome smelting. (*In* Barcza, N.A., *ed*. Proceedings of The 12th International Ferroalloys Congress organised by Cape Town, South Africa. p. 68-77)

Nunnington, R.C. & Barcza, N.A. 1989. Pre-reduction of fluxedchromite-ore pellets under oxidizing conditions. (*In*. Proceedings of the 5th International Ferroalloys Congress organised by New Orleans,USA. p. 55-68)

NWU. 2015. General Academic Rules. http://www.nwu.ac.za/sites/www.nwu.ac.za/files/files/i-governance-management/policy/7P-Arules2015_e_1.pdf Date of access: 12 November 2016.

NWU. 2016. Manual for Master's and Doctoral Studies. http://www.nwu.ac.za/sites/www.nwu.ac.za/files/files/library/documents/manualpostgrad.pdf Date of access: 12 November 2016.

Oberholzer, J. & Daly, K. 2014. SA Chrome & Ferrochrome - Tug-of-war with a giant. Johannesburg, South Africa. Macquarie First South Securities (Pty) Ltd

OCC. 2014. Beneath the Surface - Uncovering the Economic Potential of Ontario's Ring of Fire. Ontario, Canada: Ontario Chamber of Commerce. Ontario Chamber of Commerce (OCC). http://www.occ.ca/Publications/Beneath_the_Surface_web.pdf Date of access:

Osborne, D. 2013. The Coal Handbook: Towards Cleaner Production. Vol. 2. Cambridge, United Kingdom: Woodhead Publishing Limited.

Outotec. 2015. Ferrochrome. http://www.outotec.com/en/Products--services/Ferrous-metals-and-ferroalloys-processing/Ferrochrome/ Date of access: 6 July 2015.

Owada, S. & Harada, T. 1985. Grindability and magnetic properties of chromites. *Journal of The Mining and Metallurgical Institute of Japan*, 101:781.

Paktunc, A.D.a. 1990. Origin of podiform chromite deposits by multistage melting, melt segregation and magma mixing in the upper mantle. *Ore Geology Reviews*, 5(3):211-222.

Pan, X. 2013. Effect of South Africa Reductants on Ferrochrome Production. *IFAC Proceedings Volumes*, 46(16):352-358.

Papp, J.F. 2008. Chromium. Minerals Yearbook–2008 (Chromium – Advance release). *U.S. Geological Survey Minerals*. http://minerals.usgs.gov/minerals/pubs/commodity/chromium/myb1-2008-chrom.pdf Date of access: 2 February 2011.

Papp, J.F. 2009a. 2009 Minerals Yearbook Chromium [Advance Release]. *USGS Chromium Statistics and Information*. http://minerals.usgs.gov/minerals/pubs/commodity/chromium/myb1-2009-chrom.pdf Date of access: 19 October 2011.

Papp, J.F. 2009b. *Chromium. USGS Chromium Statistics and Information*. http://minerals.usgs.gov/minerals/pubs/commodity/chromium/mcs-2009-chrom.pdf Date of access: 2 February 2011.

Papp, J.F. & Lipin, B.R. 2000. Chromium and Chromium Alloys. Kirk-Othmer encyclopedia of chemical technology. John Wiley & Sons, Inc.

Pariser, G.C. 2013. *Chromite: World Distribution, Uses, Supply & Demand, Future*. http://www.boldventuresinc.com/news_pdf/uploaded/2013-Mar3-PDAC-Pariser-Chrome-Presentation.pdf Date of access: 10 Nov 2015.

Pfister, J. 2006. The Eskom plan to meet Government's 6% GDP aspiration. Johannesburg, South Africa. Eskom

Pokorny, E.A. 1957. Studies in the chlorination of some complex ores—wolframite, vanadinite, and chromite. Paper presented at the Extraction and Refining of the Rare Metals: a Symposium, London, United Kingdom.

Riekkola-Vanhanen, M. 1999. Finnish expert report on best available techniques in ferrochromium production. Helsinki, Finland. Finnish Environment Institute

Roza, G. 2008. Understanding the Elements of the Periodic Table – Chromium. New York, USA: The Rosen Publishing Group, Inc. 49p.

Sahoo, A. 1988. Physico-chemical Beneficiation of Low Grade Chromite, DISM Project Report. Dhanbad, India. I.S.M.

Schroeder, H.A. 1970. Chromium. Air Quality Monograph #70-15. Washington D.C., USA: American Petroleum Institute. 28p.

Sen, M.C. & Chatterjee, A.B. 1957. Chemical Beneficiation of Indian Chromites. *Indian Mining Journal*(Special Issue):85-94.

Serov, G.V. 2010. A century of Russian electroferroalloy production. *Steel in Translation*, 40(7):647-654.

Sharma, T. 1990. The kinetics of iron dissolution from chromite concentrate. *Minerals Engineering*, 3(6):599-605.

Shen, S.-B., Bergeron, M. & Richer-Laflèche, M. 2009a. Effect of sodium chloride on the selective removal of iron from chromite by carbochlorination. *International Journal of Mineral Processing*, 91(3-4):74-80.

Shen, S.-B., Hao, X.-F. & Yang, G.-W. 2009b. Kinetics of selective removal of iron from chromite by carbochlorination in the presence of sodium chloride. *Journal of Alloys and Compounds*, 476(1-2):653-661.

Shi, P.Y. & Liu, S.L. 2002. Experimental study on sulphuric acid leaching of chromite. *Journal of the Chinese Rare Earth Society*, 20:472-474.

Snow, D.A. 2013. Plant Engineer's Reference Book. Oxford, United Kingdom: Butterworth-Heinemann.

Soykan, O., Eric, R.H. & King, R.P. 1991a. Kinetics of the reduction of Bushveld Complex chromite ore at 1416 C. *Metallurgical Transactions B*, 22B(December):801-810.

Soykan, O., Eric, R.H. & King, R.P. 1991b. The reduction mechanism of a natural Chromite at 1416 C. *Metallurgical Transactions B*, 22B(February):53-63.

Sun, Z., Zheng, S.-l., Xu, H.-b. & Zhang, Y. 2007a. Oxidation decomposition of chromite ore in molten potassium hydroxide. *International Journal of Mineral Processing*, 83(1-2):60-67.

Sun, Z., Zheng, S.L. & Zhang, Y. 2007b. Thermodynamics Study on the Decomposition of Chromite with KOH. *Acta Metallurgica Sinica (English Letters)*, 20(3):187-192.

Sundar Murti, N.S. & Seshadri, V. 1979. On the improvement in Cr/Fe ratio of Byrapur chromite. *Transactions of The Indian Institute of Metals*, 32(3):239-243.

Sundar Murti, N.S., Shah, V.L., Gadgeel, V.L. & Seshadri, V. 1983. Effect of lime addition on rate of reduction of chromite by graphite. *Institution of Mining and Metallurgy (Great Britain) Transactions. Section C, Mineral processing & extractive metallurgy*, 98C:C172-C174.

Takano, C., Zambrano, A.P., Nogueira, A.E.A., Mourao, M.B. & Iguchi, Y. 2007. Chromites reduction reaction mechanisms in carbon–chromites composite agglomerates at 1 773 K. *ISIJ International*, 47(11):1585-1589.

Tarasova, I.I., Dudeney, A.W.L. & Pilurzu, S. 2001. Glass sand processing by oxalic acid leaching and photocatalytic effluent treatment. *Minerals Engineering*, 14(6):639-646.

Tathavakar, V.D., Antony, M.P. & Jha, A. 2005. The physical chemistry of thermal decomposition of South African chromite minerals. *Metallurgical and Materials Transactions B*, 36(1):75-84.

Taxiarchou, M., Panias, D., Douni, I., Paspaliaris, I. & Kontopoulos, A. 1997. Removal of iron from silica sand by leaching with oxalic acid. *Hydrometallurgy*, 46(1):215-227.

Tripathy, S.K., Banerjee, P.K. & Suresh, N. 2015. Magnetic separation studies on ferruginous chromite fine to enhance Cr:Fe ratio. *International Journal of Minerals, Metallurgy, and Materials*, 22(3):217-224.

Udy, M. 1956. Recovery of chromium from its ores. *(In* Udy, M., *ed.* Chromium. New York, USA: Reinhold - USGS (United States Geological Survey). p. 3-4).

Ugwuegbu, C. 2012. Technology Innovations in the Smelting of Chromite Ore. *Innovative Systems Design and Engineering*, 3(12):48-55.

USGS. 2015. Mineral commodity summaries 2015. Reston, VA: U.S. Geological Survey. http://pubs.er.usgs.gov/publication/70140094 Date of access: 29 October 2016.

Van Deventer, J.S.J. 1988. The effect of additives on the reduction of chromite by graphite. *Thermochimica Acta*, 127:25-35.

Vardar, E., Eric, R.H. & Letowski, F.K. 1994. Acid leaching of chromite. *Minerals Engineering*, 7(5/6):605-617.

Veglió, F., Passariello, B., Barbaro, M., Plescia, P. & Marabini, A.M. 1998. Drum leaching tests in iron removal from quartz using oxalic and sulphuric acids. *International Journal of Mineral Processing*, 54(3–4):183-200.

Venmyn Rand Pty Ltd. 2010. Independent Technical Expert Report on the Mineral Assets of Sylvania Resources Limited in the form of a Competent Person Report by Vemyn (Pty) Limited. Johannesburg,South Africa: Ltd, S.R. Silvania Resources Ltd

Wait, M. 2011. Xstrata opens new mining complex in Steelpoort. *Mining Weekly*. March 4.

Wang, Y., Wang, L. & Chou, K.C. 2015. Effects of CaO, MgO, Al2O3 and SiO2 on the carbothermic reduction of synthetic FeCR2O4. *Journal of Mining and Metallurgy, Section B: Metallurgy*, 51(1):8pp.

Weber, P. & Eric, R.H. 1992. Solid state fluxed reduction of LG-6 chromite from the bushveld complex. (*In* Barcza, N.A., *ed.* Proceedings of the 6th International Ferroalloys Congress organised by Cape Town, South Africa: SAIMM. p. 71-77)

Weber, P. & Eric, R.H. 1993. The Reduction Mechanism of Chromite in the Presence of a Silica Flux. *Metallurgical Transactions B*, 24B(December):987-995.

Weber, P. & Eric, R.H. 2006. The reduction of chromite in the presence of silica flux. *Minerals Engineering*, 19(3):318-324.

Xiao, Z. & Laplante, A. 2004. Characterizing and recovering the platinum group minerals – a review. *Minerals Engineering*, 17:961-979.

Xu, H.B., Zheng, S.L., Zhang, Y., Li, Z.H. & Wang, Z.K. 2005. Oxidative leaching of a Vietnamese chromite ore in highly concentrated potassium hydroxide aqueous solution at 300 °C and atmospheric pressure. *Minerals Engineering*, 18(5):527-535.

Yousef, A., Boulos, T. & Arafa, M. 1970. Concentration of low-grade chromite ores for metallurgical and chemical purposes. *Journal of Mines, Metals and Fuels*, 12(January).

Yuksel, R. 2013. Ferrochrome Market Outlook - Supply & Demand Shifting East. (*In*. 12th International Stainless & Special Steel Summit organised by London, United Kingdom: MetalBulletin. http://www.metalbulletin.com/events/download.ashx/document/speaker/6572/a0ID000000X0jdUMAR/Presentation Date of access: 3 November 2016.

Zhang, B., Shi, P. & Jiang, M. 2016. Advances towards a Clean Hydrometallurgical Process for Chromite. *Minerals*, 6(1):7.

Zhang, Y., Zheng, S.-l., Du, H., Xu, H.-b. & Zhang, Y. 2010a. Effect of mechanical activation on alkali leaching of chromite ore. *Transactions of Nonferrous Metals Society of China*, 20(5):888-891.

Zhang, Y., Zheng, S.-l., Xu, H.-b., Du, H. & Zhang, Y. 2010b. Decomposition of chromite ore by oxygen in molten NaOH–NaNO3. *International Journal of Mineral Processing*, 95(1–4):10-17.

Zhao, B. & Hayes, P.C. 2010. Effects of oxidation on the microstructure and reduction of chromite pellets. Paper presented at the The Twelfth International Ferroalloys Congress (INFACON XII). Helsinki, Finland.

Zhao, Q., Liu, C.J., Shi, P.Y., Zhang, B., Jiang, M.F., Zhang, Q.S., et al. 2014. Sulfuric acid leaching of South African chromite. Part 1: Study on leaching behavior. *International Journal of Mineral Processing*, 130:95-101.

Zhao, Q., Liu, C.J., Shi, P.Y., Zhang, B., Jiang, M.F., Zhang, Q.S., et al. 2015. Sulfuric acid leaching kinetics of South African chromite. *International Journal of Minerals, Metallurgy and Materials*, 22(3):233-240.